



University
of Glasgow

Gould, Matthew K (2009) *Putative phosphodiesterase inhibitors as potential new chemotherapies against African Trypanosomiasis*. PhD thesis

<http://theses.gla.ac.uk/1410/>

Copyright and moral rights for this thesis are retained by the author

A copy can be downloaded for personal non-commercial research or study, without prior permission or charge

This thesis cannot be reproduced or quoted extensively from without first obtaining permission in writing from the Author

The content must not be changed in any way or sold commercially in any format or medium without the formal permission of the Author

When referring to this work, full bibliographic details including the author, title, awarding institution and date of the thesis must be given

Putative Phosphodiesterase Inhibitors as Potential New Chemotherapies against African Trypanosomiasis

Matthew K. Gould

Division of Infection and Immunity
Faculty of Biomedical and Life Sciences

This thesis is submitted for the degree of Doctor of Philosophy

Faculty of Biomedical and Life Sciences

University of Glasgow

September, 2009

Abstract

African trypanosomiasis is a disease caused by the Kinetoplastida parasites *Trypanosoma brucei rhodesiense* and *T. b. gambiense*. The distribution of the disease is split geographically with *T. b. rhodesiense* found in eastern sub-Saharan Africa and *T. b. gambiense* in the west of the continent. Current treatment for this fatal disease is wholly unsatisfactory with problems such as extreme toxicity, affordability and the emergence of resistance. The case for the generation of new potential chemotherapies is compelling and urgent.

Phosphodiesterase (PDE) enzymes degrade the secondary signalling molecule cyclic adenosine monophosphate (cAMP) to AMP by hydrolysis, thereby modulating and regulating the signal transduction to the effector proteins. The phosphodiesterase enzymes in the PDEB family in *T. brucei* were shown to be essential to the host-infective bloodstream forms and validated as good drug targets using RNA-interference (Zoraghi, R. and Seebeck, T., 2002; Oberholzer, M., 2007). Prompted by these findings, two series of putative trypanosomal PDE inhibitors, from different sources, were thoroughly assessed in this project for their anti-trypanosomal activity and their intracellular effects on the trypanosome.

The whole-cell *in vitro* efficacy for each compound, against *T. brucei* wildtype and the drug-resistant strain TbAT1 knockout, was established by the standard resazurin reduction assay. 25 compounds from Series 1 had EC₅₀ values below 0.5 μ M, with 7 under 100 nM and the most active having an EC₅₀ value of 5.8 ± 3.4 nM. For the much smaller Series 2 (GJS Compounds), the most active compound was GJS-128 with an EC₅₀ value of 79.4 ± 10.3 nM. This demonstrates that a number of compounds from both series have potent *in vitro* activity against trypanosomes that is better than or equal to the current chemotherapeutic compound diminazene, and some Series 1 compounds are on a par with pentamidine and melarsoprol. No major cross-resistance was displayed by the TbAT1 knockout strain to either Series 1 or the GJS series. Similarly, a panel of Series 1 compounds tested against the B48 strain (resistant to pentamidine and melaminophenyl arsenical drugs), and also against *Trypanosoma equiperdum* wildtype and diminazene resistant (PBR) strains, showed no major cross-resistance displayed by the other resistant strains. This suggests that there

would also be little or no cross-resistance from refractory strains in the field, and also that the compounds are active against multiple *Trypanosoma* species. A small panel of Series 1 compounds were also tested for efficacy against trypanosomes in infected mice. 4 daily doses of 20 mg/kg bodyweight of Compound 48 significantly reduced parasitaemia by approximately 60% compared to untreated controls, however higher concentrations were not tolerated by the mice so a cure could not be demonstrated.

A high-throughput method for monitoring the speed of action of test compounds on trypanosomes in real time was developed, based on the fluorescence of propidium iodide when bound with DNA. Optimisation of the protocol to 96-well plates and low cell densities provided higher resolution and accurate traces of the lysis of trypanosomes in a cell suspension compared to previously used methods, as well as a greatly increased capacity. The propidium iodide assay could also be converted to provide end-point EC_{50} values that were directly comparable to those established by the standard resazurin reduction assay.

The majority of Series 1 compounds did not increase the intracellular concentration of cAMP on incubation with bloodstream form trypanosomes; those that did only induced a minor elevation of the intracellular concentration of the signalling molecule. Since genetic disruption to phosphodiesterase enzymes resulted in large increases in cAMP levels (Oberholzer, M. et al, 2007; Zoraghi, R. and Seebeck, T., 2002), the lack of increase in cAMP by the Series 1 compounds strongly suggest that they do not sufficiently inhibit the PDEs in live trypanosomes and kill the cells via an alternative pathway.

In contrast, incubation with the GJS compounds did result in significant increases in intracellular cAMP concentration with the most active being GJS-128 recording an approximately 3-fold increase in cAMP over 3 hours at just 30 nM. The concentrations that begin to increase cAMP level are consistent with the EC_{50} values for trypanosomes cultured *in vitro* (this study), and is also in line with inhibition data of recombinant TbrPDEB enzymes (work conducted by Dr. Herrmann Tenor, ALTANA Pharma, and Prof. Thomas Seebeck, University of Bern). This gives a clear and consistent link between the cause of cAMP rise (inhibition of PDEB by GJS compounds) and the effect of that concentration increase on bloodstream form trypanosomes (cell death), demonstrating that the

GJS series are inhibitors of trypanosomal PDEs and chemically validate PDEs as drug targets for potential new chemotherapies against African trypanosomiasis.

The effect of PDE inhibition on the physiology of the bloodstream form trypanosomes was also investigated. Flow cytometry analysis and the assessment of DNA configuration by fluorescence microscopy after DAPI staining determined that PDE inhibition by GJS-128 resulted in a precise block of the cell cycle in cytokinesis. The replicating trypanosome synthesized and segregated its DNA into two nuclei and kinetoplasts as normal and proceeded to initiate the physical separation of mother and daughter cells. The cleavage furrow between the old and new flagella progressed normally until the point of abscission, at which point division was halted with only a small section of plasma membrane connecting the two almost separated cells. Both cells appeared viable and underwent subsequent rounds of DNA replication, segregation and attempted physical separation that was always blocked near completion. This indicates cAMP signalling plays an important role in the correct physical separation of the replicating bloodstream form trypanosomes.

A trypanosome cell line resistant to GJS-128 was developed by chemical mutagenesis and continuous culture with gradually increasing, but sub-lethal concentrations of the PDE inhibitor. This cell line, termed R0.8, was >15-fold less sensitive to GJS-128 and displayed significant cross-resistance to the other GJS compounds, as well as to stable, membrane permeable cAMP analogues. The mode of resistance was investigated by comparing the cAMP profile of the R0.8 and parental wildtype strains on incubation with GJS-128. No major differences were observed suggesting that both the adenylyl cyclase and phosphodiesterase activities remained unchanged in the PDE inhibitor-resistant strain. In support of this, the sequencing of TbrPDEB1 and TbrPDEB2 in both strains, while uncovering the loss of heterozygosity in the R0.8 line, revealed no mutations that would impact on enzyme function or inhibitor binding in the resistant cell line. These data strongly suggest that the adaptation resulting in resistance to PDE inhibitors is located in the effector proteins downstream of the PDEs and adenylyl cyclases in the cAMP signalling pathway.

Identifying a compound that inhibits phosphodiesterases in trypanosomes and elevates cAMP concentrations, along with the generation of a PDE inhibitor-

resistant cell line will allow more detailed examination of all aspects of the cAMP signalling pathway in *T. brucei* and across the Kinetoplastida. Phosphodiesterases have also been demonstrated to be chemically inhibitable in trypanosomes and could prove to be the target of a new generation of chemotherapies against African trypanosomiasis.

Table of Contents

Abstract	2
Chapter I	21
1 General Introduction.....	21
1.1 African trypanosomes and human African trypanosomiasis (HAT)	22
1.1.1 Classification and epidemiology	22
1.1.2 Life cycle and morphology	24
1.1.3 Clinical manifestations and pathology of HAT	28
1.1.4 Diagnosis of HAT	29
1.1.5 Treatment of HAT	31
1.1.6 Modes of action and limitations of current chemotherapies.....	33
1.1.6.1 Pentamidine	33
1.1.6.2 Suramin	35
1.1.6.3 Melarsoprol.....	36
1.1.6.4 Eflornithine	38
1.1.6.5 Nifurtimox.....	39
1.2 Cyclic-nucleotide signalling in protozoa: adenylyl cyclases (AC)	41
1.2.1 Kinetoplastids.....	41
1.2.1.1 Calcium mediated adenylyl cyclase regulation.....	41
1.2.1.2 Isolation and biochemical characterisation of adenylyl cyclase genes and their proteins.....	44
1.2.1.3 Adenylyl cyclase protein structure	47
1.2.1.4 Why such diversity of adenylyl cyclase?	50
1.2.2 Apicomplexans	52
1.2.2.1 Identification of non-mammalian AC in infected erythrocytes	52
1.2.2.2 Affect of AC on gametocytogenesis	53
1.2.2.3 cAMP and calcium cross-talk	54
1.2.2.4 Isolation and characterisation of <i>Plasmodium</i> ACs.....	56
1.3 Cyclic-nucleotide signalling in protozoa: guanylyl cyclases (GC)	60
1.3.1 Apicomplexans	60
1.3.1.1 Role of cGMP in exflagellation	60
1.3.1.2 Isolation and characterisation of ciliate and <i>Plasmodium</i> GCs	61
1.4 Cyclic-nucleotide signalling in protozoa: phosphodiesterase (PDE) enzymes	64
1.4.1 Kinetoplastids.....	64
1.4.1.1 Kinetoplastid PDEA.....	66
1.4.1.2 PDEB	68
1.4.1.3 PDEC	78
1.4.1.4 PDED	80
1.4.2 Apicomplexans	80
1.4.2.1 PfPDE α	81
1.4.2.2 PfPDEB.....	84
1.4.2.3 PfPDE γ	84
1.4.2.4 PfPDE δ	85
1.5 Cyclic-nucleotide signalling in protozoa: protein kinases (PK).....	87
1.5.1 Kinetoplastid PKA.....	87
1.5.1.1 <i>Trypanosoma brucei</i>	87
1.5.1.2 <i>Trypanosoma cruzi</i>	89
1.5.1.3 <i>Leishmania</i>	95
1.6 Aims.....	99

Chapter II	100
2 Putative PDE inhibitor screening.....	100
2.1 Introduction	101
2.2 Materials and Methods	104
2.2.1 Whole-cell in vitro efficacy assay	104
2.2.2 Proliferation assay.....	105
2.2.3 Spectrophotometric lysis assay.....	105
2.2.4 In vivo compound tolerance testing	106
2.2.5 In vivo efficacy testing	106
2.3 Results.....	108
2.3.1 Whole-cell in vitro efficacy testing.....	108
2.3.2 Effect of test compounds on trypanosome proliferation	115
2.3.3 Dynamics of test compounds' lethal effects	117
2.3.4 In vivo efficacy testing	120
2.3.5 Screening of putative phosphodiesterase inhibitors from a secondary source	124
2.4 Discussion	127
Chapter III.....	133
3 Validation of a propidium iodide based method for monitoring drug action on the kinetoplastidae	133
3.1 Introduction	134
3.2 Materials and Methods	135
3.2.1 Materials and Culturing.....	135
3.2.2 Standard Curves	136
3.2.3 Effect of Propidium Iodide on Bloodstream Form <i>T. b. brucei</i> ...	137
3.2.4 Cell Lysis Assays	137
3.2.5 Comparison of the use of propidium iodide as an endpoint assay with the whole-cell resazurin reduction assay for in vitro compound efficacy 138	
3.2.6 Rates of Resazurin Metabolism.	138
3.3 Results.....	140
3.3.1 Standard Curves and Assay Sensitivity.....	140
3.3.2 Effect of propidium iodide on cell viability and growth.	142
3.3.3 Real-time monitoring of cell lysis.	143
3.3.4 Resazurin metabolism by protozoan parasites.	146
3.3.5 Propidium iodide as an endpoint-assay indicator; comparison with the whole-cell in vitro efficacy assay.	148
3.4 Discussion	150
Chapter IV	153
4 cAMP levels in trypanosomes incubated with putative PDE inhibitors.....	153
4.1 Introduction	154
4.2 Materials and Methods	156
4.2.1 Materials and trypanosome culturing.....	156
4.2.2 Monitoring of intracellular cAMP using tritiated adenine.....	157
4.2.2.1 Cell preparation.....	157
4.2.2.2 Assay set up.....	158
4.2.2.3 [³ H]-cAMP extraction	158
4.2.3 Direct quantification of intracellular cAMP concentration using enzyme-linked immunosorbant assay (ELISA) kits	159
4.2.4 Induction of resistance to a panel of selected putative phosphodiesterase inhibitors.	159

4.2.5	Resistance and cross-resistance profiling using the resazurin reduction assay	161
4.3	Results	162
4.3.1	Monitoring of the immediate cAMP response after treatment with potential PDE inhibitors	162
4.3.2	Long-term effects of PDE inhibitors on intracellular cAMP.....	164
4.3.3	Induction of resistance to a panel of putative phosphodiesterase inhibitors.	168
4.3.4	Resistance and cross-resistance characterization of the GJS-128 resistant R0.8 cell line	169
4.3.5	cAMP response in <i>T. b. brucei</i> lines adapted to high concentrations of GJS-128.....	171
4.4	Discussion	173
Chapter V		177
5	Further investigations into the mode of action of a panel of compounds & mode of resistance of the GJS-128 resistant R0.8 cell line	177
5.1	Introduction	178
5.2	Materials & Methods.....	180
5.2.1	Electron microscopy	180
5.2.2	Cell cycle analysis using flow cytometry.....	181
5.2.3	DNA configuration assessment using fluorescence microscopy ...	182
5.2.4	Sequencing of the <i>TbrPDEB1</i> and <i>TbrPDEB2</i> genes in the R0.8 cell line and its parental <i>T. b. brucei</i> 427 wildtype strain	183
5.2.4.1	Genomic DNA extraction	183
5.2.4.2	Amplification of <i>TbrPDEB1</i> and <i>TbrPDEB2</i>	183
5.2.4.3	Sequencing of the amplified <i>TbrPDEB1</i> and <i>TbrPDEB2</i> DNA..	185
5.3	Results	186
5.3.1	Electron Microscopy	186
5.3.2	Cell cycle analysis using flow cytometry.....	192
5.3.3	Assessment of DNA configuration using the fluorescent stain DAPI	198
5.3.4	Comparison of the gene sequences of <i>TbrPDEB1</i> and <i>TbrPDEB2</i> between the resistant R0.8 cell line and its parental Tb427 wildtype strain	201
5.4	Discussion	206
Chapter VI		211
6	General Discussion	211
References:		262

List of Tables

Table 1.1: Table showing chemotherapies for Human African Trypanosomiasis and their dosing protocols and side-effects	32
Table 1.2: <i>Trypanosoma brucei</i> phosphodiesterase revised nomenclature	68
Table 2.1: Average EC ₅₀ values for Series 1 compounds with sub-micromolar activity against Tb427 wild type and TbAT1 knockout bloodstream form trypanosomes, with standard errors	111
Table 2.2: Average EC ₅₀ values for a panel of Series 1 compounds against the B48 strain derived from TbAT1 knockout cell line	112
Table 2.3: Average EC ₅₀ values for a panel of Series 1 compounds assayed against procyclic forms of the Tb427 wild type strain, with standard errors.	113
Table 2.4: Average EC ₅₀ values for a panel of Series 1 compounds with sub-micromolar activity against <i>Trypanosoma equiperdum</i> wild type and the diminazene resistant PBR strain bloodstream form trypanosomes, with standard errors.	114
Table 2.5: Panel of compounds tested for <i>in vivo</i> tolerance in mice	121
Table 2.6: Average EC ₅₀ values for GJS compounds assayed against Tb427 wild type and TbAT1 knockout bloodstream form trypanosomes, with standard errors	124
Table 4.1: Table showing the average intracellular cAMP concentration in bloodstream-form Tb427 wildtype trypanosomes after incubation with various compounds for 3 hours.....	166
Table 4.2: <i>In vitro</i> efficacy values of putative phosphodiesterase inhibitors, and a range of known trypanocides and cAMP analogues, against Tb427 wildtype and the GJS-128-resistant R0.8 strain, as assessed by the resazurin reduction method.	169

List of Figures

Figure 1.1: The epidemiological status and distribution of the causative species of human African trypanosomiasis	23
Figure 1.2: Life cycle of <i>Trypanosoma brucei</i> in the mammalian and insect host	25
Figure 1.3: Diagram showing the principle structures of the <i>Trypanosoma brucei</i> bloodstream form.....	27
Figure 1.4: An example of a CATT conducted on 10 serum samples	30
Figure 1.5: Structures of the drugs used to treat Human African Trypanosomiasis	34
Figure 1.6: Overall structure of GRESAG4.1	50
Figure 1.7: The structure of LmjPDEB1 bound with IBMX.....	77
Figure 2.1: Representative graphs showing whole-cell <i>in vitro</i> efficacy assays for a number of putative phosphodiesterase inhibitors and diminazene against Tb427 wild type, TbAT1 knockout, and strain B48 bloodstream form trypanosomes..	109
Figure 2.2: Representative graph showing the range of average EC ₅₀ values of putative PDE inhibitors against Tb427 wild type bloodstream form trypanosomes	110
Figure 2.3: Representative graphs showing the effect of a selection of Series 1 compounds and diminazene on Tb427 wild type bloodstream form trypanosome proliferation	116
Figure 2.4: Representative graphs showing the effects of various compounds on the speed of cell death	118
Figure 2.5: Representative graphs showing the effect of removing drug pressure on cell death after limited incubations of the test compounds with Tb427 wild type bloodstream form trypanosomes.....	119
Figure 2.6: Histograms showing the mean parasitaemia, with standard error bars, of female ICR strain mice infected with Tb427 wild type bloodstream form trypanosomes and treated with a panel of Series 1 compounds.....	122
Figure 2.7: Graphs showing the effect of treatment with Series 1 compounds on the mean parasitaemia of female ICR strain mice infected with Tb427 wild type bloodstream form trypanosomes	123
Figure 2.8: Representative graphs showing the effect of GJS compounds on Tb427 wild type bloodstream form trypanosome proliferation	125
Figure 3.1: Standard curves of fluorescence signal generated by the interactions of various concentrations of <i>T. b. brucei</i> genomic DNA with propidium iodide.	140

Figure 3.2: Standard curves of trypanosome-associated propidium iodide fluorescence after cell permeabilisation with digitonin	141
Figure 3.3: Effect of the continuous exposure to propidium iodide on trypanosome viability	142
Figure 3.4: Effects of pentamidine and melarsen oxide on <i>T. b. brucei</i> survival	144
Figure 3.5: Effects of various concentrations of Series 1 compounds and GJS-128 on <i>T. b. brucei</i> survival	145
Figure 3.6: Development of fluorescence due to resazurin metabolism over 24 hours.....	146
Figure 3.7: Rate of fluorescence development during incubation of parasites with resazurin	147
Figure 3.8: Trypanocidal effects of melarsen oxide on <i>T. b. brucei</i> bloodstream forms measured by propidium iodide or resazurin reduction assay at different seeding densities	148
Figure 4.1: Graphs showing the effects of various compounds on intracellular cAMP levels in bloodstream-form Tb427 wildtype trypanosomes pre-labelled for 2 hours with tritiated adenine	163
Figure 4.2: Graphs showing the average intracellular cAMP concentration in bloodstream-form Tb427 wildtype cells incubated with various compounds for 3 hours.....	165
Figure 4.3: Graph of <i>in vitro</i> efficacy of selected compounds against the GJS-128 resistant R0.8 cell line and the parental Tb427 wildtype strain.....	170
Figure 4.4: Graphs showing the effect of various concentrations of GJS-128 on the intracellular cAMP concentration in Tb427 wildtype and the GJS-128 resistant R0.8 cell line	172
Figure 5.1: Cell division in procyclic form <i>Trypanosoma brucei</i>	179
Figure 5.2: Transmission electron micrograph of a Tb427 wildtype bloodstream form trypanosome incubated for 20 hours with 0.625 μ M Compound 37	188
Figure 5.3: Transmission electron micrograph of a Tb427 wildtype bloodstream form trypanosome incubated for 24 hours with 0.25 μ M Compound 48	189
Figure 5.4: Transmission electron micrograph of a Tb427 wildtype bloodstream form trypanosome incubated for 24 hours with 1 μ M Compound 72	190
Figure 5.5: Transmission electron micrograph of a Tb427 wildtype bloodstream form trypanosome incubated for 24 hours with 0.5 μ M Compound 139	191
Figure 5.6: Transmission electron micrograph of a Tb427 wildtype bloodstream form trypanosome incubated for 20 hours with 1 μ M GJS-128.....	192

Figure 5.7: Transmission electron micrograph of a Tb427 wildtype bloodstream form trypanosome incubated for twenty hours with DMSO only as a No-Drug Control.	187
Figure 5.8: Flow cytometry analysis of the DNA content of Tb427 wildtype trypanosomes treated and untreated with 0.25 μ M Compound 48, 1 μ M Compound 72 and 0.5 μ M Compound 139	193
Figure 5.9: Flow cytometry analysis of the DNA content of Tb427 wildtype trypanosomes treated and untreated with 1 μ M GJS-128 and 0.625 μ M Compound 37.	195
Figure 5.10: Graphs showing the percentage of the Tb427 wildtype culture in particular ploidy cell cycles.....	197
Figure 5.11: Example images of Tb427 wildtype trypanosomes, and the categories they were scored as, with their DNA stained with DAPI and inspected by fluorescent microscope	199
Figure 5.12: Graphs showing the percentage of Tb427 wildtype trypanosomes, in categories scored for number and configuration of nuclei and kinetoplasts, after 12 hours of incubation with or without test compound.....	200
Figure 5.13: Diagram showing the open reading frame of TbrPDEB1 (+/- 200 base pairs).	203
Figure 5.14: Diagram showing the open reading frame of TbrPDEB2 (+/- 200 base pairs).	204

Acknowledgements

Firstly, I would like to thank my supervisor Dr. Harry De Koning. Without his advice, guidance, seemingly infinite patience and encouragement, this thesis may not have been completed. His support has been deeply appreciated.

I would also like to thank my parents for being there for me when I needed home comfort the most and putting up with my grumpy moods. I know they have always wanted the best for me and to see me succeed. I hope I have repaid their faith in me.

My brother and sister have also been particularly supportive; their encouragement and good humour has helped to lift me over the finish line.

There are many people in the old North Lab and in the GBRC who have given freely of their time to show me how to do things (and how not to!). To thank them all would take another thesis. I really could not have done this without them.

The person who has put up with the most over the course of the project has been Laura. She is the one whose opinion matters most to me and reminds me to be the person I want to be. I hope she knows how much of her is in this thesis, as well as in me, and I thank her for it.

Thanks must also go to my sponsors, Otsuka Maryland Medicinal Laboratories who funded this project.

Author's Declaration

I declare that the results presented in this thesis are my own work and that, to the best of my knowledge, it contains no material previously substantially overlapping with material submitted for the award of any other degree at any institution, except where due acknowledgment is made in the text.

Matthew K. Gould

Abbreviations

A	Axoneme
AA	Amino acid
AB	Assay buffer
AC	Adenylyl cyclase / Acidocalcisome
Ado-MetDC	S-adenosyl methionine decarboxylase
AMP	Adenosine monophosphate
ATP	Adenosine triphosphate
AU	Arbitrary units
BAL	British antilewisite
BB	Basal body
BBB	Blood-brain barrier
8-bromo-cAMP	8-bromo-cyclic adenosine monophosphate
6-Bz-cAMP	N6-benzoyl cAMP
cAMP	Cyclic adenosine monophosphate
CATT	Card agglutination test for trypanosomiasis
CD	Cytosolic disruption
cGMP	Cyclic guanosine monophosphate
CNS	Central nervous system

CSF	Cerebro-spinal fluid
DABCO	1,4-diazabicyclo[2.2.2]octane
DAPI	4,6-diamidino-2-phenylindole
DFMO	DL-alpha-difluoromethylornithine
DMSO	Dimethyl sulphoxide
DNA	Deoxyribonucleic acid
EC ₅₀	Effective concentration inhibiting 50% cell proliferation
ELISA	Enzyme-linked immunosorbant assay
ER	Endoplasmic reticulum
ERK	Mitogen-activated extracellular signal-regulated kinase
ESAG	Expression-site associated gene
F	Flagellum
FAZ	Flagellar attachment zone
FBS/FCS	Foetal bovine serum/foetal calf serum
FP	Flagellar pocket
G	Golgi apparatus
GAF-domain	Allosteric binding domain named after cGMP-specific and binding phosphodiesterases, <u>a</u> denylyl cyclase of <i>Anabaena</i> and <u>F</u> hIA of <i>E. coli</i>
GC	Guanylyl cyclase

Gly	Glycosome
GPI	Glycophosphatidylinositol
GPI-PLC	Glycophosphatidylinositol-phospholipase C
GRESAG	Gene related to expression-site associated gene
GTP	Guanosine triphosphate
HAPT1	High-affinity pentamidine transporter 1
HAT	Human African trypanosomiasis
[³ H]-adenine	Tritiated adenine
[³ H]-cAMP	Tritiated cyclic adenosine monophosphate
IBMX	Isobutylmethylxanthine
IC ₅₀	50% inhibitory concentration
K	Kinetoplast
K _i	Inhibition constant
K _m	Michaelis-Menten constant
LAPT1	Low-affinity pentamidine transporter 1
LBP	Leucine-binding protein
LDL	Low-density lipoprotein
LdPDE	<i>Leishmania donovani</i> phosphodiesterase enzyme
LmjPDEB	<i>Leishmania major</i> phosphodiesterase enzyme B
MMS	Methyl methane sulphonate

mRNA	Messenger-ribonucleic acid
N	Nucleus
ODC	Ornithine decarboxylase
ORF	Open reading frame
PBR	Diminazene resistant <i>Trypanosoma equiperdum</i>
PBS	Phosphate-buffered saline
PSG	Phosphate-buffered saline plus glucose
pCMPS	<i>p</i> -chloromercuriphenylsulfonic acid
PCR	Polymerase chain reaction
PDE	Phosphodiesterase enzyme
PfAC	<i>Plasmodium falciparum</i> adenylyl cyclase
PFR	Paraflagellar rod
PI	Propidium iodide
PK	Protein kinase
PKA	Cyclic adenosine monophosphate-specific protein kinase
PKA-C	Catalytic subunit of PKA
PKA-R	Regulatory subunit of PKA
PKC	Calcium/calmodulin-specific protein kinase
PKG	Cyclic guanosine monophosphate-specific protein kinase
PKI	Specific peptide inhibitor of PKA

PLC	Phospholipase C
p[NH]ppG	Guanyl-5'-yl imidodiphosphate
PPi	Pyrophosphate
PtdIns(3)P	Phosphatidylinositol-3-phosphate
RBC	Red blood cell
RNAi	RNA interference
RSMD	Root-mean-squared-deviation
RT-PCR	Reverse transcription polymerase chain reaction
SIF	Stumpy induction factor
SMA	Subpellicular microtubule array
Tb427	<i>Trypanosoma brucei</i> strain 427
TbAT1	<i>Trypanosoma brucei</i> adenosine transporter 1
TbrPDEB	<i>Trypanosoma brucei</i> phosphodiesterase enzyme B
TcAQP	<i>Trypanosoma cruzi</i> aquaporin
TcrPDEB	<i>Trypanosoma cruzi</i> phosphodiesterase enzyme B
TcAC	<i>Trypanosoma cruzi</i> adenylyl cyclase
TcADC	<i>Trypanosoma cruzi</i> adenylyl cyclase
TEM	Transmission electron microscopy/micrograph
THG	Thapsigargin
TM	Trans-membrane

UD	Uracil-derived
UDP	Uracil diphosphate
UMP	Uracil monophosphate
UTP	Uracil triphosphate
V	Clathrin-coated Vesicle
V_{\max}	Maximum velocity
VSG	Variant surface glycoprotein
WHO	World Health Organization

Chapter I

1 General Introduction

1.1 African trypanosomes and human African trypanosomiasis (HAT)

1.1.1 Classification and epidemiology

African trypanosomes are flagellated protozoans that belong to the genus *Trypanosoma* and are part of the subphylum Kinetoplasta. All members of this subphylum share a distinguishing organelle called the kinetoplast, which can be found close to the flagella. This organelle contains DNA that is ordered into linked circles of differing sizes. The small circles (minicircles) can number up to 20,000 while there are usually between 20 and 50 larger circles (maxicircles)(Roberts, L. S. and Janovy, J., 2000). The position of the kinetoplast in relation to other organelles forms the basis for identification of different stages of the life cycle.

Trypanosomes are part of the family termed the Trypanosomatidae and share many morphological and biochemical features with other important pathogenic members, like the American trypanosomes and the leishmanias. For example they all are either elongated with a single flagellum or are more spherical with a flagellum that does not extend past the end of its body. Many of the members of the family, including African trypanosomes, have more than one host in their life cycle and as such are termed heterozenous; they usually require blood or blood components when cultured in the laboratory and are, therefore, also called hemoflagellates (Roberts, L. S. and Janovy, J., 2000).

Human African Trypanosomiasis (HAT), or 'sleeping sickness' is caused by the trypanosome species *Trypanosoma brucei* which is generally accepted as having three subspecies: *Trypanosoma brucei gambiense*, *T. b. rhodesiense* and the animal infective *T. b. brucei* (Gilles, H. M., 1999). The parasite is spread to humans by the bloodsucking tsetse fly that lives in areas ideal for agricultural cultivation and habitation, that is: close to rivers and lakes, and in the vast savannahs (WHO, 2001).

T. b. brucei, while infectious to a large number of mammalian hosts, cannot infect humans as it is killed by a haptoglobin-like molecule in human serum (Smith, A. B. et al, 1995); *T. b. gambiense* and *rhodesiense*, on the other hand,

are both resistant to this lysing action of human serum and so can be transmitted to man. Not only can they infect man but they both have animal reservoir hosts as well: *T. b. gambiense* can live in domestic pigs and cattle while *T. b. rhodesiense* can also infect game and savannah cattle, amongst others (Pépin, J. and Méda, H. A, 2001).

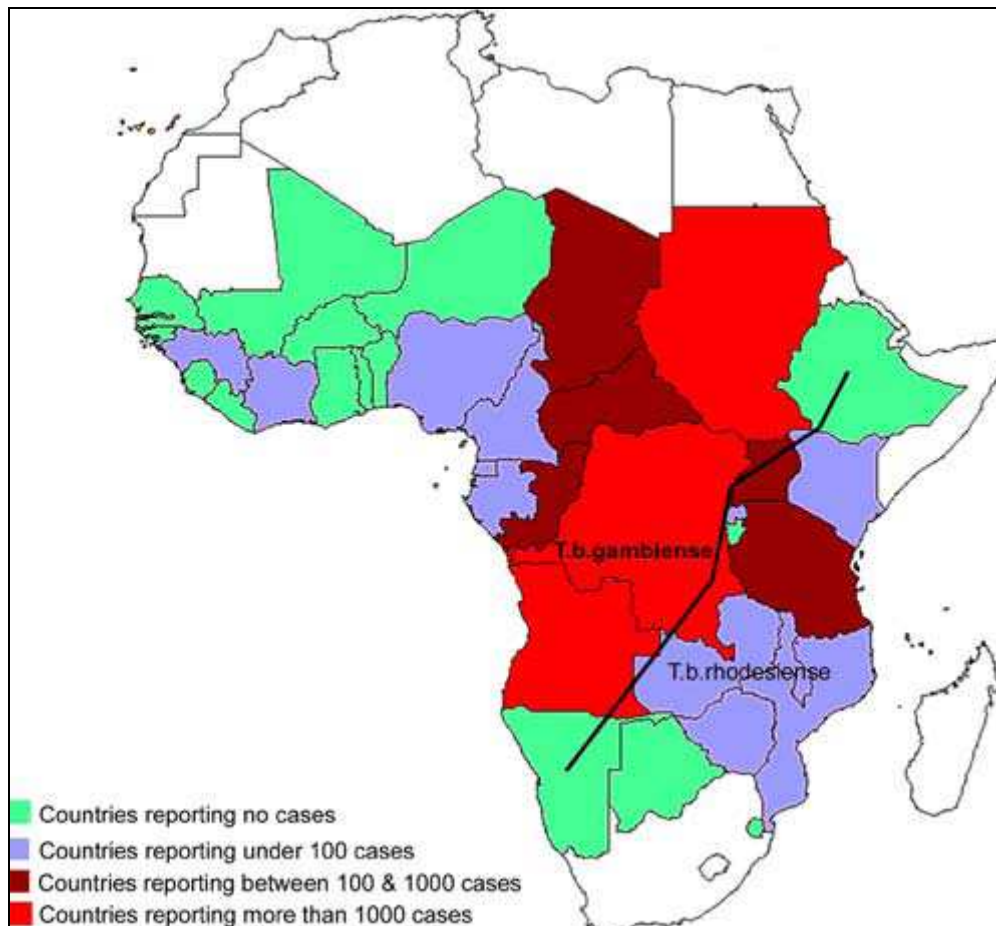


Figure 1.1: The epidemiological status and distribution of the causative species of human African trypanosomiasis. The black line denotes the approximate geographical separation of species endemicity. Reproduced from Simarro, P. P. et al, 2008.

As their names suggest *T. b. rhodesiense* and *gambiense* have different geographical distributions. *T. b. gambiense* is generally found in the tropical areas of West and Central Africa while *T. b. rhodesiense* is usually located in the wooded areas of East Africa (WHO, 2000; Simarro, P. P. et al, 2008)(Figure 1.1).

Human African trypanosomiasis cases were greatly reduced and well under control by the 1960s (Kennedy, P. G. E., 2004), however factors such as the withdrawal of the old colonial powers leading to social, political and economic instability led to a disruption of the surveillance and disease control strategies previously adopted (Abel, P. M. et al, 2004). As a result an epidemic began in

the 1970s and continues, over 30 years later, to the turn of the millennium (WHO, 2000). In 1999 there were nearly 45,000 reported cases of HAT but according to the World Health Organization the real number could be between 300,000 and 500,000 due to a severe lack of screening in the countries affected (WHO, 2001). HAT cases have been recorded in over 35 countries in sub-Saharan Africa leaving over 60 million people at risk of infection (Barrett, 1999). In Sudan, the Democratic Republic of Congo, Angola, and Uganda the prevalence has risen to over 20% in the worst afflicted areas (Bouteille et al, 2003). In 2006, the actual prevalence of infected cases was estimated at between 50,000 and 70,000 (WHO, 2006), with recent control strategies having reduced the prevalence greatly from its peak (Simarro, P. P. et al, 2008).

1.1.2 Life cycle and morphology

T. brucei is obliged to infect a mammalian host and an insect vector in order for it to complete its life cycle (Neva, F. A. and Brown, H. W., 1994). Multiplying stages alternate with differentiating stages where the cell changes its structure and the orientation and location of some of the organelles within (Figure 1.2).

As the tsetse fly feeds, it infects the host with metacyclic form trypanosomes via the insect's saliva, which are pre-adapted, metabolically, for life inside a mammalian host. Once inside the mammalian host the metacyclics differentiate to form trypomastigotes, or 'slender bloodstream forms,' and proliferate rapidly in the blood and lymph (Roberts, L. S. and Janovy, J., 2000).

When the number of parasites begins to reach the maximum density, the long slender form trypomastigotes begin to transform into non-dividing, short 'stumpy forms' giving a population of trypanosomes with two differing morphologies, which is termed pleiomorphic. The stumpy forms appear like their name suggests: shorter and fatter than the slender bloodstream forms, with their flagellum greatly shortened so that it barely protrudes past the main body of the cell. It appears that the trypomastigotes secrete a molecule called Stumpy Induction Factor (SIF), which, when accumulated, triggers cell cycle arrest via the cyclic AMP (cAMP) signalling pathway in the cell and may instigate differentiation (Vassella, E. et al, 1997). This density sensing mechanism allows the parasites to transform into a pre-adapted stage ready for ingestion in a

blood meal by the tsetse fly. It may also help control the parasitaemia in order to prevent the host dying from the infection before transmission to the insect vector.

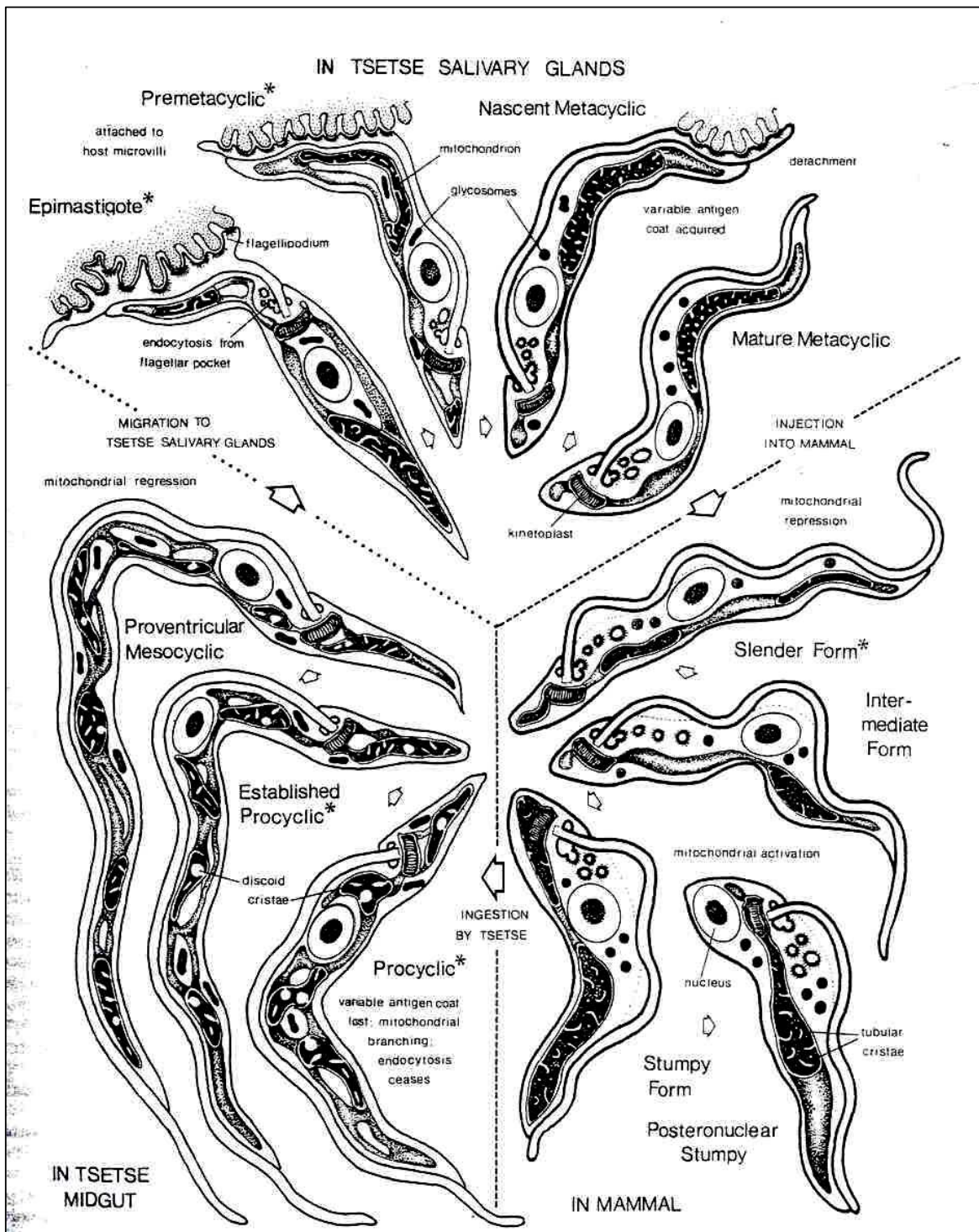


Figure 1.2: Life cycle of *Trypanosoma brucei* in the mammalian and insect host. Reproduced from Vickerman, K., 1985.

The stumpy forms are ideally prepared for the abrupt change in environment found in the midgut of the tsetse fly, and differentiate into the procyclic trypomastigotes forms between 48 -72 hours after ingestion. The procyclics cross

the peritrophic matrix, a bag like structure that surrounds the blood bolus, where they grow and multiply over the period of about a week, then transform again to become proventricular mesocyclic forms that do not divide. After this they begin a migration through the body of the tsetse fly to the salivary glands, probably via the oesophagus and mouthparts, which can take between 3 and 5 weeks from the initial blood meal. Once in the salivary glands the trypanosomes undergo four further differentiations. The stage that does most of the proliferating is the epimastigote form, which has attached itself, by its flagellum, to the microvilli of the gland. The final stage in the tsetse fly occurs when the trypanosome disengages from the microvillus as a mature metacyclic, the only form in the fly that is infective to mammals, and is ready for inoculation of the host via saliva secreted by the fly during feeding.

The bloodstream form trypomastigotes of *T. b. gambiense* and *T. b. rhodesiense* are difficult to tell apart morphologically. The flagellum and main body of the cell are coated in a plasma membrane with the flagellum being anchored along the length of the cell so that, when thrashing, it forms an 'undulating membrane' (Figure 1.3). The part of the flagellum extending past the anterior of the cell rotates in a flailing, corkscrew fashion and pulls the body of the cell through the medium, however, the origin of the flagellum is to be found near the posterior of the trypanosome in close proximity to the kinetoplast. Surrounding the basal body of the flagellum is the flagellar pocket through which receptor-mediated endocytosis can take place (Vickerman, K. et al 1993; Gilles, H. M., 1999; Roberts, L. S. and Janovy, J., 2000; Garcia, L. S., 2001).

Variant surface glycoproteins (VSGs) are extruded from the flagellar pocket after synthesis in the Golgi apparatus and transportation through the cytosol on vesicles (Vickerman, K. et al, 1993). VSGs form a dense coat covering the entire plasma membrane and flagellum of the metacyclic and bloodstream forms, and are thought to protect the trypanosome from the innate and acquired immune response of the mammalian host (Sternberg, J. M., 1998). The coat may act as a shield by preventing antibodies from recognizing some of the invariant molecules necessary for survival which are attached to the surface of the cell; molecules like receptors and essential nutrient transporters.

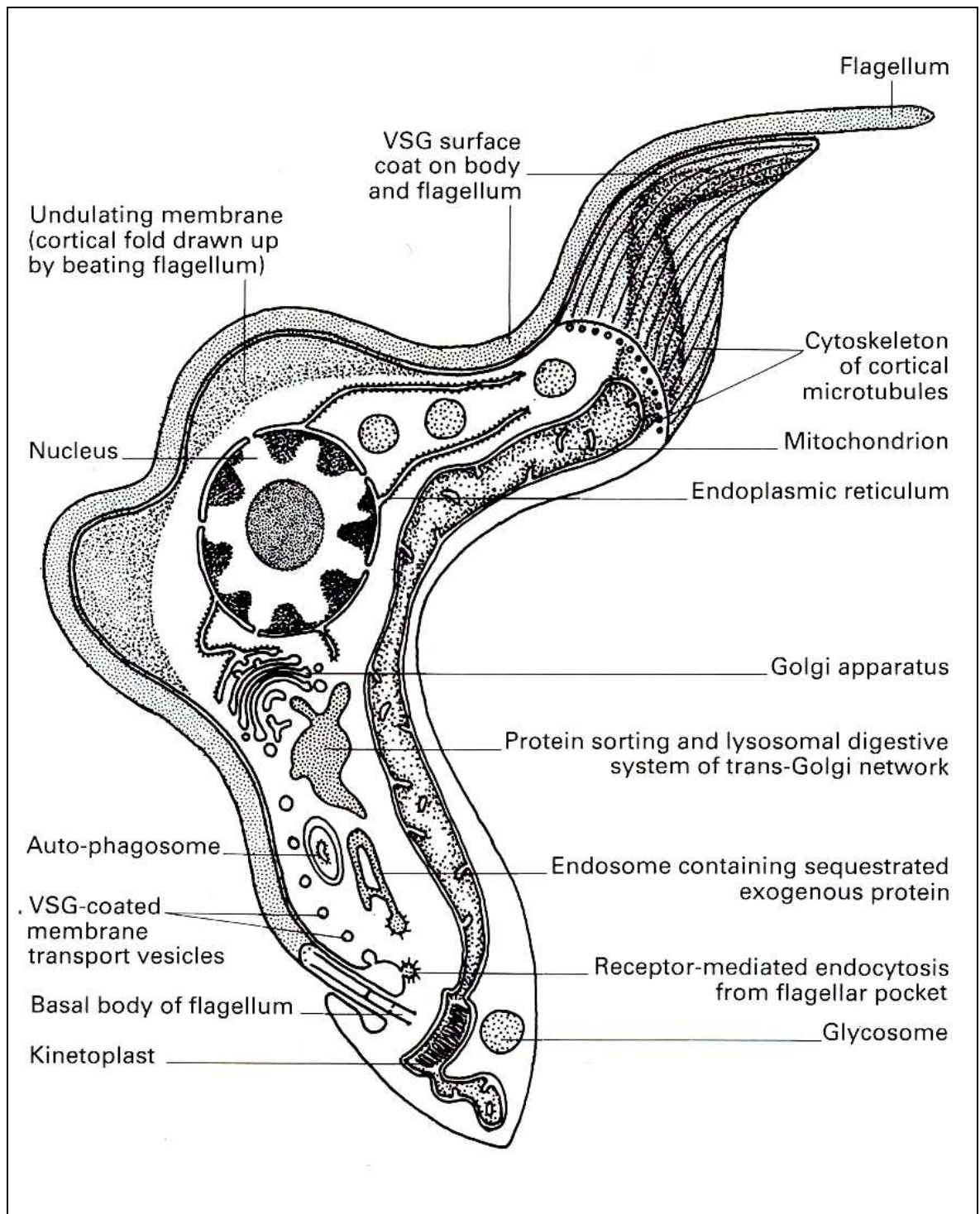


Figure 1.3: Diagram showing the principle structures of the *Trypanosoma brucei* bloodstream form. Reproduced from Vickerman, K. et al, 1993.

The VSG molecule is made up of two domains: the more conserved carboxyl terminal domain and the highly variable amino terminal domain. Although there are up to 1000 differing genes, each coding for a different VSG in the trypanosome's repertoire, only one variant is expressed at a time coating the entire surface membrane (Barry, J. D. and McCulloch, R., 2001). A population of trypanosomes with the same VSG being expressed will continue to proliferate until an antibody is raised to recognize that particular protein coat. Once

recognized by the host's immune system the parasite numbers will 'crash' until a mutant arises with a different VSG coat that is not recognized by the host; then the parasite population will proliferate again. This system of controlled switching is called antigenic variation and gives rise to the characteristic fluctuating parasitaemia seen in cases of HAT.

1.1.3 Clinical manifestations and pathology of HAT

The two causative species of HAT give rise to slightly differing symptoms. *T. b. gambiense* generally produces a chronic illness that gradually increases in severity from the almost asymptomatic incubation period of the first couple of months, to the severe neurological problems and terminal coma after, sometimes, several years. *T. b. rhodesiense*, on the other hand, is more acute and the onset of noticeable symptoms can occur within one to four weeks from the initial inoculation by the tsetse fly. The span of the *rhodesiense* infection ends fatally, usually within a year (Garcia, L. S., 2001).

After an infective bite from a feeding fly a swelling, called a chancre, may develop a few days later at the location of the bite. This sore usually resolves itself within one or two weeks. The metacyclic stage makes its way from the bite site into the bloodstream and lymph and starts differentiating and proliferating, marking the onset of stage one of the infection sometimes known as hemolymphatic trypanosomiasis. During stage one, many patients display non-specific symptoms such as an irregular or intermittent fever, tiredness, myalgia, aching joints and a general malaise. The periodicity of these symptoms correlates to the fluctuating parasitaemia levels brought on by the antigenic variation of the VSG protective coat. Some of the afflicted show swelling of the posterior cervical lymph nodes, termed Winterbottom's sign, and is noticeable in up to 85% of patients hospitalized. 10 to 20% have enlarged spleens or livers and others have areas of edema and facial puffiness (Pépin, J., 2000).

The crossing of the blood-brain barrier by the trypanosomes and entry into the cerebro-spinal fluid (CSF) and central nervous system (CNS) denotes the onset of stage two, or meningoencephalitic trypanosomiasis. This can occur as quickly as within a few weeks with *T. b. rhodesiense* and as much as years later with *T. b. gambiense*. Headaches increase and become prolonged and more severe;

patients become more apathetic and show changes in their personalities presenting paranoid and antisocial behavior. Characteristic disruption of the circadian rhythms and other sleep problems give the disease its colloquial name of 'sleeping sickness'. Muscle tremors and muscle rigidity and tone increase, with changes in gait and speech also apparent. Eventually the deterioration of neurological function leaves the patient in an ever-deepening coma until death (Lalloo, D. G., 2004).

1.1.4 Diagnosis of HAT

The diagnosis of HAT caused by *T. b. gambiense* has three main steps: suspicion aroused by symptom history or screening, trypanosome detection, and determination of stage of infection. The clinical presentations of early stage HAT are easily confused with a variety of ailments. The chancre, visible at the bite site of the tsetse fly, not only can be mistaken for the bites of other insects but, as it spontaneously resolves itself after a few weeks, is sometimes not present when the patient seeks medical help. The relapsing fever, caused by the fluctuating parasitaemia, can often be mistaken for malaria, typhoid and other febrile diseases (Gilles, H. M., 1999). Even the neurological impairment caused by late stage HAT can be confused with other psychiatric illnesses. Nevertheless, these symptoms, combined with local knowledge of endemic diseases and their epidemiology, may help to point in the right direction and prompt serological screening or inspection of body fluids by microscopy for trypanosomes.

The definitive diagnosis of stage one trypanosomiasis is ideally done by the identification of trypanosomes in samples from blood, lymph nodes and, rarely, bone marrow. However due to the irregular parasitaemia of *T. b. gambiense*, there are usually relatively few parasites in the peripheral blood circulation and a false negative diagnosis results in 20 to 30% of patients using this technique (Chappuis, F. et al, 2005). For that reason multiple samples over a long period of time, especially at times of fever which are indicative of high parasitaemia, are required to give a reliable diagnosis. This is time consuming and requires skilled workers with laboratory facilities. Consequently, simple and easy to perform tests are of vital importance in determining HAT when screening large populations.

The Card Agglutination Test for Trypanosomiasis (CATT) is now the diagnostic tool of choice in the field as it is simple to use, reliable and quick. It was developed in the late 1970s by the Institute of Tropical Medicine in Antwerp, Belgium, and works by inducing antibodies from a sample from an infected patient to agglutinate to a stained antigen derived from *in vivo* cultured trypanosomes of variant antigen type LiTat 1.3 (Figure 1.4). The reported sensitivity is between 87 and 98% with a specificity of around 95% when whole blood is assayed, however this can be improved further by using the blood serum only and diluting 1:4 (Chappuis, F. et al, 2005). Although the CATT technique does not give a definitive diagnosis it saves valuable resources by narrowing down those that need further investigation from a large population, given that the incidence of HAT is usually less than 5%.

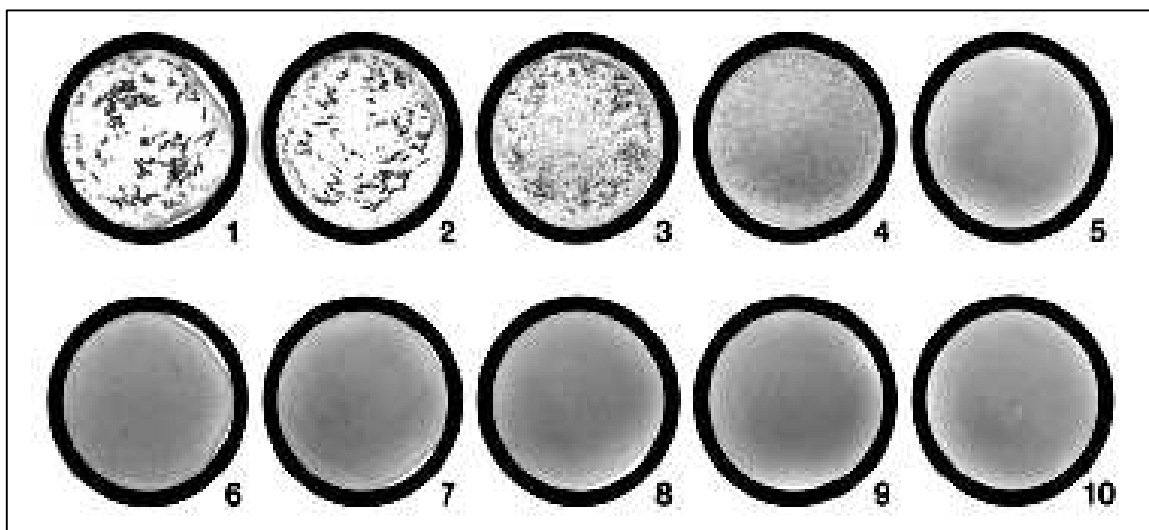


Figure 1.4: An example of a CATT conducted on 10 serum samples. Samples 1 – 3 are strongly positive, sample 4 is weakly positive and samples 5 – 10 are negative. Reproduced from Chappuis, F. et al, 2005.

Determining whether the patient is in stage one of the infection or if the trypanosomes have crossed into the cerebro spinal fluid to give stage two is of critical importance in deciding on a course of treatment. The only way to do this reliably is to examine the CSF by lumbar puncture after a single dose of suramin or pentamidine, which clears the parasites from the blood and prevents contamination of the CSF by the sampling procedure. The World Health Organization defines late stage HAT as a patient having at least one from three observations: (1) having live trypanosomes in the CSF sample, (2) a white blood cell count greater than 5 cells/ μ l, and (3) a protein content greater than 370 mg/litre, measured by the dye-binding protein assay. Apart from (1), these

defining thresholds are controversial and hotly debated as they could be achieved by other CSF infections and some countries have set their own limits in the light of recent findings (Chappuis, F. et al, 2005). For *T. b. rhodesiense* field screening, before parasitological confirmation, is based solely on case history and symptoms. This is because there is no comparable CATT serological assay available. Conversely definitive diagnosis is more straightforward with *T. b. rhodesiense* than with *gambiense* as the trypanosomes are more readily detected in the blood samples due to the generally higher parasitaemia of a *rhodesiense* infection. Stage determination is carried out in the same way as for *T. b. gambiense*.

At present the two species causing human trypanosomiasis do not coexist in the same geographical areas. Detecting trypanosomes in the blood and knowledge of the endemicity of an area has been enough to differentiate between the acute and chronic forms of infection, allowing determination of specific treatment schedules tailored to the species infecting the patient. This natural separation of the two species cannot be relied upon in the future. Evidence from molecular identification of human infective parasites in domestic herds of cattle indicates that *T. b. rhodesiense* is spreading north in Uganda towards an area already endemic for *T. b. gambiense* (Welburn, S. C. and Odiit, M., 2002). Should the two forms mix then confusion over diagnosis is bound to arise since the species are indistinguishable morphologically, resulting in incorrect treatment decisions and treatment failures. CATT screening could no longer be relied upon, as it cannot detect *T. b. rhodesiense*, forcing control programs to resort to the time consuming and expensive diagnosis by microscopy placing an added burden on the overstretched and under funded health services in sub-Saharan Africa.

1.1.5 Treatment of HAT

The treatment strategies and chemotherapies used against HAT are dependant on the stage of the infection presented to the clinician. Some of the drugs cannot cross the blood-brain barrier so cannot kill the trypanosomes in the CSF, whereas the main drug used against stage two infections can be extremely toxic, occasionally resulting in death from the side-effects, and so is only used once CNS involvement has been established.

Stage one or hemolympathic trypanosomiasis is treated with pentamidine if the patient is infected with *T. b. gambiense* and with suramin if infected with *T. b. rhodesiense* (Table 1.1). Pentamidine is given intramuscularly at a recommended dosage of 4 mg/kg either daily or on alternating days for a total of seven to ten administrations (Bouteille, B. et al, 2003). Suramin's treatment protocol is usually a 5 mg/kg test dose on day one to check for allergic reactions, followed by 10 mg/kg on day 3 of treatment. 20 mg/kg is given on days 5, 11, 23, and 30 (Legros, D. et al, 2002). Each dispensation of drug is given by a slow intravenous infusion to reduce the risk of anaphylactic shock and other side-effects.

Drug	Species Range	Stage	Dosage	Route	Side-Effects
Pentamidine	<i>T. b. gambiense</i>	Early	7-10 doses @ 4mg/kg daily or on alternate days	Intra-muscularly (i.m.)	Hypotension, hypoglycaemia
Suramin	<i>T. b. gambiense</i> <i>T. b. rhodesiense</i>	Early	Day 1: 5mg/kg Day 3: 10mg/kg Days 5, 11, 23 & 30: 20mg/kg	Slow intravenous (i.v.) infusion	Anaphylaxis, fever, nausea, mucocutaneous eruptions
Melarsoprol	<i>T. b. gambiense</i> <i>T. b. rhodesiense</i>	Late	3 series of 4 daily doses @ 1.2-3.6mg/kg separated by 7-10 days	I.v. injection	Encephalopathy, cardiac, renal and hepatic toxicity
Eflornithine	<i>T. b. gambiense</i>	Late	400mg/kg daily over 4, 2hr infusions for 7-14 days	I.v. infusion	Pancytopenia, diarrhoea, convulsions
Nifurtimox	<i>T. b. gambiense</i>	Late	15-20mg/kg daily over 3 doses for 14-21 days	Orally	Anorexia, neurological dysfunction

Table 1.1: Table showing chemotherapies for Human African Trypanosomiasis and their dosing protocols and side-effects. Compiled from Legros, D. et al, 2002; Bouteille, B. et al, 2003 and Fairlamb, A. H., 2003.

Melarsoprol is the drug of choice for treating late stage HAT, however there is no standard protocol for dosage or length of treatment. The most commonly used strategy is made up of three series, between seven and ten days apart, of three or four-day courses at a dosage of 3.6 mg/kg per day by single intravenous injection. Melarsoprol is active against both stage one and stage two infections however, since 5-10% of cases suffer from a serious reactive encephalopathy, half of which die as a result, it is only used for late stage trypanosomiasis as other less toxic drugs are available for stage one (Fairlamb, A. H., 2003).

Eflornithine can be used against late stage *T. b. gambiense* infections as it is less toxic than melarsoprol, but it is very expensive and difficult to administer so is generally only used in cases resistant to melarsoprol. The regimen for this drug is 400 mg/kg per day, which is spread over four 2 hour infusions, for seven to fourteen days.

Nifurtimox is a drug used against the American trypanosome *T. cruzi*, which causes Chagas disease, but has not been approved for use against African trypanosomes. Nevertheless it has been used when patients have not been cured by melarsoprol or eflornithine and is under going clinical trials with conflicting results (Bouteille, B. et al, 2003).

Due to the recrudescence abilities of human African trypanosomes it is recommended that patients should be reviewed periodically for 2 years after treatment to detect those that relapse. Those relapsing after treatment with suramin or pentamidine, having been infected with *T. b. gambiense*, can be treated with melarsoprol or eflornithine, while those infected with *T. b. rhodesiense* can be given a course of melarsoprol. Nifurtimox can be used as a last resort if all previous treatments fail (Lalloo, D. G., 2004).

1.1.6 Modes of action and limitations of current chemotherapies

1.1.6.1 Pentamidine

Pentamidine is a water-soluble aromatic diamidine (Figure 1.5), which has been used as a chemotherapy since 1937. Not only is it effective against *T. b. gambiense*, but it is also used as a drug against antimony-resistant leishmaniasis and also *Pneumocystis carinii* pneumonia (Docampo, R. and Moreno, S. N., 2003). An analogue of insulin, it was hoped that pentamidine would be active against trypanosomes after a related compound, synthalin, was shown to induce hypoglycaemia in humans. The idea was to deprive the parasites of their source of glucose in the blood and essentially starve them to death, however pentamidine's mode of action is independent of its effects on the physiology of the patient (Denise, H. and Barrett, M. P., 2003).

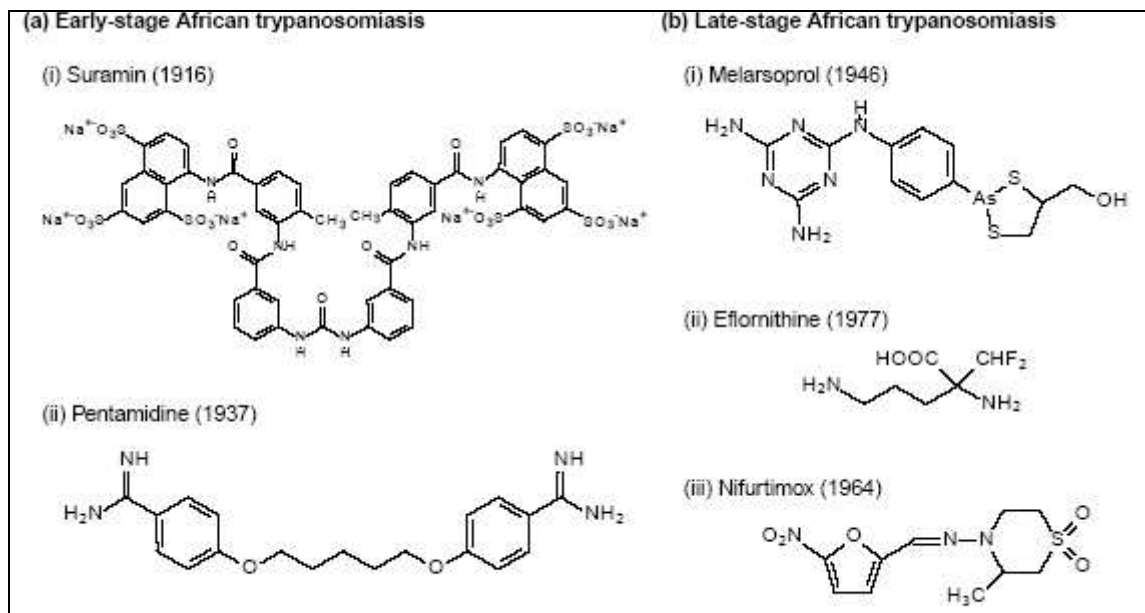


Figure 1.5: Structures of the drugs used to treat Human African Trypanosomiasis. Dates first synthesized in brackets. Reproduced from Fairlamb, A. H., 2003.

Pentamidine is actively taken up by the parasite to millimolar levels inside the cell, however there is more than one transporter involved in the accumulation of the drug to such high concentrations. Uptake inhibition experiments have shown that the P2 aminopurine transporter mediates between 50 - 70% of pentamidine uptake by *T. b. brucei*, with a high-affinity (HAPT1) and a low-affinity pentamidine transporter (LAPT1) also implicated (De Koning, H. P., 2001). These transporters are essential for the survival of the parasite under normal conditions as they import purines scavenged from the host. Trypanosomes cannot synthesize purines *de novo* so have to rely completely on efficient uptake of the molecules by their transporters. The transporters recognize specific regions of the purine structure, which are also present on pentamidine and some other trypanocides, and so take up the drug along with the natural substrate.

The specific target of pentamidine, once inside the cell, has not been definitively determined. It binds tightly to the circular DNA of the kinetoplast, however the parasite can still survive when the kinetoplast has been removed (Denise, H. and Barrett, M. P., 2003). Pentamidine can also affect the mitochondrion by acting as an uncoupler of oxidative phosphorylation, inhibit the S-adenosyl methionine decarboxylase (Ado-MetDC) enzyme perhaps preventing polyamine synthesis, and interfere with trypanothione metabolism (Docampo, R. and Moreno, S. N., 2003; Nok, A. J., 2003). The high intra-cellular

concentrations reached by the drug means it may be acting on more than one, or all of the above processes or targets. The unpleasant side effects of pentamidine can result in poor completion of treatment schedules giving rise to relapse. The drug can cause nausea, rash, tachycardia, pruritus and extreme tenderness at the site of injection. More seriously kidney failure, diabetes mellitus caused by the hypoglycaemic effects to the host, not to mention death from hypotension, mean that a course of treatment can leave serious, long-term damage to the patient.

Resistance to pentamidine does not appear to be a major problem, even after massive prophylaxis use in the 1950s and '60s (Fairlamb, A. H., 2003). This is because of the multiple transporters used to accumulate the drug; a mutation or loss of one would not lower the intra-cellular concentration to a sub-therapeutic level; disruption of the TbAT1 purine transporter only results in a minor resistance to the drug (Matovu, E. et al, 2003). However a TbAT1 knockout cell line that was made further resistant to pentamidine by gradually increasing the maximum tolerated concentration in *in vitro* culturing was also shown to have lost the transport activity associated with HAPT1 (Bridges, D. J. et al, 2007).

In spite of this resistance has been induced in the laboratory that does not involve the loss of uptake, signifying that other mechanisms of resistance can arise (Berger, B. J., et al, 1995).

1.1.6.2 Suramin

Suramin is the drug of choice for stage one *T. b. rhodesiense* infections as pentamidine was found not to be as reliable. It was first used as a trypanocide in the early 1920s when German scientists developed it after similar dyes were shown to have remarkable activity against trypanosomes. Suramin is a water soluble, polysulfonated naphthylamine (Figure 1.5) and is highly ionic, having six positive charges at a physiological pH. Its ionic character means it cannot cross the blood-brain barrier (BBB) and so is not used to target trypanosomes in the CNS during the late stage of infection.

The charged nature of the drug may explain how it is taken into the cell; its positive charge makes it bind to many plasma proteins including low-density lipoproteins (LDLs) allowing it to be accumulated by receptor-mediated

endocytosis at the flagellar pocket of the trypanosome. Recent evidence (Pal, A. et al, 2002) casts doubt on this hypothesis, however, inferring accumulation may occur by a totally different process.

Excretion of the drug is extremely slow; it has a half-life of 44-54 days and can still be detected in the blood between five and eight months after the final injection. Again this is probably due to its high charge with 99.7% of the drug found bound to plasma proteins after pharmacokinetic analysis (Pépin, J. and Milord, F., 1994).

The mode of action of suramin has not been fully elucidated. The compound binds electrostatically to numerous enzymes, such as dihydrofolate reductase and thymidine kinase, consequently inhibiting them; nevertheless, this does not prove it is the process responsible for the death of the parasite. The reduced growth rate suggests interference in glycolysis by the inhibition of glycolytic enzymes, which might explain the slow death of the parasite over several days (Fairlamb, A. H., 2003; Docampo, R. and Moreno, S. N., 2003); however, any evidence is only inferential. More research is required before any firm conclusions can be drawn on a definitive mode of action for the drug.

Anaphylactic shock is a risk with treatment with suramin although rare, having an incidence of less than 1 in 2000 patients (Pépin, J. and Milord, F., 1994). More common is renal toxicity, however it is usually mild. Other side effects are fever, perhaps due to the lysing of the trypanosomes, nausea, vomiting and mucocutaneous eruptions. Despite being in use for over eighty years resistance to suramin is not a serious problem (Delespaux, V. and De Koning, H. P., 2007).

1.1.6.3 Melarsoprol

Also known as Mel B, melarsoprol was first used as a trypanocide in 1949. It is one of a class of compounds called the trivalent melaminophenyl arsenicals and was synthesized by the addition of British antilewisite (BAL) to the arsenic of melarsen oxide (Figure 1.5). It is insoluble in water, and so is administered dissolved in propylene glycol. Melarsoprol itself, while active against trypanosomes in its own right, may not be the actual compound killing the trypanosomes. Mel B is rapidly metabolised to melarsen oxide in the patient,

reaching a maximum plasma concentration in 15 minutes after injection, with a half-life of nearly four hours (Nok, A. J., 2003).

Evidence points to the adenosine P2 transporter being responsible for the uptake of the arsenicals into the trypanosome. Melarsen oxide and melarsoprol have been shown to inhibit the uptake of adenosine by the P2 transporter (Carter, N. S. and Fairlamb, A. H., 1993; De Koning, H. P. and Jarvis, S. M., 1999; De Koning, H. P., 2001), and only compounds that specifically inhibit P2 reduced the lysing affect of melarsen oxide on the trypanosome. More information came to light when an arsenical resistant *T. brucei* clone was investigated and a mutant TbAT1 gene, which is normally an adenosine P2 type transporter, was found; it had point mutations leading to six amino acid changes and an inability to transport adenosine (Mäser, P. et al, 1999). Furthermore, in northwestern Uganda 38 isolates out of 65 *T. b. gambiense* infected patients who had relapsed after treatment with melarsoprol had mutated TbAT1 genes, all of which had the same nine mutations in the gene (Matovu, E. et al, 2001). Not only does this data add weight to the importance of the P2 transporter in the accumulation of arsenicals to lethal concentrations inside the cell, but also its loss of function may be responsible for increasing resistance to melarsoprol. The high-affinity pentamidine transporter (HAPT1) appears to provide a secondary mode of uptake into the trypanosome. A TbAT1 knockout cell line made further resistant to pentamidine was also cross resistant with arsenical class compounds and was demonstrated to have lost HAPT1 activity (Bridges, D. J., et al, 2007).

The incidence of melarsoprol treatment failure has risen from a standard 5-8% to an alarming 30% in Uganda in 1999, with a reported 40% treatment failure in the late 1970s. A detailed investigation of the drug sensitivities of isolates from these outbreaks produced a confused picture (Brun, R. et al, 2001): the 1970s isolates showed a sensitivity one-tenth of that of non-relapse inducing isolates, with mouse infections also not being cured by previously therapeutic concentrations of drug; the recent Ugandan isolates, however, showed no change in sensitivity between isolates from relapsed and curable patients, with no difference in plasma concentrations of melarsoprol between the patients. This suggests that treatment failure is not just down to the sensitivity of the parasite to the drug but that a range of factors may be involved.

The exact mode of action of melarsoprol or its metabolite melarsen oxide has not been determined yet. The trypanosomes rapidly lose motility and lyse in the bloodstream. This has been put down to inhibition of the pyruvate kinase enzyme and, consequently, interference with the glycolytic pathway that produces the energy, in the form of ATP, that is required for movement; however it appears that the cells lyse well before the ATP levels are critically depleted (Denise, H. and Barrett, M. P., 2001). Another potential target is the trypanothione reductase enzyme, which is essential for maintaining a redox balance intracellularly. Melarsen oxide can react with trypanothione to form Mel T that can inhibit the trypanothione reductase (Fairlamb, A. H., 2003).

The most important side effect of treatment with melarsoprol is reactive encephalopathy. It occurs in between 5-10% of patients and is defined as a rapid decline in the level of consciousness and/or seizures; followed by pulmonary edema and death in over half of those affected within 24-48 hours (Pépin, J. and Milord, F., 1994). Suspending the treatment and giving high doses of corticosteroids and anticonvulsants can help to reduce the severity of the reaction. Once the encephalopathy has been resolved it is possible to continue treatment with melarsoprol without recurrence (Bouteille, B. et al, 2003). Other side effects are abdominal and chest pain, skin rashes, headaches, fever, tremors, and cardiac, renal and liver toxicity.

1.1.6.4 Eflornithine

An analogue of ornithine, eflornithine, sometimes known as DFMO from its chemical structure and name DL-alpha-difluoromethylornithine (Figure 1.5), is the first and only new drug to be approved for use in humans against Human African Trypanosomiasis since 1949.

It is thought to accumulate intracellularly in the trypanosome by passive diffusion although evidence for mediated uptake has been shown (De Koning, H. P., 2001). The pharmacokinetics shows that after intravenous infusion the serum concentration of eflornithine in patients was 49.2 nmol/ml for children and 87.5 nmol/ml for adults. The ratio of eflornithine in the cerebro spinal fluid to that in the blood plasma was 0.91 for adults and 0.58 for children (Milord, F., et al, 1993).

It acts as a suicide inhibitor of ornithine decarboxylase (ODC), a key enzyme in the synthesis of the polyamines spermidine, spermine, and putrescine that are essential for cell proliferation (Burri, C. and Brun, R., 2003). DFMO inhibits both the trypanosomal and mammalian ODC enzymes, however its selectivity of effect is brought about by the fact that humans degrade and replace their ODC enzyme much more rapidly than the trypanosome. DFMO is only efficacious against *T. b. gambiense* because *T. b. rhodesiense* has a much shorter half-life for its ODC meaning it replaces its enzyme faster than *T. b. gambiense*, and also fast enough to avoid the chemotherapeutic effects of eflornithine. It has been noted that DFMO is not trypanocidal; rather it merely prevents the growth and proliferation of the trypanosomes in the bloodstream and cerebrospinal fluid long enough for the patient's immune system to kill the parasites. This is backed up by the fact that eflornithine does not cure patients that are also HIV-positive, indicating that a competent immune system is vital for treatment success.

Resistance to DFMO can be relatively easily induced, at least in the procyclic forms, in *in vitro* culture by gradually increasing the sub-lethal concentration of the drug. However, the mode of resistance has not definitively been identified. There are conflicting reports about whether transport of the drug into the cell is responsible (Iten, M. et al, 1997; Phillips, M. A. and Wang, C. C., 1987), with others suggesting an increased level of ornithine, which competes with DFMO for the binding site of ODC, gives rise to the resistance (Bellofatto, V. et al, 1987).

Adverse reactions to eflornithine are similar to those of cancer treatments, for which DFMO has also undergone trials, and are reversible after treatment is completed. Nausea, vomiting and diarrhea are often reported with hair loss in 5-10% (Burri, C. and Brun, R., 2003). Convulsions can occur but are of a different type to those caused by the melarsoprol-induced encephalopathy.

1.1.6.5 Nifurtimox

Nifurtimox is a 5-nitrofurant derivative (Figure 1.5) that was developed in the 1960s for use against Chagas disease, which is caused by the American trypanosome *Trypanosoma cruzi*. It has not yet been registered for use against African trypanosomiasis but permission has been given on compassionate grounds to treat those where melarsoprol and eflornithine have both failed in late-stage infections (Bouteille, B. et al, 2003).

In *T. cruzi* nifurtimox enters the cell by passive diffusion and it seems likely that this would be the mode of uptake by African trypanosomes although no work has been carried out on *T. brucei* in this respect (Denise, H. and Barrett, M. P., 2001). Nifurtimox is a prodrug and its toxicity is thought to be derived from the production of free radicals after metabolism of the compound by nitroreductases (NTRs) (Wilkinson, S. R. et al, 2008). Free radicals are extremely reactive and could cause damage to multiple processes and pathways in the cell (Fairlamb, A. H., 2003).

Recently nifurtimox resistance was induced in *T. cruzi* parasites *in vitro* by culturing the parasites in 10 μM of the drug. This concentration inhibits the growth of more than 99% of the trypanosome population. The surviving parasites were shown to have a reduction in nifurtimox reducing activity and were 4-fold less sensitive to the drug (Wilkinson, S. R. et al, 2008). A type I NTR from *T. cruzi*, recombinantly expressed, was demonstrated to be able to metabolize nitrofurans including nifurtimox, and null TcNTR mutants were approximately 4-fold resistant to the drug. In the same study one allele of the homologous gene in *T. brucei* was disrupted, with the heterozygous TbNTR^{+/-} parasites also showing resistance to nifurtimox; overexpression of the same gene in bloodstream form *T. brucei* resulted in a marked increase in sensitivity to all nitroaromatic compounds tested. These data strongly implicate the type I nitroreductase in metabolising the prodrug to its toxic, free radical producing metabolite and that mutation or differential regulation of the NTR can result in resistance to the drug (Wilkinson, S. R. et al, 2008).

Side effects to nifurtimox in patients treated for Chagas disease are very common with 50% not able to complete a full course of treatment. Since treatment in patients with HAT is limited to those in late stage and also refractory to melarsoprol and eflornithine it is difficult to differentiate between side effects and natural symptoms to the terminal stages of the infection (Bouteille, B. et al, 2003).

1.2 Cyclic-nucleotide signalling in protozoa: adenylyl cyclases (AC)

1.2.1 Kinetoplastids

Adenylyl cyclase activity was first reported in trypanosomes in 1974 in *T. gambiense* (Walter, R. D., 1974), followed quickly by the first measurement of cyclic-AMP in trypanosomes in different life cycle stages, where it was observed that in *T. lewisi* the cAMP concentration in the non-reproducing adult form was approximately twice that of the reproducing form (Strickler, J. E. and Patton, C. L., 1975). Further changes in intracellular cAMP concentration were measured in *T. brucei*: as the parasitaemia in rats increased, the cAMP concentration rose with it. In strains that caused a relapsing parasitaemia, the same initial change in cAMP was observed, however, as the proportion of trypanosomes in the long slender form decreased to give way to the short stumpy forms, so the intracellular cAMP concentration fell too, until a basal level was reached when short stumpy forms were predominant. When the next parasitaemic wave of long slender forms grew, cAMP concentration in the trypanosomes rose also, suggesting a link between morphological form of bloodstream trypanosome and cAMP response to changing cell density (Mancini, P. E. and Patton, C. L., 1981).

1.2.1.1 Calcium mediated adenylyl cyclase regulation

Adenylyl cyclase (AC) activity was found to be predominantly localised to the membrane portion of sub-cellular fractions of *T. cruzi* (Pereira, N. M. et al, 1978) and *T. brucei* (Martin, B. R. et al, 1978). Further characterisation of the AC activity in *T. brucei* membrane fractions revealed that it is constitutively active in the presence of Mg^{2+} and completely unaffected by the usual mammalian AC effectors glucagon, guanyl-5'-yl imidodiphosphate (p[NH]ppG), adrenaline or adenosine; and is inhibited by pyrophosphate (PP_i), the secondary product of adenylyl cyclase (Martin, B. R., et al, 1978). The AC activity in the membrane fraction was also inhibited by Ca^{2+} ; however, measuring its effect in whole, intact cells showed that calcium actually stimulated AC activity, reaching a maximum effect at a concentration of 300 μM before gradual attenuation of activation at concentrations up to 2 mM (Voorheis, H. P. and Martin, B. R., 1980).

To investigate the effects of calcium *in situ*, Voorheis and Martin developed a technique, termed 'swell dialysis', whereby membrane permeability was achieved by carefully lowering the osmotic strength of the cell suspension medium, disrupting the membrane enough to allow small molecular weight compounds or molecules to cross the lipid bi-layer and enter the cytoplasm. Using this technique it was observed that calcium crossed the plasma membrane and equilibrated with the external concentration within just 30 seconds, however, there was a time-lag of several minutes (depending on Ca^{2+} concentration) before the adenylyl cyclase activity was stimulated (Voorheis, H. P. & Martin, B. R., 1981). The addition of the ionophore A-23187 hastened the Ca^{2+} stimulation in osmotically swollen cells. This seems somewhat strange since the accumulation of calcium intracellularly in swollen cells is so rapid: the authors hypothesized that the ionophore allows Ca^{2+} to access the lipid bi-layer plasma membrane faster than just swelling alone and that the calcium receptor is located in the membrane, possibly located in the part of the membrane-embedded region of the adenylyl cyclase. More circumstantial evidence of the AC-stimulating calcium receptor being located in the plasma membrane comes from the fact that the local anaesthetic benzyl alcohol can activate adenylyl cyclase in the presence of Ca^{2+} (Voorheis, H. P. & Martin, B. R., 1982). Benzyl alcohol is a membrane perturbing agent in mammals and it may act by disrupting the plasma membrane of trypanosomes allowing faster access to the putative membrane embedded receptor for calcium.

The addition of calcium and the ionophore A-23187 also result in the shedding of the variant surface glycoprotein (VSG) coat by the bloodstream form trypanosomes (Bowles, D. J. & Voorheis, H. P., 1982; Voorheis, H. P., et al 1982). Indeed VSG shedding and adenylyl cyclase stimulation appear to share numerous characteristics in common: the activation by calcium and ionophore; stimulation by the rupturing or perturbation of the plasma membrane; and blocking of stimulation by the addition of Zn^{2+} (Voorheis, H. P. et al, 1982), all suggesting a link between AC activation and VSG shedding. The investigation of the calcium-mediated activation of adenylyl cyclase in the differentiation of bloodstream form trypanosomes to procyclics appeared to substantiate this connection. Swell dialysis of both forms showed that Ca^{2+} stimulated the AC of bloodstream forms only, having no apparent effect on procyclic AC which have a different type of outer surface protein coat from the VSG of bloodstream forms

(Rolin, S. et al, 1990). AC activity and VSG shedding were monitored after triggering differentiation of bloodstream to procyclic forms by lowering the incubation temperature from 37 °C to 27 °C and adding citrate/*cis*-aconitate to pleomorphic trypanosomes harvested from the rodent host after 8 days post-infection (where more than 90% of the trypanosomes are non-proliferative intermediate and stumpy forms). After 4 hours post differentiation induction transforming cells began to appear with 100% of the trypanosomes transforming after 9 hours; procyclic forms began to appear at 12 hours with virtually all having fully differentiated by 22 hours (Rolin, S. et al, 1993). VSG was rapidly shed with around 50% released after 5 hours post induction and only a residual level remaining after 10 hours; AC activity began to rise sharply 4-6 hours after triggering differentiation and peaking around 7-8 hours before falling to a basal level after 10 hours, a further transient peak spanned the 20-40 hour time period where the procyclics were reproducing. These data suggest that AC stimulation does not appear to be responsible for the release of VSG, as the first peak in activity only appears after VSG shedding is well under way, but may be modulating the subsequent stages of differentiation since this peak coincides with the appearance of transforming trypanosomes. Interestingly, it was observed that for cultures that did not appear to be differentiating together, the addition of 1 mM cAMP to the triggering conditions synchronised the transformation of the whole cell population (Rolin, S. et al, 1993), lending weight to the above hypothesis.

It was also speculated that it may be the release of VSG itself that might stimulate the adenylyl cyclase enzymes. Bloodstream form trypanosomes were treated with trypsin, which cleaves VSG from the plasma membrane by proteolysis, and VSG shedding and AC activity were monitored over time. The result was a lag of 15 minutes between the detection of the N-terminal domain of cleaved VSG in the medium by anti-VSG antibody and the stimulation of adenylyl cyclase (Rolin, S. et al, 1996). Treating the trypanosomes with trypsin for 15 minutes then adding soybean trypsin inhibitor resulted in a slightly different picture: the N-terminal domain of VSG was detected as before, with a lag phase until the activation of AC, however, detection of the C-terminal domain of VSG in the medium by anti-CRD antibodies was paralleled by the stimulation of adenylyl cyclase. The C-terminal domain of VSG is released only by the cleavage of the glycoposphatidylinositol (GPI) anchor by GPI-

phospholipase C (GPI-PLC). Incubating the trypanosomes at pH 5.5 also resulted in VSG release and AC activation; again the AC stimulation paralleled the release of the C-terminal domain of VSG by GPI-PLC (Rolin, S. et al, 1996).

Similar experiments conducted on a pleomorphic line of *T. brucei* highlighted the different responses to the same type of stress conditions by long slender and stumpy bloodstream forms. Trypanosomes harvested on differing days post infection from infected rodents were subjected to pH 5.5 medium: only the trypanosomes taken early in the infection, when the majority are long slender forms, activated their adenylyl cyclase and triggered GPI-PLC mediated VSG release (Nolan, D. P. et al, 2000). Likewise, incubation with trypsin resulted in only the predominantly long slender form cultures activating AC and releasing C-terminal VSG. This suggests that only the long slender forms are sensitive to stress-activated AC stimulation and GPI-PLC mediated VSG release. Exposure to Ca^{2+} under swell dialysis conditions however, showed an equal activation of AC by both long slender and stumpy forms.

The data above suggest that the release of the C-terminal domain of VSG by GPI-PLC directly stimulates adenylyl cyclase activity. However, further investigation with GPI-PLC null mutants and PKC inhibitors showed both effects were simultaneous but independent. Incubation of the mutant trypanosomes at pH 5.5 resulted in AC stimulation but no release of VSG. Also, it had been observed that PKC inhibitors also induced GPI-PLC mediated VSG release and AC stimulation. Total inhibition of adenylyl cyclase with *p*-chloromercuriphenylsulfonic acid (pCMPS) and incubation with the PKC inhibitor Myr- ψ -PKC- α resulted in the release of C-terminal domain VSG but no activation of AC (Rolin, S. et al, 1996). While it is now apparent that VSG release and AC activation are independent processes, they may be triggered by the same stimuli and resulting signalling cascade.

1.2.1.2 Isolation and biochemical characterisation of adenylyl cyclase genes and their proteins

The first identification of a putative kinetoplastid adenylyl cyclase gene occurred when the gene expression site of an active VSG was sequenced in *T. brucei* (Pays, E. et al, 1989). The sequencing revealed that there were multiple genes in the expression site transcribed at the same time as the VSG gene,

termed expression-site associated genes (ESAGs), and one of them, ESAG4, showed homology with an adenylyl cyclase from yeast. The sequence homology was mostly restricted to two regions in the C-terminal end of the gene which, in the yeast AC, is responsible for enzyme activity. ESAG4 is expressed in the bloodstream form only by an α -amanitin resistant polymerase; however, sequences similar to that of ESAG4 can be detected in the procyclic form as well as the bloodstream form, having been transcribed by an α -amanitin sensitive polymerase (Pays, E. et al, 1989; Alexandre, S. et al, 1990). Hybridization with an ESAG4 probe of a procyclic cDNA library could not pick out a single clone identical to ESAG4, but detected several related sequences. Restriction mapping of the clones separated them into two categories, with the largest from each further characterised and named GRESAG4.1 and GRESAG4.2 (for genes related to ESAG4). Southern blots using 5' and 3' regions of ESAG4 showed that related genes were also found in *Trypanosoma gambiense*, *T. congolense*, *T. mega* and *T. vivax* (Alexandre, S. et al, 1990). Specific antibodies against ESAG4 and GRESAG4.1 showed differential expression in transforming bloodstream forms, with most of the ESAG4 AC lost around 9 hours after differentiation was triggered, paralleling the decline in the proportion of stumpy forms; while the level of GRESAG4.1 remained constant from stumpy form through to reproducing procyclics (Rolin, S. et al, 1993). A further GRESAG4 was found by using the cDNA of GRESAG4.1 and GRESAG4.2 as probes against bloodstream form cDNA. The GRESAG4.1 probe identified an identical clone from the bloodstream cDNA library while the GRESAG4.2 probe picked up a slightly different clone and the gene contained within was termed GRESAG4.3. The sequences of the GRESAG4 genes were aligned with that of ESAG4: this revealed a highly homologous region in the C-terminal, located immediately after a hydrophobic stretch big enough to be membrane spanning. This strongly conserved region also shares a high degree of homology to the catalytic domains of adenylyl cyclase in *Saccharomyces cerevisiae* and also the guanylyl cyclase found in the rat brain (Alexandre, S. et al, 1990).

Proof that the putative AC genes actually coded for adenylyl cyclase enzymes came when ESAG4 and GRESAG4.1 were transfected into a temperature sensitive *cyr1* yeast mutant, which lacks adenylyl cyclase activity at 34 °C (Paindavoine, P. et al, 1992). Both ACs complemented the yeast mutant and were detected by antibodies in the membrane fraction of transformed yeast. They were also

activated by Mg^{2+} , but more so by Mn^{2+} ; however, ESAG4 is stimulated by Ca^{2+} , whereas GRESAG4.1 is not, indicating that ESAG4 may be responsible for the calcium mediated activation of AC activity observed by Voorheis and Martin in intact bloodstream form *T. brucei* (Voorheis, H. P. and Martin, B. R., 1980; 1981; 1982). Similar work using the related parasite *Trypanosoma equiperdum* also uncovered a homologous AC gene in the VSG expression site (Ross, D. T. et al, 1991). This gene shared 92% homology with ESAG4 and, when transfected into a yeast mutant with its *cyr-1* AC gene almost completely deleted, also displayed constitutive adenylyl cyclase activity.

In *Leishmania donovani* a tightly clustered family of at least five adenylyl cyclase genes were identified, and two sequenced and characterised (Sanchez, M. A. et al, 1995). Sequence alignment showed the putative ACs, termed *rac-A* and *rac-B*, shared a high degree of homology with GRESAG4.3 from *T. brucei*, being over 50% identical in the C-terminal catalytic domain and also sharing the transmembrane domain immediately before the catalytic region. Attempts to transform and complement yeast AC mutants were unsuccessful, however, but functional expression in *Xenopus laevis* oocytes showed that *rac-A* could produce cAMP whereas *rac-B* could not, or at least not in this expression system.

A GRESAG 4.3 fragment from *T. brucei* was used to screen a *T. cruzi* cosmid library: again a multi-gene family of putative adenylyl cyclases was identified and two were sequenced and characterised and termed *TcADC 1* and *TcADC 4* (Taylor, M. C. et al, 1999). The catalytic domain of *TcADC 1* was expressed in, and complemented, an *E. coli cya* AC mutant; AC activity was measured in the presence of Mg^{2+} and Mn^{2+} with a preference shown for the latter by a 6-fold increase in activity at 10mM. No guanylyl cyclase activity was detected indicating that *TcADC 1*, at least, is specific for ATP over GTP. Sequence analysis determined that they shared the same predicted protein architecture as in *T. brucei* and *L. donovani* having a transmembrane domain followed by a highly conserved cytosolic catalytic domain. The regions responsible for the binding of the $G_{s\alpha}$ and $G_{\beta\gamma}$ subunits of the heterotrimeric G-proteins that regulate mammalian adenylyl cyclases were not conserved in *TcADC 1* or *TcADC 4* or any of the other kinetoplastid AC genes, suggesting that trypanosomal ACs are not regulated or activated by G-proteins homologous to those of mammals. Indeed, while some characteristics of G-protein subunit activity have been reported in *T.*

cruzi (Eisenschlos, C. et al, 1986; Coso, O. A. et al, 1992), no homologous sequences homologous to the G-protein subunits have been identified in the genomes of any of the kinetoplastids sequenced to date.

Interestingly, the change of one residue, from serine in the mammalian adenylyl cyclases to aspartic acid in *TcADC 1* or *TcADC 4*, at the position corresponding to amino acid 942 of the C2 domain of rat type II AC, predicts that the binding of forskolin to kinetoplastid ACs would be impeded. Forskolin is a stimulator of mammalian ACs and has been used uncritically in investigations of protozoal AC activity, including kinetoplastids, on the unproven assumption that its effects in mammalian cells would be replicated in other systems. Functional characterisation of the two *T. cruzi* AC genes in *E. coli* back up the sequence observation, as forskolin had no effect on *T. cruzi* AC activity (Taylor, M. C. et al, 1999), in agreement with an early report on activity in *T. cruzi* AC purified with the aid of monoclonal antibodies which also failed to see an effect from forskolin (Torruella, M. et al, 1986). Similarly, another *T. cruzi* AC gene (*TczAC*) was identified and characterised and was also shown to be insensitive to forskolin and mammalian G-protein regulators (D'Angelo, M. A. et al, 2002). Work published previously with the effects of forskolin on trypanosomes as a component, while probably genuinely observed and diligently reported, will need to be reappraised in the light that forskolin-mediated effects may be due to non-adenylyl cyclase or non-cAMP signalling effects.

1.2.1.3 Adenylyl cyclase protein structure

As became apparent from the sequencing of numerous ACs from several species, the adenylyl cyclase enzymes from kinetoplastids all share a similar over-arching protein structure. They all have a large extracellular N-terminal domain with low homology between individual genes and/or species, and a single membrane spanning region that connects to the catalytic domain. This is in stark contrast to mammalian ACs that generally have 12 transmembrane domains, with the exception of the soluble AC. Until recently it was thought that the N-terminal extracellular domain of trypanosomal adenylyl cyclases had no similarity with any other protein domains, although it had been suggested that since there were no G-protein coupled receptors in the kinetoplastid genomes this region may act as a receptor itself (Paindavoine, P et al, 1992; Seebeck, T. et al, 20004;

Laxman, S. and Beavo, J. A., 2007). A Blast search and hidden Markov modelling revealed a relationship with an *E. coli* L-leucine-binding protein with the N-terminal of a representative AC from *T. brucei* (Emes, R. D. and Yang, Z., 2008). In *Pseudomonas aeruginosa* a leucine-binding protein (LBP) acts as an amide receptor (O'Hara, B. P. et al, 2000).

The C-terminal region of the ACs is highly conserved between kinetoplastids and is also highly related to that of the mammalian Class I adenylyl cyclase catalytic domain and to the receptor guanylyl cyclase. A C-terminal extension, found after the catalytic domain, appears to be unique to kinetoplasts and has a large amount of sequence variation. The cytosolic domains of *T. brucei* AC genes GRESAG4.1 and GRESAG4.3, with 110 residues of the C-terminal extension removed, were crystallized and their structures solved by high resolution X-ray analysis of the crystals formed (Bieger, B. and Essen, L.-O., 2000; 2001). As expected from the sequence analysis, the structures of the crystallized trypanosomal ACs are very similar to that of the C1A domain of dogs and the C2A domain found in rats, with overall structural differences equal between the *T. brucei* ACs and the mammalian and those between the mammalian ACs themselves.

The crystals of the catalytic domain of GRESAG4.1 and GRESAG4.3 were formed exclusively in a monomeric state. However, there is evidence to suggest that the active forms of the trypanosomal ACs are dimers. In *L. donovani* RAC-A was expressed in *Xenopus laevis* oocytes and was shown to produce cAMP; co-expression with RAC- Δ (RAC-A with part of its catalytic domain removed) resulted in a dramatic reduction in cAMP production (Sanchez, M. A. et al, 1995). Also, co-expression of RAC-A with RAC-B - an apparently non-functional pseudogene - also resulted in the inhibition of cAMP production. This suggests that RAC-A can interact with the other non-active gene products, possibly oligomerizing. Gel filtration analysis of a new family of *T. brucei* AC, GRESAG4.4 confirmed that trypanosomal adenylyl cyclase catalytic domains could spontaneously and stably dimerise. The addition of a leucine zipper to the N-terminal of the catalytic domain increased the V_{max} of the enzyme 20-fold, while the K_m remained constant (Naula, C. et al, 2001). This implies that dimerisation is linked to increased cyclase activity, or that by slightly altering the conformation of the AC dimer the rate of cAMP production can be greatly

increased. The authors suggest that this could act as a form of AC regulation, speculating that a small ligand molecule could alter the conformation of the dimer by binding and thereby stimulate the AC. The predicted substrate binding and active sites indicated that two molecules of ATP would be bound per catalytically active homodimer (Liu, Y. et al, 1997), in contrast to the one active site in mammalian Class I ACs. This was confirmed by heterodimerization with differential active site mutants of GRESAG4.1: a single site mutant in a dimer with the wildtype resulted in a loss of 60% of the activity, consistent with the loss of one active site; whereas a differential double mutant dimer results in the activity falling below 10%. Dimers made from complementary mutants could restore the activity of one active site (Bieger, B. and Essen, L.-O., 2001). Superimposition of the active site of GRESAG4.1, GRESAG4.3 and the mammalian C1A, as well as a common key-residue active site mutagenesis profile all suggest that the actual mechanism of catalysis of ATP to cAMP in trypanosomal ACs is very similar to that of mammalian Class I ACs.

The major structural difference between the *T. brucei* adenylyl cyclases and Class I ACs is the insertion of a 36 amino acid region in the loop between the $\alpha 3$ helix and the $\beta 4$ sheet (Figure 1.6). This insertion forms two extra helices called $\alpha 3A$ and $\alpha 3B$ and together have been called the Δ -subdomain. In Class I ACs the $\alpha 3$ - $\beta 4$ loop is involved in the interaction of G-protein subunits; that trypanosomal ACs have such a variation at that particular point suggests the Δ -subdomain may have a regulatory role and gives a structural reason for the inability of G-protein subunits to affect kinetoplastid ACs. Further analysis of the crystal structure of GRESAG4.1 and GRESAG4.3 show that together with the $\alpha 4$ - $\beta 7$ loop and parts of $\beta 4$ and $\beta 8$, the Δ -subdomain forms a cavity of 95 \AA^3 , large enough to be a binding pocket for a small molecule or protein co-factor that may exert an allosteric or regulatory effect on the enzyme (Bieger, B. and Essen, L.-O., 2001). Interestingly, a recent analysis of the kinetoplastid genomes published to date, investigating adaptive evolution in a number of large multigene families, identified 29 trypanosomal adenylyl cyclases as having sites of predicted positive selection (Emes, R. D. and Yang, Z., 2008). The majority were located in the N-terminal extracellular region, whereas only 4 codons were predicted to have been subject to positive selection in the catalytic domain. These 4 amino acid changes are all apparently located on the $\alpha 4$ helix, possibly capable of interacting with the cavity enclosed by the Δ -subdomain.

However, a number of candidates have been uncovered. It was observed that preparations from the hindguts of the insect host of *T. cruzi*, that had been fed chicken blood, activated the epimastigotes form's adenylyl cyclase as well as stimulate differentiation to the metacyclic form (Fraidenraich, D. et al, 1993). After HPLC and reverse-phase chromatography singled out a 10 kDa molecule which, when the first 20 amino acids were sequenced, was identified as part of chicken α^D -globin and the peptide was designated Globin-Derived Factor (GDF). A synthetic peptide made from amino acids 1 - 40 of chicken α^D -globin also stimulated AC activity, as did peptides 30 - 49 and 35 - 73 (Garcia, E. S. et al, 1995). Similarly, for *T. brucei*, the crude membrane fraction of the proventriculus/esophagus of tsetse flies apparently activates the adenylyl cyclase enzymes of both bloodstream forms and procyclics (Van Den Abbeele, J. et al, 1995). However these observations do not appear to have been followed up.

The cellular localization of the adenylyl cyclases of kinetoplastids may also impact on their diversity. In characterizing ESAG4 and GRESAG4.1, antibodies raised against recombinant ESAG4 were used in conjunction with immunogold staining to identify the localization of the AC families (Paindavoine, P. et al, 1992). The antibodies used were not specific for ESAG4 over GRESAG4 related peptides, however they did show a specific cellular region with which they react: the cell surface and only along the flagellum. Interestingly the localization of ACs in bloodstream forms was apparently identical to that of procyclics. Similarly, in *T. cruzi* epimastigotes, the calcium-stimulatable TcAC was also found to be associated with the flagellum (D'Angelo, M. A. et al, 2002). In the TcAC characterization a yeast 2-hybrid system was developed to demonstrate dimerisation of the catalytic domain: if the TcAC domains, transfected into yeast in two different plasmids, closely interacted with each other the two reporter genes, also on the plasmids, would be expressed and would rescue the mutant yeast. Dimerisation of the catalytic domains was inferred in this manner. In addition, the yeast 2-hybrid approach was also used to identify putative regulators of the ACs by screening a cDNA library generated from epimastigotes. One of eight that rescued the mutant yeast phenotype encoded a portion of the protein paraflagellar rod, an integral component of the flagellum. A full length copy of the identified gene was transformed into the 2-hybrid system and confirmed the interaction with TcAC by complementation of

the yeast mutant, implying that the flagellar protein may have a role in regulation of the adenylyl cyclase activity (D'Angelo, M. A. et al, 2002).

The localization of kinetoplastid ACs on the cell surface is the logical expected home for these proteins if they are the sensory receptors they are hypothesised to be, and the exposure to panoply of small host molecules and immunologically active components may have driven the sequence diversity of the N-terminal domain and helped generate the multiple gene families of ACs found in the respective genomes. As mentioned above, a study investigating adaptive evolution in *T. brucei* identified 29 ACs of having regions of positive selection (Emes, R. D. and Yang, Z., 2008). The majority of these regions can be found in the N-terminal domain homologous to the leucine-binding protein, specifically on the regions predicted to come into close contact with a putative ligand. The sequence diversity may give rise to the specificity of ligand recognition requiring a multitude of ACs to allow specific activation and cellular response due to a specific ligand found in the very different host environments.

1.2.2 Apicomplexans

1.2.2.1 Identification of non-mammalian AC in infected erythrocytes

Early observations of adenylyl cyclase activity in *Plasmodium*-infected red blood cells (RBCs) attributed the changes in cAMP concentration to the host cell cyclases. It was noted that erythrocytes infected with strains of *P. berghei* had approximately 2-fold the concentration of cAMP compared to uninfected cells (Hertelendy, F. et al, 1979). Also, an investigation of the membrane-bound adenylyl cyclase activity of infected and uninfected RBCs suggested that the parasitised erythrocyte membranes displayed a 130% increase in AC activity compared to those of RBCs from an uninfected host; the AC activity of uninfected erythrocytes from an infected host was also raised, but only by 33% (Khare, S. et al, 1984).

However, a more detailed study of the membranes of infected erythrocytes and of the isolated parasites identified an adenylate cyclase with characteristics different from those displayed by the ACs of the host RBC (Read, L. K. and Mikkelsen, R. B., 1991a). Parasites were separated from the host erythrocytes by N₂ cavitation and Percoll gradient centrifugation and the AC activity profile of

the parasite was compared with that of uninfected RBC membranes, as well as the AC activity from infected RBCs. The erythrocyte membrane ACs showed a marked stimulation of activity on incubation with G protein activators whereas the parasites did not show any effect; forskolin also greatly stimulated erythrocyte ACs but did not significantly increase the activity of the parasite's cyclase. The two adenylyl cyclase profiles also displayed a differential preference for cation co-factor and optimal pH with the parasite ACs working better with Mn^{2+} and maximally at pH 8.0 and the erythrocytes preferring Mg^{2+} and pH 9.0. When the AC profile of the isolated parasite was compared to that of the erythrocyte still infected with *Plasmodium* it was found that the two profiles were highly similar suggesting that it is the parasite adenylyl cyclase that predominantly contributes to the intracellular cAMP of infected RBCs and not the host cell's. This apparent contradiction of earlier work was explained by the authors as a function of the techniques used to separate the erythrocyte membranes from that of the parasites, with the methods used previously not being as discriminatory as thought at the time.

1.2.2.2 Affect of AC on gametocytogenesis

Reports as to the effect of cAMP and its signalling cascade on the differentiation of blood-stage malaria to gametocytes are also somewhat contradictory. 1 mM cAMP added to 4 day old cultures of *Plasmodium falciparum* in human erythrocytes resulted in 5 - 10 times more parasites transforming into gametocytes, with similar results for the cAMP analogue dibutyryl cAMP (Kaushal, D. C. et al, 1980). The effect of cAMP was narrowed down to the stationary phase of growth in culture when nearly 100% of parasites were stimulated to differentiate to gametocytes with cAMP, whereas the proportion induced to transform was much lower when cAMP was added to cultures in rapid growth. In stark contrast to the results above, cAMP was shown to have an inhibitory effect on gametocytogenesis in a different strain of *Plasmodium falciparum*, as well as inhibiting asexual growth in the ring-stage but not maturation in subsequent stages (Inselburg, J., 1983).

Comparisons between two more strains of *P. falciparum* with differing abilities to produce gametocytes also implicated cAMP signalling. The parasites were isolated from their erythrocyte host cells and their adenylyl cyclase and cAMP-

dependent protein kinase activities assessed. Both strains had a similar AC activity; however the protein kinase activities differed, with the strain that could produce gametocytes *in vitro* (LE5) being 3-fold higher than the strain that could not (T9/96) (Read, L. K. and Mikkelsen, R. B., 1991b). The data suggest that it is the inability of the cAMP-dependent protein kinase of strain T9/96 to respond to cAMP fluctuations caused by activation of the adenylyl cyclase that results in the inhibition of gametocytogenesis.

1.2.2.3 cAMP and calcium cross-talk

cAMP signalling has also been linked with the regulation of the synchronisation of the *Plasmodium* cell cycle in the mammalian host, in conjunction with the Ca^{2+} signalling cascade. The symptomatic periodic fever of sufferers infected with malaria is caused by the synchronised rupturing of parasitized erythrocytes and the release of merozoites into the bloodstream. The mammalian hormone melatonin, which is synthesised in the pineal gland when the host is in darkness, has been implicated in the synchronisation of the maturation of parasites in the erythrocyte (Hotta, C. T. et al, 2000). Melatonin was shown to increase the cytosolic concentration of Ca^{2+} in saponin-isolated *Plasmodium* trophozoites, probably via the activation of phospholipase C (PLC) and its production of inositol triphosphate (InsP_3) resulting in the mobilisation of Ca^{2+} from the endoplasmic reticulum (Hotta, C. T. et al, 2000). However, melatonin also stimulates an increase in the intracellular cAMP concentration in saponin-isolated trophozoites, which can be blocked by the PLC inhibitor U73122, the calmodulin inhibitor calmidazolium and also by the calcium chelator BAPTA (Beraldo, F. H. et al, 2005). The hormone affects the maturation rate of blood stage malaria by speeding up transformation to the schizont stage (Hotta, C. T. et al, 2000). This stimulation can be mimicked by the cAMP analogue and PKA activator N6-benzoyl cAMP (6-Bz-cAMP), as well as the phosphodiesterase inhibitor IBMX. Furthermore, the melatonin stimulation can be completely abolished by the addition of PKA inhibitors providing strong evidence of cAMP signalling regulating cell cycle synchrony and sharing a common pathway with the calcium cascade (Beraldo, F. H. et al, 2005). While the cell cycle experiments were necessarily conducted with *P. falciparum*-infected erythrocytes, creating potential difficulties in the interpretation of signalling, the fact that melatonin was shown to act directly on the parasites (Hotta, C. T.

et al, 2000; Beraldo, F. H. et al, 2005) is consistent with the PKA modulators also acting on the Plasmodium enzyme.

Continued exploration of the effects of cAMP and melatonin on the cytosolic Ca^{2+} concentration of *Plasmodium* unveiled a complex mechanism of cross-talk between the two signalling systems via PKA. The rise in cytosolic Ca^{2+} due to exposure to melatonin is independent of the extracellular Ca^{2+} concentration and of PKA, as the same level of calcium stimulation is achieved when melatonin is assayed against the parasite in Ca^{2+} free medium and also in the presence of the PKA inhibitor PKI. The cAMP analogue and PKA activator 6-Bz-cAMP also increases cytosolic Ca^{2+} ; however, unlike melatonin treatment, this rise is transient in calcium free medium, and is blocked by PKI, suggesting that the cAMP-induced Ca^{2+} increase is mediated by PKA but different from the melatonin response. The PLC inhibitor U73122 had no effect on the Ca^{2+} increase induced by 6-Bz-cAMP, again opposite to what happened with melatonin, but the addition of 6-Bz-cAMP after melatonin did not result in a further increase in Ca^{2+} in the cytosol, suggesting that while the mobilisation of cytosolic Ca^{2+} by melatonin and cAMP is triggered independently of each other, the two pathways utilise the same intracellular source of the calcium (Beraldo, F. H. et al, 2005).

Further evidence of the identity of the intracellular calcium store utilized by both melatonin and cAMP pathways came with the use of thapsigargin (THG). THG inhibits the sarco-endoplasmic reticulum Ca^{2+} ATPase (Pozzan, T, et al, 1994) and caused a depletion of cytosolic Ca^{2+} stores in *Plasmodium*. Pre-treatment with THG thus prevented the cytosolic Ca^{2+} increase caused by melatonin (Hotta, C. T. et al, 2000). 6-Bz-cAMP also could not increase cytosolic calcium after the THG-induced transient increase and *vice versa* when assayed in Ca^{2+} free medium. However, 6-Bz-cAMP did induce a second rise in cytosolic calcium after that induced by thapsigargin (THG) when calcium was present in the assay medium (Beraldo, F. H. et al, 2005). The data suggest that cAMP and melatonin utilize the same intracellular store of calcium, but also that cAMP can mobilise calcium from the external environment of the parasite while melatonin cannot.

1.2.2.4 Isolation and characterisation of *Plasmodium* ACs

Preliminary release of the *Plasmodium falciparum* genome database facilitated the identification of putative genes coding for the adenylyl cyclase activity. The conserved motifs of the catalytic domains from many diverse species were used to BLAST search the *P. falciparum* genome yielding two potential AC genes; one on chromosome 14 (PfAC α) and the other on chromosome 8 (PfAC β). RT-PCR on total RNA from blood stage parasites and examination of upstream and downstream sequence data revealed PfAC α to have 22 exons, with at least 3 splice variations at the N-terminal end. Variant 1 was predicted to code for an 81.2 kDa protein with 2 transmembrane (TM) domains, variant 2 coded for a 98.2 kDa protein with 5 TM domains and variant 3, made up of all 22 contiguous exons, gave a full length 108 kDa protein with 6 TM domains (Muhia, D. K. et al, 2003).

PfAC β appears to be quite different from PfAC α , having a double catalytic domain (C1 and C2) in comparison to the single catalytic domain of PfAC α . Both the soluble and membrane-bound mammalian adenylate cyclases also have a pair of catalytic domains (Sunahara R. K. et al, 1996). Phylogenetic analysis of PfAC β puts it into a group containing all known soluble ACs including the mammalian bicarbonate sensor and a hypothetical protein from the mosquito *Anopheles gambiae*; PfAC α clusters with putative adenylyl cyclases from other apicomplexans as well as prokaryotic organisms. Sequence alignments with a range of AC catalytic domains show the majority of conserved residues essential for catalytic function are present in both genes with the substrate specificity residue being lysine for the two *Plasmodium* genes and in all other known ACs (Muhia, D. K. et al, 2003). Interestingly both PfAC α and PfAC β have amino acid inserts in the catalytic domain in the same position as the Δ -subdomain insert found in all kinetoplastid ACs, which has been hypothesized to have a regulatory ligand binding role (Bieger, B. and Essen, L.-O., 2001).

Northern blot analysis of total RNA extracted from asexual and sexual blood stage parasites, at various time points after synchronisation with sorbitol or N-acetylglucosamine (GlcNAc), respectively, showed that PfAC α blood stage expression is confined to the gametocyte forms, maximally at stages II and III of development. PfAC α mRNA was also detected in gametocytes stimulated to

gametogenesis, indicating that AC activity may be necessary in the mosquito forms as well as mammalian forms (Muhia, D. K. et al, 2003).

In order to express PfAC α in a heterologous organism the entire gene was resynthesized with the codon bias of *Xenopus laevis*. This was due to the extremely high A/T base-pair percentage, in common with all other *Plasmodium* genes, which can interfere with correct expression in other systems. The full length splice variant 3 of PfAC α was expressed in *Xenopus* oocytes resulting in a 2.5 - 3-fold increase in intracellular cAMP in comparison to the control, demonstrating that PfAC α is a functional adenylyl cyclase. Variants 1 and 3 (fused with Yellow Fluorescent Protein) were similarly expressed in *Dictyostelium discoideum*, also resulting in an increase in intracellular cAMP. Cell lysates of the transformed *D. discoideum* showed that the highest AC activity was displayed in the presence of Mn²⁺ for both variants rather than Mg²⁺ as usual for mammalian ACs (Muhia, D. K. et al, 2003).

Further characterisation of a resynthesized PfAC α catalytic domain, using mammalian codon bias and expression in Sf9 insect cells, confirmed the preference for Mn²⁺ over Mg²⁺ and determined the K_m at 115 μ M ATP. Furthermore GTP was not a substrate and forskolin could not stimulate the AC activity (Weber, J. H. et al, 2004). The data from the heterologous expression of studies with PfAC α are thus strikingly in agreement with the observations of Read and Mikkelsen (1991a) on increased AC activity in *P. falciparum*-infected erythrocytes (see section 1.2.2.1).

Evidence that the N-terminal region of PfAC α , which contains the transmembrane domains, acts as a putative ion channel emerged from work carried out on the homologous adenylyl cyclase genes in ciliates (Weber, J. H. et al, 2004). Primers designed from the PfAC α genome sequence were used to produce a DNA fragment from *Paramecium* genomic DNA; this was then used to probe a *Paramecium* cDNA library and two clones were identified. Sequence analysis combined with membrane topology predictions unveiled a potential voltage gated ion channel in *Paramecium* and also in *Tetrahymena*, both organisms grouped into the Alveolata with the apicomplexans. The N-terminal region was made up of two blocks of transmembrane helices: block one contained four TM helices (S1 - S4), with S4 containing conserved residues for

voltage gating; block two contained the remaining two TM helices (S5 and S6) which are predicted to form the ion pore. The putative ion pore is connected to the AC catalytic domain by a short 18 amino acid linker region suggesting the regulation of the cyclase activity by the ion channel. The ion pore region also contains the signature motif found in potassium channels, indicating the possible ion specificity reminiscent of the bifunctional AC/ion-channel activity reported earlier in *Paramecium tetraurelia*, which was blocked by potassium channel inhibitors (Schultz, J. E. et al, 1992).

The domain structure of PfAC α is predicted to be topologically identical to the ciliate AC with a high degree of conservation in the ion pore region and AC catalytic domain; some differences in the S4 transmembrane domain may indicate a difference in the range of voltage sensitivity, however. Homologous genes were identified in a range of *Plasmodium* species genome databases as well as in that of *Toxoplasma gondii* and *Cryptosporidium parvum*, however no such bifunctional ACs were spotted in other protozoa such as kinetoplastids, or in metazoan, eubacteria, archaea or plants - suggesting this protein arrangement may be unique to the Alveolata (Weber, J. H. et al, 2004). Attempts to express a resynthesized version of the *Paramecium* AC/ion-channel in heterologous systems did not result in any detectable cyclase or ion conductance activity, as did similar attempts to express the full length resynthesized PfAC α . Expression of a PfAC α catalytic domain fused to an N-terminal hexahistidine tag was successful and the results were described above (Weber, J. H. et al, 2004).

Knock-out of the PfAC α homologous gene in *P. berghei* revealed an essential role for this protein in exocytosis and hepatocyte infection by sporozoites, although the PbAC α mutants were identical to wildtype in blood stages in mice and were unimpeded in the generation of gametocytes; similarly in the mosquito, oocysts and salivary gland sporozoite numbers were the same as wildtype. (Ono, T. et al, 2008). The active invasion of a host hepatocyte is brought about by apically regulated and expressed TRAP/SSP2 proteins. The expression of the exocytosis proteins is stimulated by migration through the cytoplasm of other host cells on the way to the hepatocytes and can also be stimulated by uracil and its derived nucleotides UMP, UDP and UTP. The membrane permeable cAMP analogue 8-bromo-cAMP also induced exocytosis to a similar extent as the uracil derived compounds (UD) and UD can increase the intracellular cAMP content in

sporozoites. 8-bromo-cAMP and UD compounds incubated together with sporozoites did not result in an increased stimulation suggesting they use the same pathway to activate the expression of proteins involved in exocytosis. Interestingly, the uracil derivative induced stimulation of exocytosis protein expression was inhibited when the assays were carried out in potassium-free medium, as well as by incubation with K^+ channel inhibitors; however, 8-bromo-cAMP could stimulate exocytosis protein expression in potassium-free medium suggesting that K^+ is required upstream of cAMP activated effectors, and is consistent with the hypothesis that the AC activity of PfAC α can be regulated by an N-terminal potassium specific ion channel. Re-introduction of PbAC α into the knockout clone fully restored the phenotype to that of the wildtype with respect to infectivity and exocytosis protein expression stimulated by uracil derivatives (Ono, T. et al, 2008).

1.3 Cyclic-nucleotide signalling in protozoa: guanylyl cyclases (GC)

1.3.1 *Apicomplexans*

1.3.1.1 Role of cGMP in exflagellation

Early reports of cyclic nucleotide signalling involvement in exflagellation by the male gametocytes were somewhat equivocal. In *Plasmodium gallinaceum* the phosphodiesterase inhibitors 8-bromo-cAMP, Squibb 20009 and caffeine initiated exflagellation at pH 8.0; however, cyclic AMP analogues dibutyryl cAMP and 8-OH-cAMP did not (Martin, S. K. et al, 1978). Caffeine also stimulated exflagellation at pH 7.4, unlike the other two inhibitors (Martin, S. K. et al, 1978). In marked contrast, caffeine resulted in strongly inhibited exflagellation in *P. berghei* at both pHs (Kawamoto, F. et al, 1990). Cyclic GMP signalling was implicated when IBMX, cGMP, 8-bromo-cGMP and the guanylyl cyclase (GC) activator nitroprusside increased exflagellation in *P. berghei* and *P. falciparum* at pH 7.3 - a pH that is not normally permissive of exflagellation. Also, the GC inhibitor N-methylhydroxylamine inhibited exflagellation at the permissive pH of 8.0 (Kawamoto, F. et al, 1990).

Further evidence of a role for cGMP signalling in exflagellation came with the identification of xanthurenic acid as the gametocyte activating factor that triggered exflagellation *in vivo*. Purification of homogenates by HPLC followed by analysis of exflagellation-inducing fractions using mass spectrometry identified a molecule with a molecular weight of approximately 204, suggesting a molecular composition of $C_{10}H_7NO_4$ (Billker, O. et al, 1998; Garcia, G. E. et al, 1998). This formula is consistent with Xanthurenic acid, which displayed an identical mass spectrometry profile and induced exflagellation at concentrations in the same range as purified gametocyte activating factor. Purified membranes from gametocytes showed a markedly increased guanylyl cyclase activity compared to asexual blood stage membranes with a preference for Mg^{2+} over Mn^{2+} and that was inhibited by Ca^{2+} . Xanthurenic acid also stimulated GC activity in gametocyte membranes in a dose dependent manner, reaching a plateau of stimulation at 500 μM suggesting that the signal to exflagellate may be transduced by the cGMP signalling cascade (Muhia, D. K. et al, 2001).

1.3.1.2 Isolation and characterisation of ciliate and *Plasmodium* GCs

A guanylyl cyclase gene was identified in ciliates with sequence and topology homology to a GC found in the then unfinished *Plasmodium* genome database. Originally an attempt to identify the ciliate adenylyl cyclase gene described above, a 328 base-pair PCR product presumed to partly code for a mammalian-type AC was used to clone a guanylyl cyclase from a *Paramecium* cDNA library (Linder, J. U. et al, 1999). The gene coded for a large protein of 2412 amino acids with a calculated molecular mass of 282.6 kDa. Hydrophobicity analysis predicted five regions containing a total of 22 transmembrane domains; topology modelling predicted the protein consisted of two units: an N-terminal P-type ATPase-like region and a C-terminal with topology similar to mammalian membrane-bound adenylyl cyclases. Further analysis identified a double catalytic domain (C1a and C2a), similar to metazoan ACs, but the units appear to have switched position. Conserved motifs found in the C1a unit in mammals were found in the C2a unit in *Paramecium* and *vice versa*. All residues essential for catalytic function were conserved, with the substrate specificity residues suggesting guanylyl cyclase activity. The N-terminal P-type ATPase segment had several deviations from conserved regions in mammalian homologues, suggesting the function of the region has changed in *Paramecium* (Linder, J. U. et al, 1999).

The *Paramecium* GC was resynthesized according to mammalian codon bias and expressed in HEK293 cells, showing GC activity in the membrane fraction of cell lysates. Expression in Sf9 cells gave similar results with a K_m for MgGTP of 32 μM and specificity for GTP over ATP; however, some AC activity was observed in the presence of Mn^{2+} . Expression in the Sf9 cells resulted in proteolytic cleavage of the protein in the region linking the cyclase to the ATPase unit, suggesting that GC activity is not dependent on the presence of the ATPase-like section. Interestingly, expression of catalytic domain chimeras of *Paramecium* C1a and C2a subunits with bovine type VII AC showed that GC activity is preserved irrespective of the order of the catalytic subunits (Linder, J. U. et al, 1999).

Two guanylyl cyclase genes were identified, isolated and analysed from *Plasmodium falciparum* and termed PfGCa and PfGCB (Carucci, D. J. et al, 2000). They both coded for large, apparently bifunctional proteins homologous to those of the ciliates *Paramecium* and *Tetrahymena* with RT-PCR showing that

PfGC α was had one contiguous, intron-free open reading frame. PfGC β , however had 12 introns - all confined to the N-terminal region, which has homology with P-type ATPase. The N-terminal domain showed most sequence similarity with a Ca²⁺ ion pump, indicating that calcium may regulate cGMP production. The cyclase catalytic domain is well conserved between genes and across the Alveolata, with both displaying the switched catalytic subunits of *Paramecium* and *Tetrahymena*. Interestingly, PfGC α has an amino acid insert in the catalytic domain in the same relative position as the Δ -subdomain of trypanosomatid ACs (see section 1.2.1.3); PfGC β does not, possibly inferring some degree of differential regulation. Northern blot analysis of RNA from blood stages showed that both genes appear to be specific for the sexual stages. Immunoelectron microscopy localised PfGC α to either the parasitophorous vacuole or the plasma membrane of the gametocyte; extracellular gametes did not appear to show any reactivity to the specific antibodies (Carucci, D. J. et al, 2000).

Resynthesis and expression of the catalytic domains fused with a hexahistidine tag on the N-terminal in *E. coli* allowed limited characterisation of the *Plasmodium* guanylyl cyclases (Carucci, D. J. et al, 2000). No AC activity was found with either Mn²⁺ or Mg²⁺ but PfGC α showed no GC activity either. PfGC β catalytic domains did show GC activity when assayed as individual domains, which was greatly increased when assayed in combination and entirely dependent on the presence of Mn²⁺.

Recently the homologous gene to PfGC β was identified and knocked out in *Plasmodium berghei* (PbGC β). Sequence analysis and RT-PCR indicated PbGC β had 7 introns with the fully spliced transcript encoding a 2952 amino acid protein with a molecular weight of approximately 348 kDA. Topologically PbGC β and PfGC β are identical having 22 transmembrane domains and a P-type ATPase-like region at the N-terminal linked to a C1a, C2a catalytic domain at the C-terminal. Both genes share 68% identity and 82% similarity in the ATPase-like region and 84% and 89% identity and similarity respectively in the C1a, C2a cyclase domain. The PbGC β gene was disrupted by a double crossover with *T. gondii* DHFR/TS replacing the C1 and C2 domains. 3 knockout clones were obtained which showed normal development in mice and normal exflagellation and zygote to ookinete transformation after fertilisation *in vitro*. In mosquitoes,

however no oocysts could be found indicating an essential role for PbGCB in the insect vector stage of the parasite's life cycle (Hirai, M. et al, 2006).

Further investigation using confocal microscopy showed that the number of knockout ookinetes in the midgut of mosquitoes was approximately the same as for the wildtype indicating that *in vivo* the mutants can correctly differentiate to that stage. However, while the knockout mutants could cross the peritrophic matrix of the midgut, invasion of the epithelial cells appeared to be severely inhibited. Horizontal motility of the ookinetes is also inhibited with the wildtype moving at a velocity of $5.7 \pm 1.4 \mu\text{m}/\text{min}$ and the knockout moving much slower at $0.6 \pm 0.1 \mu\text{m}/\text{min}$ (Hirai, M. et al, 2006). *In vitro* the PbGCB knockout parasites could form oocysts and transform into infective sporozoites indicating that the GC is not involved in further development. It thus seems likely that disruption of PbGCB and the resultant inability to penetrate the epithelial cell layer of the mosquito midgut may be directly attributable to the parasite's severely reduced motility, ultimately leading to an inability to complete its life cycle.

1.4 Cyclic-nucleotide signalling in protozoa: phosphodiesterase (PDE) enzymes

1.4.1 Kinetoplastids

The first phosphodiesterase activity identified in kinetoplastids was observed in *Trypanosoma brucei gambiense* (Walter, R. D., 1974), and was subsequently discovered in *T. b. brucei*, *Trypanosoma cruzi* and *Leishmania* species (Walter, R. D. and Opperdoes, F. R., 1982; Goncalves, M. F. et al, 1980; Al-Chalabi, K. A. K. et al, 1989). Attempts to purify the PDE activity from cell lysates showed that the vast majority of cAMP-PDE was contained in the soluble fraction of *T. cruzi* and *T. brucei* and *L. mexicana* (Goncalves, M. F. et al, 1980; Walter, R. D. and Opperdoes, F. R., 1982; Rascon, A. et al, 2000) and both cAMP and cGMP hydrolysing PDE activity was found in the soluble fraction of *L. tropica* (Al-Chalabi, K. A. K. et al, 1989).

The *T. cruzi* cAMP-PDE activity from lysed epimastigote forms was active in the presence of divalent cations, showing a preference for Mn^{2+} , giving a K_m of 40 μM for cAMP; the PDE activity was not inhibited by theophylline or caffeine (Goncalves, M. F. et al, 1985). Later investigators, however, found two distinct peaks of activity after further purification of NaCl-gradient DEAE-cellulose column eluent by brain calmodulin-Sepharose affinity chromatography. The purified PDE was activated by Ca^{2+} /calmodulin and displayed a dual affinity profile with K_m values of 2.5 μM and 100 μM in the presence of 5 mM Mg^{2+} (Tellez-Inon, M. A. et al, 1985). The calmodulin/calcium activation could be inhibited by the Ca^{2+} chelator EGTA and also by the calmodulin antagonists chlorpromazine, fluphenazine and compound 48/80 (Tellez-Inon, M. A. et al, 1985).

The *Leishmania tropica* PDE activity from promastigote cell lysates also separated into two peaks of activity after column fractionation and required Mg^{2+} to function optimally but was independent of Ca^{2+} (Al-Chalabi, K. A. K. et al, 1989). The K_m values for cAMP for both peaks were reported as being very high: 1.43 mM and 4.1 mM respectively and both peaks were capable of utilising cGMP as well as cAMP with the second peak displaying a slight preference for cGMP and the first a small preference for cAMP. The methylxanthines

theophylline and caffeine appeared to be better inhibitors of leishmanial PDEs than of *T. cruzi* PDEs, showing similar effects as on mammalian PDEs.

Similar studies of the PDE activity of promastigote studies of *L. mexicana* identified and characterised different activities in cytosolic and purified plasma membrane fractions (Rascon, A. et al, 2000). The majority of the activity (~95%), like that found in *T. cruzi*, *T. brucei* and *L. tropica*, was cytosolic; however the remainder found in the plasma membranes was purified and enough protein was produced to characterise its hydrolyzing properties. Both PDE activities were cAMP specific with cGMP unable to stimulate or inhibit cAMP hydrolysis up to 1 mM; the K_m for cAMP for the soluble activity was 200 μM while that of the particulate fraction was considerably higher at 700 μM . The sensitivities to PDE inhibitors were also divergent with the soluble fraction having an IC_{50} for PDE inhibition by theophylline, caffeine and zaprinast of 30 mM, >50 mM and 2.8 mM respectively compared to the IC_{50} values for the particulate fraction of 3 mM (theophylline), 19 mM (caffeine) and 0.04 mM (zaprinast). The most potent inhibitor of both fractions, cibacron blue ($\text{IC}_{50} = 8 \mu\text{M}$ and 20 μM for soluble and particulate fractions, respectively), along with the pyridazine fragment of the methylxanthines, was used as the structural basis for the creation of a series of analogues which, unfortunately, were no more potent (Dal Piaz, V. et al, 2002). Further characterisation of the soluble fraction's PDE activity showed increased cAMP hydrolysis in the presence of Mn^{2+} or Mg^{2+} , with a slight preference for magnesium with no stimulation by calmodulin/ Ca^{2+} (Rascon, A. et al, 2000).

The utilization of molecular techniques combined with the recent releases of the genome databases of a range of kinetoplastids resulted in a major spur in cyclic nucleotide signalling research. Many phosphodiesterase genes were identified, cloned, sequenced, recombinantly expressed and biochemically characterised, in a relatively short space of time by multiple laboratories and collaborations. Unfortunately each group adopted a different naming convention for the publication of their identified enzyme resulting in a confusion of species abbreviations, numbers and letters threatening to slow and obfuscate scientific discourse on the subject. To rectify this, a unified nomenclature was published (Kunz, S. et al, 2006) laying down a straight-forward naming convention based on grouping phosphodiesterases by gene sequence homology and biochemical characteristics. Four families of class I phosphodiesterases have been identified

in kinetoplastids (PDEA-D), all of which are present as homologues in the genome databases of *Trypanosoma brucei*, *T. cruzi* and *Leishmania*.

1.4.1.1 Kinetoplastid PDEA

In *Trypanosoma brucei*, PDEA was identified by complementation screening of a cDNA library in a yeast mutant deficient in phosphodiesterase enzymes and sensitive to heat shock. A single plasmid clone was isolated containing the majority of the open reading frame representing TbrPDEA (formerly termed TbPDE1) (Kunz, S. et al, 2004). The full sequence was later determined, predicting a 620 amino acid protein and a molecular mass of approximately 70,000. The gene is located on chromosome 10 and is a single copy, but allelic polymorphism was uncovered by restriction enzyme digestion with *Bam*HI. Sequence analysis indicated that the catalytic domain was well conserved between TbrPDEA and human PDEs, sharing approximately 30 - 40% identity with the eleven class I PDEs in humans and conserving the key signature motif of all class I PDEs His-Asp-[Leu/Ile/Val/Met/Phe/Tyr]-X-His-X-[Ala/Gly]-X-X-Asn-X-[Leu/Ile/Val/Met/Phe/Tyr]. The almost complete absence of sequence identity in the N-terminal region outside the catalytic domain confirms TbrPDEA as being in a distinct family of class I PDEs separate from all other PDE families identified (Kunz, S. et al, 2004).

Homologues of TbrPDEA have also been identified and characterised in *Leishmania major* and *T. cruzi*, having similar sequence characteristics (Johner, A. et al, 2006; Alonso, G. D. et al, 2007). Screening of the *L. major* genome database identified LmjPDEA, which is found on chromosome 18 and is also a single copy gene. The gene sequence predicts a protein of 631 amino acids and has the class I PDE signature motif conserved in the catalytic domain (Johner, A. et al, 2006). TcrPDEA was also identified by genome database mining and has 48.2% amino acid sequence identity with TbrPDEA, being a single copy gene coding a protein of 619 amino acids and containing the class I PDE signature motif (Alonso, G. D. et al, 2007).

Northern blots and RT-PCR identified expression of TbrPDEA mRNA in the slender and stumpy forms of bloodstream trypanosomes isolated from infected rats, as well as in procyclic forms cultured *in vitro*. Expression of the full length gene, and an N-terminally truncated form, complemented heat-shock sensitive S.

cerevisiae mutants lacking endogenous PDEs, confirming TbrPDEA is capable of phosphodiesterase activity. In spite of restoring the wild type phenotype in the yeast strain no significant PDE activity was measurable from cell lysates with either TbrPDEA construct. A similar lack of PDE activity in cell lysates was also observed after complementation of yeast PDE mutants with LmjPDEA and TcrPDEA suggesting a common feature of the gene which results in low expression in yeast (Johner, A. et al, 2006; Alonso, G. D. et al, 2007). However, expression of the N-terminally truncated form of TbrPDEA in the bacteria *E. coli* did produce an active enzyme in lysates, although the presence of Mg^{2+} in the purification steps was essential in maintaining conformational stability as well as enzyme activity (Kunz, S. et al, 2004).

As inferred from the purification requirements, divalent cations are necessary for optimal activity of TbrPDEA, with a preference for Mn^{2+} over magnesium shown in the kinetic assays. The K_m for cAMP in the presence of 10 mM Mg^{2+} was surprisingly high at over 600 μM ; a 100-fold excess of cGMP did not inhibit or stimulate cAMP hydrolysis designating TbrPDEA cAMP specific (Kunz, S. et al, 2004). Most class I PDEs characterised from other organisms have a much lower K_m , usually below 50 μM . However, expression of the full length TcrPDEA in *E. coli* confirmed the lower than usual affinity for cAMP in *Trypanosoma* PDEAs: TcrPDEA required a divalent cation for activity and had a K_m of around 200 μM for cAMP in the presence of 10 mM Mg^{2+} which was neither inhibited nor stimulated by cGMP (Alonso, G. D. et al, 2007). Interestingly calmodulin/ Ca^{2+} did not affect enzyme activity either indicating that TcrPDEA is not responsible for the calmodulin/ Ca^{2+} -dependent PDE activity described earlier (Tellez-Inon, M. A. et al, 1985). The two recombinant *Trypanosoma* PDEA enzymes diverge with respect to inhibitor sensitivities, as the N-terminal truncated TbrPDEA is inhibited by sildenafil, trequinsin, ethaverine, dipyridamole and papverine with IC_{50} values below 30 μM . The full length TcrPDEA, on the other hand, was insensitive to any inhibitor up to 100 μM , although sildenafil, the most potent inhibitor of TbrPDEA ($IC_{50} = 1 \mu M$), was not tested. Theophylline and IBMX did not inhibit either recombinant protein (Kunz, S. et al, 2004; Alonso, G. D. et al, 2007).

A double knock out of PDEA by sequentially replacing both alleles in *Trypanosoma brucei* with phleomycin and neomycin resistance markers

demonstrated that the gene was non-essential for *in vitro* differentiation of bloodstream forms to procyclics or for procyclic infestation of the tsetse fly midgut (Gong, K. W. et al, 2001). Total PDE activity was reduced by approximately 20 - 30% in the mutant procyclic and bloodstream forms compared to wild type, which was restored almost exactly to wild-type levels by the ectopic expression of TbrPDEA from the procyclin locus. The resultant effect of the TbrPDEA knockout on the steady state level of intracellular cAMP was to increase it by approximately one third but morphology and motility of the knock out mutants were indistinguishable from the wild type. However, the procyclic generation time was increased by around 2.5 hours. No change was observed in a heterozygous knock out retaining one copy of the TbrPDEA gene or in the bloodstream form generation time. (Gong, K. W. et al, 2001).

In *Leishmania donovani* promastigotes, overexpression of PDEA produced a 3 - 3.5 fold increase in LdPDEA mRNA and protein levels. The resultant reduction in intracellular cAMP concentration was concomitant with a reduction in the level of upregulation of genes coding for oxidative stress-protection proteins that is associated with the differentiation to amastigote form upon entering the macrophage (Bhattacharya, A. et al, 2008). What is not clear is whether the overexpression of any other *L. donovani* PDE would have had the same effect or if it is solely limited to that of PDEA. Curiously, the inhibition of upregulation of the genes after temperature and pH shift is entirely reversed on addition of 20 μ M IBMX to the overexpressing promastigotes. This is surprising considering IBMX does not inhibit recombinant *T. cruzi* or *T. brucei* PDEA up to 1 mM (Kunz, S. et al, 2004; Alonso, G. D. et al, 2007), suggesting that the effects of PDEA overexpression were compensated by the inhibition of an IBMX-sensitive PDE, increasing overall cAMP content.

1.4.1.2 PDEB

Old name	New name	GeneDB assignment
PDE1	PDEA	Tb10.389.0510
PDE2A	none	Not in genome
PDE2B	PDEB2	Tb09.160.3630
PDE2C	PDEB1	Tb09.160.3590
PDEC	PDEC	Tb927.3.3070
PDED	PDED	Tb927.3.3340

Table 1.2: *Trypanosoma brucei* phosphodiesterase revised nomenclature

Basic gene features and enzyme characterisation

The PDEB family contains two tandemly arranged genes, termed PDEB1 and PDEB2 (previously TbPDE2C and TbPDE2B, see Table 1.2). Both phosphodiesterase enzymes were first cloned and sequenced from *T. brucei* and share 99.6% amino acid identity in the catalytic core region (Zoraghi, R. and Seebeck, T., 2002; Rascon, A. et al, 2002). The open reading frames predict proteins of 930 amino acids in length and contain the class I PDE signature motif in the catalytic domains. Highly homologous genes were identified in *T. cruzi* with TcrPDEB1 being 918 amino acids in length (Diaz-Benjumea, R. et al, 2006) and TcrPDEB2 (previously termed TcPDE1) having 929 amino acids (D'Angelo, M. A. et al, 2004); the catalytic domains share 90 and 88% amino acid identity with *T. brucei* PDEB1 and PDEB2, respectively, and even higher identity within the N-terminal region, each displaying 93% identity (Diaz-Benjumea, R. et al, 2006). Similar homology is evident in the *Leishmania major* PDEB1 and LmjPDEB2 proteins, being 940 and 930 amino acid polypeptides (82% identical on amino acid sequence), respectively, and also presenting the canonical class I PDE motif. Interestingly, when the catalytic domains of LmjPDEB1 and LmjPDEB2 were compared, a small stretch of 24 divergent amino acids was observed in the almost perfectly conserved remainder. The position of this non-conserved region, spanning predicted helices 12 and 13, is the same as a similar divergent sequence in *T. brucei* and *T. cruzi* (Johner, A. et al, 2006). The functional significance of this hypervariable patch in the middle of the highly conserved catalytic domain is unclear and the authors speculate that this stretch might confer specific regulational or functional differences in the isoenzymes (Johner, A. et al, 2006).

Full length protein expression of TbrPDEB1 in the phosphodiesterase knockout *S. cerevisiae* mutant resulted in complementation of the heat shock phenotype. In contrast to PDEA, PDEB1 activity was readily recovered from cell lysates and kinetic characterisation revealed the recombinant enzyme was cAMP specific with a K_m of $\sim 8 \mu\text{M}$; cGMP did not compete with cAMP as substrate nor did it stimulate enzyme activity (Zoraghi, R. and Seebeck, T., 2002). Similar heat shock complementation and kinetic activity was observed for the *L. major*

homologue, which was cAMP-specific and yielded a K_m value of $\sim 1 \mu\text{M}$ (Johner, A. et al, 2006). TcrPDEB1 was expressed in HEK-293 cells, and parameters similar to TbrPDEB1 were measured from the lysates: specificity for cAMP with a K_m of $\sim 11 \mu\text{M}$ and neither inhibited or stimulated by cGMP (Diaz-Benjumea, R. et al, 2006).

In view of the sequence similarity of PDEB1 with PDEB2, it is not surprising that the kinetic parameters of expressed PDEB2 proteins are very similar to those of the PDEB1s. TbrPDEB2 complements heat shock sensitive yeast, is cAMP specific with a K_m of $\sim 2.5 \mu\text{M}$, and is neither inhibited nor stimulated by cGMP (Rascon, A. et al, 2002). Likewise, TcrPDEB2 is cAMP specific with a K_m of $\sim 7 \mu\text{M}$ (D'Angelo, M. A. et al, 2004), as is LmjPDEB2, also with a K_m of $\sim 7 \mu\text{M}$ (Johner, A. et al, 2006).

The inhibitor profiles for both PDEB1 and PDEB2 are also similar across the kinetoplastid species. TbrPDEB1 was inhibited by trequinsin and dipyridamole with IC_{50} values of 13.3 and 14.6 μM respectively, and also by ethaverine, etazolate and sildenafil ($IC_{50} = 26.8, 30.6$ and $42.2 \mu\text{M}$ respectively); whereas the non-specific PDE inhibitor IBMX displayed an IC_{50} in the milli-molar range (Zoraghi, R. and Seebeck, T., 2002). Of the compounds tested against TcrPDEB1 only dipyridamole had an inhibitory effect ($IC_{50} = 11.3 \mu\text{M}$) with IBMX ineffective up to 300 μM (Diaz-Benjumea, R. et al, 2006). This is in good agreement with the values for TcrPDEB2 which is also inhibited by dipyridamole with an IC_{50} of 17 μM (D'Angelo, M. A. et al, 2004). Both LmjPDEB1 and LmjPDEB2 are inhibited more than 50% by 100 μM etazolate, trequinsin and dipyridamole, with the latter being the most effective; again IBMX does not inhibit (Johner, A. et al, 2006). There appears to be some divergence between TbrPDEB1 and TbrPDEB2 with respect to inhibitor profile as sildenafil and etazolate inhibited TbrPDEB2 with IC_{50} values greater than 100 μM and dipyridamole displayed an IC_{50} of 27 μM - approximately 2-fold that of TbrPDEB1; IBMX, however, remained non-inhibitory (Rascon, A. et al, 2002).

Effects of RNA-interference of the PDEB family

RNA-interference of the TbrPDEB family demonstrated that these enzymes are essential in bloodstream form trypanosomes. Initial attempts to generate bloodstream form RNAi inducible mutants resulted in trypanosomes that survived

antibiotic selection but only lived for approximately 3 weeks (Zoraghi, R. and Seebeck, T., 2002). Under light microscopy the cells were oddly shaped and multinucleated before they died. Expression of the RNAi constructs in procyclic trypanosomes resulted in a lower proportion of similarly misshapen, multi-nucleated cells. Induction of the RNAi construct against TbrPDEB1 or TbrPDEB2 resulted in a strong and specific reduction in mRNA levels for each gene, with a construct designed to target all TbrPDEB genes showing a complete loss of PDEB mRNA. The PDE activity was lowered upon induction of interference against the individual genes with a cumulative reduction of activity displayed on induction of the pan-TbrPDEB construct. The intracellular cAMP concentrations in procyclic cells were unaffected, however, by induction against TbrPDEB2 or against TbrPDEA. In contrast, cAMP levels were increased in the TbrPDEB1 RNAi mutants even without induction - with a 15-fold increase after induction compared to wild type control cells. Global induction against the TbrPDEB genes even resulted in a greater than 30-fold increase in intracellular cAMP, which was not lethal to the procyclic trypanosomes (Zoraghi, R. and Seebeck, T., 2002). One of the clear conclusions from this study is that bloodstream forms are highly sensitive to increased levels of cAMP, whereas the insect forms are relatively resistant to the cyclic nucleotide. A further indication for this is the much higher sensitivity of bloodstream forms to membrane permeable cAMP analogues (Oberholzer, M. et al, 2007).

The inability to produce stable bloodstream form trypanosomes transfected with RNAi constructs against either PDEB1 or PDEB2 or both was ascribed to the vector used being slightly 'leaky', in that it may have produced some RNA interference without induction by the addition of tetracycline. This low level interference seems to have been sufficient to result in the lethal phenotype in bloodstream forms described above. In a follow-up study a different vector was used that maintained a much tighter control of the induction of RNA interference (Oberholzer, M. et al, 2007). As in the Zoraghi and Seebeck paper, RNAi against TbrPDEB1, TbrPDEB2 or both, had no effect on the survival or proliferation of procyclic *T. b. brucei*. Northern blot analyses showed that the constructs in both procyclic and bloodstream forms were effective at reducing target mRNA levels, and also that the knockdown of either TbrPDEB1 or TbrPDEB2 does not result in the upregulation of the other PDEs to compensate (Oberholzer, M. et al, 2007). Induction of interference against both TbrPDEB1

and TbrPDEB2 in bloodstream forms also resulted in strong reduction of both genes' mRNA and no compensatory upregulation of genes from the other trypanosomal PDE families (PDEA, PDEC and PDED). The effect on the phenotype of the bloodstream forms is emphatic, with the double-RNAi construct resulting in the cells rounding up and becoming multinuclear, multikineto-plastic and multiflagellar; RNAi against TbrPDEB1 and TbrPDEB2 individually had no apparent phenotypic effect. The ratio of the multiple nuclei to kinetoplasts in the double-RNAi induced cells was maintained at one, suggesting that DNA replication and segregation occur as normal, but that separation of the mother and daughter cells is blocked, apparently as a result of a cytokinesis defect. Normal proliferation of the bloodstream forms was completely disrupted, resulting in eventual cell death approximately 50 hours after double-RNAi induction. The effect on intracellular cAMP mirrored that of the morphological phenotype in that RNAi against the individual TbrPDEB genes did not result in a change in cAMP level in comparison to the control, but induction of the construct against both genes produced an approximately 100-fold increase in cAMP in the bloodstream forms. In procyclics the double induction only resulted in an approximately 10-fold increase in intracellular cAMP (Oberholzer, M. et al, 2007). It would thus seem that bloodstream form trypanosomes can compensate for (most of) the loss of either PDEB activity but not for the loss of both simultaneously.

Further investigation into the effects of inducing RNAi against PDEB genes in infected mice elegantly highlighted the essential nature of these proteins *in vivo*. Mice were infected with bloodstream form trypanosomes transfected with TbrPDEB1, TbrPDEB2 or the double-RNAi construct; all strains had a similar virulence without antibiotic RNAi induction, producing high parasitaemias after 3 - 4 days post inoculation. Mice pre-treated with doxycycline in the drinking water for 2 - 3 days before and during the course of infection had similar parasitaemia levels when infected with the individual-gene RNAi-induced trypanosomes as the parental NYSM wild type control strain. In contrast those mice pre-treated with doxycycline and infected with the generic PDEB-RNAi transfected trypanosomes had no sign of parasitaemia for the entire duration of the experiment (35 days). The same effect was seen when the mice were immunocompromised with either cyclophosphamide or rolipram before infection ruling out the necessity for an intact immune system to clear the trypanosomes

with the double-RNAi construct. Induction of the double RNA interference after infection had reached a moderate level of parasitaemia also allowed the mice to overcome the initial wave of parasitaemia. The mice eventually relapsed, although analysis of trypanosomes extracted from the relapsed mice showed they no longer responded to RNAi induction, possibly due to spontaneous mutation (Oberholzer, M. et al, 2007). This study, in conjunction with the earlier RNAi experiments, clearly show that TbrPDEB1 and TbrPDEB2 together are absolutely essential for the proliferation of bloodstream form trypanosomes, *in vitro* and *in vivo*, and that inhibition of both proteins results in cell death, validating the genes as excellent drug targets for future chemotherapies.

GAF domains of PDEB

The N-terminal region of PDEB1 and PDEB2, of all species in which they have been sequenced, contain two regions known as GAF domains. These domains, named after the first proteins in which they were identified - cGMP-specific and binding phosphodiesterases, adenylyl cyclase of *Anabaena* and FhlA of *E. coli*, have been shown to function as regulatory, small ligand-binding entities and in mammalian PDEs 2, 5 and 6 binds cGMP to modulate enzyme activity (Aravind, L. and Ponting, C. P., 1997). Since the characterisation of the recombinantly expressed PDEB1 and PDEB2 proteins ruled out modulation by cGMP the properties of the two GAF domains (GAF-A and GAF-B) were investigated further. Full length TbrPDEB2 and the N-terminally truncated TbrPDEB2 catalytic domain were expressed with a C-terminal epitope tag, allowing immunoprecipitation. A filter-binding assay with radio-labelled cAMP was then conducted on the two proteins in the presence of > 5 mM EDTA, which inactivates the nucleotide hydrolysis capabilities of the proteins by chelating the divalent cations essential for substrate binding and enzyme function. The [³H]-cAMP bound only to the full length TbrPDEB2 protein and not to the catalytic domain protein (or control cell lysates) indicating that the two GAF domains present in the full length enzyme and not just the catalytic domain, bind cAMP (Laxman, S. et al, 2005). To verify this, the N-terminal section of TbrPDEB2 up to the end of the GAF-A domain was expressed and immunoprecipitated with [³H]-cAMP, clearly demonstrating binding of the nucleotide. Affinity purification and assaying with labelled and unlabelled cAMP in a competition binding assay showed that cAMP bound to GAF-A with an IC₅₀ of ~17 nM. Binding of cGMP was also observed but with a 15-fold

higher IC_{50} of ~ 290 nM; subsequent competition binding assays with the full length enzyme under non-catalytic conditions gave an IC_{50} for cAMP of ~ 60 nM, whereas for cGMP the IC_{50} had increased to ~ 12 μ M indicating that the full length enzyme can discriminate between nucleotides even more efficiently than the GAF domains alone (Laxman, S. et al, 2005). Introduction of a point mutation in a conserved residue in GAF-A that was thought to be critical for ligand binding by homology modelling with the crystal structure of murine PDE2A GAF-B, resulted in a total loss of cAMP binding by TbrPDEB2 in the presence of EDTA, and also a four fold increase in the K_m of the enzyme under normal PDE assay conditions. Not only does this indicate that the second GAF domain, GAF-B, does not bind cAMP as a point mutation in GAF-A completely abolishes cAMP binding of the whole enzyme in the presence of EDTA, but also that GAF-A can modulate the activity of the catalytic domain by binding cAMP resulting in more hydrolysis at lower concentrations of cAMP (Laxman, S. et al, 2005).

Similar binding of cyclic nucleotides was also observed by the GAF-A domains of TcrPDEB1 and TcrPDEB2, albeit with lower affinities. The N-terminal region, including the GAF-A domain, of both genes were expressed in *E. coli* and purified and competitive binding assays carried out. TcrPDEB2 GAF-A had a binding affinity of ~ 190 nM for cAMP. No binding of labelled cAMP could be detected with this method for TcrPDEB1 GAF-A. However, a calorimetric binding method assigned TcrPDEB1 GAF-A a binding affinity of ~ 1 μ M and TcrPDEB2 GAF-A an affinity of ~ 0.5 μ M. cGMP binding was also observed for TcrPDEB2 GAF-A, again with a much lower affinity than for cAMP (~ 2.5 μ M); no cGMP binding could be measured with TcrPDEB1 GAF-A, however (Diaz-Benjumea, R. et al, 2006).

Gene expression profiles and cellular localisation

The mRNA of PDEB1 and PDEB2 appear to be expressed in both mammalian and insect host forms, as determined by RT-PCR and Northern blots in *Leishmania major* and *T. brucei*, and by Western blots of whole cell lysates from epimastigotes and trypomastigote forms in *T. cruzi* (Johner, A. et al, 2006; Zoraghi, R. and Seebeck, S., 2002; Oberholzer, M. et al, 2007; Diaz-Benjumea, R. et al, 2006). Subcellular localization experiments were first conducted in *T. cruzi*: successive centrifugation fractions from whole cell epimastigotes lysates followed by Western blot analysis showed TcrPDEB2 had the same fraction

distribution as paraflagellar rod protein from the flagellum (D'Angelo, M. A. et al, 2004). Confirmation of the flagellar localization of PDEB1 and PDEB2 in *T. cruzi* came from immunofluorescent microscopy. The protein remained associated with the flagellum after treatment with Triton X-100 to remove cytoplasmic enzymes and NP-40 to prepare a cytoskeleton preparation, consistent with TcrPDEBs being integral membrane proteins of the flagellum or paraflagellar rod (D'Angelo, M. A. et al, 2004).

Similar results were also observed in *T. brucei* where one allele of TbrPDEB1 and TbrPDEB2 was tagged with a triple HA tag and a triple c-Myc tag, respectively. Immunofluorescence microscopy of TbrPDEB1 in procyclics showed the protein was localized along the flagellum but only where the flagellum had exited the cell body. TbrPDEB2 had a minor fraction co-localized with TbrPDEB1, however the majority was distributed throughout the cytoplasm. Extraction with Triton X-100 failed to release TbrPDEB1 and the flagellar associated TbrPDEB2, whereas the cytoplasmic TbrPDEB2 was easily removed. RNA-interference of PFR2, a major structural protein of the paraflagellar rod results in proteins normally associated with the structure amassing at the tip of the flagellum in a droplet shape. Tagged TbrPDEB1 accumulates in the tip of the flagellum on induction of RNAi against PFR2, as does a small portion of TbrPDEB2, clearly indicating that both are integrated into the paraflagellar rod structure. The remainder of the TbrPDEB2, however, is distributed normally in the cytoplasm showing dual localization of this isoform (Oberholzer, M. et al, 2007).

Further sequencing and restriction enzyme profile analysis identified two alleles for TbrPDEB2 in the strain used in the protein localization studies (Lister 427). TbrPDEB2b has its GAF-A domain apparently replaced by the GAF-A from TbrPDEB1, whereas TbrPDEB2a corresponds to the sequence published in the genome database. TbrPDEB2b has 26 base-pair changes, compared to TbrPDEB2a, resulting in 9 amino acid substitutions, of which seven are conservative and two non-conservative (Kunz, S. et al, 2009). This allelic variation appears to be specific to those strains derived from the Lister 427 strain; and the triple c-Myc tag used in the localization study was shown to be integrated into the B2b allele leading the authors to postulate that the dual localization of the protein may be allele specific. However, they disproved that hypothesis by showing that integration of the Myc tag into the TbrPDEB2 gene in

procyclic cells of the STIB 247 strain, which did not have a GAF-A identical to that of TbrPDEB1 as in Lister 427, resulted in an identical dual localization of the protein. A similar distribution was observed in bloodstream form BS221 strain trypanosomes, derived from Lister 427 and retaining the PDEB1 GAF-A in the PDEB2 gene allele. Both alleles were independently tagged giving the same localization for one allele as the other (Kunz, S. et al, 2009).

The crystal structure of PDEB1 catalytic domain of *L. major*

A major advance in the quest for specific inhibitors of kinetoplastid PDEB genes came with the solving of the crystal structure of the catalytic domain of *Leishmania major* PDEB1 in complex with the non-specific inhibitor IBMX (Wang, H. et al, 2007). The PDEB1 fragment forms an apparent dimer on crystallization, with the catalytic domain made up of 16 α -helices and no β -sheets. The bottom of the catalytic pocket is taken up by two divalent metal ions which were assigned, without verification, to be Zn^{2+} and Mg^{2+} and form an octahedral binding configuration similar to that found in human phosphodiesterases. A low root-mean-squared-deviation (RMSD) for the position of the C_{α} atoms of selected amino acid residues indicates similar folding of the polypeptide compared to those of human PDEs; however four regions have significant differences. Two of these are in positions that have divergent insertions or deletions in almost every class I PDE characterised to date, but the other two are in the H9 helix of the H-loop (residues 729 - 752) and in the M-loop (residues 858 - 882) (Figure 1.7), resulting in a positional shift compared to human PDEs of up to 3 Å. This is predicted to significantly alter interactions with inhibitors (Wang, H. et al, 2007), which is of obvious pharmacological interest.

The binding of IBMX with the LmjPDEB2 catalytic pocket has two elements in common with almost all PDEs: the H-bond formed between the O6 atom of the xanthine ring and the invariant glutamine (residue 887) and the π -stacking of the ring of phenylalanine residue 890 and the xanthine ring of IBMX. The xanthine ring also forms weaker van der Waals' contacts with amino acids Tyr680, Asn838, Val853 and Phe857. The isobutyl group from IBMX also interacts with Tyr680, Asn838 and Val853 as well as His681. Interestingly, IBMX only forms one H-bond, in common with human PDEs 4D, 7A and 9A, whereas hPDE3B and hPDE5A form

two; IBMX is bound by LmjPDEB1 in the same orientation as PDE3B, PDE5A and PDE9A, whereas it is rotated 180° in PDE4D and PDE7A (Wang, H. et al, 2007).

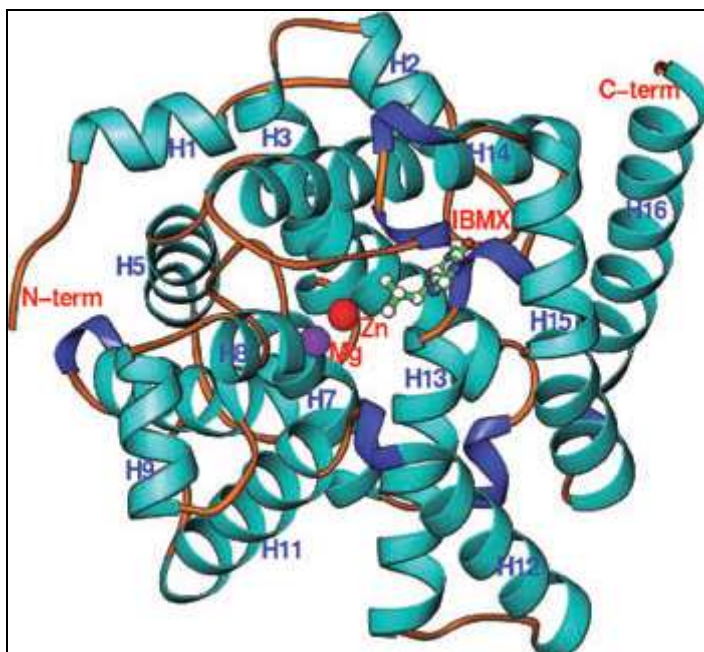


Figure 1.7: Reproduced from Wang, H. et al, 2007. The structure of LmjPDEB1 bound with IBMX

The 3-D structure of LmjPDEB1 was superimposed over those human PDEs that have solved crystal structures in order to identify aspects of the catalytic domain unique to the parasitic PDE that may be utilized in the development of chemical inhibitors specific to the parasite. Generally, the catalytic pockets are quite similar, with the metal-binding residues His685, His721, Asp722 and Asp835, inhibitor-interacting Phe890 and catalytically important His681 and His725 being well conserved. Some subtle and not so subtle differences were identified, however, with glycine (886) and the invariant glutamine (residue 887) displaying the largest positional displacement compared to representatives of all eleven human PDEs. The invariant glutamine is conserved across the class 1 PDEs and plays an essential role in substrate and inhibitor binding; large positional changes may allow structural engineering of inhibitors to capitalise on this distinctive difference and confer selectivity for that compound over human PDEs. Other residues with significant differences in their positions, which could potentially interact with inhibitors are Asn838, Val839, Ser846 and Met874.

The most unique feature of the crystal structure of LmjPDEB1, however, is the identification of a sub-pocket, within the active site, unenclosed at the bottom

and essentially forming a pore or channel through the enzyme. The pocket (dubbed the 'L-pocket' by the paper's authors) is gated by the residues Thr854, Met874 and Gly886. The latter, being conserved in four out of the five identified *Leishmania major* phosphodiesterases but found only in PDE10 of the human PDEs, can bend to accommodate any conformation due to its flexible backbone. The walls of the channel are formed by Thr854 and Tyr858 of the H14 helix and Leu883 and Gly886 of helix H15, with Asn881 of the M-loop making up the third wall. Met874 and Gly886 are separated by 7.5 Å to leave the pocket open at the active site. The L-pocket has hydrophobic as well as hydrophilic characteristics and is large enough to accommodate a structure the size of a five-membered ring (Wang, H. et al, 2007).

1.4.1.3 PDEC

The TcrPDEC gene has some unusual characteristics for a kinetoplastid phosphodiesterase enzyme. It was identified by screening the *T. cruzi* genome database, amplified from genomic DNA by PCR and sequenced for analysis (Kunz, S. et al, 2005). Two different alleles were detected with 38 amino acid residues different between them: 21 conservative substitutions and 17 non-conserved. Although six amino acid differences were located in the catalytic domain none of them were predicted to be essential for the catalytic function of the enzyme. Southern blot analysis of restriction digested genomic DNA indicate TcrPDEC is a single copy gene. The open reading frame predicts a polypeptide of 924 amino acids with the catalytic domain situated in the middle of the protein (Thr291 - Ser657), whereas all other class I PDEs contain a C-terminal catalytic domain. The catalytic core contains the canonical class I PDE signature motif, confirming its grouping, in spite of its non-conforming functional domain arrangement. Amino acids important for catalytic function are all conserved. However, one of the residues conferring substrate specificity (Asn395) is substituted for alanine which, as is the case for human PDEs 5 and 6, might allow it to hydrolyse cGMP instead of cAMP. Indeed, it was demonstrated that TcrPDEC displays dual selectivity for cAMP and cGMP in the presence of Mg^{2+} , with K_m values of $32 \pm 9 \mu M$ and $78 \pm 25 \mu M$, respectively - a unique feature for kinetoplastid PDEs characterised to date.

The N-terminal contains a FYVE-type domain (Pro10 - Gly73), along with two coiled-coil regions (Asp144 - Asp179 and Lys207 - Glu264) (Kunz, S. et al, 2005). Classical FYVE-domains bind to phosphatidylinositol-3-phosphate (PtdIns(3)P) embedded in the membrane, however, the FYVE-like domain of TcrPDEC has significant changes resulting in a decrease of the net charge of the region, making it unlikely that it binds to PtdIns(3)P. This opinion appears to be confirmed by the recombinant FYVE-domain of TcrPDEC not binding to PtdIns(3)P, or to a series of other phospholipids in a dot-spot assay (Kunz, S. et al, 2005). Investigation of the coiled-coil regions indicate they may be important to the quaternary structure of the protein. Gel filtration of recombinantly expressed TcrPDEC's FYVE domain on its own indicates it migrates as a stable dimer. When the experiment is repeated with the addition of the coiled-coil regions to the recombinantly expressed FYVE domain the polypeptide is eluted with an apparent mass of ~200 kDa (calculated mass = 30.5 kDa), indicating a higher order complex is formed (Kunz, S. et al, 2005). Expression of the full length TcrPDEC in PDE-deficient yeast mutants complemented the heat-shock phenotype; as did expression of the TcrPDEC catalytic domain with the N- and C-terminals truncated (Kunz, S. et al, 2005). Not only does this confirm that TcrPDEC is an active phosphodiesterase enzyme that can hydrolyse cAMP, but also that the FYVE domain and the coiled-coil regions are not essential for catalytic activity. The PDE inhibitors etazolate, trequinsin and dipyridamole all inhibit TcrPDEC with IC_{50} values of 0.7 μ M, 3.9 μ M and 6.9 μ M, respectively, with papaverine having an IC_{50} of 25 μ M. Interestingly IBMX inhibits TcrPDEC with an IC_{50} of 68 μ M - by a large margin the lowest value seen for any of the kinetoplastids characterised so far.

A similar characterisation of TcrPDEC independently confirmed much of the data presented in the previous study, with a few notable exceptions. TcrPDEC (named in TcPDE4 in this study) contains a FYVE-like domain, complements heat-shock sensitive yeast, prefers Mg^{2+} over Mn^{2+} , has a K_m for cAMP of ~20 μ M, is inhibited by etazolate, trequinsin and dipyridamole with IC_{50} values in the single-figure μ M range and IBMX being a much more potent inhibitor of TcrPDEC than any other kinetoplastid PDE, in agreement with Kunz et al, 2005 (Alonso, G. D., et al, 2006). The second study, however, identified rolipram as a reasonable inhibitor of TcrPDEC, with an IC_{50} of ~10 μ M, in contrast to no effect observed at up to 100 μ M in the first characterisation. Also, the recombinant TcrPDEC in yeast

lysates was localised to the membrane extracts by Western blot analysis, as well as PDE activity being characterised only in the membrane lysates (Alonso, G. D. et al, 2006); Kunz, et al, found and characterised their TcrPDEC in the soluble extract. However, the biggest difference between the two studies is in the substrate specificity; although Alonso, et al, did not directly attempt to measure cGMP hydrolysing activity directly, cGMP did not compete with cAMP as a substrate for TcrPDEC up to a concentration of 2 mM, in contrast to Kunz, et al, determining a K_m of $\sim 80 \mu\text{M}$ for cGMP. The differences highlighted here may represent the differences between the two alleles of TcrPDEC, with the data from Kunz, et al, relating to TcrPDEC-1, and that of Alonso, et al, coming from characterisation of TcrPDEC-2. That two alleles of the same gene might code for proteins with such different characteristics is curious, and further investigation is required to confirm and expand on the work carried out so far.

PDEC has also been identified in the genomes of *T. brucei* and *Leishmania major*, although apart from a cursory analysis of the predicted amino acid sequence confirming its belonging to the class I PDEs, no in-depth characterisation has yet been published. It was noted, however, that the *L. major* version, at least, had conserved the 'dual-specificity' alanine residue, indicating that in leishmania, the protein might also be able to hydrolyse cGMP (Johner, A. et al, 2007).

1.4.1.4 PDED

So far, PDED has not been cloned and recombinantly characterised from any of the kinetoplastids, although it does appear to be in the genome databases of all those kinetoplastids published. It is predicted that PDED is a single copy gene coding for a protein of approximately 700 amino acids, with its catalytic domain containing the conserved class I PDE signature motif and being C-terminally located (Kunz, S. et al, 2006; Johner, A. et al, 2007).

1.4.2 Apicomplexans

Characterisation of apicomplexan phosphodiesterase enzymes had been fairly limited in the pre-genomic era, other than to infer their modulatory presence being necessary due to the observation of adenylyl and guanylyl cyclase activity, as well as that of cyclic nucleotide specific effector-proteins protein kinase A

(PKA) and protein kinase G (PKG). However, four putative *Plasmodium falciparum* PDEs have now been identified, containing the class I signature motif and sharing approximately 40% amino acid identity (Yuasa, K. et al, 2005; Wentzinger, L. et al, 2008). A general naming convention was adopted and the four PfPDEs are now termed PfPDE α , β , γ and δ (Wentzinger, L. and Seebeck, T., 2007). All four genes are predicted to contain between four and six transmembrane domains, unique amongst the class I PDEs, suggesting that they are all integral membrane proteins (Wentzinger, L. et al, 2008).

1.4.2.1 PfPDE α

The first apicomplexan PDE to be characterised, PfPDE α , is represented by at least two splice variants, PfPDE α A and PfPDE α B. The first investigation found an open reading frame made from two exons and predicted to code for a protein of 884 amino acids (Yuasa, K. et al, 2005), whereas a second study identified the ORF as starting 210 base-pairs upstream, giving a protein of 954 amino acids (PfPDE α A) with a splice variant of 892 amino acids (PfPDE α B) (Wentzinger, L. et al, 2008). PfPDE α A is predicted to have six transmembrane domains in the N-terminal, while PfPDE α B has helices 4 and 5 removed to give four membrane-spanning domains. Although no other functional domains were identified, apart from the catalytic domain, a potential phosphorylation motif was found which could be phosphorylated by PKA, casein kinase II and/or tyrosine kinase, as well as a casein kinase II-specific motif after the last transmembrane helix and before the catalytic domain. These motifs are also present in *Plasmodium vivax*, *P. yoelii* and *P. knowlesi* homologues, indicating a possible conserved regulatory function (Wentzinger, L. et al, 2008).

Producing a recombinant version of PfPDE α proved to be difficult, with attempts at expression of full length or N-terminally truncated catalytic domains in *S. cerevisiae*, and COS cells failing. However, expression of the hexahistidine-tagged catalytic domain in *E. coli* was successful, and partially purified proteins from cells transformed with this fragment of PfPDE α showed 135-fold higher cGMP hydrolysing activity compared to the same fractions from control cells, with no cAMP hydrolytic activity observed. Divalent cations were necessary for proper catalytic function, with Mn²⁺ preferred over Mg²⁺ and Ca²⁺; a K_m of 0.65 μ M for cGMP in the presence of manganese indicates PfPDE α is a high affinity

class I PDE (Yuasa, K. et al, 2005). Similar data was recorded when the catalytic domain was resynthesized using bacterial codon preferences and N-terminally tagged with GST, giving a K_m of 2 μM for cGMP in the presence of 5 mM Mg^{2+} (Wentzinger, L. et al, 2008). The PDE inhibitor profile from both approaches at recombinant expression were also in good agreement, with zaprinast being the only compound tested with an IC_{50} below 10 μM ($\sim 3.5 \mu\text{M}$) with dipyrindamole, E4201 and sildenafil, all three human PDE5 inhibitors, having IC_{50} values of 22 μM , 46 μM and 56 μM , respectively (Yuasa, K. et al, 2005; Wentzinger, L. et al, 2008).

Further investigation into the inhibition of PfPDE α was carried out by individually mutating Asp762 and Gly788 to alanine, two residues reported to be essential for substrate binding as well as that of the inhibitor zaprinast, in bovine PDE5A. The PfPDE α D762A mutant displayed no cGMP-PDE activity, in spite of recombinant production of the protein at the same level as the un-mutated catalytic domain, suggesting Asp762 is essential for the hydrolyzing activity of the enzyme in PfPDE α . PfPDE α G788A, on the other hand, maintained its PDE activity unchanged (K_m for cGMP was 0.77 μM), and was inhibited by zaprinast with similar potency ($\text{IC}_{50} = 5.6 \mu\text{M}$). Since the glycine residue in bovine PDE5A is necessary for zaprinast binding, and no difference in inhibition by the compound is reported in the alanine-substituted mutant, this observation implies that there may be sufficient divergence in the catalytic domain of PfPDE α to allow the chemical engineering of a specific inhibitor (Yuasa, K. et al, 2005). Expression in the intraerythrocytic stages was investigated using reverse-transcriptase PCR. The abundance of PfPDE α transcripts mirrored the proportion of ring stages in the cultures, inferring stage-specific regulation of PfPDE α production (Yuasa, K. et al, 2005).

The presence of the N-terminal transmembrane domains in the *Plasmodium* PDEs is highly unusual in class I PDEs, with no other family identified so far having similar regions. In order to determine if the PDEs are located in the membranes, as predicted, cytosolic and membrane fractions were purified from mixed blood stage cultures. The vast majority of cGMP-PDE activity was localized in the membrane fraction (Yuasa, K. et al, 2005; Wentzinger, L. et al, 2008), with an identical profile for cAMP-PDE activity (Wentzinger, L. et al, 2008).

The endogenous cGMP-hydrolysing activity could be inhibited by zaprinast with an IC_{50} of $4.1 \mu\text{M}$, similar to the inhibition of the recombinant PfpPDE α catalytic fragment. Treatment of asexual blood stage *P. falciparum* *in vitro* resulted in growth inhibition of the parasite with an ED_{50} value of $\sim 35 \mu\text{M}$, implying that cGMP-PDE activity is essential for the development and proliferation of blood stage *Plasmodium* parasites (Yuasa, K. et al, 2005). Interestingly, the effects of dipyridamole on *P. falciparum* infected erythrocytes had been investigated earlier, with the compound giving an IC_{50} for growth and development arrest of just 30 nM, and also inhibiting the invasion of erythrocytes by merozoites (Akaki, M. et al, 2002). The authors of that paper appeared to have overlooked dipyridamole's PDE-inhibitory properties as they hypothesized that the mode of action of the drug was for it to bind to the erythrocyte surface, preventing the binding of the merozoite with its erythrocyte receptor. They further discussed the growth arrest of the parasites inside the host erythrocytes in terms of nucleoside and anion transport inhibition and antioxidant effects. However inhibition of PfpPDE α by dipyridamole has been demonstrated (Yuasa, K. et al, 2005), albeit with an IC_{50} value of $22 \mu\text{M}$ rather than in the mid-nanomolar range, and part of the effects described in the Akaki paper may be due to inhibition of one, or more, of the other three PfpPDEs.

As a means of further characterising the function of PfpPDE α , knock out mutants were derived by a double cross-over, replacing the PDE gene with human DHFR, which confers resistance to dihydrofolate reductase inhibitors. Two clonal lines were derived with no obvious morphological changes or disruption of the blood stage asexual cell cycle after the knock out of PfpPDE α . However, it was observed that ring stages always appeared slightly sooner after synchronisation of the culture compared with the parental strain (Wentzinger, L. et al, 2008). RT-PCR determined that the other three PfpPDEs were not upregulated to compensate for the loss of PDE activity and that PfpPDE γ and PfpPDE δ are only expressed at very low levels in blood stages. These data suggest that PfpPDE α is not an essential enzyme in blood stage *Plasmodium*, at least during *in vitro* culture, and that the other PDE that is highly expressed in intraerythrocytic stages, PfpPDE β , may be more important for controlling cyclic nucleotide levels. The effect of the knock out on overall PDE activity showed an approximately 20% reduction in cGMP hydrolysis with no effect on cAMP-PDE activity. This confirms the data from the characterisation of the recombinant catalytic domain showing cGMP

specificity, and also implies that at least one other PfPDE is capable of cGMP-PDE activity and that it is (they are) expressed at the same time. 10 μM of zaprinast reduces cGMP-PDE activity by ~50% in both the knock out and its parental strain suggesting that at least one of the remaining PDEs is not sensitive to the inhibitor and that one is. Furthermore, when cAMP was present in excess, cGMP-PDE activity was reduced by 20% in the membrane fraction of wild-type parasites compared to more than 60% in the knockout suggesting that at least one of the remaining PfPDEs is inhibitable by cAMP. When cGMP was present in excess cAMP-PDE activity was also reduced in both wild type and PfPDE α knock out strains. Taken together with the fact that PfPDE α is cGMP-specific, the above data suggests that at least one out of PfPDE β , γ , or δ is a dual substrate phosphodiesterase enzyme (Wentzinger, L. et al, 2008).

1.4.2.2 PfPDE β

The PDE β gene is located on chromosome 13 of *Plasmodium falciparum*. Sequencing of PfPDE β after PCR amplification from cDNA extracted from asynchronous blood stage culture revealed a gene of 3420 base-pairs coding for a protein of 1139 amino acids. The catalytic domain is located at the C-terminal end of the polypeptide and the N-terminal contains six transmembrane domains suggesting it is an integral membrane protein. Interestingly, Hidden Markov Modelling of the transmembrane regions predicts that PfPDE β is oriented in the membrane so that the catalytic domain is not exposed in the parasite cytosol but is actually projecting into the parasitophorous vacuole; this may allow the parasite to modulate the cyclic nucleotide milieu of the host erythrocyte. RT-PCR of total RNA extracted from blood stages, in combination with knocking out PfPDE α , indicates it is the predominantly expressed PDE in these stages. So far, recombinant expression of PfPDE β has proved unsuccessful in numerous systems and with different methodologies (Wentzinger, L. et al, 2008).

1.4.2.3 PfPDE γ

PDE γ is also found on chromosome 13 of *Plasmodium falciparum*, approximately 3000 base-pairs downstream of PfPDE β and transcribed from the opposite strand of DNA. Sequencing of PfPDE γ identified an open reading frame of 2310 base-pairs made from nine exons and coding for a protein of 769 amino acids, a slightly larger gene than published in *Plasmodium* genome database

(Wentzinger, L. et al, 2008). PfPDE γ is predicted to have six transmembrane helices, with Hidden Markov Modelling indicating a normal, i.e. cytosolic, orientation of the catalytic domain (Wentzinger, L. et al, 2008). In an investigation into gametogenesis (see below), PfPDE γ was knocked out as an experimental control. No aberrant phenotype in gametocytes was observed, with normal rounding up and exflagellation upon stimulation by xanthurenic acid, and displayed unchanged phosphodiesterase activities for cGMP and cAMP. It was concluded that this protein is not essential in gametogenesis (Taylor, C. J. et al, 2008).

1.4.2.4 PfPDE δ

PDE δ , an open reading frame of 2448 base-pairs made from six exons coding for a protein of 815 amino acids, is located on chromosome 14 of *Plasmodium falciparum*. PfPDE δ also contains six transmembrane regions in the N-terminal and, like PfPDE β , is predicted to have its C-terminal catalytic domain exposed to the parasitophorous vacuole (Wentzinger, L. et al, 2008).

Previous work had observed that cGMP-PDE inhibitor zaprinast could stimulate rounding up and exflagellation of gametocytes in the absence of xanthurenic acid, implicating the cGMP signalling pathway in male gametocyte exflagellation (McRobert, L. et al, 2008). However, knocking out guanylyl cyclase PfGCB failed to produce any significant change in gametocyte phenotype, leading to the hypothesis that cGMP degradation rather than production was critical in gametogenesis. Because of the high level of PfPDE δ mRNA expression, compared to the other PfPDEs, in developing and mature gametocytes, PfPDE δ knock outs were generated in order to investigate the involvement of cGMP metabolism further (Taylor, C. J. et al, 2008). Analysis of the particulate fractions of lysed stage V gametocytes showed an approximately 50% reduction in cGMP-PDE activity compared to wild type, indicating PfPDE δ does hydrolyse cGMP and also that at least one other cGMP-PDE is expressed in this parasite stage. Zaprinast reduced the wild type PDE activity by approximately 75%, whereas in the knock out parasites the activity was removed completely, indicating PfPDE δ is at least partly resistant to the inhibitor and also that the residual PDE activity is made up of zaprinast-sensitive enzymes, possibly PfPDE α (Taylor, C. J. et al, 2008).

Phenotypically, the PfPDE δ mutants generated normal gametocytes. However, their ability to round up and exflagellate on stimulation by xanthurenic acid was significantly reduced. A similar effect was observed on treatment with zaprinast. On examination of the ability of the gametocytes to emerge from infected erythrocytes, less than 20% of the PfPDE δ mutants emerged after stimulation with XA compared to nearly 60% emergence by the control strain, as measured by reactivity to a Band 3 antibody. This indicates that PfPDE δ is important for both male and female gametogenesis (Taylor, C. J. et al, 2008). The authors of this study propose that xanthurenic acid stimulates guanylyl cyclase activity, thereby increasing the cGMP level which, in turn, activates PKG to trigger gametogenesis. PfPDE δ , in conjunction with other minor PDEs in this stage, degrade the cGMP signal allowing further gametocyte development, eventually resulting in full gametogenesis. A sustained increase in cGMP, for example by inhibiting PfPDE δ , retards development once gametogenesis has been initiated (Taylor, C. J. et al, 2008). A specific PfPDE δ inhibitor would have the effect of blocking transmission of *Plasmodium* to the insect vector.

1.5 Cyclic-nucleotide signalling in protozoa: protein kinases (PK)

1.5.1 Kinetoplastid PKA

1.5.1.1 *Trypanosoma brucei*

Cyclic AMP-dependent protein kinase (PKA) activity has been associated with a number of processes in *Trypanosoma brucei*, but mostly by inference from the presence of adenylyl cyclases and cAMP-specific phosphodiesterases in the parasites, as well as by analogy with mammalian systems which use PKA as the main cAMP signalling effector protein. One such study implicates PKA in inhibition of disaggregation of *T. brucei* from anti-VSG antibodies in the mammalian bloodstream (O'Beirne, C. et al, 1998). Incubation of bloodstream forms with anti-VSG antibodies results in the cells clumping together; these clumps quickly disaggregate in an energy dependent fashion which does not result in the release of VSG nor damages the viability of the parasite. This disaggregation can be inhibited by the addition of extracellular cGMP or cAMP and its membrane-permeable analogues, and also by 5 mM of the PDE inhibitor theophylline and several protein kinase inhibitors. The authors concluded that an increase in intracellular cAMP concentration activates a cAMP-dependent protein kinase that inhibits the disaggregation process (O'Beirne, C. et al, 1998).

The first actual measurement of cyclic nucleotide-dependent protein kinase activity in *Trypanosoma brucei* came with the identification and sequencing of a trypanosomal PKA regulatory subunit. In mammals the PKA holoenzyme is found in an inactive state, with two catalytic subunits (PKA-C) bound in a heterotetramer to two regulatory subunits (PKA-R). When cAMP binds to the regulatory subunits, a conformational change activates the phosphorylating catalytic domain by releasing the PKA-C subunit from the holoenzyme. In *T. brucei*, a fragment of protein with high homology to eukaryotic regulatory subunits of PKA was identified by searching the draft genome database for proteins containing putative cAMP-binding domains (Shalaby, T. et al, 2001). PCR amplification of the sequence allowed screening of genomic and procyclic cDNA libraries, which uncovered the entire open reading frame of the gene, as well as hybridization of genomic blots of *T. brucei* DNA which established the regulatory

subunit was probably a single-copy gene. The gene, named *TbRSU*, encodes a protein of 499 amino acids giving a predicted molecular weight of approximately 57 kDa. The protein has the usual two cyclic nucleotide-binding domains (residues 243 - 360 and 363 - 483) which are predicted to retain all the conserved residues necessary for function, as well as a pseudo-inhibitor site which interacts with the catalytic subunit. Despite this broad homology with type I mammalian PKA regulatory subunits, some sequence deviations are apparent. Arginine residues conserved in both cyclic nucleotide-binding domains are replaced by threonine and asparagine (residues 318 and 442, respectively); also, eight residues before each of these substitutions a conserved alanine is replaced by glutamic acid (residues 311 and 435). A third difference in the nucleotide-binding region is a substitution at residue 319: in all cAMP-binding domains this residue is alanine, whereas in cGMP-binding domains of cyclic GMP-dependent protein kinase (PKG) this amino acid is either a serine or threonine. Uniquely, this amino acid is valine in *TbRSU* (Shalaby, T. et al, 2001).

The recombinant expression in *E. coli*, and subsequent purification, of a fragment of *TbRSU* allowed antibodies to the full-length protein to be raised. Immunoblots of whole cell lysates with the anti-*TbRSU* antibodies detected the protein in both bloodstream and procyclic forms; however, *TbRSU* protein levels were higher in the bloodstream forms than in procyclics. This confirmed Northern blot analysis of total RNA that showed an approximately five times higher level of messenger RNA for *TbRSU* in the former rather than in the latter trypanosome life cycle stage (Shalaby, T. et al, 2001).

Native *TbRSU* was immunoprecipitated from whole cell lysates using the polyclonal antibodies against the protein fragment. Immunoprecipitation using antibodies generated against the bovine catalytic subunit of PKA co-precipitated a protein of approximately 40 kDa, indicating that the trypanosomal PKA-C subunit co-precipitates with *TbRSU*. The co-precipitates displayed phosphorylating activity, transferring a phosphate to classical PKA-specific substrates, as well as being inhibited by the peptide inhibitor PKI (also specific for PKA). Surprisingly, however, cAMP did not stimulate phosphorylating activity of the purified lysates, and in some assays may actually have been inhibitory. Even more unexpected was the finding that cGMP stimulated kinase activity by 3 - 4 times that of controls, with 20 μM of the nucleotide giving the maximum

activity, an observation unique to *T. brucei* out of all the eukaryotic PKA homologues characterised at that point (Shalaby, T. et al, 2001).

To investigate the cNMP binding further, the binding domains were individually expressed in *Drosophila* S2 cells and purified. Domain A had a dissociation constant for cGMP of 7.5 μM while domain B had a K_d of 11.4 μM . cAMP did not compete with cGMP up to concentrations 100-fold in excess, confirming the binding substrate-specificity of the regulatory subunit in purified whole cell lysates (Shalaby, T. et al, 2001). It thus appears that *T. b. brucei* expresses a PKG activity, but no functional PKA activity has been demonstrated to date.

1.5.1.2 *Trypanosoma cruzi*

cAMP-dependent PKA activity was characterised in *T. cruzi* epimastigotes cell lysates after DEAE-cellulose and affinity chromatography with histone IIA and cAMP. A cAMP-stimulated protein kinase fraction was identified, with a half-maximal effect at approximately 1 nM cAMP; the kinase was not affected by cGMP but its phosphate-acceptor preferences were as expected for a cyclic AMP-dependent protein kinase (Ulloa, R. M. et al, 1988).

The apparent holoenzyme was then separated into the catalytic and regulatory subunits by further chromatography in the presence of cAMP which, when bound by the nucleotide binding domains of the regulatory subunit, releases the catalytic protein from the holoenzyme. Experiments with and without the regulatory fraction showed that the catalytic subunit was only activated by cAMP in the presence of the regulatory fraction. The same results were obtained when the *T. cruzi* catalytic fraction was reconstituted with bovine heart regulatory subunit, and *vice versa*. Immunoblotting of purified epimastigote cell lysates using anti-bovine type-II regulatory subunit antibodies also identified a 56 kDa band from both bovine heart and *T. cruzi* extracts, confirming the kinase activity isolated from *T. cruzi* was that of PKA and that similar functional subunits are employed to make up similar holoenzymes in the parasite and mammalian systems (Ulloa, R. M. et al, 1988).

A follow up study which further characterised the catalytic subunit of cAMP-dependent PKA from *T. cruzi* confirmed the similarity of subunit makeup of the holoenzyme. Estimates of the size of the PKA-C of *T. cruzi* were calculated from

the sedimentation constant, Stokes' radius and partial specific volume, giving a relative molecular weight of around 40 000 (Ochatt, C. M. et al, 1993). This figure was substantiated by SDS-PAGE of the parasite catalytic subunit and Western blots using anti-bovine heart PKA-C. Similar calculations from data for *T. cruzi* PKA-C reconstituted with the PKA-R subunit estimated the holoenzyme in *T. cruzi* to have a relative molecular weight of approximately 200 000. This figure, when also taking into account the size of monomeric *T. cruzi* PKA-R being ~ 57 kDa (Ulloa, R. M. et al, 1988), is consistent with a tetrameric molecule made up of two catalytic subunits bound with, and inhibited by, two regulatory subunits (Ochatt, C. M. et al, 1993). The kinetics of the native PKA catalytic subunit were observed to give K_m values of 40 μM for ATP and of 48.6 μM and 26 μM for histone IIA and kemptide as phosphate acceptors, respectively (Ochatt, C. M. et al, 1993).

The gene encoding the *T. cruzi* PKA catalytic subunit was identified after degenerate PCR primers were designed from conserved domains of the ACG serine/threonine protein kinase family and the resulting product was used to screen genomic DNA libraries. The full-length *TcPKA-C* gene encoded a protein 329 amino acids long, sharing 80% and 57% sequence identity with two putative *Leishmania* PKAs, as well as 67% identity with the PKA-C of *Euglena gracilis* (Huang, H. et al, 2002). Further sequence analysis identified all necessary residues and signature motifs of the catalytic core of a PKA; however, the FXXF motif is uniquely situated at the extreme C-terminal end of the parasite protein, and the N-terminal lacked the myristoylation motif usually found in mammalian PKA-Cs. A potential proteolytic cleavage site, relatively well conserved in *L. major* and *E. gracilis*, was also detected, and may allow another mode of regulation of the protein kinase activity. Northern blot analysis identified *TcPKA-C* in all stages of the parasite's life cycle albeit at a relatively low level in the mammalian forms. Southern blotting of restriction digests of *T. cruzi* DNA gave a banding pattern consistent with either allelic variation of a single copy of *TcPKA-C*, or the presence of a second related *TcPKA-C* gene in the parasite's genome (Huang, H. et al, 2002). A BLAST search with the original sequence for *TcPKA-C* from this paper identifies at least three separate isoforms with P values below e^{-100} of PKA-C in the *T. cruzi* database (www.genedb.org).

TcPKA-C was recombinantly expressed in *E. coli* and cell lysates were assayed for phosphorylating activity. TcPKA-C could phosphorylate kemptide, and was inhibited by the PKA-specific peptide inhibitor PKI, suggesting the *T. cruzi* protein is a homologue of PKA. GST-tagged recombinant TcPKA-C was affinity purified and used to raise polyclonal antibodies against the parasite protein. The antibodies detected an approximately 40 kDa protein in epimastigote forms only; similar results were obtained using antibodies raised against a fragment from the PKA-C from *C. elegans* which also cross-reacts with mammalian PKA-Cs. Confirmation of the differential expression of *T. cruzi* PKA-C came from measuring the protein kinase activity in the differing life cycle forms, determined as the difference between phosphorylating activity with or without PKI in the presence of 1 mM cAMP. The PKA activity was approximately 4 times higher in the epimastigote forms than in mixed lysates of trypomastigote and amastigote forms. Immunohistology using the anti-TcPKA-C antibodies localised the protein to the cytosol in all life cycle stages (Huang, H. et al, 2002). The activity of recombinant TcPKA-C was completely inhibited by the peptide inhibitor PKI; specific inhibitors of PKC/CaMK had no effect on the kinase activity of the recombinant *T. cruzi* catalytic subunit (Huang, H. et al, 2006).

Recently the *T. cruzi* PKA regulatory subunit was also cloned and characterised. The deduced open reading frame encodes a protein of 503 amino acids, containing all the domains and motifs of known PKA-R subunits including two cyclic nucleotide-binding domains and an autophosphorylation site (Huang, H. et al, 2006). Sequence analysis showed the protein shares 72% identity with the PKA-R from *T. brucei* and 63% identity with that from *L. major*. Southern blots of restriction digests show that in *T. cruzi* the PKA regulatory subunit is probably a single copy gene.

TcPKA-C kinase activity was completely inhibited by the addition of the recombinant TcPKA-R subunit, with the catalytic activity being partially restored by 100 μ M cAMP (Huang, H. et al, 2006), seemingly substantiating the classical PKA-C/R holoenzyme modulation by cAMP. However, the data presented in this study shows cAMP dramatically stimulating the kinase activity of the recombinant TcPKA catalytic subunit on its own, to many times that of the basal activity without cAMP. This is at odds with the native kinase characterisation where cAMP has no stimulatory effect on the separated catalytic fraction from

epimastigote lysates, and that addition of cAMP to the reconstituted catalytic and regulatory fractions only serves to return the kinase activity to the basal, catalytic subunit-only level (Ulloa, R. M. et al, 1988). It is also at variance with the mammalian PKA holoenzyme paradigm where cAMP does not act on PKA-C, but essentially de-represses the inhibitory effect of the regulatory subunit by binding to specific PKA-R domains. The nucleotide binding by the R-subunit results in conformational change and release of the catalytic subunit, thereby allowing the full phosphorylating activity of the catalytic peptide. It is unclear how cAMP would stimulate the recombinant *T. cruzi* PKA catalytic subunit on its own and what this implies for cyclic nucleotide regulation of the holo-enzyme. If cAMP stimulates the catalytic subunit directly, might the regulatory subunit be regulated by a different factor, such as cGMP in *T. brucei* PKA-R (Shalaby, T. et al, 2001), allowing cross-talk between signalling pathways.

Evidence of cAMP-dependent protein kinase activity has also been uncovered in *Trypanosoma evansi* lysate fractions. Intriguingly, cAMP had no effect on phosphorylating activity of whole cell lysates or particulate fractions, but a doubling of kinase activity was recorded in the soluble fraction. This stimulation could be inhibited almost completely by the addition of PKI (Galan-Caridad, J. M. et al, 2004). The results could be interpreted as evidence for the presence of kinase inhibitory factors that are not sensitive to cAMP in whole cell lysates, but have been removed by fractionation of the soluble extracts.

In order to show that the two characterised *T. cruzi* PKA subunits interact in their native state, specific monoclonal antibodies to both peptides were generated. Individual immunoprecipitates of epimastigote lysates using the anti-TcPKA-C and anti-TcPKA-R antibodies pulled down complexes which were then immunoblotted to identify their components. Those complexes precipitated by anti-TcPKA-C antibodies reacted with anti-TcPKA-R, and *vice versa*, demonstrating that the two subunits do interact with each other in *T. cruzi* whole cell lysates. Also, the complex precipitated by the anti-TcPKA-R antibodies was assayed for kinase activity showing stimulation on addition of cAMP which was greatly inhibited by the further addition of PKI, showing the immunoprecipitate contains protein kinase A activity (Huang, H. et al, 2006).

Immunoblots with anti-TcPKA-R antibodies of whole cell lysates from trypanosomes from all three life cycle stages showed differential expression. The highest expressing stage was the trypomastigote form, followed by the epimastigotes, with amastigotes having the least TcPKA-R. This pattern was similar as for TcPKA-C (Huang, H. et al, 2002). Immunofluorescence using anti-TcPKA-R showed a cytosolic location in all three stages; however, in trypomastigotes significant fluorescence was also detected in the flagellum and plasma membrane (Huang, H. et al, 2006).

The importance of PKA activity in *T. cruzi* was clearly demonstrated by the transfection of the PKA-specific peptide-inhibitor PKI into epimastigotes, which displayed a delayed lethal phenotype, with the majority of selected parasites dying within a month; control lines transfected with the empty vector, or with vector plus GFP, resulted in normal growth (Bao, Y. et al, 2008). Inhibition of PKA activity using the inhibitor H89 also resulted in slow cell death, with 10 μ M of the inhibitor killing all parasites in 10 days.

Having demonstrated that PKA is essential in *T. cruzi* the authors attempted to identify the proteins that it interacts with and phosphorylates using a yeast 2-hybrid system; 38 candidate proteins were identified (Bao, Y. et al, 2008). Of these, 18 could not be named or given a hypothetical function as they did not contain any recognized functional domains, although 12 proteins of this group contained putative PKA phosphorylation motifs. A second group of 12 genes were tentatively identified from putative domains, allowing prediction of their function but no biochemical characterisations have been conducted to date to confirm or reject these preliminary annotations. Half of this second group of candidate PKA-C interacting proteins contained recognizable PKA phosphorylation motifs, with one of them predicted to be an adenylyl cyclase. A third group consisting of 8 out of the 38 candidate proteins had a known and defined function, or were deemed to have important functions for the parasite based on putative domains, 5 of which displayed known PKA phosphorylation motifs (Bao, Y. et al, 2008).

To confirm the TcPKA-C interactions with the identified proteins were not quirks of exogenous expression of the partial proteins encoded by the DNA library constructs, full-length open reading frames for each of the 8 group 3 proteins

were subcloned and transformed into the yeast 2-hybrid system. Again, all showed positive for interaction with the 'Bait' TcPKA-C. The 8 genes were then His-tagged and recombinantly expressed and purified. Each protein could be phosphorylated by bovine heart PKA-C, which could be inhibited by PKI, demonstrating that TcPKA-C is also likely to interact with the proteins in order to phosphorylate them (Bao, Y. et al, 2008).

The authors speculate that three of the identified and putative proteins that interact with TcPKA-C may be involved in adaptation to environmental stress. The *T. cruzi* aquaporin (TcAQP) has been shown, previously to be involved in osmoregulation with cAMP inducing translocation to the contractile vacuole complex (Rohloff, P. et al, 2004). Osmoregulation may also be aided by the ATPase that interacts with TcPKA-C. DNA damage due to the host's immune response mounting attacks on the parasite with free radicals could be repaired by the DNA excision repair protein (DERP) after activation by TcPKA-C. A hexokinase also interacted with TcPKA-C. The *T. cruzi* PKA catalytic subunit has been shown to have a PST1 motif which may allow entry of the protein into the glycosome. Hexokinase is recognized as a marker for the glycosome and regulation of the activity of the hexokinase by TcPKA-C is likely to modulate glucose metabolism (Bao, Y. et al, 2008).

Two phosphatidylinositol 3 (PI3) kinases were also detected by the yeast 2-hybrid system as interacting with TcPKA-C. One of them is putatively annotated as such, however, the other is a type III PI3 kinase, termed Vps34, which has been demonstrated to be associated with autophagy and other intracellular trafficking processes (Bao, Y. et al, 2008).

The possibility of a negative-feedback loop to modulate the cAMP signal was also brought to light. A putative mitogen-activated extracellular signal-regulated kinase (ERK) and the phosphodiesterase TcPDEC-2 were also shown to interact with TcPKA-C (Bao, Y. et al, 2008). In *Dictyostelium*, ERK activity has been shown to activate adenylyl cyclases and inhibit phosphodiesterases. The resulting rise in cAMP activates PKA which inhibits ERK and stimulates PDE activity, thereby lowering the cAMP concentration again (Loomis, E. F., 1998). The components of this kind of feedback system appear to be in place in *Trypanosoma cruzi* as well, since TcERK and TcPDEC-2 were demonstrated to

interact with each other, as well as with TcPKA-C, again using the yeast 2-hybrid system (Bao, Y. et al, 2008).

In similar experiments, the localisation of the TcPKA holoenzyme was further investigated using the TcPKA regulatory subunit instead of TcPKA-C as 'Bait' in the yeast 2-hybrid system. Three P-type ATPases were shown to interact with TcPKA-R; one a putative cation-transporting ATPase, the second a putative calcium-motive P-type ATPase, and the third a Na⁺-ATPase (Bao, Y. et al, 2009). Furthermore, immunocomplexes precipitated from trypomastigote lysates using anti-TcPKA-R monoclonal antibodies were recognized by anti-Na⁺ ATPase antibodies in a 120 kDa band, and by anti-cation transporting ATPase antibodies in a 140 kDa band. Unsurprisingly, a 56 kDa band was recognized by anti-TcPKA-R antibodies from immunoprecipitates using anti-Na⁺ ATPase and anti-cation transporting ATPase antibodies, confirming the interaction between the TcPKA regulatory subunit and the P-type ATPases. The identical experiment with the catalytic sub unit revealed no interactions with the ATPases.

Immunofluorescence using anti-TcPKA-R monoclonal antibodies demonstrated that the regulatory subunit of TcPKA was associated with the flagellum and plasma membrane of trypomastigotes, as well as in the cytosol of all three *T. cruzi* life cycle stages. Subcellular fractionation analysis by immunoblot confirmed the presence of TcPKA-R in the membrane fraction (Bao, Y. et al, 2009), in good agreement with previous investigations (Huang, H. et al, 2006). Since Na⁺-ATPases are also upregulated in trypomastigotes (Iizumi, K. et al, 2006), it was hypothesized that TcPKA-R may be localised to the plasma membrane and flagellum in trypomastigotes by binding to this, or the other, P-type ATPases already located there. This would then recruit the PKA catalytic subunit to the same location and could serve as a useful reservoir of effector proteins capable of responding rapidly, and perhaps more specifically than cytosolically located PKA-C, to the signals induced by the stresses of being released from the host cell and the environmental changes associated (Bao, Y. et al, 2009).

1.5.1.3 *Leishmania*

A *Leishmania* catalytic subunit of PKA was first isolated and characterised in the early 1990s. Protein kinase activity resembling that of mammalian PKA was

purified from *L. donovani* promastigotes by centrifugal fractionation of lysates and sequential column chromatography (Banerjee, C. and Sarkar, D., 1992). Kinase activity eluted as a single peak with SDS-PAGE analysis of the final preparation showing a product with a molecular weight of approximately 34 kDa. The purified molecule was constitutively active and shared peptide phosphorylation preferences with that of mammalian PKA, phosphorylating kemptide over histone H1 and only phosphorylating mixed histones and protamine at a much lower level. Acid hydrolysis of protamine phosphorylated by the leishmanial extract, followed by separation of the phosphoamino acids on cellulose-layer plates, indicated that only serine amino acids were acceptors of the phosphate. The fact that cAMP, cGMP, calcium and calmodulin had no effect on the kinase activity, combined with the size of the eluted molecule, indicated that the catalytic subunit of the *Leishmania* PKA had been purified on its own without a regulatory subunit. The addition of bovine heart regulatory subunit type II inhibited the *Leishmania* kinase activity; however cAMP increased the protein kinase activity back to the basal level. Furthermore both purified and cell lysate activity was inhibited by the PKA-specific peptide inhibitor PKI, purified from pig heart, indicating that the *Leishmania* enzyme is topologically similar to mammalian PKA (Banerjee, C. and Sarkar, D., 1992).

A gene with high homology to other protein kinase A sequences was cloned and sequenced from *L. major* with a PCR-based strategy utilising degenerate primers based on conserved domains of known PKA gene sequences. This identified a gene, designated *LmPKA-C1*, which displayed 64% identity with the catalytic subunit of PKA from the fungi *Blastocladiella* and encodes a protein of 332 amino acids and approximately 38 kDa molecular mass (Siman-Tov, M. M. et al, 1996). All the important conserved features involved in ATP and phosphate-acceptor binding are present, including the RDLKPEN motif indicative of serine/threonine phosphorylating protein kinases. Some deviations from the typical PKA-C sequence were observed, with the *LmPKA-C1* protein having a relatively short N-terminal region of just 11 residues until the first conserved amino acid of the catalytic core, and lacking a site for potential myristoylation. In addition, *LmPKA-C1* has an 8 amino acid, C-terminal extension beyond the usually final FXXF motif, compared to most other PKA-C subunits (Siman-Tov, M. M. et al, 1996 and 2002).

Southern blots with genomic DNA from *L. major*, *L. donovani* and *L. amazonensis* indicate that the leishmanial *PKA-C1* gene is present in all three species as a single copy gene. Northern blot analysis showed that expression of *LmPKA-C1* by promastigote forms is essentially halted on change of temperature from 26 °C to 35 °C, with hybridization levels dropping to less than 30% after just one hour and undetectable after four hours. The change in temperature also triggers differentiation from promastigote to amastigote forms indicating that expression of *LmPKA-C1* is down-regulated on initiation of the transformation process and the kinase appears to play no role in the amastigote form (Siman-Tov, M. M. et al, 1996).

Two further isoforms of PKA-C were later identified, cloned and sequenced in *Leishmania major*. *LmPKA-C2a* and *LmPKA-C2b* are highly homologous genes sharing 96.6% identity overall at the amino acid level, and 100% identity at the DNA base-pair level in the catalytic core (Siman-Tov, M. M. et al, 2002). While both are found on chromosome 35 they are not tandemly arranged, having approximately 36 kb between them. *LmPKA-C1*, on the other hand is located on chromosome 18 and shares only 59.4 % and 58.9% amino acid identity, respectively, with the two *LmPKA-C2* isoforms, rising to 62.2% in the catalytic core. The open reading frames of the two isoforms predict proteins of 381 and 371 amino acids for -C2a and -C2b, with approximate molecular masses of 43 kDa and 42 kDa, respectively. All conserved domains and invariant residues of eukaryotic PKA-Cs are found in the *LmPKA-C2* proteins; however, the PKI binding motif is somewhat different from that of mammalian PKA-C (FDDYEEE compared to FDKYPDS in *LmPKA-C1* and FEKYPDS in *LmPKA-C2* isoforms), possibly reflecting differences in leishmanial PKI. The C-terminal of the two isoforms is similar to that of the mammalian PKA-C in size, having no amino acids after the FXXF motif, although in *LmPKA-C2a* the motif is LXXF (Siman-Tov, M. M. et al, 2002) - possibly reducing catalytic activity, based on studies with mouse PKA-C (Batkin, M. et al, 2000).

Three-dimensional models of the *LmPKA-Cs* based on mammalian PKA-C α crystal structures indicate only minor topological differences with the majority of non-conserved substitutions found on the protein surface and not in the catalytic core. The N-terminal of the *LmPKA-C2* isoforms is predicted to form an α -helix like mammalian PKA-Cs whereas the truncated region in *LmPKA-C1* does not. In

addition LmpKA-C1 has an extra C-terminal loop compared to typical eukaryotic PKA-Cs, due to its eight amino acid extension (Siman-Tov, M. M. et al, 2002).

Attempts to identify a leishmanial PKA regulatory subunit have, so far, drawn a blank. Three cAMP binding proteins were isolated from promastigotes after separation on DEAE-cellulose columns but no protein kinase activity was associated with the three peaks in cAMP binding activity and the proteins did not cross-react with antisera against bovine type I and II PKA regulatory subunits (Banerjee, C. and Sarkar, D., 2001), in contrast to similar experiments using *Trypanosoma cruzi* extracts which did cross-react (Ochatt, C. M. et al, 1993). Yet, protein kinase A activity in *L. amazonensis* promastigotes was observed to be stimulated by cAMP in crude soluble and membrane-enriched protein extracts, with highest activity in metacyclic cells. Fractions obtained from axenic amastigote cultures of *L. amazonensis* displayed equivocal, at most, cAMP stimulation of protein kinase activity (Genestra, M. et al, 2004).

Recent experiments appeared to confirm a role for cyclic nucleotide regulated protein kinase activities in promastigote proliferation and infectivity: PKA inhibitors PKI and H89 and PDE inhibitors dipyrindamole, rolipram and IBMX all clearly affected both parameters. However, the addition of cAMP did not affect kinase activity whereas cGMP, increased activity by nearly 250%. This increase could not be inhibited by PKI, although PKI inhibited the base-line activity by more than 50% (Malki-Feldman, L. and Jaffe, C. L., 2009). This suggests that the cGMP stimulated kinase activity is independent of the PKI-inhibitable activity and that at the life cycle stages investigated a cGMP-dependent kinase activity may contribute more to phosphorylation of kemptide, the substrate used in this study. Even though cAMP itself did not detectably stimulate kemptide phosphorylation under the assay conditions, non-hydrolysable analogues did - probably suggesting high PDE activity in the lysates.

1.6 Aims

This thesis will investigate the anti-trypanosomal action of putative phosphodiesterase inhibitors in relation to current chemotherapies against human African trypanosomiasis (HAT). It will devise, validate and optimise new techniques to aid the more efficient screening of large compound libraries; and it will investigate the mode of intracellular action of selected compounds through biochemical analyses and the characterisation of resistant trypanosome strains.

Chapter II

2 Putative PDE inhibitor screening

2.1 Introduction

The chemotherapeutic control of African trypanosomiasis relies on a group of drugs that can be toxic to the patient, and are becoming less effective, with only pentamidine having no reliable reports of resistance arising in the field (Delespaux, V. and De Koning, H. P., 2007). Unfortunately pentamidine is unable to cross the blood-brain barrier rendering it ineffective against late-stage trypanosomiasis. Only one new drug has been licensed in the past 50 years for the treatment of sleeping sickness, eflornithine (or DFMO), which is only efficacious against the *T. b. gambiense* parasite. This compound also causes severe side-effects such as vomiting, diarrhoea, hair loss and convulsions (Burri, C. and Brun, R., 2003). The need for a new class of chemotherapy is urgent.

The development of new lead compounds against trypanosomiasis requires reliable and informative *in vitro* assays for the screening of test compounds. This is equally true for the monitoring of drug resistance and the study of resistance mechanisms. The current assay of choice is based on the blue and non-fluorescent dye Alamar Blue[®] (resazurin) (Rätz, B. et al, 1997), and is based on the fact that live cells take up resazurin and reduce it to resorufin (pink and fluorescent). Owing to the fact that resazurin can be reduced by many different mitochondrial and cytosolic enzymes (Gonzalez, R. J. et al, 2001), this protocol has been adapted to monitor viability in many different cell types, including hepatocytes (Slaughter, M. R. et al, 1999), neuronal cells (White, M. J. et al, 1996), *Candida* (Pfaller, M. A. et al, 1994) and *Leishmania* promastigotes (Mikus, J. and Steverding, D., 2000) and amastigotes (Al-Salabi, M. I. and De Koning, H. P., 2005). Its results are widely accepted as accurate. The assay is considered cheap, versatile in that it can be used both colourimetrically and fluorescently, and is reproducible. In this chapter, compounds from two sources were assessed for their activity against trypanosomes in *in vitro* culture, using the standard whole-cell efficacy assay.

Since strains refractory to some of the standard chemotherapies have been identified in the field it is essential to ascertain if cross-resistance to any potential new drug is likely to be displayed. In order to examine this, the test compounds were screened against *Trypanosoma brucei brucei* Tb427 wildtype, as well as against strains that are resistant to the diamidine and melaminophenyl

arsenical class compounds and also to pentamidine. The TbAT1 knock out strain has a disrupted P2 adenosine transporter resulting in significant resistance to diamidines like diminazene, as well as having minor resistance to pentamidine and arsenicals (Matovu, E. et al, 2003). Resistance to current chemotherapies against trypanosomiasis in the field has been shown to be linked to adaptations in the P2 adenosine transporter (Mäser, P. et al, 1999; Matovu, E. et al, 2001), and so this strain can be used as a model to test for likely cross-resistance to new compounds by diamidine refractory strains in endemic regions.

Some compounds were tested against the B48 strain which also has the P2 transporter knocked out. However, this cell line has been made further resistant to pentamidine by gradually increasing the maximum tolerated concentration in *in vitro* cultures. The resulting strain also has additional cross-resistance to the melaminophenyl arsenicals (Bridges, D. J. et al, 2007). A small panel of selected compounds were also tested for efficacy *in vivo* in a murine model of trypanosomiasis.

In order to test for efficacy against trypanosomiasis in domestic animals that result in an economic morbidity in endemic regions, compounds were screened against the animal infective species *Trypanosoma equiperdum*. As against the *T. brucei* strain, a drug resistant strain (PBR) was also be tested against. Like the TbAT1 knockout, the PBR strain has been shown to express a modified P2 transporter thought to give rise to the diminazene resistance (Barrett, M. P. et al, 1995).

For some chemotherapies merely inhibiting the increase in parasites in the host is sufficient to result in eventual cure, for example: eflornithine (Burri, C. and Brun, R., 2002). However, a fully competent host immune system is required to prevent relapse, meaning this treatment is inappropriate for those patients also infected with HIV/AIDS, or having some other immune deficiency. It is therefore vital to establish the effect the test compounds have on a population of trypanosomes to see if they kill or inhibit replication. In this chapter, two methods were employed to assess the action of the compounds. The first was to simply count the number of cells in a culture of bloodstream trypanosomes incubated with the test compound over a period of days. The second utilised the

absorbance of light by a dense culture, with the absorbance dropping as the trypanosomes in suspension die.

2.2 Materials and Methods

2.2.1 Whole-cell *in vitro* efficacy assay

Test compounds were provided by Otsuka Maryland Medicinal Laboratories (Series 1 compounds) and by Dr. Geert-Jan Sterk (GJS compounds). A test compound was doubly diluted in a white-bottomed 96-well plate (Greiner) in HMI-9 (Invitrogen) supplemented with 10% foetal calf serum (FCS; Biosera). Bloodstream form *T. b. brucei* strain 427 wild type trypanosomes, cultured *in vitro* at 37 °C in a 5% CO₂ atmosphere, were taken at the late logarithmic phase of growth and the cell density measured using a haemocytometer and adjusted to the desired concentration in HMI-9/FCS. An equal volume (100 µl) of the trypanosomes was added to each well of diluted test compound to give a final cell density of 10⁵ trypanosomes/ml. The plates were incubated for 48 hours at 37 °C and 5% CO₂, after which 20 µl of 0.5 M resazurin sodium salt in phosphate-buffered saline (PBS) was added to each well, followed by a further 24 hour incubation under the same conditions. Fluorescence was measured using either a LS55 luminescence spectrometer (PerkinElmer Life Sciences) with the excitatory wavelength set at 530 nm and the emission wavelength at 590 nm, or a FLUOstar OPTIMA fluorimeter (BMG Labtech) with excitation and emission filters of 544 nm and 590 nm respectively. Data was analyzed using GraphPad Prism software and EC₅₀ values (Effective Concentration that inhibits 50% of maximal growth) were derived from sigmoidal dose-response curves with variable slopes. EC₅₀ values reported in this thesis are the averages of at least three independent experiments.

An identical protocol was employed when assaying bloodstream form TbAT1 knockout (Matovu, E. et al., 2003) and B48 (Bridges, D. J., et al., 2007) strains that are derived from the wild type s427. However, for the *Trypanosoma equiperdum* wild type and PBR strains (Barrett, M. P. et al., 1995) the HMI-9 was supplemented with 20% FCS instead of 10%. When using Tb427 wild type procyclic form trypanosomes, the assays were performed using SDM79 (Gibco) supplemented with 7.5 µg/ml haemin (Sigma) and 10% FCS, with the incubations at 27 °C and atmospheric CO₂ levels.

2.2.2 Proliferation assay

Tb427 wild type bloodstream form trypanosomes were taken from culture in the late logarithmic phase of *in vitro* growth and diluted in fresh HMI-9/FCS medium to a cell density of 5×10^5 trypanosomes/ml. 10 ml aliquots were dispensed into 25 cm³ tissue culture flasks (Corning), to which the required volume of test compound, diluted in DMSO, was added so as to give the desired final concentration, and gently mixed. Test cultures were incubated at 37 °C and 5% CO₂. 10 µl samples were taken periodically by Gilson pipette, after gentle agitation of the culture flask to homogenize the trypanosome suspension, and assessed for cell density using a haemocytometer and a phase-contrast microscope at 40-fold magnification.

2.2.3 Spectrophotometric lysis assay

Tb427 wild type bloodstream form trypanosomes were taken in the late logarithmic phase of *in vitro* growth and centrifuged at 610 rcf for 10 minutes at room temperature. The supernatant was carefully removed and the cell pellet resuspended in fresh HMI-9/FCS medium. The trypanosomes were washed twice more by centrifugation and resuspension in HMI-9/FCS, as above, with the final resuspension giving a cell density between 10^7 and 10^8 cells/ml. After washing, the trypanosomes were left to recover in a water bath for 15 minutes at 37 °C before the commencement of the lysis assay.

The HP8453 spectrophotometer (Hewlett-Packard) was calibrated using HMI-9/FCS medium without test compound or trypanosomes, and set to measure absorbance at a wavelength of 750 nm. 950 µl of the cell suspension was added to each heated 1 ml cuvette, continuously warmed to 37 °C by circulating water, and readings were taken every 30 seconds. After 15 minutes of recording reference traces, 50 µl of test compound, diluted in HMI-9/FCS to 20 times the final desired concentration, was added to each cuvette. Absorbance measurements were taken every 30 seconds for approximately 8 hours.

A similar protocol was followed when assessing the effects of the test compounds on trypanosome survival after short periods of exposure, with a deviation after the washing steps. Before starting measuring absorbance, 960 µl

of cell suspension was added to pairs of eppendorfs. 40 µl of test compound, diluted in HMI-9 at 25 times the desired final concentration, was added to the eppendorf pairs and incubated for the stated period of time at 37 °C. After incubation the eppendorfs were centrifuged at 610 rcf for 10 minutes at room temperature and the supernatant removed. One pellet was resuspended in 1 ml of the HMI-9-diluted test compound at the desired final concentration and the other was resuspended in fresh HMI-9 with no added compound, as a control. The cell suspensions were then transferred to the cuvettes preheated to 37 °C and absorbance measuring commenced as before.

2.2.4 In vivo compound tolerance testing

Before efficacy trials against murine trypanosomiasis were conducted, each selected lead compound was assessed for tolerance by individual mice at increasing concentrations.

The compounds were first tested at a dose of 1 mg/kg in a single uninfected mouse. All mice used were female, ICR strain (Harlan, UK), 10 - 12 weeks old and weighing between 25 - 30 g, and fed a normal diet throughout the tests. Each mouse was weighed and injected intraperitoneally with the required volume of compound dissolved in dimethyl sulphoxide (DMSO), and monitored periodically for adverse reactions. If no overt toxicity was observed after 48 hours, a second mouse was injected with a dose of 10 mg/kg in the same manner, and monitored for signs of discomfort. If after 5 days none were observed in the second mouse, and no severe discomfort was displayed by the first mouse, a third mouse was then injected intraperitoneally with a dose of 50 mg/kg. Each mouse was monitored for a total of 10 days for signs of overt toxicity, with the experiment being terminated at any sign of severe discomfort. For compounds tolerated at 10 mg/kg, but not 50 mg/kg, the dose was increased by 10 mg/kg for each fresh mouse until the maximum tolerated dose was established.

2.2.5 In vivo efficacy testing

Female ICR mice were infected with 10⁴ Tb427 wild type bloodstream form trypanosomes, in 200 µl HMI-9, by intraperitoneal injection. 6 hours later the

first dose of test compound at 50 mg/kg, or the maximum tolerated concentration, was administered by intraperitoneal injection on the opposite side from the parasite inoculation site. Subsequent doses were given at the same concentration and in the same manner, spaced 24 hours apart.

Parasitaemia was monitored daily by sampling blood from the tail of each mouse. A small gauge needle was used to prick the tip of the tail which was gently massaged to produce a sufficient quantity of blood. 2 μ l was taken using a Gilson pipette and mixed with an equal volume of heparin (at a concentration of 500 International Units/ml Carter's Balanced Salt Solution) in a microfuge tube. The remaining blood was smeared onto a glass microscope slide and covered with a cover slip. The slides were screened by light microscopy for the presence of trypanosomes in 40 fields of view at 40x magnification and those that were positive for parasites were quantified using the blood sample from the microfuge tube. The sample was diluted 1:25 with 0.85% ammonium chloride in PBS, which lyses the red blood cells but not the trypanosomes, making the quantification of parasitaemia using a haemocytometer markedly easier.

A preliminary study was carried out first with groups of three mice per compound tested and with three doses of test compound. A larger study was then conducted with groups of six infected mice for compounds 37 and 48, along with control groups; mice were treated with four doses, 24 hours apart, instead of the three doses in the first trial.

2.3 Results

2.3.1 Whole-cell *in vitro* efficacy testing

Over 200 compounds were identified from compound libraries as putative inhibitors of *Trypanosoma brucei* PDEB by Otsuka Maryland Medicinal Laboratories (Series 1 compounds), and dispatched for further screening for efficacy against live trypanosomes. All compounds were assayed for their effect on cell growth using a protocol based on the Alamar Blue[®] method developed by Rätz et al, (1997). The ability to inhibit cell growth was determined by the amount of fluorescence developed through metabolism of the dye resazurin by any surviving trypanosomes after 24 hours of incubation with the test compound. In cultures where parasites were killed by a particular concentration of compound, the amount of fluorescence measured was minimal, whereas at concentrations that did not kill the parasites considerable fluorescence was observed (Figure 2.1). Plotting the relative fluorescence against the log of the test compound concentration gives a sigmoidal dose response curve (Figure 2.1), from which the EC₅₀ value (Effective Concentration which inhibits growth by 50%) can be determined.

Each compound was screened against the *Trypanosoma brucei brucei* Tb427 wild type strain, as well as the TbAT1 knockout strain which is strongly resistant to diminazene and some other diamidine class compounds, as well as mildly resistant to arsenicals and pentamidine (Matovu, E. et al, 2003). Resistance to current chemotherapies against trypanosomiasis in the field is linked to adaptations in the P2 adenosine transporter that is disrupted in the TbAT1 knockout strain (Mäser, P. et al, 1999; Matovu, E. et al, 2001). This strain can be used as a model to test for likely cross-resistance to new compounds by diamidine refractory strains in endemic regions. As well as testing against this mutant strain, a panel of compounds was also tested against the B48 strain. This cell line exhibits additional cross-resistance to pentamidine and melaminophenyl arsenicals, and was derived from the TbAT1 knockout strain by gradually increasing the maximum tolerated concentration of pentamidine in *in vitro* cultures (Bridges, D. J. et al, 2007).

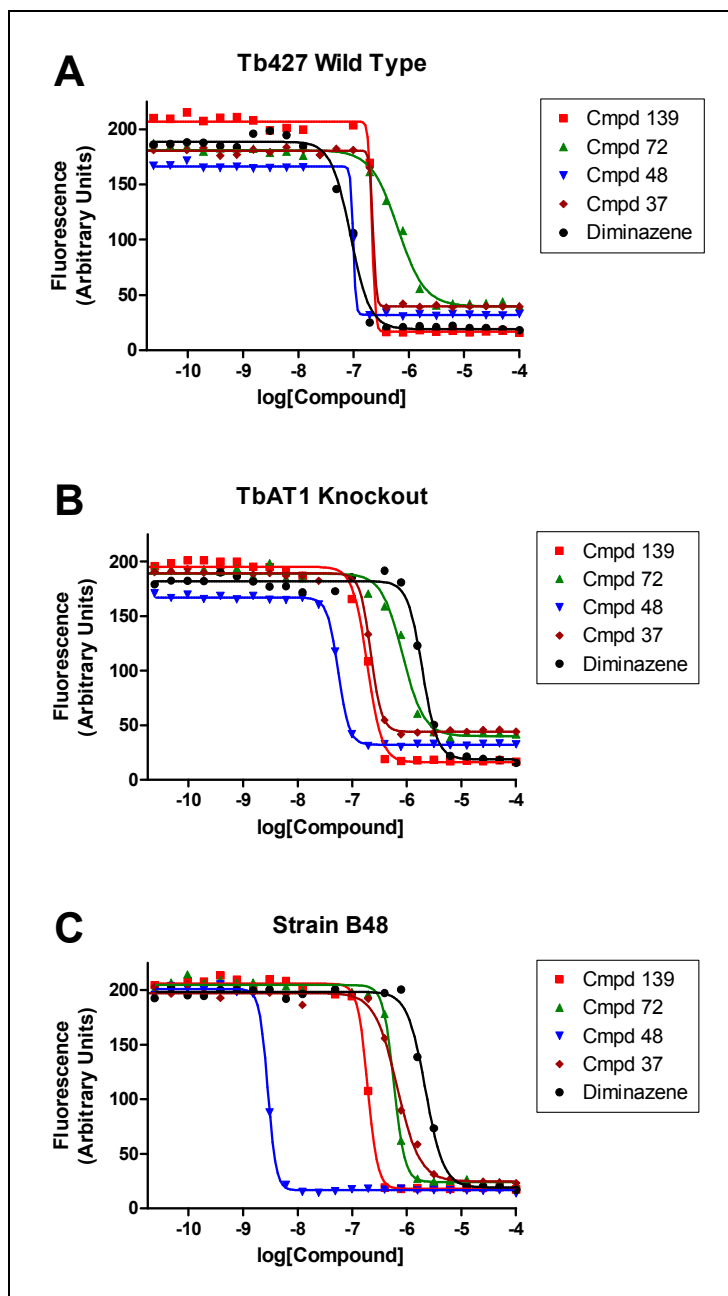


Figure 2.1: Representative graphs showing whole-cell *in vitro* efficacy assays for a number of putative phosphodiesterase inhibitors and diminazene against (A): Tb427 wild type, (B): TbAT1 knockout, and (C): strain B48, bloodstream form trypanosomes. Cells were incubated with the respective test compound at a series of concentrations for 48 hours at 37 °C, 5% CO₂ and in the culture medium HMI-9, before the addition of resazurin and a further incubation of 24 hours. Cell growth was assessed as the amount of fluorescence produced from an excitation wavelength of 530 nm and emission wavelength of 590 nm from the metabolism of resazurin by living trypanosomes.

Representative graphs of the whole-cell *in vitro* efficacy assay, for a number of compounds, against the three strains of *T. brucei* 427 are shown in Figure 2.1. Against Tb427 wild type, diminazene and compound 48 are the most active, with concentrations in the tens of nanomolars being sufficient to kill the trypanosome cultures as measured by the metabolism of resazurin. In the TbAT1 knockout and the B48 strains the curve for diminazene has moved markedly to the right in

comparison to the wild type, demonstrating that these strains are resistant to the diamidine compound. For TbAT1 knockout, the activities of the remaining compounds are broadly equivalent to those against Tb427 wildtype, indicating no cross-resistance by the diamidine-refractory strain, whereas for the B48 strain a dramatic increase in sensitivity is displayed to compound 48 and slight resistance shown to compound 37.

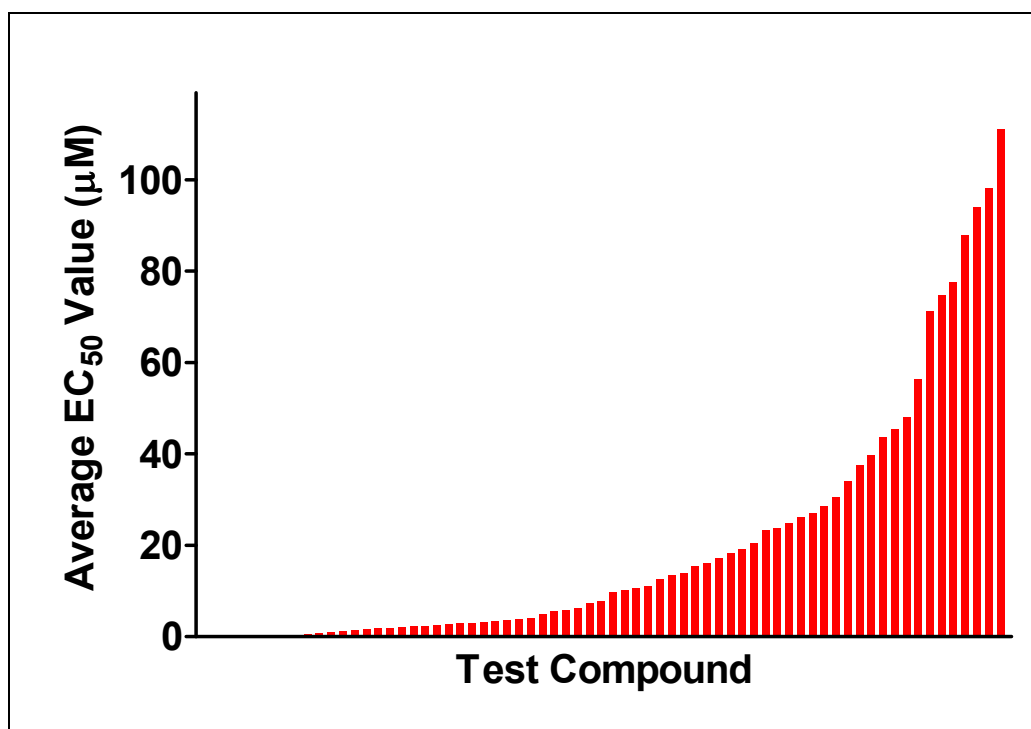


Figure 2.2: Representative graph showing the range of average EC₅₀ values of putative PDE inhibitors against Tb427 wild type bloodstream form trypanosomes. Compounds were ranked by ascending EC₅₀ value, and the value of every third compound was plotted.

The EC₅₀ values were determined for each compound in a minimum of 3 independent experiments, and the averages determined. The values ranged from the highly active, with an EC₅₀ average of just 5.8 ± 3.4 nM for compound 129 against Tb427 wild type, to the much less active compounds, such as compounds 208 - 212, with *in vitro* efficacy values over 100 µM (Table 2.1, Appendix 1 and Figure 2.2). 32 compounds had EC₅₀ values under 1 µM, 7 of which had activity below 100 nM, against Tb427 wild type bloodstream forms. Although significant resistance was displayed against 26 compounds by the TbAT1 knockout trypanosomes, only 6 showed more than 2-fold resistance, with 4-fold being the maximum significant resistance for any Series 1 compound (Compound 124), compared with the 21-fold resistance shown for diminazene (Table 2.1 and Appendix 1).

University of Glasgow Compound Code	EC ₅₀ Value (M) Tb427 WT		EC ₅₀ Value (M) TbAT1 KO		TbAT1 KO Resistance Factor	P Value: Significantly Resistant
	Average	S.E.	Average	S.E.		
129	5.8E-09	3.4E-09	7.8E-09	4.2E-09	1.3	0.373
197	1.2E-08	2.1E-09	5.2E-08	1.8E-08	4.4	0.103
140	3.3E-08	1.8E-08	3.0E-08	1.6E-08	0.90	
141	3.6E-08	2.1E-08	3.2E-08	1.8E-08	0.89	
48	7.0E-08	2.8E-08	4.2E-08	2.9E-08	0.60	
82	7.0E-08	1.6E-08	4.7E-08	1.4E-08	0.67	
137	8.1E-08	4.3E-08	7.2E-08	4.1E-08	0.89	
Diminazene	8.6E-08	1.2E-08	1.8E-06	1.1E-07	21	0.000
138	1.2E-07	1.4E-08	9.1E-08	2.5E-08	0.75	
143	1.6E-07	1.9E-08	5.7E-07	5.0E-08	3.6	0.002
198	1.6E-07	2.1E-08	2.6E-07	4.7E-08	1.6	0.064
124	1.8E-07	2.4E-08	7.0E-07	4.4E-08	4.0	0.000
199	1.8E-07	3.0E-08	1.5E-07	4.2E-09	0.84	
128	1.9E-07	9.7E-08	3.1E-07	3.3E-08	1.6	0.169
114	2.0E-07	2.3E-08	4.7E-07	4.7E-09	2.4	0.004
142	2.0E-07	9.8E-09	3.3E-07	5.1E-08	1.7	0.078
139	2.3E-07	4.3E-08	1.9E-07	4.7E-09	0.84	
113	2.6E-07	2.7E-09	6.4E-07	2.5E-08	2.5	0.003
80	2.7E-07	2.9E-08	3.5E-07	3.6E-08	1.3	0.113
79	2.9E-07	4.5E-08	3.1E-07	6.2E-08	1.1	0.421
104	3.4E-07	4.1E-08	5.3E-07	4.8E-08	1.6	0.033
37	3.5E-07	7.5E-08	3.3E-07	8.0E-08	0.93	
111	3.9E-07	3.8E-08	4.9E-07	1.5E-08	1.3	0.058
83	4.4E-07	1.9E-08	5.1E-07	3.6E-08	1.2	0.126
107	4.4E-07	4.7E-09	4.9E-07	2.2E-08	1.1	0.093
130	4.8E-07	6.8E-08	4.3E-07	2.4E-08	0.89	
158	5.7E-07	4.5E-08	5.3E-07	1.1E-08	0.92	
72	5.8E-07	4.2E-08	8.5E-07	4.8E-08	1.5	0.013
105	5.9E-07	9.7E-08	8.5E-07	7.2E-08	1.4	0.080
103	6.6E-07	8.6E-08	1.1E-06	1.6E-07	1.6	0.069
77	7.6E-07	7.1E-08	5.7E-07	7.5E-08	0.75	
10	8.3E-07	1.7E-07	9.5E-07	2.0E-07	1.2	0.354
121	9.2E-07	7.3E-08	1.2E-06	2.2E-08	1.3	0.022
6	1.0E-06	2.3E-07	1.4E-06	4.7E-07	1.3	0.314
74	1.0E-06	4.7E-08	8.9E-07	1.1E-08	0.86	

Table 2.1: Average EC₅₀ values for Series 1 compounds with sub-micromolar activity against Tb427 wild type and TbAT1 knockout bloodstream form trypanosomes, with standard errors. Values were derived from whole-cell *in vitro* efficacy assays and calculated from sigmoidal dose-response curves, with variable slopes, using GraphPad Prism software. Averages are taken from at least 3 independent experiments. Also shown is the resistance factor of the TbAT1 knockout strain compared to Tb427 wild type for each compound. Statistical significance was calculated after an F-test was conducted to determine which one-tailed, unpaired Student's T-test was most appropriate: that for equal or unequal variances. Those compounds for which the TbAT1 knockout strain is statistically resistant are highlighted with red text.

The B48 strain of the TbAT1 knockout cell line showed a similar resistance profile to the panel of compounds assayed against it. No significant resistance was shown for the majority of Series 1 compounds against B48, with only Compound 113 having more than a 3-fold increase in EC₅₀ value (12.8-fold

increase) (Table 2.2). In spite of the large apparent resistance factor produced from the mean EC₅₀ values of Compound 37, statistical analysis did not determine the difference as significant. Interestingly, 11 out of the 27 compounds assayed against B48 were significantly more active compared to the Tb427 wild type, with 6 of them having EC₅₀ values more than 10-fold lower than against the wildtype (Table 2.2).

University of Glasgow Compound Code	EC ₅₀ Value (M) TbAT1 KO B48		Resistance Factor	P Value:Significantly Resistant compared to Tb427 WT	P Value:Significantly Sensitive compared to Tb427 WT
	Average	S.E.			
129	6.7E-11	1.2E-11	0.01		0.105
48	2.1E-09	6.8E-10	0.03		0.063
82	2.2E-09	6.4E-10	0.03		0.038
80	8.7E-09	1.7E-09	0.03		0.009
111	1.8E-08	7.6E-10	0.05		0.008
79	2.1E-08	1.4E-09	0.07		0.020
112	1.2E-07	2.7E-08	0.08		0.000
110	1.7E-07	3.7E-08	0.07		0.011
139	1.8E-07	4.4E-08	0.81		0.299
83	2.2E-07	1.3E-08	0.50		0.001
77	4.5E-07	3.7E-08	0.60		0.018
74	4.7E-07	7.5E-08	0.45		0.003
114	4.8E-07	3.5E-08	2.45	0.003	
107	5.0E-07	9.4E-08	1.13	0.339	
72	5.9E-07	8.1E-08	1.01	0.485	
10	9.5E-07	1.6E-07	1.15	0.342	
84	9.6E-07	1.2E-07	0.58		0.019
63	1.3E-06	1.2E-07	0.64		0.112
64	1.5E-06	2.5E-08	0.72		0.189
Diminazene	1.6E-06	6.2E-07	18.31	0.049	
73	1.7E-06	6.2E-08	0.89		0.050
7	2.0E-06	3.9E-07	0.90		0.438
6	2.4E-06	4.6E-07	2.29	0.051	
98	2.8E-06	3.5E-08	1.12	0.011	
113	3.3E-06	2.1E-07	12.81	0.004	
4	3.5E-06	5.5E-07	2.26	0.032	
37	3.7E-06	1.5E-06	10.50	0.106	
27	5.7E-06	1.0E-06	2.79	0.049	

Table 2.2: Average EC₅₀ values for a panel of Series 1 compounds against the B48 strain derived from TbAT1 knockout cell line. Values were derived from whole-cell *in vitro* efficacy assays and calculated from sigmoidal dose-response curves, with variable slopes, using GraphPad Prism software. Averages are taken from at least 3 independent experiments. Also shown is the resistance factor of the B48 strain compared to Tb427 wild type for each compound. Statistical significance was calculated using the one-tailed, unpaired Student's T-test after an F-test was conducted to determine which was most appropriate: that for equal or unequal variances. Those compounds for which the TbAT1 knockout B48 strain is statistically resistant are highlighted with red text and those that are statistically more active against the B48 strain are highlighted with blue.

Since procyclic form trypanosomes had been shown to be much more resistant to increases in intracellular cAMP (Zoraghi, R. and Seebeck, T. 2002), it was

hypothesized that phosphodiesterase inhibitors would be less active in this life cycle stage than in bloodstream forms. A panel of 25 Series 1 compounds was assayed against the procyclic form trypanosomes of the Tb427 strain (Table 2.3). As expected, the majority of the compounds were less active in the procyclic form with only Compounds 82 and 77 being more active, compared to activity against bloodstream forms. Five compounds were 10 - 20-fold less active, and Compound 129 was 175-fold less active in the procyclic form suggesting that the target(s) of these compounds may be differentially expressed in the life cycle stages of the trypanosome.

University of Glasgow Compound Code	EC ₅₀ Value (M) Tb427 WT Procyclic Form		Efficacy Factor (Tb427 WT PCF / Tb427 WT BSF)	P Value: Significantly Different compared to Tb427 WT
	Average	S.E.		
82	2.0E-08	6.2E-10	0.28	0.128
48	1.5E-07	1.6E-08	2.08	0.130
111	4.6E-07	5.5E-08	1.19	0.431
80	4.6E-07	6.1E-08	1.71	0.080
79	5.7E-07	8.4E-08	1.98	0.072
77	6.1E-07	5.9E-08	0.80	0.249
129	1.0E-06	6.6E-08	175.69	0.006
114	1.1E-06	3.7E-08	5.52	0.000
83	1.2E-06	8.9E-08	2.84	0.015
10	2.2E-06	5.6E-07	2.67	0.127
6	2.5E-06	1.1E-07	2.39	0.010
110	2.5E-06	7.9E-08	1.07	0.684
107	2.6E-06	5.3E-08	6.00	0.001
112	3.2E-06	2.0E-07	2.17	0.003
64	3.5E-06	2.5E-07	1.67	0.082
139	4.3E-06	3.0E-07	19.08	0.007
37	4.9E-06	3.1E-07	13.81	0.000
72	5.1E-06	2.3E-07	8.71	0.003
74	5.2E-06	1.1E-07	4.99	0.000
98	5.5E-06	4.4E-08	2.25	0.000
73	6.5E-06	3.1E-07	3.38	0.007
63	7.4E-06	2.5E-07	3.62	0.001
84	1.6E-05	8.0E-07	9.70	0.005
4	2.5E-05	2.1E-06	15.66	0.011
27	2.8E-05	1.2E-06	13.62	0.003
Diminazene	9.5E-05	6.8E-06	1103.53	0.008

Table 2.3: Average EC₅₀ values for a panel of Series 1 compounds assayed against procyclic forms of the Tb427 wild type strain, with standard errors. Values were derived from whole-cell *in vitro* efficacy assays and calculated from sigmoidal dose-response curves, with variable slopes, using GraphPad Prism software. Averages are taken from at least 3 independent experiments. Also shown is the fold increase in EC₅₀ value for the procyclic form compared to that of the bloodstream form, expressed as the efficacy factor.

Compounds with a significantly different EC₅₀ value compared to that against Tb427 wild type bloodstream forms are highlighted with red text. Statistical significance was calculated using the two-tailed, unpaired Student's T-test after an F-test was conducted to determine which was most appropriate: that for equal or unequal variances.

University of Glasgow Compound Code	EC ₅₀ Value (M) <i>T. equiperdum</i> WT		EC ₅₀ Value (M) <i>T. equiperdum</i> PBR		PBR Resistance Factor	P Value: Significantly Resistant	Efficacy Factor (Tb427 WT / <i>T. equiperdum</i> WT)	P Value: Significantly Different
	Average	S.E.	Average	S.E.				
82	3.5E-09	2.1E-09	3.7E-09	9.8E-10	1.0	0.478	20	0.077
48	5.4E-09	1.3E-09	5.7E-09	1.6E-09	1.1	0.452	13	0.140
80	1.9E-08	1.9E-09	2.0E-08	4.7E-09	1.1	0.420	14	0.019
111	1.9E-08	2.9E-09	2.5E-08	8.2E-10	1.3	0.088	20	0.015
Diminazene	2.8E-08	4.9E-09	2.0E-06	2.9E-07	71	0.003	3.1	0.002
107	3.2E-08	1.4E-08	2.9E-08	1.2E-08	0.90		14	0.000
197	3.5E-08	1.4E-08	2.5E-08	2.2E-09	0.73		0.35	0.326
79	4.2E-08	6.8E-09	4.3E-08	2.7E-09	1.0	0.445	6.9	0.043
199	6.2E-08	8.9E-09	6.0E-08	4.6E-09	0.97		2.9	0.037
139	1.1E-07	4.9E-09	1.0E-07	3.2E-09	0.98		2.1	0.144
72	1.1E-07	2.0E-08	1.7E-07	1.3E-08	1.5	0.045	5.4	0.000
112	1.3E-07	1.4E-08	1.4E-07	1.4E-08	1.0	0.442	11	0.004
83	1.6E-07	2.1E-08	1.4E-07	2.3E-08	0.90		2.8	0.001
104	2.0E-07	1.5E-08	1.5E-07	4.7E-09	0.76		1.7	0.058
198	2.0E-07	3.2E-09	1.8E-07	2.0E-08	0.88		0.80	0.151
84	2.2E-07	2.7E-09	2.3E-07	5.4E-09	1.0	0.125	7.7	0.000
114	2.3E-07	2.0E-08	2.1E-07	1.8E-08	0.94		0.87	0.466
37	2.5E-07	1.4E-08	2.9E-07	2.5E-08	1.2	0.160	1.4	0.323
110	2.5E-07	4.3E-08	2.6E-07	3.3E-08	1.0	0.469	9.3	0.023
10	3.6E-07	1.4E-08	4.5E-07	2.7E-09	1.3	0.015	2.3	0.151
74	3.9E-07	9.0E-08	3.7E-07	7.4E-08	0.94		2.7	0.004
103	4.1E-07	1.2E-07	4.7E-07	1.0E-07	1.1	0.388	1.6	0.247
105	4.3E-07	1.2E-07	3.7E-07	7.7E-08	0.85		1.4	0.437
64	4.4E-07	3.6E-08	6.4E-07	4.8E-08	1.4	0.028	4.8	0.086
4	4.9E-07	4.7E-08	6.7E-07	5.0E-08	1.4	0.052	3.2	0.103
77	5.2E-07	1.2E-07	4.9E-07	1.3E-07	0.94		1.5	0.234
113	5.2E-07	3.7E-08	6.6E-07	1.2E-08	1.3	0.022	0.49	0.027
98	5.3E-07	3.8E-08	8.1E-07	5.9E-08	1.5	0.014	4.7	0.000
6	8.1E-07	1.9E-07	9.3E-07	1.6E-07	1.1	0.352	1.3	0.547
158	8.3E-07	3.4E-08	8.8E-07	3.9E-08	1.1	0.254	0.69	0.014
63	8.5E-07	9.3E-08	1.0E-06	1.1E-07	1.2	0.206	2.4	0.072

Table 2.4: Average EC₅₀ values for a panel of Series 1 compounds with sub-micromolar activity against *Trypanosoma equiperdum* wild type and the diminazene resistant PBR strain bloodstream form trypanosomes, with standard errors. Values were derived from whole-cell *in vitro* efficacy assays and calculated from sigmoidal dose-response curves, with variable slopes, using GraphPad Prism software. Averages are taken from at least 3 independent experiments. Also shown is the resistance factor of the PBR strain compared to *T. equiperdum* wild type, as well as the efficacy factor between species, comparing the average EC₅₀ values against Tb427 and *T. equiperdum* wild type strains for each compound. Statistical significance for the presence of resistance was calculated using the one-tailed, unpaired Student's T-test after an F-test was conducted to determine which was most appropriate: that for equal or unequal variances. A two-tailed, unpaired Student's T-test was carried out to determine the presence of significant differences between species, again after the use of the F-test to determine the correct T-test to use. Those compounds for which the PBR strain is statistically resistant are highlighted in red text, and those showing significant inter-species difference in EC₅₀ values are highlighted in blue.

A selection of Series 1 compounds were also tested for *in vitro* efficacy against the wild type and diminazene resistant (PBR) strains of the animal infective species *Trypanosoma equiperdum*. Like diamidine resistant *T. b. brucei*, the PBR strain also expresses a modified P2 transporter thought to give rise to the diminazene resistance (Barrett, M. P. et al, 1995). The most active compound was Compound 82 with EC₅₀ values of 3.5 ± 2.1 nM and 3.7 ± 1.0 nM against the wild type and diminazene resistant strains, respectively (Table 2.4 & Appendix 2). For the majority of Series 1 compounds, no cross-resistance was displayed by the diminazene resistant PBR strain. Only five out of the sixty two compounds

assayed against the *T. equiperdum* strains gave statistically significant increases in EC₅₀ value in the PBR strain *versus* the wild type; however, similar to the *T. brucei* wild type *versus* TbAT1 knockout cell lines, none of these showed more than a two-fold difference in efficacy, compared to the greater than 70-fold resistance seen for diminazene.

When the EC₅₀ values against the wild type strains of the two species were compared 18 out of the 62 compounds assayed were significantly different from each other. Most notably, Compounds 80, 111, 107, and 112 were more than 10-fold more active (P-value < 0.05) against *T. equiperdum* than *T. brucei* (Table 2.4 & Appendix 2), suggesting either differential expression of, or significant modification to, the target protein(s) of these compounds across the two species.

2.3.2 Effect of test compounds on trypanosome proliferation

Since the whole-cell *in vitro* efficacy assay with resazurin essentially only gives a snapshot of metabolic activity at the end of a particular incubation period, it was not possible to determine, by using this method, how quickly the test compound acts on the cells at a specific concentration. It is also very difficult to establish if the effect of the test compounds is lethal to the trypanosomes, or merely inhibits proliferation. In order to examine these aspects of the compounds' action, cell density in cultures with and without the test compounds was monitored over time by manually counting the trypanosomes, using a haemocytometer.

Figures 2.3A and 2.3B show representative graphs of Tb427 wild type bloodstream form trypanosomes incubated with 15 µM of various test compounds. Compounds 4 and 7 are relatively slow acting at concentrations of approximately 10 and 7-fold the EC₅₀ values, respectively, only killing all the trypanosomes after more than 3 days incubation. Similarly, diminazene is a slow acting compound, taking up to 34 hours to kill wild type Tb427 bloodstream forms at a concentration over 100-fold its EC₅₀ value. In spite of having similar EC₅₀ values, Compounds 27 and 55 appear to act much more quickly than Compounds 4 and 7, killing all the trypanosomes in the culture in less than 24

hours at 15 μM , suggesting either faster uptake of the compounds, or a different mode of action within the cell.

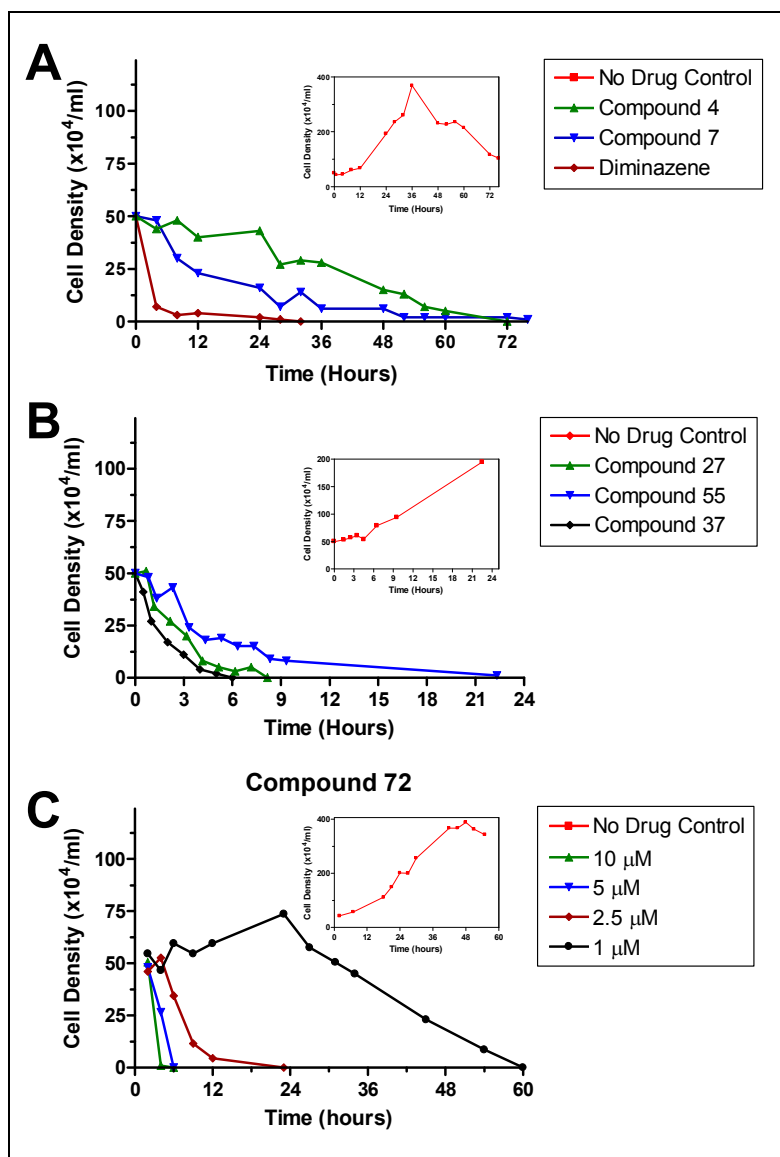


Figure 2.3: Representative graphs showing the effect of a selection of Series 1 compounds and diminazene on Tb427 wild type bloodstream form trypanosome proliferation. 15 μM of each compound was incubated with the trypanosomes, beginning at a density of 5×10^5 cells/ml, at 37 $^\circ\text{C}$, 5% CO_2 , and cell counts conducted periodically using a haemocytometer for up to (A): 72 hours or (B): 24 hours. (C): The effect of Compound 72 at various concentrations on trypanosome proliferation over 60 hours. *Insets:* control cultures without test compound shown separately for reasons of scale.

Compound 37 appears to be the fastest acting compound tested at 15 μM , with complete cell death within 6 hours (Figure 2.3B). However, Compound 72 killed all cells over the same time-frame at just 5 μM (Figure 2.3C), while having an EC_{50} value approximately twice that of Compound 37 (Table 2.1), again suggesting alternative modes of action within the trypanosomes.

All the compounds tested in this way show that they are lethal to the trypanosomes and result in cell death, instead of merely inhibiting cell proliferation while not ultimately killing the cell. The multiple concentrations of Compound 72 assayed also show that, for this compound at least, there is a clear dose-response, with increasing concentrations resulting in faster cell death (Figure 2.3C).

2.3.3 Dynamics of test compounds' lethal effects

One major drawback to using the proliferation assay, above, is the amount of time involved in conducting cell counts of the sampled cultures, thereby limiting the number of samples that can be taken and the number of test conditions assayed in any one set of experiments.

In order to overcome this, the monitoring of the cell density of a test culture was automated by the use of a spectrophotometer. In a dense culture of trypanosomes light is absorbed or refracted by the living cells in suspension. If the cells die, they lose the ability to maintain their osmotic stability and swell up and lyse. Therefore, light absorption can be used as a proxy measure of the cell density of a culture: as the cell density of a suspension becomes less, the light absorption at a specific wavelength (750 nm) is also lowered (Fairlamb, A. H. et al, 1992; Bridges, D. J. et al, 2007). A potential confounding factor, however, is that loss of motility by the flagellated trypanosomes may produce a similar effect: reduced light scatter and fewer cells in the light beam due to slow precipitation.

Figure 2.4A shows the effect on cell density, as measured by light absorbance, of incubating Tb427 wild type bloodstream form trypanosomes with various concentrations of Compound 48. 10 μM of the test compound appears to kill the majority of cells within minutes of addition to the cell suspension. 8 and 6 μM of Compound 48 appear to produce a biphasic curve. The first, and steepest, slope of the curve could be due to the killing of a sub population of the trypanosomes by the initial shock of the addition of the compound, followed by a period where the compound acts on its intracellular target(s), resulting in a more gradual slope later on as the secondary action of the compound takes effect. At 4 and 2 μM of Compound 48, the concentration may not be enough to generate the

initial toxic shock and the steep slope seen for the higher concentrations is missing resulting in a single, more gradual slope as the secondary effects begin to take hold.

In Figure 2.4B, Compound 111 shows a similar lysis profile, with high concentrations resulting in almost immediate lysis of all the cells. However, at 16 μM , a biphasic lysis curve is displayed, with a steep initial slope followed by a period of approximately 1 hour where next to no lysis occurs and a more gradual second slope coming later. At lower concentrations only one slope is evident, with a similar gradient to that of the second slope at 16 μM . The observation that higher concentrations of Compound 111 are required to produce the same effects of Compound 48 is consistent with the higher EC_{50} value of the former compared to the latter (Table 2.1).

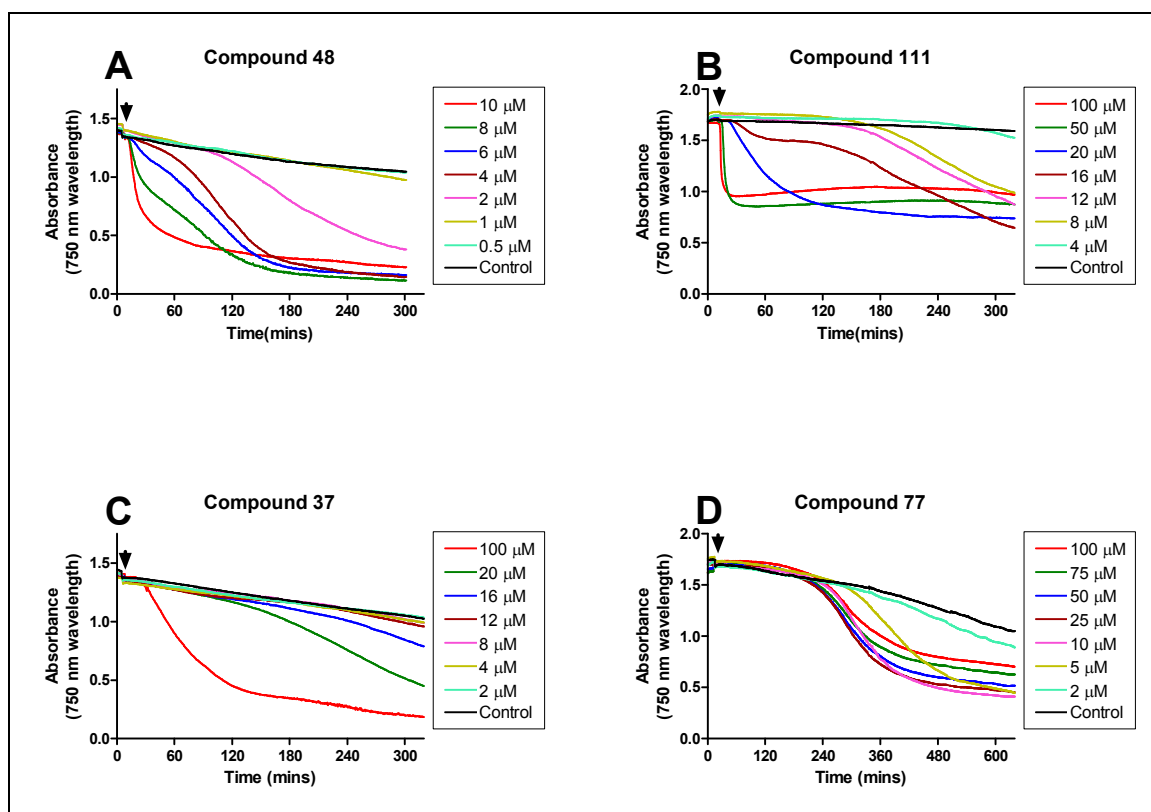


Figure 2.4: Representative graphs showing the effects of (A): Compound 48, (B): Compound 111, (C): Compound 37 and (D): Compound 77, at various concentrations, on the speed of cell death. Between 10^7 and 10^8 cells/ml of Tb427 wild type bloodstream form trypanosomes were incubated at 37 °C with the respective concentrations of test compound in HMI-9/FCS. Arrowheads denote the time-point when the test compound was added. The cell suspensions were monitored for cell death by measuring light absorbance at a wavelength of 750 nm every 30 seconds.

In spite of having a very similar *in vitro* efficacy value to Compound 111 (Table 2.1), Compound 37 appears to lyse the trypanosome suspension much more

slowly (Figure 2.4C). Even at 100 μM there is a lag phase of approximately 30 minutes from addition of Compound 37 to the beginning of the lysis of the cells, whereas for Compound 111, lysis occurred almost instantaneously at the same concentration.

For Compounds 48, 111 and 37, a dose-response relationship is apparent, with higher concentrations lysing the trypanosome suspensions faster than lower concentrations. However, the same cannot be said for Compound 77: concentrations of 10 μM and above appear to lyse the cells with equal rapidity, beginning after approximately 3 hours incubation (Figure 2.4D). A dose-response relationship appears to resume below 10 μM , with 5 μM of Compound 77 beginning lysis of the cells after approximately 5 hours incubation.

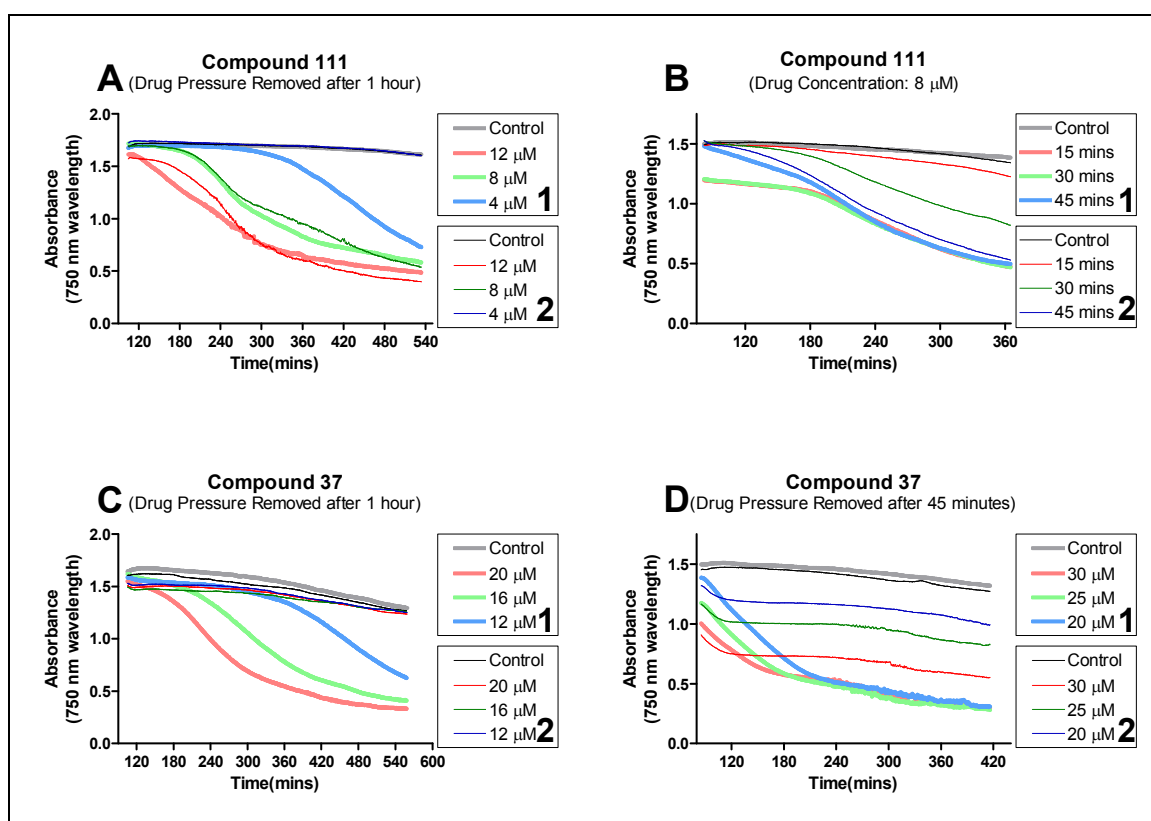


Figure 2.5: Representative graphs showing the effect of removing drug pressure on cell death after limited incubations of the test compounds with Tb427 wild type bloodstream form trypanosomes. Between 10^7 and 10^8 cells/ml were incubated with the various concentrations of test compound for the stated lengths of time in HMI-9/FCS and at 37 °C. The cell suspensions were washed once by centrifugation and resuspension of the cell pellet in an equal volume of either (Group 1): 1 ml of the test compound at the initial concentration dissolved in fresh HMI-9/FCS, or (Group 2): 1 ml of fresh HMI-9/FCS only. After washing, the trypanosome suspension was maintained at 37 °C and monitored for cell death by measuring light absorbance at a wavelength of 750 nm in a spectrophotometer every 30 seconds. (A): The effect of various concentrations of Compound 111 with drug pressure removed after 1 hour incubations in Group 2. (B) The effect of 8 μM of Compound 111 with drug pressure removed after various incubation lengths in Group 2. (C) and (D) The effect of various concentrations of Compound 37 with drug pressure removed after 1 hour, and 45 minutes, respectively, in Group 2. Higher concentrations of the drug were used in panel D than in panel C.

The spectrophotometric lysis assay was also used to investigate whether the trypanosomes were committed to cell death after removing drug pressure before the toxic effects became apparent. For concentrations of Compound 111 at 8 and 12 μM , a 1 hour exposure of the trypanosomes appears to be sufficient to commit the cells to death even if drug pressure is removed (Figure 2.5A). However at 4 μM , removing the drug pressure after 1 hour by centrifugation and resuspension in fresh HMI-9 medium appears to prevent the onset of cell lysis, at least over the time-frame monitored. When the concentration of Compound 111 is maintained at 8 μM and the exposure time to the trypanosomes is varied a similar result is given. Exposure for 45 minutes is sufficient to result in the onset of cell lysis at the same time as a cell suspension with drug pressure maintained throughout (Figure 2.5B). Reducing the exposure time to 30 minutes results in a delayed onset of cell lysis, whereas a 15 minute exposure does not appear to have been sufficient to commit the trypanosomes to lyse over the time period monitored. The obvious conclusion is that Compound 111 is rapidly accumulated into the cells where it triggers events that will eventually lead to cell death over a period of several hours.

In contrast to Compound 111, removal of drug pressure after a 1 hour exposure to Compound 37 appears to entirely prevent cell lysis (Figure 2.5C). Indeed, even removing drug pressure after the onset of cell death can prevent the remaining trypanosomes from lysing (Figure 2.5D).

2.3.4 *In vivo efficacy testing*

A panel of compounds with the highest *in vitro* activity that were available at the time were selected to undergo preliminary *in vivo* efficacy trials against trypanosomiasis in mice. Before investigating the effects of the compounds on parasitaemia in infected mice, each compound was tested to ensure the mice tolerated the treatment without signs of acute toxicity. Single mice were injected intraperitoneally with a single dose of 1 mg/kg bodyweight for each compound. If no adverse effects were observed after 48 hours another mouse was injected with a single dose of 10 mg/kg. Again, if no signs of severe discomfort were observed after 5 days post-injection, another mouse was given

the maximum allowed dose of 50 mg/kg. Each mouse was monitored for 10 days in total for any adverse effects or signs of discomfort.

Table 2.5 shows the 10 compounds tested for tolerance in mice and the maximum tolerated doses. For Compounds 4, 7, 24, 27, 37, 38, 43 and 55, no severe discomfort was observed in the mice over 10 days after a dose of 1, 10 or 50 mg/kg. However, for Compounds 5 and 48, while well tolerated at 1 and 10 mg/kg, a dose of 50 mg/kg resulted in severe discomfort and the test was aborted immediately by terminal anaesthesia with a rising concentration of CO₂. Since Compound 5 only displayed moderate *in vitro* activity in the whole-cell efficacy assays, no further *in vivo* testing was carried out with this compound. Compound 48, on the other hand, showed remarkable activity, with an EC₅₀ value of just 70 nM (\pm 28) against Tb427 wild type (Table 2.1) so it was decided to determine the maximum tolerated dose by increasing the concentration by increments of 10 mg/kg bodyweight. The maximum dose that was well tolerated by the mouse was 20 mg/kg (Table 2.5) and this concentration was used in subsequent *in vivo* efficacy trials.

University of Glasgow Compound Code	Compound Dose (mg/kg bodyweight)				
	1	10	20	30	50
4	OK	OK			OK
5	OK	OK			Aborted
7	OK	OK			OK
24	OK	OK			OK
27	OK	OK			OK
37	OK	OK			OK
38	OK	OK			OK
43	OK	OK			OK
48	OK	OK	OK	Aborted	Aborted
55	OK	OK			OK

Table 2.5: Panel of compounds tested for *in vivo* tolerance in mice. Single female ICR strain mice were given a single dose at the concentration stated by intraperitoneal injection and monitored for signs of severe discomfort for 10 days. Conditions that were tolerated by the mice are marked OK; those that were not tolerated are marked Aborted.

A preliminary investigation into the effect of 5 compounds on the parasitaemia of infected mice was carried out on groups of 3 mice per compound. Female ICR mice were first inoculated with 10⁴ bloodstream form Tb427 wild type trypanosomes by intraperitoneal injection. 6 hours later the first of three doses were given at 50 mg/kg, again by intraperitoneal injection, with the remaining two doses administered 24 hours apart. The parasitaemia was monitored by

microscopic inspection of blood smears as well as cell counts, using a haemocytometer, on small samples of blood taken from each mouse.

Three days post-infection, those mice treated with Compounds 4, 27 and 55 did not appear to show a difference in the level of parasites in the blood compared with the untreated, infected controls (Figure 2.6A). Those mice treated with 7 mg/kg of diminazene had no sign of infection after the same time period. Mice treated with Compounds 37 and 7, however, did appear to have greatly reduced parasitaemia, but statistical testing using the 1-tailed, paired Student's T-test showed the differences were not significant compared to the untreated control.

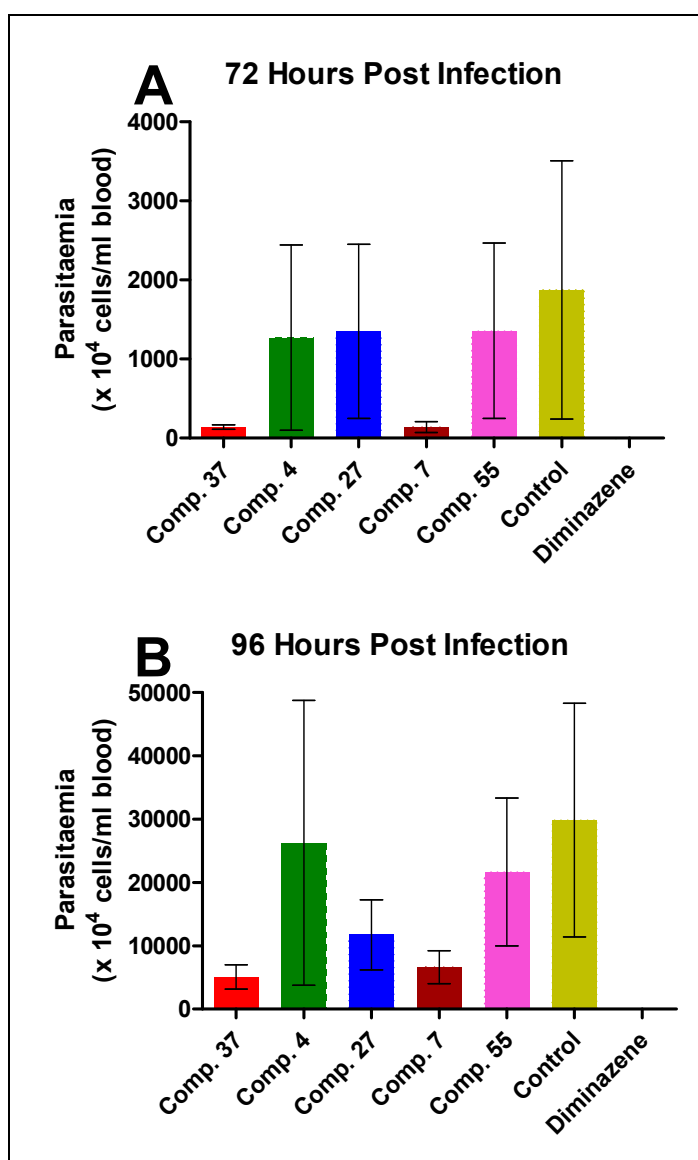


Figure 2.6: Histograms showing the mean parasitaemia, with standard error bars, of female ICR strain mice infected with Tb427 wild type bloodstream form trypanosomes and treated with a panel of Series 1 compounds after (A) 72 hours, and (B) 96 hours post infection. For each compound, 3 mice were infected and treated with 3 doses of 50 mg/kg by intraperitoneal injection, 24 hours apart. The mice treated with the positive control, diminazene, were also given 3 doses 24 hours apart but at a concentration of 7 mg/kg. Blood samples were taken daily and parasitaemia quantified by haemocytometer.

24 hours later, the parasitaemias of mice treated with Compounds 4 and 55, again show no apparent difference to those of the untreated controls (Figure 2.6B). The group of mice given Compound 27 appear to have a reduced parasitaemia, with those treated with Compounds 37 and 7 showing an even more pronounced reduction. While the average parasite levels in the blood appear to show an effect for these compounds, the 1-tailed, paired Student's T-test again showed the differences were not significant compared to the control.

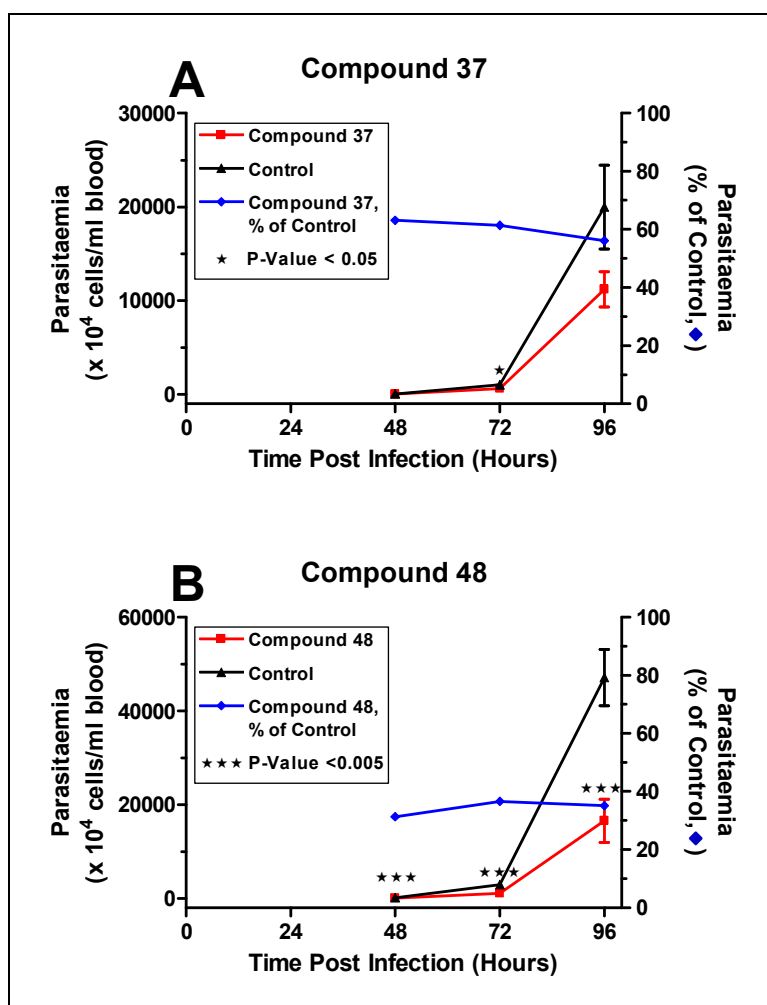


Figure 2.7: Graphs showing the effect of treatment with Series 1 compounds on the mean parasitaemia of female ICR strain mice infected with Tb427 wild type bloodstream form trypanosomes. (A): Average parasitaemia after daily doses of Compound 37 at 50 mg/kg for 4 days starting 6 hours post-infection. (B): Average parasitaemia after daily doses of Compound 48 at 20 mg/kg for 4 days starting 6 hours post-infection. The left-hand axis expresses the parasitaemia as the number of trypanosomes per ml of blood and the right-hand axis expresses it as a percentage of the parasitaemia in the infected, untreated, control group. Each point is the mean parasitaemia, with standard errors, of 6 mice and those that are significantly different from the control are marked with asterisks. P-values were calculated using a one-tailed, unpaired, Student's T-test. Parasitaemia levels were not quantifiable before 48 hours post-infection.

In order to establish if there was a genuine reductive effect on the level of parasites in the blood of infected mice treated with Compound 37 at 50 mg/kg,

a larger trial with groups of 6 mice was conducted, as well as a fourth dose of the compound added to the treatment regimen. After 48, 72 and 96 hours post infection, there was a consistently lower average number of trypanosomes present in the group of treated mice than in the untreated controls (Figure 2.7A). When converted to a percentage, the parasitaemia in the treated group remained at approximately 60% of that of the control over the days when the parasite numbers were measurable. While the lower level of parasites appeared consistent over the course of the trial, the difference was only significant at the 72 hour time-point ($P = 0.044$; 1-tailed, paired Student's T-test).

A similar *in vivo* efficacy trial was also conducted for Compound 48. 2 groups of 6 mice were infected with bloodstream form trypanosomes: one group was left untreated while the mice in the other group were given 4 doses of Compound 48 at 20 mg/kg 24 hours apart, commencing 6 hours post-infection. At all time points where the parasitaemia was quantifiable, the average number of parasites in the treated group was less than 40% of that of the control (Figure 2.7B). At the 48, 72 and 96 hour time points, the reduction in parasitaemia was strongly significant, with P-values for each less than 0.005 (1-tailed, paired Student's T-test), suggesting Compound 48, while not curative, can reduce the parasite burden in infected mice at a concentration of 20 mg/kg via the intraperitoneal route.

2.3.5 Screening of putative phosphodiesterase inhibitors from a secondary source

University of Glasgow Compound Code	EC ₅₀ Value (M) Tb427 WT		EC ₅₀ Value (M) TbAT1 KO		TbAT1 KO Resistance Factor	P Value: Significantly Resistant
	Average	S.E.	Average	S.E.		
GJS-128	7.94E-08	1.03E-08	9.16E-08	5.20E-09	1.2	0.186
GJS-446	1.31E-07	3.11E-08	1.60E-07	1.59E-08	1.2	0.248
GJS-2011	2.11E-07	1.37E-08	2.65E-07	1.94E-08	1.3	0.083
GJS-2358	3.67E-07	1.69E-08	3.34E-07	1.74E-08	0.91	

Table 2.6: Average EC₅₀ values for GJS compounds assayed against Tb427 wild type and TbAT1 knockout bloodstream form trypanosomes, with standard errors. Values were derived from whole-cell *in vitro* efficacy assays and calculated from sigmoidal dose-response curves, with variable slopes, using GraphPad Prism software. Averages are taken from at least 3 independent experiments. Also shown is the resistance factor of the TbAT1 knockout strain compared to Tb427 wild type for each compound. Statistical significance was calculated after an F-test was conducted to determine which one-tailed Student's T-test was most appropriate: that for equal or unequal variances.

A batch of four putative phosphodiesterase inhibitors, synthesized by Dr. G.-J. Sterk of Mercachem, The Netherlands, was made available and dispatched for preliminary screening against trypanosomes using the whole-cell *in vitro* efficacy assay. These compounds proved to be highly efficacious against the bloodstream form Tb427 wild type strain, with EC₅₀ values in the nanomolar range and no cross-resistance displayed by the TbAT1 knockout cell line (Table 2.6). The most active compound was GJS-128 with an EC₅₀ value of 79.4 ± 10.3 nM.

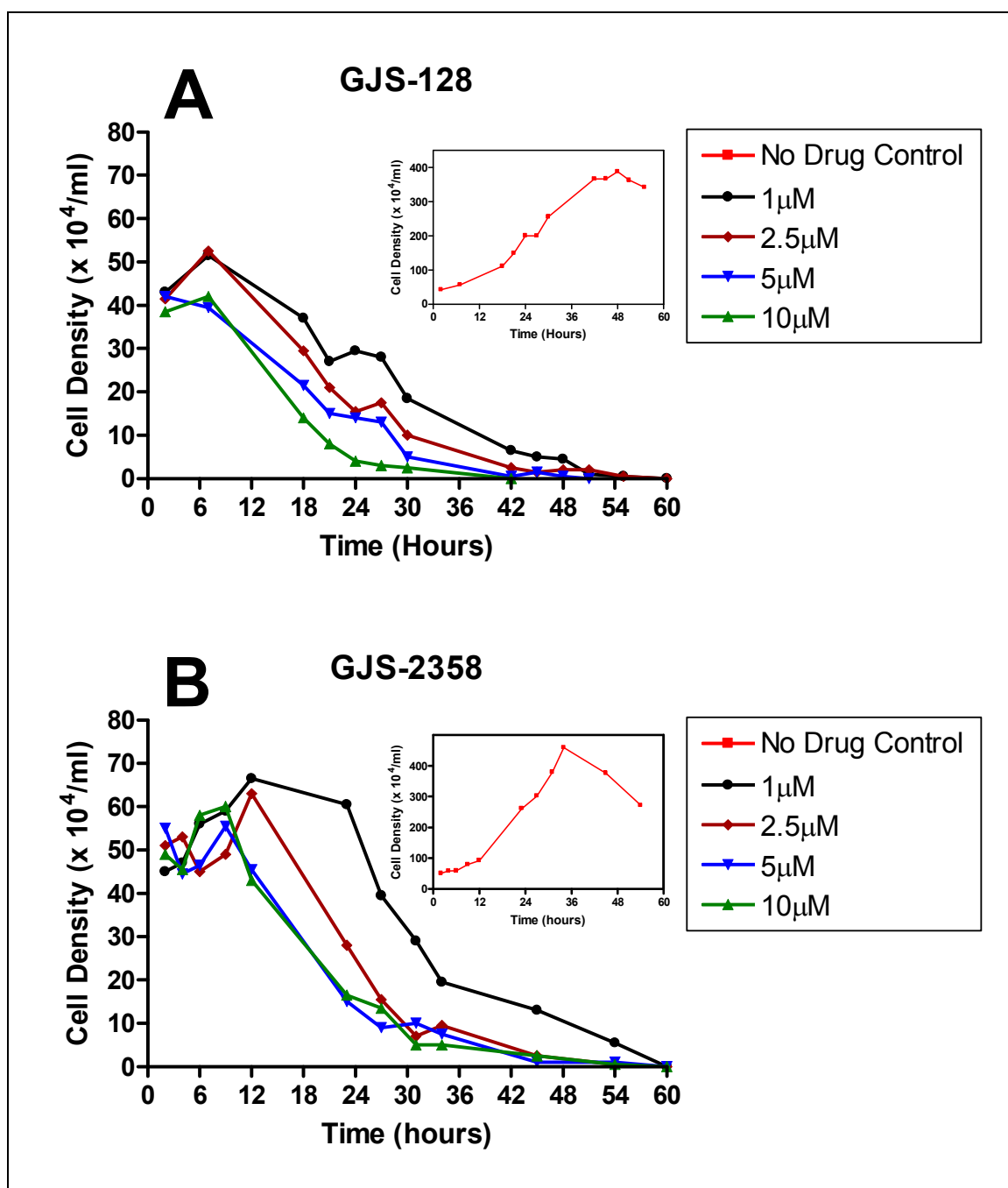


Figure 2.8: Representative graphs showing the effect of GJS compounds on Tb427 wild type bloodstream form trypanosome proliferation. Various concentrations of (A): GJS-128 and (B): GJS-2358 were incubated with the trypanosomes, beginning at a density of approximately 5×10^5 cells/ml, at 37 °C, 5% CO₂, and cell counts conducted periodically using a haemocytometer for up to 60 hours.

Proliferation assays with various concentrations of GJS-128 and GJS-2358 demonstrate that the compounds are relatively slow acting compared to the putative PDE inhibitors of Series 1 (Figures 2.8A and 2.8B). For both compounds there is a dose-dependent effect, with higher concentrations of drug resulting in faster rate of trypanosome population decline. However there appears to be a considerable lag-phase between addition of compound and the beginning of cell lysis: for GJS-128 at least 6 hours elapses before cell density begins to decrease, even at over 100-fold the EC_{50} value (Figure 2.8A). The cell density graphs show a similar, if slightly longer, lag-phase for GJS-2358 (Figure 2.8B), consistent with it being a less active compound as determined by the whole-cell *in vitro* efficacy assays (Table 2.6).

2.4 Discussion

The Series 1 compounds display a wide range of activity against *T. b. brucei* and *T. equiperdum* with the most active compounds having EC₅₀ values below 10 nM and the least active above 100 µM. Thus, a number of Series 1 compounds have activities in the same range, or better, than the current clinical or veterinary chemotherapies. Against *T. b. brucei*, seven compounds are more active than diminazene (Table 2.1), with Compounds 129, 197, 140 and 141 having EC₅₀ values roughly equivalent to those reported for pentamidine, melarsoprol and suramin (Lanteri, C. A. et al, 2006). Against *T. equiperdum*, four of the compounds tested were more active than diminazene (Table 2.4) with seven having EC₅₀ values lower than suramin, and Compound 82 just ~ 2-fold less active than cymelarsen (Gillingwater, K. et al, 2007).

Resistant *T. b. brucei* strains isolated from relapsing, treated animals or patients have been shown to have modifications in the parasite TbAT1/P2 transporter that takes up diamidine class drugs in addition to its physiological role in purine salvage (Mäser, P. et al., 1999; Matovu, E. et al., 2001b). This transporter has been disrupted in the TbAT1 knock out strain and has a greatly reduced substrate affinity in the *T. equiperdum* PBR strain (Barrett, M. P. et al., 1995). Induction of further resistance to pentamidine and melaminophenyl arsenical drugs resulted in the loss of the high-affinity pentamidine transporter (HAPT1) in the B48 strain and is a likely route for resistance to these compounds to arise in the field (Bridges, D. J. et al, 2007). That only a handful of compounds displayed significant resistance in the TbAT1 knockout and B48 strains, as well as the *T. equiperdum* PBR strain; and that even these compounds do not have more than a 3 - 4-fold difference from the wildtype, suggests that there would be a low chance of cross-resistance to the Series 1 compounds from refractory strains in endemic foci. Compound 113 is one exception, with minor, but statistically significant resistance shown by the TbAT1 knockout and PBR strains, and more than 10-fold resistance from B48. The greater resistance in the B48 strain suggests that for this compound the high-affinity pentamidine transporter is a major route of entry into the trypanosome. Compound 98 also has statistically significant resistance in all three resistant cell lines, however the EC₅₀ values are all less than 2-fold higher than the wildtype (Appendix 1; Tables 2.2 and 2.4). Since the resistance level is no different in the B48 strain than in the TbAT1

knockout cell line, HAPT1 is probably not a transporter of Compound 98, but TbAT1 may be one route of entry, probably alongside at least one other. Six compounds were more than 10-fold more active against the B48 strain than the wildtype (Table 2). One explanation for the greater sensitivity could be that the mutation in HAPT1 that lowers the affinity for pentamidine in B48 could also give rise to higher affinities for the Series 1 compounds. A similar phenomenon was observed with some curcumin analogues (Changtam, C. et al., 2009).

Three compounds are more than 10-fold more active against *T. equiperdum* wildtype than *T. b. brucei*. Such large variations may be a result of differing expression levels of the target protein between species, or possibly due to single nucleotide polymorphisms in the gene sequence resulting in different affinities for the target protein.

The proliferation assays highlight an apparently different mode of action between the two sources of putative phosphodiesterase inhibitors: the GJS compounds and those from Series 1. The GJS compounds have a lag phase of at least one generation time after the addition of test compound before the trypanosomes start to die, even at concentrations 100-fold higher than the EC₅₀ value (Figure 2.8). Some of the Series 1 compounds, on the other hand, begin to lower the cell density almost straight away (Figures 2.3B and 2.3C). To achieve the same lag period with Compound 72 the concentration must be lowered to just 5-fold that of the EC₅₀, indicating that either Compound 72 enters the cell faster than the GJS compounds or the intracellular mode of action is different resulting in much faster cell death. When RNA interference was used to knock down the PDEB family of enzymes in bloodstream form trypanosomes, the intracellular cAMP concentration had risen to ~100-fold that of the basal level after 18 hours post-induction (Oberholzer, M. et al, 2007). In spite of the large increase in cAMP, cell lysis did not begin until approximately 24 - 30 hours after RNAi induction, and total population death was not complete until after approximately 50 hours. While the half-life of PDEB enzymes in trypanosomes is not known, and the long lag period between RNAi induction and the start of cell death may be a result of the slow degradation of the enzyme, the timing of cell death matches that caused by the GJS compounds better than that by the Series 1 compounds tested. This indicates that the Series 1 compounds may not act by inhibiting the trypanosomal PDEB enzymes.

This hypothesis is also supported by the efficacy data for the procyclic forms. This life cycle stage of the trypanosome has been shown to be resistant to knock down of the PDEB genes by RNAi, showing abnormalities in only a small percentage of the population due to the resultant increase in intracellular cAMP concentration (Zoraghi, R. and Seebeck, T., 2002; Oberholzer, M. et al, 2007). Although approximately two thirds of the compounds tested have EC₅₀ values significantly higher in procyclics than bloodstream forms only 20% show greater than a 10-fold resistance in the insect stage, with just Compound 129 being more than 20-fold less active (Table 2.3). Since procyclics appear to be almost unaffected by the knockdown of the PDEB genes one would expect a very large degree of resistance to PDE inhibitors in this stage, suggesting the majority of Series 1 compounds tested are not trypanosomal PDE inhibitors. For the five compounds that do show major resistance from procyclic forms either the intracellular target protein or pathway is differentially expressed in the life cycle stages or, as is the case for diminazene, the transporter that allows entry to the cell is expressed at a lower level in the insect form (De Koning, H. P. et al., 1998; De Koning, H. P. et al., 2004).

Both the proliferation assay and the spectrophotometric lysis assay suggest that differing modes of action or of cellular entry are utilised by different Series 1 compounds. Compounds 7 and 27 have almost identical EC₅₀ values (Appendix 1); however Compound 27 only takes approximately nine hours to kill all the trypanosomes whereas Compound 7 takes three days (Figures 2.3A and 2.3B). Either Compound 27 is accumulated to a lethal concentration inside the cell much faster than Compound 7, or the target proteins/pathways of the two compounds are different resulting in slower death for those trypanosomes incubated with Compound 7. Similarly, Compounds 37 and 111 have statistically identical EC₅₀ values (Table 2.1); however, at 20 µM, cell lysis begins after 2 hours of incubation with Compound 37, whereas lysis begins mere minutes after the addition of the same concentration of Compound 111 (Figures 2.4B and 2.4C). There also appears to be a difference in the length of exposure time necessary to result in cell death for these two compounds. While exposure to 8 µM of Compound 111 for 1 hour is sufficient to bring about the onset of cell death 2 hours later, toxic pressure needs to be maintained right up until the trypanosomes lyse for Compound 37 (Figures 2.5A, 2.5B and 2.5C). Again, the

lysis assays could indicate alternative modes of action or of uptake of the compounds.

At high concentrations, both Compounds 48 and 111 appear to be acutely toxic to the trypanosome (Figures 2.4A and 2.4B); however, after some time, the rate of population lysis appears to slow before gathering pace again. At low concentrations the lysis curve has one slope instead of the two seen at high concentrations. This could be the result of the compounds disrupting multiple proteins or pathways within the cell with differing affinities. The acute toxicity could be the result of a low affinity target which, possibly after some response to the toxin, can be overcome to halt or retard the lethal effects. The later slope may be due to the inhibition of a second target protein or pathway with a higher affinity for the inhibitor but which kills the cell more slowly than the acute mode. At high concentrations both routes to cell death can be taken, but at lower concentrations only the high affinity target may be disrupted, giving the single slope. Another explanation for the biphasic lysis curves could be that instead of the initial lowering of absorbance being due to cell death, the compounds may be paralysing the cells resulting in less diffraction of light from the non-motile flagella compared to the moving, unaffected flagella. In this instance the second slope would correspond to either the trypanosomes falling below the light beam through the effect of gravity on the non-motile cells, or actual cell death as a result of the toxic effects of the compounds.

Compound 77 also appears to display a unique lysis profile compared to the other compounds, with the lack of a dose-response above 10 μM (Figure 2.4D). This could be due to the target being saturated at that concentration, with higher concentrations having no greater impact on the target and the onset of cell lysis. A more likely alternative is that Compound 77 is not entirely soluble in the HMI-9 medium at higher concentrations. It was observed that on addition of the compound stock, dissolved in DMSO, to HMI-9, the medium would initially turn cloudy before the compound apparently went back into solution as the medium was heated to 37 °C. It may be that at higher concentrations some of Compound 77 was merely in a fine suspension and not available for uptake or diffusion into the cell.

While both the proliferation and spectrophotometric lysis assays provide valuable information on the relative speeds of action of particular compounds against trypanosomes, there are a number of drawbacks and confounding factors that limit their usefulness. Using a haemocytometer to assess the effects of compounds on cell density is slow and labour-intensive; because of this it is not possible to assay many variations on incubation conditions at one time. It is also difficult to provide accurate timings for compounds that act in minutes as opposed to hours. The spectrophotometric lysis assay overcomes some of these problems by automating the cell density assessment meaning many more readings can be taken than by haemocytometer. This gives higher resolution and accuracy for fast acting compounds as to the beginning of cell lysis in the population of trypanosomes, providing useful information for the set up of future biochemical analyses of the compounds' intracellular effects. However, since the cell densities required to provide a measurable drop in absorbance due to cell lysis are an order of magnitude higher than can be achieved through normal *in vitro* culture, questions are raised as to whether the effects observed can be directly translated to experiments conducted at lower cell densities. Another confounding factor already alluded to is whether the lowering of absorbance is always due to cell lysis or to loss of motility, which would result in the cells accumulating at the bottom of the cuvette and below the beam of measured light. A higher through-put assay that can more accurately determine the point of cell lysis at less physiologically stressful trypanosome densities is much needed and we describe the development and characterization of such an assay in Chapter 3.

The *in vivo* trials indicate that at least for Compound 48, the Series 1 compounds can have an effect on the parasitic burden in the host. Pharmacokinetic analysis of the half-life of the compound in the blood plasma indicates that at 10 mg/kg bodyweight, the concentration of Compound 48 rapidly drops below the *in vitro* EC₅₀ value (Shota Yamanaka, personal communication, Otsuka Japan). This suggests that at the maximum tolerated dose, Compound 48 does not stay at a high plasma concentration for long enough to kill all of the trypanosomes and result in a cure. Chemical modification of the compound to prevent rapid clearance by the host could be possible, although this may result in a compound more toxic to the mammalian host.

Compound 37 did not suffer from the same problem of toxicity and appeared to be well tolerated by the mice. The maximum dose allowed under the Home Office Project license of 50 mg/kg, while consistently lowering the parasitaemia compared to untreated mice, was not sufficient to produce a statistically significant difference from the controls. Although far from ideal, higher concentrations may provide statistical evidence for an effect for Compound 37 *in vivo* and possibly cure. As a comparison, the current treatment regimen for Eflornithine stipulates a daily dose of 400 mg/kg per day for two weeks to provide a cure for late stage *T. b. gambiense* infections (Bouteille, B. et al, 2003).

Chapter III

3 Validation of a propidium iodide based method for monitoring drug action on the kinetoplastidae

3.1 Introduction

As has been described in the previous chapter (2.1) the Alamar Blue[®] assay is the standard assay used to determine *in vitro* efficacy of test compounds. Based on the method developed by Rätz, et al (1997), the metabolism of non-fluorescent resazurin to its fluorescent metabolite resorufin by living cells is utilised as a means of monitoring the effects of test compounds on trypanosome growth *in vitro*. It is cheap, versatile and reproducible, yet it suffers from a number of limitations that are not always appreciated.

The rate of resorufin formation logically depends on both the rate by which resazurin enters the cell and the rate by which this dye is reduced once inside. Neither parameter can be assumed to be constant between different cell types or species, leading to different incubation conditions that make comparisons difficult. For instance, Mikus and Steverding (2000) noted that *Leishmania* promastigotes metabolise resazurin much more slowly than bloodstream form trypanosomes, and assume the difference stems from different incubation temperatures (27 versus 37 °C). However, Al-Salabi and De Koning (2005) found that in order to produce a sufficient fluorescent signal they had to incubate *L. mexicana* amastigotes (seeded at 10⁶/ml, 32 °C in a CO₂ incubator) for 72 hours in the presence of the dye, as opposed to a two-hour incubation with *Trypanosoma brucei* bloodstream forms, seeded at 2×10³ cells/ml and cultured at 37 °C Rätz, B. et al, 1997). In addition, Rolón et al. (2006) found a resazurin incubation time of 5 hours at 28 °C sufficient for *Trypanosoma cruzi* epimastigotes.

More importantly, in some cases the test substance itself can reduce resazurin (Eichler, H., 1934) yielding a false positive. In addition, the fluorescent resorufin can be further reduced to the colorless, non-fluorescent metabolite hydroresorufin. This can result in metabolically active, living cells that produce hardly any fluorescent signal as a result of over-incubation. On the other hand, dead cells that fail to further reduce resorufin can produce a strong fluorescent signal, normally taken to indicate live cells (O'Brien, J. et al, 2000). Moreover, resazurin lends itself poorly to analysis of the dynamics of drug action, being very much an end-point indicator (O'Brien, J. et al, 2000; personal observations) and monitors metabolic activity rather than cellular survival. It is thus very hard,

using this assay, to distinguish between test compounds that induce growth arrest or cell death (Rodenko, B. et al, 2007). A test compound might also affect the metabolic activity or growth rate of cells rather than their survival, creating further uncertainty. Finally, the validity of comparison of different strains of the same species relies on the assumption that they metabolize resazurin at the same rate. However, in two different isogenic pairs of melarsen-resistant trypanosomes, the resistant cells' capacity to reduce resazurin was diminished and there was no clear correlation between cell survival and fluorescence (Foucher, A. L., 2003).

While the resazurin reduction assay has undoubtedly allowed the screening of potential new lead compounds against diverse protozoan pathogens and cancer cell lines, it would be highly beneficial to have a well-validated alternative protocol that does not suffer from the same drawbacks. In this chapter the fluorescent dye propidium iodide (PI) is evaluated as an alternative monitor for assessing drug action on trypanosomes. This dye, which becomes fluorescent upon binding to nucleic acids and which does not cross intact plasma membranes or even membranes of cells in the early stage of apoptosis (Ferlini, C. et al, 1996), can be used either in an end-point or a real-time assay.

3.2 Materials and Methods

3.2.1 Materials and Culturing

Propidium iodide was supplied by Fluka; digitonin, resazurin sodium salt and pentamidine were obtained from Sigma Aldrich; melarsen oxide was a gift from Sanofi-Aventis.

Bloodstream forms of *Trypanosoma brucei brucei* strain 427 were grown at 37 °C in a 5% CO₂ atmosphere in HMI-9 medium (BioSera) supplemented with 10% foetal bovine serum (FBS, Biosera). Cells in the mid to late logarithmic stage of growth were collected and centrifuged at 610 rcf for 10 minutes and either resuspended in HMI-9 to the required cell density, or washed once and resuspended in assay buffer (AB) (33 mM Hepes, 98 mM NaCl, 4.6 mM KCl, 0.3 mM CaCl₂, 0.07 mM MgSO₄, 5.8 mM NaH₂PO₄, and 14 mM glucose, pH 7.3) for

those experiments not conducted in HMI-9 medium. Cell counts were carried out using a haemocytometer.

T. b. brucei procyclics were grown in SDM79 (Gibco) supplemented with 7.5 µg/ml haemin (Sigma) and 10% FBS at 27 °C. *Leishmania mexicana* promastigotes were grown at 25 °C in HOMEM (Gibco) supplemented with 10% FBS and harvested for experiment at a density of $\sim 10^7$ cells/ml. *L. mexicana* amastigotes were cultured at 32 °C in Schneider's *Drosophila* medium (Gibco) supplemented with 20% FBS.

3.2.2 Standard Curves

Genomic DNA from bloodstream form *T. b. brucei* strain 427 was extracted using a method based on that described by Medina-Acosta and Cross (1993). A 50 ml culture was centrifuged at 610 rcf and resuspended in 1 ml HMI-9 before being transferred to a 1.5 ml eppendorf; this was centrifuged again at 380 rcf for 10 minutes. The supernatant was discarded and the pellet gently resuspended in 150 µl of TELT lysis buffer (50 mM Tris-HCl (pH 8.0), 62.5 mM EDTA (pH 9.0), 2.5 M LiCl, 4% (v/v) Triton X-100) and left for 5 minutes at room temperature. 150 µl equilibrated phenol:chloroform (Sigma-Aldrich) was added and mixed, then the eppendorf was centrifuged at 16060 rcf for 5 minutes. The upper, aqueous phase was removed and placed in a new eppendorf to which 300 µl of absolute ethanol was added, gently swirled and left for 5 minutes to precipitate the DNA. The eppendorf was then centrifuged at 16000 rcf for 10 minutes and the supernatant removed; the pellet was washed once with 70% (v/v) ethanol and re-pelleted at 16000 rcf for 10 minutes after which the ethanol was removed by pipette and the pellet left to air dry. The DNA was then dissolved in 100 µl TE buffer (10 mM Tris-HCl (pH 8.0), 1 mM EDTA (pH 8.0)) with RNaseA. The DNA was quantified using a Nanodrop spectrophotometer (Thermo Fisher Scientific) and stored at 4 °C.

The Tb427 gDNA was doubly diluted in assay buffer in a 96-well plate and an equal volume (100 µl) of assay buffer containing propidium iodide at twice the final desired concentration was added to each well. Fluorescence was measured using a PerkinElmer LS55 Luminescence Spectrometer at an excitation wavelength of 535 nm and an emission wavelength of 617 nm.

Live Tb427 bloodstream forms were harvested as described above and resuspended to a cell density of 4×10^8 trypanosomes/ml in either assay buffer or HMI-9 medium, as indicated. Serial two-fold dilutions of the cell suspension were made in a 96-well plate and to each well an equal volume (100 μ l) of assay buffer or HMI-9 containing twice the desired concentration of propidium iodide and 40 μ M digitonin was added. The 96-well plate was incubated at 37 °C for 2 hours to allow the digitonin to permeabilize the cell membranes to the propidium iodide; full lysis was confirmed by microscope. Fluorescence was then measured using a FLUOstar OPTIMA (BMG Labtech) fluorimeter with excitation and emission filters at 544 nm and 620 nm respectively.

3.2.3 Effect of Propidium Iodide on Bloodstream Form *T. b. brucei*

Propidium iodide was doubly diluted in HMI-9 medium in a 24-well plate. An equal volume (500 μ l) of HMI-9 containing bloodstream form *T. b. brucei* strain 427 trypanosomes was added to each well to give a final cell density of 2×10^5 /ml and the plate was incubated at 37 °C and 5% CO₂. Cell counts for each well were carried out in duplicate at various time points using a haemocytometer and the ED₅₀ values (the effective dose at which 50% of the cells were killed) were calculated by non-linear regression using the Prism 4 software package (GraphPad).

3.2.4 Cell Lysis Assays

100 μ l of HMI-9 containing twice the desired concentration of melarsen oxide or pentamidine and 12 μ g/ml (18 μ M) propidium iodide was pipetted into a well of a 96-well plate; a well containing 100 μ l HMI-9 with propidium iodide only was set up as a control. An equal volume of HMI-9 containing bloodstream form Tb427 trypanosomes was added to each well to give a final cell density of 5×10^6 /ml and PI concentration of 6 μ g/ml (9 μ M) and fluorescence was monitored over time at 37 °C and 5% CO₂ using a FLUOstar OPTIMA fluorimeter with the excitation and emission filters stated above. This method was compared to the standard spectrophotometric lysis assay monitored at 750 nm in a 1 ml cuvette, using $1-3 \times 10^7$ bloodstream form trypanosomes/ml in HMI-9/10% FBS, exactly as described (Chapter II).

3.2.5 Comparison of the use of propidium iodide as an endpoint assay with the whole-cell resazurin reduction assay for *in vitro* compound efficacy

The resazurin reduction assay was performed essentially as described (Chapter II) with minor modifications. Briefly, melarsen oxide was doubly diluted in HMI-9 in a 96-well plate; an equal volume (100 μ l) of HMI-9 containing bloodstream form Tb427 trypanosomes was added to give a final cell density of 10^5 trypanosomes/ml. This was repeated with final cell densities of 5×10^4 , 1×10^4 , and 5×10^3 trypanosomes/ml and the plate was incubated at 37 °C and 5% CO₂ for 48 hours. After which, 20 μ l of 0.5 mM resazurin sodium salt in phosphate-buffered saline (PBS) was added to each well and the plate was incubated for a further 24 hours. Fluorescence was measured using a FLUOstar OPTIMA fluorimeter with excitation and emission filters of 544 nm and 590 nm respectively.

The propidium iodide endpoint assay was set up in exactly the same manner as the whole-cell *in vitro* efficacy assay except that, after the trypanosomes were added to the drug dilutions, the 96-well plate was incubated for 72 hours. Subsequently, 20 μ l of 90 μ M propidium iodide and 200 μ M digitonin in PBS was added to each well and, after a further incubation of 1 hour to ensure all the trypanosomes were permeabilized, the fluorescence of the propidium iodide was measured with a FLUOstar OPTIMA fluorimeter with the excitation and emission filters at 544 nm and 620 nm respectively.

3.2.6 Rates of Resazurin Metabolism.

T. b. brucei procyclics and bloodstream forms, and *L. mexicana* promastigotes and axenic amastigotes were grown and harvested as described above, washed twice and resuspended in their respective culture media supplemented with FBS. Doubling dilutions of the cells in the same media were set up in 96-well plates, starting at 1 or 2×10^8 parasites/ml in a final volume of 200 μ l. At the start of the incubation, 20 μ l of 0.5 mM resazurin sodium salt in PBS was added to each well and the plate was incubated for a further 24 hours at 28 °C (procyclics and promastigotes), 32 °C (amastigotes) or 37 °C (*T. b. brucei* bloodstream forms). The bloodstream forms were also kept under a 5% CO₂ atmosphere throughout.

Fluorescence was monitored in real time using a FLUOstar OPTIMA fluorimeter with excitation and emission filters of 544 nm and 590 nm respectively. Initial rates of resazurin metabolism were determined using linear regression over the linear phase ($r^2 \geq 0.99$) and expressed as artificial fluorescence units (A.U.) per hour.

3.3 Results

3.3.1 Standard Curves and Assay Sensitivity.

To test whether propidium iodide could be a suitable fluorophore to use in the monitoring of a culture of trypanosomes, standard curves of fluorescence when bound to doubly diluted genomic DNA extracts or whole trypanosomes lysed with digitonin were generated. PI generates a dose-dependent fluorescence when bound to trypanosomal gDNA (Figure 3.1), with a detection limit (using a Perkin-Elmer LS55 fluorimeter) of approximately 0.5 pg/ml. At 12 µg/ml or 6 µg/ml PI the linear range was up to 12.5 pg/ml (Figure 3.1, inset) although fluorescence continued to increase up to 100 ng/ml *T. b. brucei* gDNA.

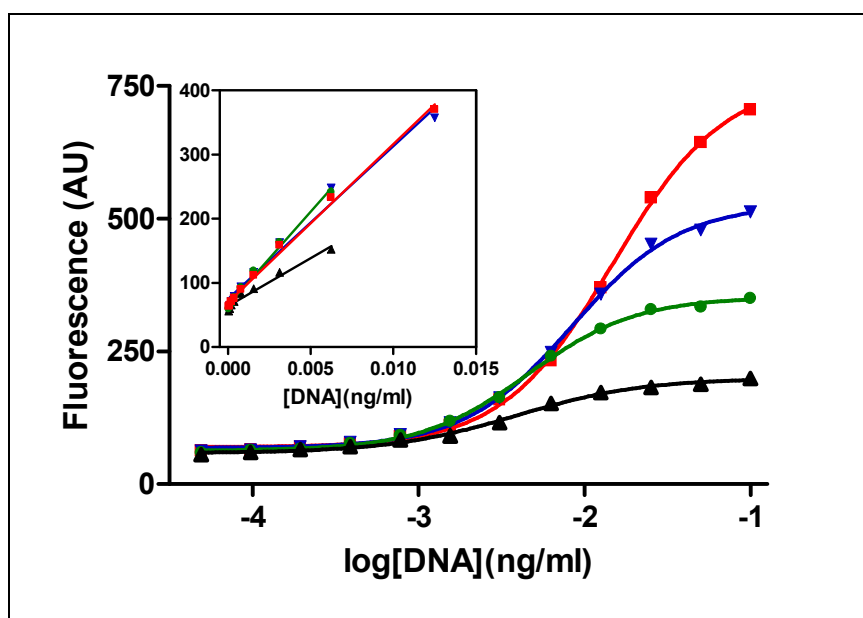


Figure 3.1: Standard curves of fluorescence signal generated by the interactions of various concentrations of *T. b. brucei* genomic DNA with propidium iodide: (■) 12 µg/ml; (▼) 6 µg/ml; (●) 3 µg/ml; and (▲) 1.5 µg/ml. The inset shows the linear part of the dose-response curve for each propidium iodide concentration, with correlation coefficients of 0.99, 0.98, 0.99 and 0.94, respectively, calculated by linear regression.

A similar signal was generated when PI was added to whole cell *Trypanosoma brucei* suspensions, lysed by digitonin (Figure 3.2A). Using the Perkin-Elmer LS55 fluorimeter, and a concentration of 6 µg/ml PI, the detection limit was below 10^6 trypanosomes/ml and the assay is linear between 1×10^6 and 5×10^7 trypanosomes/ml ($r^2 = 0.98$).

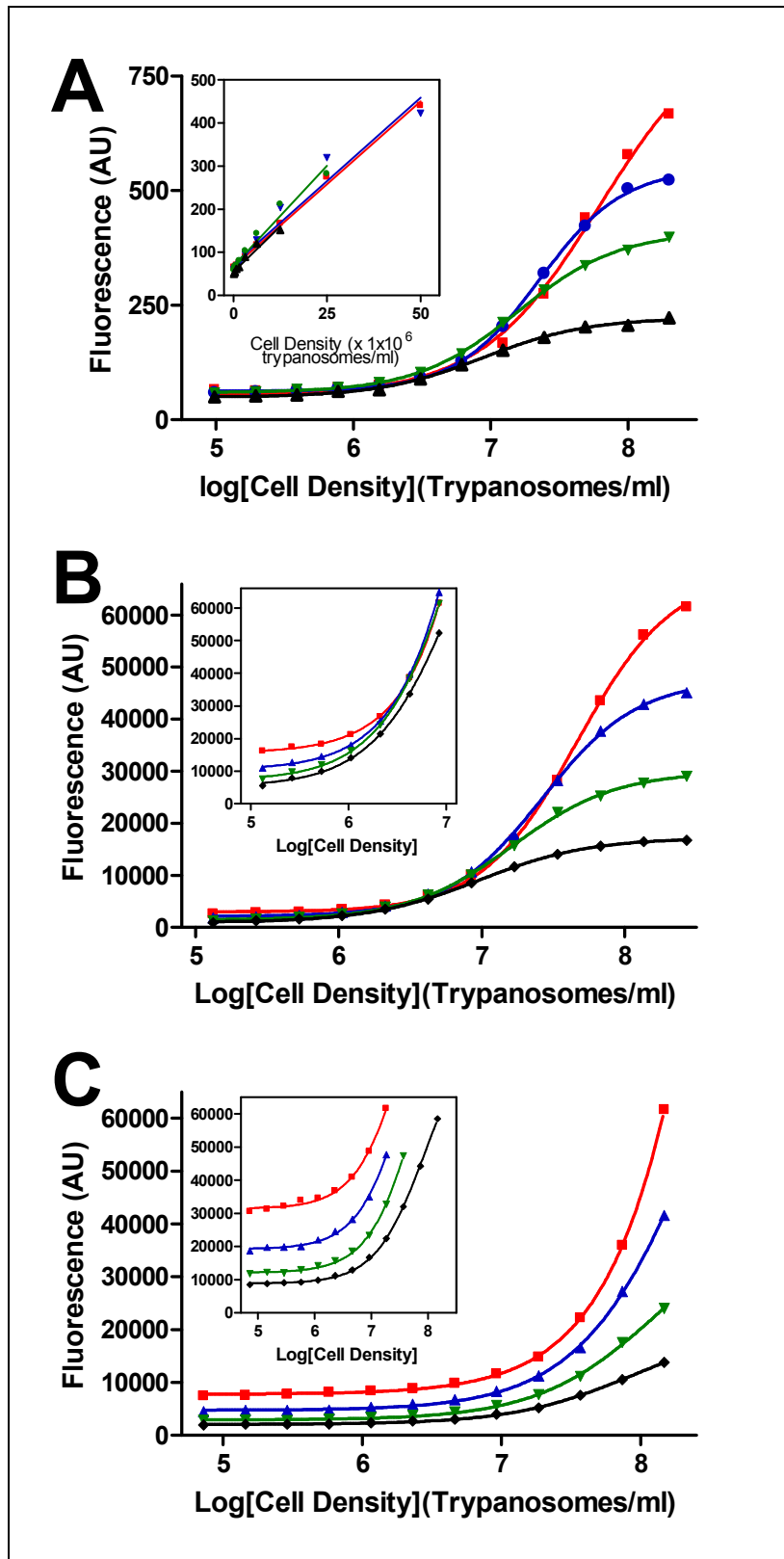


Figure 3.2: Standard curves of trypanosome-associated propidium iodide fluorescence after cell permeabilisation with digitonin. Propidium iodide concentrations: (■) 12 µg/ml; (▼) 6 µg/ml; (●) 3 µg/ml; and (▲) 1.5 µg/ml. (A): *T. b. brucei* bloodstream forms, suspended in assay buffer: fluorescence read using a Perkin-Elmer LS55. Inset shows the linear phase of the dose-response curve for each propidium iodide concentration, with correlation coefficients of 0.99, 0.95, 0.96 and 0.95, calculated by linear regression. (B), (C): *T. b. brucei* bloodstream forms suspended in assay buffer (B) or HMI-9 medium with 10% FBS (C): fluorescence read using FLUOstar OPTIMA. Insets shows fluorescence after the gain was readjusted to enhance resolution at low fluorescence levels.

Optimising the signal strength by adjusting the gain settings at 6 $\mu\text{g PI/ml}$ and in assay buffer (AB) resulted in the operational range being extended to 1.2×10^5 - 2.5×10^8 trypanosomes/ml (Figure 3.2B) and linear up to 7×10^7 trypanosomes/ml ($r^2 > 0.98$ at 12 and 6 $\mu\text{g/ml PI}$). Indeed, the improved sensitivity also allowed similar measurements in HMI-9 (Figure 3.2C), with a lower limit of $\sim 1 \times 10^6$ trypanosomes/ml.

3.3.2 Effect of propidium iodide on cell viability and growth.

The effect of propidium iodide on trypanosome viability was tested next, in order to confirm whether the dye can be used to monitor drug effects on viability without affecting this itself. The effects of varying concentrations of the compound on cultures of bloodstream trypanosomes were monitored over 34 hours by cell counts using a haemocytometer and phase-contrast microscopy. At high concentrations, PI was found to be toxic to trypanosomes over a period of 9 hours, yielding an extrapolated IC_{50} value of $76 \pm 3 \mu\text{M}$ or $51 \pm 3 \mu\text{g/ml}$ ($n = 3$; Figure 3.3). Below 10 $\mu\text{g/ml}$ no discernible growth effect was observed over 9 hours, or any effect on viability for up to 34 hours (data not shown). However, concentrations as low as 0.5 $\mu\text{g/ml PI}$ appeared to inhibit cell proliferation over 24 or 34 hours (data not shown).

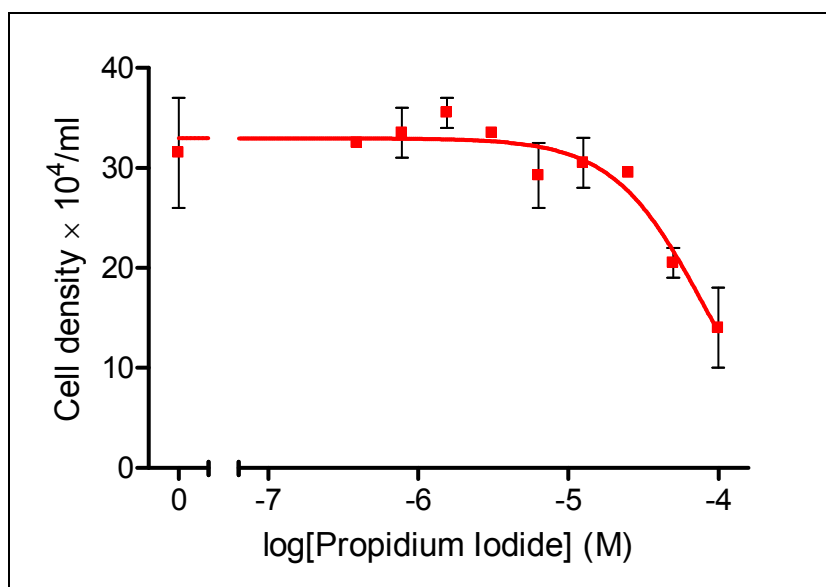


Figure 3.3: Effect of the continuous exposure to propidium iodide on trypanosome viability. *T. b. brucei* in HMI-9 with 10% FBS were incubated with serial two-fold dilutions of propidium iodide for 9 hours. Cell counts were performed in duplicate using a haemocytometer. IC_{50} value was estimated using a non-linear regression (Prism 4.0, GraphPad) and extrapolation of the sigmoidal curve to a minimum value of zero.

3.3.3 Real-time monitoring of cell lysis.

Since propidium iodide is unable to cross intact cell membranes, it can only bind to intracellular RNA and DNA and fluoresce when the cell membrane has been disrupted. Therefore, in suspensions of live cells, fluorescence of propidium iodide can be an accurate signal of the moment the cell membrane is breached and, by inference, cell death occurs. This gives an accurate depiction of the dynamics of drug action on the trypanosome.

When incubated with 10 μM of melarsen oxide, the onset of *T. brucei* cell lysis started to occur after as little as 15 minutes and was complete within 30 minutes (Figure 3.4A). The assay clearly shows a dose-dependent response to the arsenical drug: at 2.5 μM the start of cell lysis has been delayed by 15 minutes, with full lysis of the culture reached at approximately 40 minutes. With 0.5 μM melarsen oxide, 50% of trypanosomes were lysed in ~100 minutes. The action of pentamidine (a compound with an almost identical EC_{50} value to melarsen oxide as determined in a resazurin reduction assay (Matovu, E. et al, 2003)) on trypanosome viability was very much slower; the extremely high concentration of 100 μM (i.e. 50,000 \times IC_{50} (Bridges, D. J. et al, 2007)) only bringing about the onset of cell lysis after 2 hours of incubation and 25 μM of pentamidine having no apparent effect on cell survival over 6 hours (Figure 3.4A). At the end of the assay, samples from each of the cultures were inspected by microscope: no living trypanosomes were observed in any of the samples containing melarsen oxide. In contrast, no ill effects on the cells were noticeable in the 5 μM pentamidine sample or in the no-drug control. The traces due to PI fluorescence in figure 3.4A mirror those derived from the spectrophotometric assay in figure 3.4B demonstrating that the PI lysis assay produces data consistent with that from the alternative method.

Figure 3.4C shows the acute effects of melarsen oxide and pentamidine on these cells in the presence and absence of 3, 6 and 12 $\mu\text{g}/\text{ml}$ PI. No difference is shown for the onset of cell lysis due to either drug in the presence or absence of propidium iodide. Similarly, the rate of cell lysis is unaffected by the addition of PI, in comparison to drug action without the dye. This demonstrates that over at least eight hours PI did not alter the rate by which standard trypanocides cause cell death in bloodstream *T. b. brucei*.

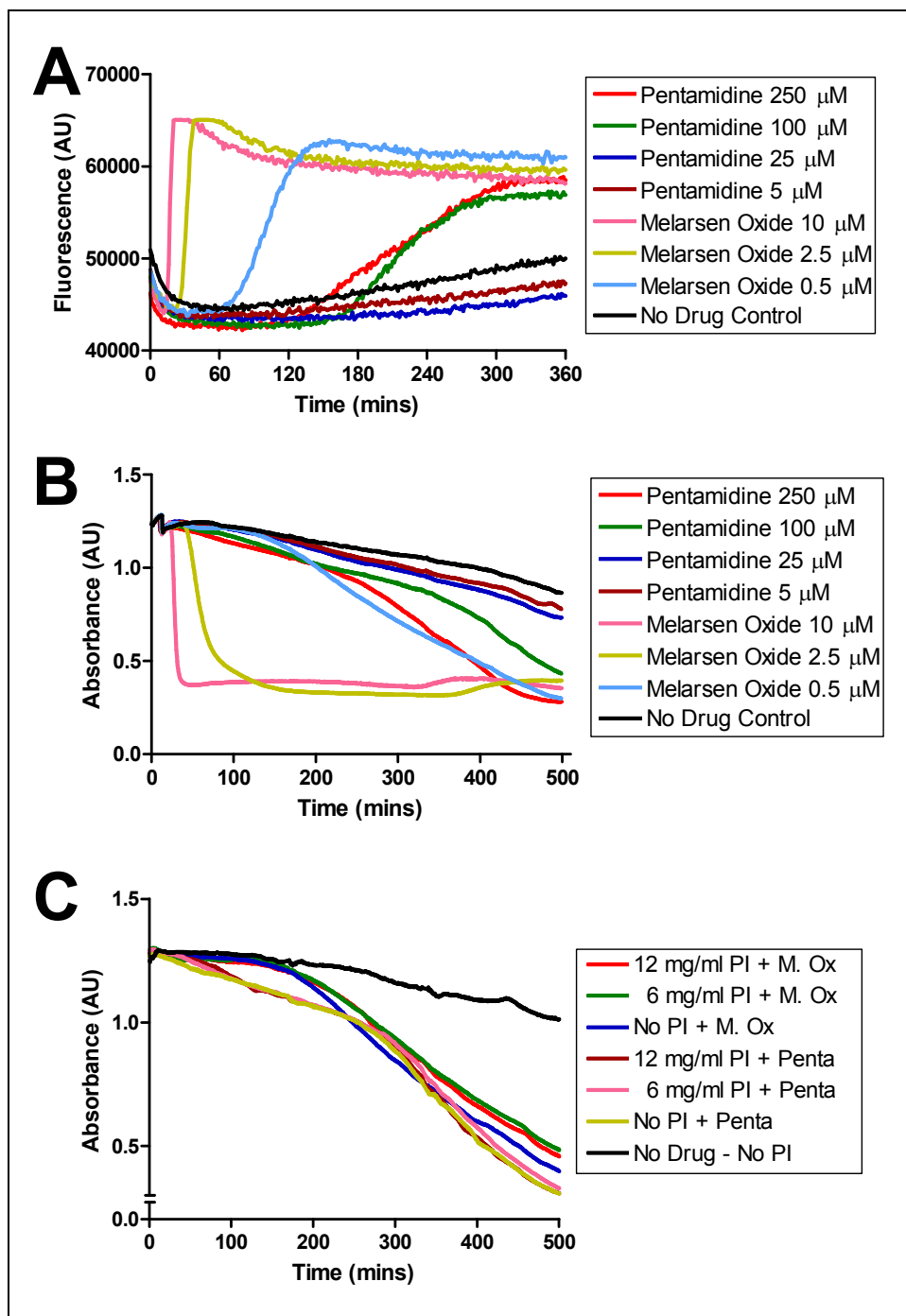


Figure 3.4: Effects of pentamidine and melarsen oxide on *T. b. brucei* survival. (A): Survival monitored by measuring fluorescence of 6 $\mu\text{g/ml}$ propidium iodide in HMI-9 with 10% FBS using a FLUOstar OPTIMA fluorimeter. All traces recorded simultaneously in a white-bottomed 96-well plate using 5×10^6 bloodstream form trypanosomes/ml. (B), (C): Survival monitored by measuring light scatter or absorbance at 750 nm.

The propidium iodide lysis assay validated in Figure 3.4 was used to monitor the effects of a number of test compounds on the survival of populations of bloodstream form trypanosomes. The timings for the onset of cell death with Compound 37 is almost identical to the data generated by the spectrophotometric lysis assay (Chapter 2, Figure 2.4C; Figure 3.5A), further validating the PI assay as a reliable means of monitoring cell death. Compound

48, on the other hand, appears to be much more active in the PI method in comparison to the spectrophotometric assay. In the PI assay Compound 48 kills trypanosomes almost instantaneously at concentrations as low as 6.25 μM (Figure 3.5B), whereas similar concentrations in the light absorbance assay result in a biphasic curve with the initial drop in absorbance becoming less steep taking approximately 3 hours to reach the base-line absorbance of total cell death (Chapter 2, Figure 2.4A). The Compound 48 analogue, Compound 139, appears to kill trypanosomes more slowly than Compound 48 (Figure 3.5C), consistent with the former having a lower EC_{50} than the latter. GJS-128, in spite of having an almost identical EC_{50} value with Compound 48, is a much slower acting compound with concentrations hundreds of times higher than the *in vitro* efficacy value not killing the trypanosomes within 8 hours (Figure 3.5D). This difference in speed emphasises a probable different mode of action between the two series of compounds.

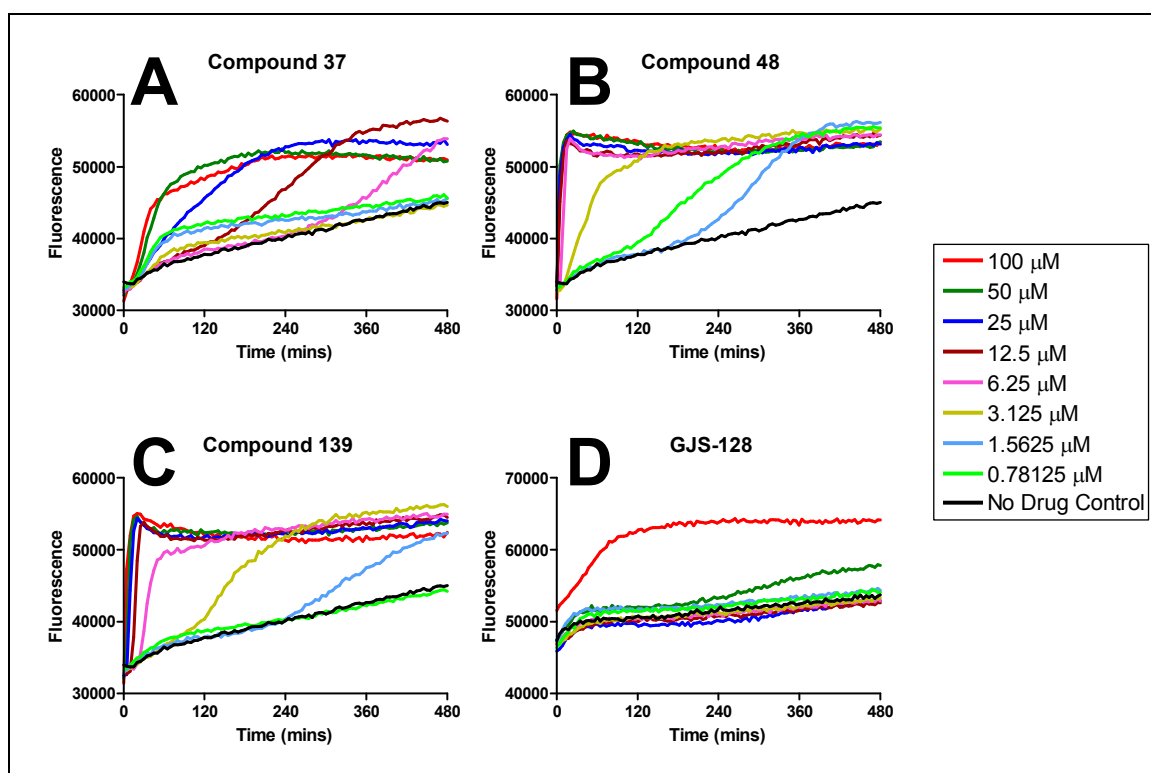


Figure 3.5: Effects of various concentrations of Series 1 compounds and GJS-128 on *T. b. brucei* survival. Survival was monitored by measuring fluorescence of 6 $\mu\text{g}/\text{ml}$ propidium iodide in HMI-9 with 10% FBS using a FLUOstar OPTIMA fluorimeter. All traces recorded simultaneously in a white-bottomed 96-well plate using 5×10^6 bloodstream form trypanosomes/ml. (A): Compound 37; (B): Compound 48; (C): Compound 139; (D): GJS-128.

3.3.4 Resazurin metabolism by protozoan parasites.

As part of the comparison between the whole-cell *in vitro* and PI assays, it was investigated whether, as reported for some mammalian cell types (O'Brien, J. et al, 2000), protozoa are able to reduce resazurin to resorufin and onwards to the non-fluorescent hydroresorufin. Figure 3.6 shows that bloodstream form *T. b. brucei*, but not *L. mexicana* amastigotes, do seem to rapidly metabolize the fluorescent compound generated upon incubation with resazurin, especially at high cell numbers, leading to a rapid decrease in net fluorescence. Some reduction in resazurin fluorescence after more than 6 hours was also noticeable with high density cultures of *T. b. brucei* procyclics and *L. mexicana* promastigotes, but this was less pronounced than with bloodstream forms (data not shown).

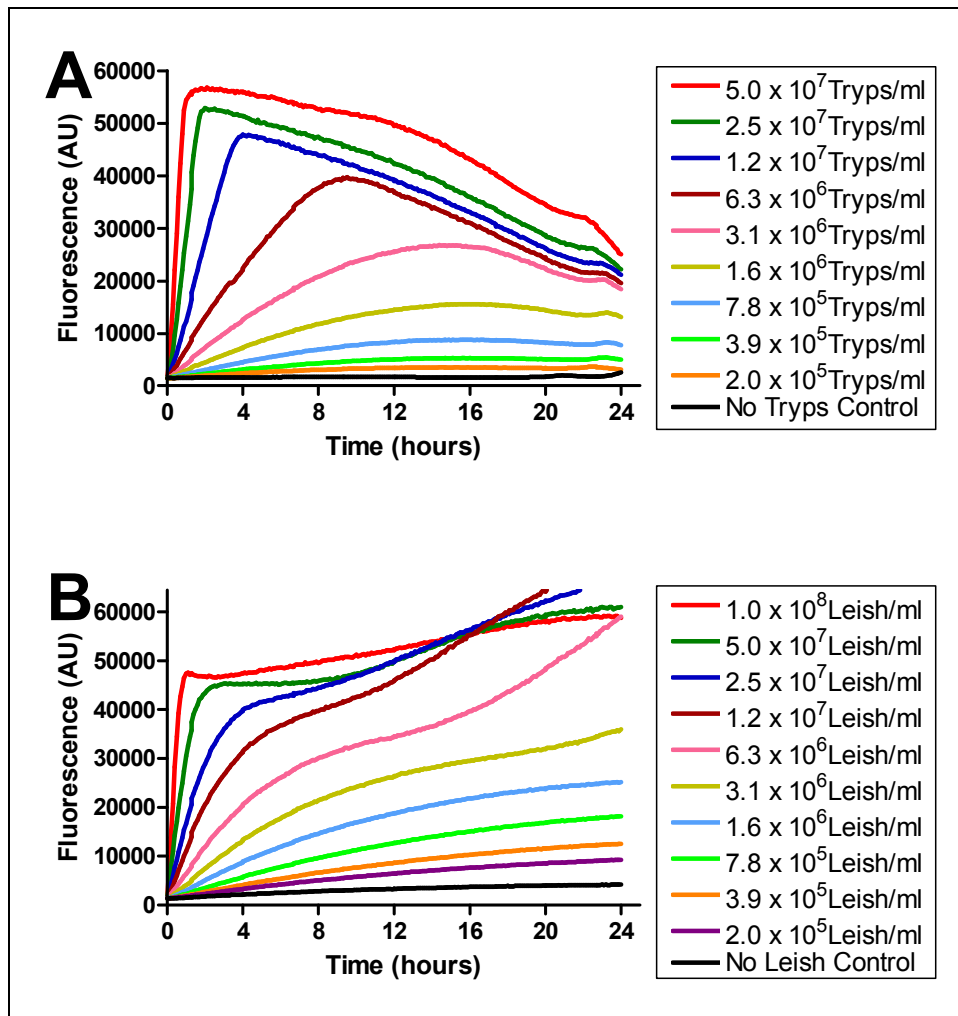


Figure 3.6: Development of fluorescence due to resazurin metabolism over 24 hours. (A): *T. b. brucei* bloodstream forms at 37 °C under 5% CO₂ atmosphere at stated seeding cell densities. (B): *L. mexicana* amastigotes at 32 °C at stated seeding cell densities. Fluorescence was measured using a FLUOstar OPTIMA fluorimeter with identical gain settings for both organisms.

The perceived differences in resazurin metabolic rates in the various parasites were addressed next. Initial rates of metabolism, rather than levels of fluorescence after a predetermined number of hours, were plotted for *T. b. brucei* procyclics and bloodstream forms as well as *L. mexicana* promastigotes and axenic amastigotes. The rate of resazurin metabolism was virtually identical in *T. b. brucei* procyclics and bloodstreams forms (Figure 3.7A), and the rate is directly proportional to cell density for all four cell types over at least three orders of magnitude (Figures 3.7A and 3.7B). However, resazurin metabolism was notably slower in *L. mexicana* amastigotes than in promastigotes (Figure 3.7B), although not to the extent expected on the basis of the incubation times required for the standard whole-cell *in vitro* efficacy assay (Al-Salabi, M. I. and De Koning, H. P., 2005; Papageorgiou, I. G. et al, 2005).

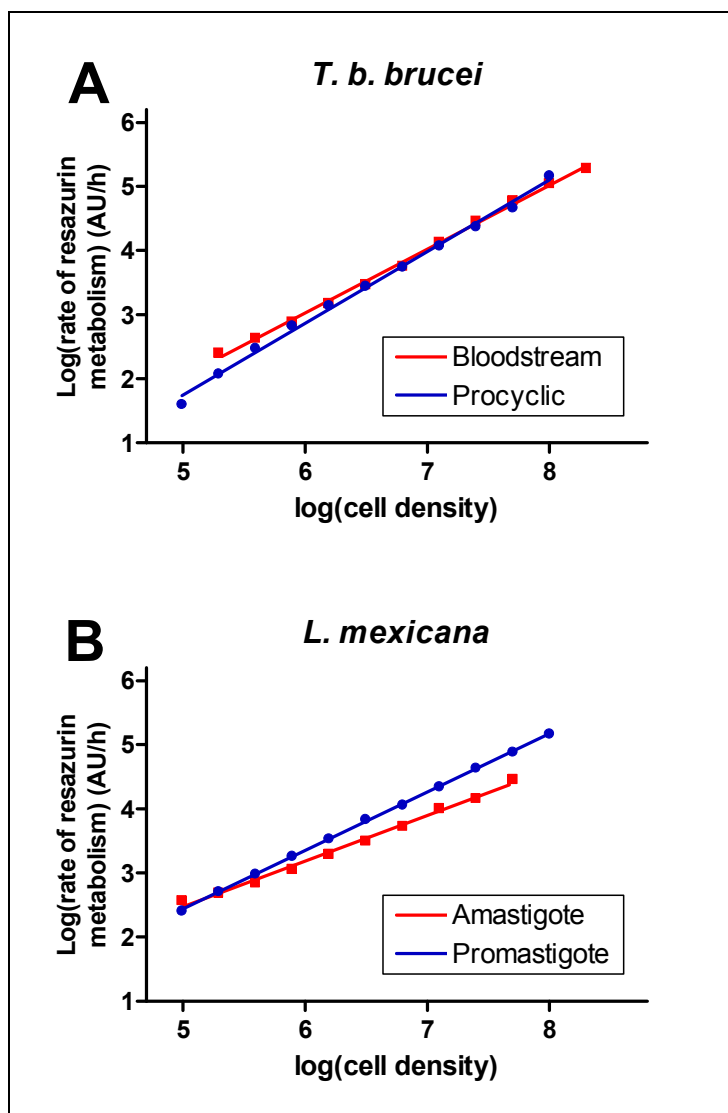


Figure 3.7: Rate of fluorescence development during incubation of parasites with resazurin. Fluorescence was monitored over 24 hours in the presence of various cell densities, the initial rate of resazurin metabolism was determined by linear regression of the first phase of increasing fluorescence (correlation coefficient ≥ 0.99). (A): *T. b. brucei* procyclics or bloodstream forms; (B): *L. mexicana* promastigote or amastigote forms.

3.3.5 Propidium iodide as an endpoint-assay indicator; comparison with the whole-cell *in vitro* efficacy assay.

In order to assess the potential for using propidium iodide fluorescence (in conjunction with digitonin as a cell lysis agent) in an *in vitro* high-throughput screening assay, a comparison with the commonly used resazurin reduction method was conducted using melarsen oxide as the test compound. Since different laboratories use differing seeding densities of trypanosomes to start their efficacy evaluations (e.g. Rätz, B. et al, 1997; Wallace, L. J. M. et al, 2002), potentially leading to different outcomes (Chris Ward and Professor Mike P. Barrett (University of Glasgow), personal communication), a range of starting densities was compared. For both assays, *T. b. brucei* bloodstream forms of strain 427 were incubated for 72 hours in HMI-9 media. To one set of cultures, resazurin was added after 48 hours, and fluorescence was read after an additional 24 hours incubation. To the second set, PI and digitonin were added to a final concentration of 6 µg/ml (9 µM) and 20 µM respectively after the cells were incubated with the differing concentrations of melarsen oxide for 72 hours. Fluorescence was then read after a further 60 minutes incubation.

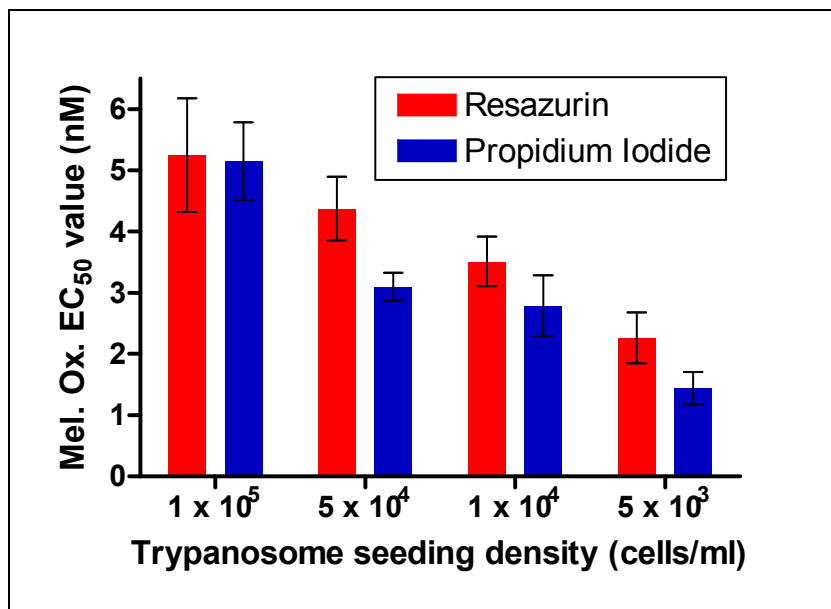


Figure 3.8: Trypanocidal effects of melarsen oxide on *T. b. brucei* bloodstream forms measured by propidium iodide or resazurin reduction assay at different seeding densities. Melarsen oxide concentrations reducing fluorescence by 50% (EC₅₀ values) were determined using the standard resazurin reduction protocol (red bars) or the propidium iodide-based protocol (blue bars), using different trypanosome densities at the start of the experiment. Results are the average of three independent determinations and error bars are standard errors.

The melarsen oxide EC_{50} values derived from the PI/digitonin method were in close agreement with those derived from the whole-cell *in vitro* method (Figure 3.8) and also similar to data previously published (Matovu, E. et al, 2003). Although some disparity was apparent when the efficacy values were compared between the differing trypanosome seed densities, the degree to which this affected the actual EC_{50} values was the same for both methods. Thus, the results derived using the propidium iodide method appear to be directly comparable to those from the whole-cell *in vitro* method as long as the starting density of trypanosomes is the same.

3.4 Discussion

The data generated from the standard curves demonstrate that propidium iodide produces a strong fluorescent signal when incubated with trypanosomal genomic DNA. There is also enough genetic material in lysed whole trypanosomes to provide PI with a substrate with which to bind and fluoresce. Based on an estimated DNA content of 7.8×10^7 bp per nucleus of *T. b. brucei* s427 (Melville, S. E. et al, 2000) and a G+C content of 46.4% (Berriman, M. et al, 2005), it can be worked out that 10^7 trypanosomes of *T. b. brucei* s427 have a theoretical content of 0.88 μ g nuclear DNA. Figures 3.1 and 3.2A show that, using 6 μ g/ml PI, the fluorescence signal of 10^7 trypanosomes was almost identical to that of 4 μ g of *T. b. brucei* genomic DNA. This probably indicates that PI binds to additional *T. b. brucei* material, possibly including RNA and kinetoplast DNA. It can be concluded that the assay is highly sensitive and linear and thus can be used for quantitative analysis of cell numbers.

The preliminary measurements were performed in a standard serum-free Assay Buffer (AB) (De Koning, H. P. et al, 1998), as sensitivity in the HMI-9 culture medium was much reduced, apparently as a result of quenching of the fluorescent signal. The use of a FLUOstar OPTIMA fluorimeter (BMG Labtech, Aylesbury, UK) greatly increased sensitivity, with the highest sensitivity achieved by using a clear buffer, such as AB, and a sensitive instrument with adjustable signal gain. This results in an operational range over three orders of magnitude and, importantly, encompassing physiologically relevant cell densities.

The observations using PI monitoring of cell survival are entirely consistent with the effects of the same drugs monitored using the classical spectrophotometric lysis assay (Fairlamb, A. H. et al, 1992) performed in parallel. However, the PI assay has several advantages over this alternative. The traditional assay monitors the scatter/absorbance of light by the rapidly moving flagellates, whereas the PI assay monitors plasma membrane integrity, which is a much better proxy for parasite survival and more universal, as well as also applicable to non-motile cells including *Leishmania* amastigotes. While the light scatter assay works well for arsenicals (Matovu, E. et al, 2003; Fairlamb, A. H. et al, 1992) and could possibly be used for the slow-acting diamidines, any test compound that depletes the parasite of ATP or otherwise acts on the flagellar

motion is indistinguishable from one that actually kills the cell. This is because loss of motility will result in live parasites disappearing from the spectrophotometer beam, as well as those cells killed outright by drug action, due to gravity-assisted precipitation. The PI assay does not suffer this drawback. Moreover, this assay is much more sensitive: the data in Figure 3.4A were obtained using 5×10^6 cells/ml or 1×10^6 cells/trace, whereas the data in Figure 3.4B were obtained using 2.7×10^7 cells/ml in a 1 ml volume.

However, it is clear that even in the absence of drug-induced cell death, a slow increase in fluorescence is observed over the course of the PI assay (Figures 3.4A and 3.5). This could be the result of either a slow rate of uptake by the parasites through endocytosis or perhaps the same transporters that mediate uptake of the dications isometamidium and pentamidine (Delespaux, V. and De Koning, H. P., 2007), or because of natural turnover of cells in the population, leading to some spontaneous cell death in the population over six hours.

The PI assay is more suited to a 96-well plate format and higher throughput, than the light scatter/absorbance assay which is performed in 1 ml cuvettes. In the case of a plate reader spectrophotometric assay the cells would still precipitate to the bottom of the well upon loss of motility as well as cell debris from lysed cells, but this would not remove them from the beam and thus reduce the observed change in absorbance in comparison to measuring horizontally through a cuvette. The PI assay is superior to the light scatter assay by more accurately monitoring cell death, requiring far fewer cells and allowing a much more efficient high-throughput system. The acute effects on parasite viability can be determined for 47 compounds (alongside positive and negative controls, and controls for autofluorescence of the test compound with PI) on a single 96-well plate.

The increased capacity of the PI assay compared to the spectrophotometric assay was utilised to help determine protocols for a large number of test compounds for further biochemical analysis (Chapter 4). The assay provided valuable information on the most appropriate concentrations and incubation times to give the best opportunity to detect intracellular changes. It also demonstrated, through the obviously different speeds of action, either alternative intracellular targets or modes of compound uptake between the

Series 1 and GJS compounds (Figure 3.5). The differences in timings between the PI and light scatter/absorbance assay for Compound 48 are probably due to the length of time required for the cell debris of the immediately lysed trypanosomes sinking below the light beam. This highlights the superiority of an assay that cannot be confounded by the time between cell death and sedimenting on the floor of the cuvette.

The metabolism of resazurin data shows that, for the endpoint *in vitro* efficacy assay, the different incubation times required for various organisms with this compound probably reflect differences in the rate of resazurin metabolism (influenced by temperature of culturing), rate of hydroresorufin formation and the doubling time of the particular cell type in culture. The rather complex interplay of these parameters makes the adaptation of this assay for new cell types rather cumbersome. The resazurin *in vitro* efficacy assay cannot be used to assess acute effects, yielding insufficient signal over short time intervals and being insufficiently sensitive to record relatively small changes in cell survival that are immediately apparent with the PI real-time assay. In addition, the resazurin-based end-point assays require a dilution range of test compound in order to yield usable information, a single concentration not distinguishing between, for instance, (a) all cells dead at the end of the assay but having survived long enough to generate a considerable signal, (b) few cells surviving to the end of the incubation time, and (c) inhibition of growth, resulting in fewer cells and hence a lower signal. The robustness of a PI based approach to assessing cell numbers allows more flexibility in assay design, with the compound being equally reliable when used as an endpoint *in vitro* efficacy assay compared to the resazurin assay.

Chapter IV

4 cAMP levels in trypanosomes incubated with putative PDE inhibitors

4.1 Introduction

In this chapter the effect on the intracellular concentration of cAMP in bloodstream form trypanosomes is monitored to determine whether the putative phosphodiesterase inhibitors can impact on the cAMP signalling pathway.

cAMP, produced by the adenylyl cyclase enzymes from ATP, activate downstream effector proteins. In mammalian cells this allows them to respond to an extracellular stimulus. In order to control the activation of these effector proteins, phosphodiesterase enzymes modulate and contain the cAMP signal by hydrolysing cAMP to the linear AMP (Seebeck, T. et al, 2001). Although it is not currently known whether the adenylyl cyclases of *T. brucei* are constitutively active or need to be activated by a stimulus to produce cAMP, it has been shown that genetic disruption to the PDEs in trypanosomes results in an elevated intracellular cAMP concentration (Zoraghi, R. and Seebeck, T., 2002; Oberholzer, M., et al, 2007). An increase in cAMP on incubation with a test compound is strong evidence that that compound is inhibiting the phosphodiesterase enzymes in the trypanosome.

Two methods were employed to monitor the intracellular cAMP concentration. The first was based on an assay developed by Salomon, Y. et al, (1974), using tritiated adenine to label the intracellular adenine pool (including cAMP) after a pre-experiment incubation period with the bloodstream form trypanosomes. After incubation with test compound, metabolic activity in the cells can be stopped immediately by adding the sample to an acidic ice-cold stop solution. The cAMP is then separated from the cell contents via a series of Dowex and alumina columns and the radioactivity measured by a scintillation counter, allowing the intracellular concentration of cAMP to be expressed as a ratio of labelled-cAMP to labelled-adenine pool. Using this protocol allows the rapid sampling of the radio-labelled intracellular cAMP over short periods of time giving information on the immediate response of the trypanosomes to the putative PDE inhibitors.

The second method uses a commercially available enzyme-linked immunosorbant assay (ELISA) kit to directly quantify the cAMP concentration from a standard curve of known cAMP concentrations. While this method is much more sensitive

and accurate than the other, the protocol does not stop metabolic activity until after a centrifugation step. This means the assay is only appropriate to assess cAMP levels over a long incubation time.

Inducing resistance to a compound or drug under controlled circumstances can further the understanding of how the compound kills the trypanosome, and also how resistance may arise in the field (Bridges, D. J. et al, 2007; Barret, M. P. et al, 1995; Matovu, E. et al, 2003). A selection of compounds was cultured with bloodstream form trypanosomes at sub-lethal concentrations. Over a prolonged period of time, attempts were made to increase the maximum tolerated concentration of the compounds. A second approach started with the screening of a chemically mutagenised culture of trypanosomes with lethal concentrations of test compound. Those trypanosomes that survived were resistant to the compound and further resistance was induced by gradually increasing the concentration of the compound as in the first method. The resultant resistant cell lines were then assayed for cross-resistance by the standard whole-cell *in vitro* efficacy assay, as well as comparing the cAMP profile on incubation with PDE inhibitors to that of the parental wildtype strain.

4.2 Materials and Methods

4.2.1 Materials and trypanosome culturing

Test compounds were provided by Geert Jan Sterk of Mercachem, The Netherlands (GJS compounds) and by Otsuka Maryland Medicinal Laboratories (Series 1 compounds). Etazolate, dipyridamole, dibutyryl cAMP, 8-bromo-cAMP, chlorophenylthio-cAMP were obtained from Sigma Aldrich and Fluka; melarsen oxide was a gift from Sanofi-Aventis; pentamidine, phenylarsine oxide and diminazene were purchased from Sigma, Suramin was a gift from Brian Cover (University of Kent at Canterbury), nifurtimox was a gift from Mike Barrett (University of Glasgow), and cymelarsan a gift from Mike Turner (University of Glasgow). [³H]-adenine was obtained from either GE Healthcare or Moravek (specific activity 20-40 Ci/mmol) and the Direct Cyclic AMP Enzyme Immunoassay kits came from Assay Designs. Resazurin sodium salt was purchased from Sigma Aldrich and DE52 cellulose came from Whatman.

Bloodstream form *Trypanosoma brucei brucei* strain 427 wildtype were cultured *in vitro* as described previously (Chapter 2.2.1) in HMI-9 (Biosera). After the GJS-128 resistant R0.8 line, derived from *T. b. brucei* strain 427 wildtype, was obtained it was also cultured under the same conditions as the wildtype except that 0.4 µM GJS-128 was added to the HMI-9 to maintain drug pressure. Before assaying, the trypanosomes were grown in HMI-9 without GJS-128 for at least 6 days (approximately 18 generations). Cells were either taken directly from a culture in the late logarithmic growth phase for experimentation or centrifuged for 10 minutes at 610 rcf and room temperature with resuspension of the pellet in fresh HMI-9 to increase the cell density above that which can be reached unassisted.

Ex vivo *T. b. brucei* strain 427 wildtype parasites were obtained from infected Wistar rats with high parasitaemia and purified from the whole blood using DE52 cellulose columns (Lanham, S. M., 1968): DE52 cellulose was washed three times with PSG (20.21 g/l Na₂HPO₄.12H₂O; 0.47 g/l NaH₂PO₄.2H₂O; 2.49 g/l NaCl; 10 g/l glucose; pH = 8.0, phosphoric acid) and the pH adjusted to 8.0. The plunger was removed from a 50 ml syringe and a fine layer of glass wool was packed in to form the base for an approximately 3 cm layer of washed DE52 cellulose; the

cellulose was then washed again in the column with 100 ml of PSG. Whole blood from an infected rat was centrifuged for 10 minutes at room temperature and 610 rcf before removal of the Buffy Coat layer containing the parasites. This was then resuspended in PSG (pH 8.0) and loaded onto the DE52 cellulose column to remove any remaining blood cells. After the mixture had entered the cellulose matrix approximately 50 ml of PSG (pH 8.0) was carefully added and the eluate containing the purified trypanosomes collected. This cell suspension was centrifuged once, as above, the supernatant removed and the cell pellet resuspended in HMI-9/10% FCS culture medium for assaying.

4.2.2 Monitoring of intracellular cAMP using tritiated adenine

4.2.2.1 Cell preparation

T. b. brucei strain 427 wildtype trypanosomes were obtained *ex vivo* as described above and resuspended in HMI-9 medium. In order to ensure the maximum uptake of radio-labeled adenine, 100 μ M inosine was substituted as the purine source instead of hypoxanthine in the HMI-9 medium, as hypoxanthine can be metabolized to adenine. Cell density was established with a haemocytometer and sufficient trypanosomes for the entire experiment were added to more HMI-9 (+ inosine, -hypoxanthine) to give two 100 ml cultures in 150 cm² flasks. 1.48 MBq (40 μ Ci) of [³H]-adenine was added to each flask and the cultures incubated at 37 °C, 5% CO₂ for 2 hours. After incubation the cultures were poured into 50 ml falcon tubes and centrifuged at room temperature for 10 minutes at 610 rcf. The supernatant was carefully removed and reserved for appropriate disposal and the pellets were resuspended in 10 ml HMI-9 (+inosine, -hypoxanthine) to wash the trypanosomes. Centrifugation and washing was repeated twice more, with the final pellet being resuspended in HMI-9 (+inosine, -hypoxanthine) so as to give a cell density of 1×10^8 trypanosomes/ml. The cell suspension was then left to recover in a water-bath at 37 °C before the commencement of the assay. Due to the trypanosomes having been radio-labeled with [³H]-adenine it was deemed unsafe to conduct cell counts with a haemocytometer; it was assumed that there was no loss of cells during the wash and centrifugation steps and the required cell density was obtained by using the cell counts from before the addition of [³H]-adenine.

4.2.2.2 Assay set up

Assays were carried out independently on at least three separate occasions; 0.5 ml samples were taken in triplicate at each time-point for both the control culture and the culture incubated with the test compound. Metabolic activity was halted by dispensing the sample into an equal volume of ice cold STOP solution (5% trichloroacetic acid (TCA), 1 mM ATP, 1 mM cAMP) in a 1.5 ml microfuge tube and vortexing briefly. Samples were placed in the refrigerator for at least 30 minutes to complete the lysis of the trypanosomes and then centrifuged at maximum speed in a bench-top microfuge for 2 minutes (13,000 rpm). The supernatant was carefully pipetted into a fresh eppendorf and stored in a freezer at -20 °C until [³H]-cAMP extraction was commenced. The cell debris pellets and contaminated eppendorfs were disposed of as appropriate for tritiated radioactive waste.

4.2.2.3 [³H]-cAMP extraction

The isolation of [³H]-cAMP from the [³H]-adenine and its metabolites was achieved by sequential chromatography on Dowex and alumina columns. The [³H]-cAMP migrates more slowly through the Dowex ion-exchange column than the adenine metabolites [³H]-ATP and [³H]-ADP, and so can be retained in the Dowex after the careful elution of the latter. The [³H]-cAMP portion of the sample is further purified from any contaminants by further chromatography through an alumina column. When the sample is eluted from the Dowex onto the alumina, the solution is slightly acidic which results in the retardation of the [³H]-cAMP. Neutralizing the alumina with imidazole allows the release of the tritiated cAMP giving a more accurate assessment of the compounds relative concentration than by Dowex or alumina chromatography alone (Salomon, Y. et al, 1974).

Columns loaded with 2 ml Dowex 50WX4-400 ion-exchange resin (Sigma) were placed above 20 ml scintillation vials and the thawed out supernatant samples were loaded onto individual columns. 3 ml of water was gently added to the column and 4 ml of scintillation fluid was added to the vials once all the eluate had been collected below, after which they were capped and vortexed; these vials now contained the [³H]-ATP and [³H]-ADP fraction. The Dowex columns were then placed directly above a corresponding set of regenerated alumina

columns washed with 0.1 M imidazole and 10 ml water was added to each. Once the water had dripped through both sets of columns the Dowex columns were removed and the alumina columns were mounted above a fresh set of 20 ml scintillation vials. The [³H]-cAMP was eluted from the alumina by adding 6 ml of 0.1 M imidazole to each column. 8 ml of scintillation fluid was added to each vial and these were then capped and vortexed. All the scintillation vials were transferred to a Becton-Dickson beta counter for determination of radioactivity. Intracellular [³H]-cAMP levels were expressed as a percentage of the total pool of [³H]-adenine nucleotides.

4.2.3 Direct quantification of intracellular cAMP concentration using enzyme-linked immunosorbant assay (ELISA) kits

Intracellular cAMP concentrations were quantified by using the Direct Cyclic AMP Enzyme Immunoassay kit made by Assay Designs. Bloodstream form trypanosomes were cultured *in vitro*, as described above, and incubated at 37 °C with or without test compound at the concentrations specified at a cell density of 5 x 10⁶ trypanosomes/ml. At specific time points 2 ml samples were pipetted into microfuge tubes and centrifuged at 855 rcf for 10 minutes at 4 °C in a Heraeus Biofuge centrifuge. The supernatant was removed, the cell pellet was resuspended in 100 µl 0.1 M HCl and left on ice for 20 minutes to complete cell lysis. The samples were centrifuged at 16,000 rcf for 10 minutes and the supernatant transferred to a new eppendorf and stored in a freezer at -20 °C. cAMP content was assessed exactly as per the ELISA kit instructions from the manufacturers. Samples were taken in duplicate and all assays were conducted independently at least 3 times.

4.2.4 Induction of resistance to a panel of selected putative phosphodiesterase inhibitors.

Series 1 compounds 37, 72, 139 and 48 were doubly diluted in HMI-9 in 24-well plates and bloodstream trypanosomes of strain Tb427 wildtype were added to give a final volume of 1 ml and cell density of ~ 5 x 10⁴ cells/ml. These were then incubated at 37 °C and 5% CO₂ for 48 hours. After the first incubation the compounds were again doubly diluted in HMI-9 in 24-well plates as before to a final volume of 1 ml; 40 µl of culture from each well of the incubated plates was

then transferred to the corresponding well of the fresh dilutions which were subsequently incubated for a further 48 hours under the same conditions as above. After the second incubation the 24-well plates were inspected by light microscopy for cell viability: the highest concentration of each compound which allowed apparently normal cell growth was taken as the initial maximum tolerated concentration. For each compound trypanosomes from these cultures were passaged into wells in 24-well plates containing 1ml of HMI-9 only, HMI-9 plus the initial maximum tolerated concentration and HMI-9 plus 2x the tolerated concentration and incubated for 48 hours. The cultures were then visually inspected for cell viability and passaged again into wells containing the (new) maximum tolerated concentration and 2x the tolerated concentration, as well as a no drug control well. The cultures were maintained in this way continuously for over 24 months.

However, after 12 months of continuous culturing in sub-lethal concentrations of test compound it became apparent that gradual accumulation of resistance to these compounds was not progressing quickly. Therefore a new approach was taken using chemical mutagenesis. Methylmethanesulphonate (MMS; Sigma) was added to a 50 ml culture of Tb427 wildtype trypanosomes in late logarithmic growth phase to give a final concentration of 0.001% (v/v) and incubated at 37 °C and 5% CO₂ for 1 hour. The culture was then centrifuged at room temperature at an RCF of 610 for 10 minutes and the supernatant carefully removed and discarded in 1 M NaOH (to deactivate the mutagen). The pellet was resuspended in fresh HMI-9 and washed twice by centrifugation and resuspension in fresh HMI-9 as above. After the final wash the pellet was resuspended in 50 ml HMI-9 and incubated at 37 °C and 5% CO₂. During this incubation approximately 95% of the trypanosomes died due to the exposure to MMS. The remaining trypanosomes proliferate, some of which will have been mutagenised.

Once the surviving culture reached the late logarithmic phase of growth the cells were washed once, as above, and resuspended in fresh HMI-9 to a final cell density of approximately 1×10^5 cells/ml. The Series 1 compounds 37, 72, 139 and 48 were diluted in HMI-9 to 2x the final desired concentration (the approximate EC₅₀ value) and GJS-128 was diluted to 2x the desired final concentration of 0.1 µM. Mutagenised trypanosomes (0.5 ml at $\sim 5 \times 10^4$ cells/ml) were added to an equal volume of test compound dilution in multiple

24-well plates and incubated at 37 °C and 5% CO₂. The plates were inspected by light microscopy every 24 hours for 5 days for cell viability. Once the trypanosomes in a well reached the late logarithmic phase of growth they were passaged into a 24-well plate with fresh HMI-9 containing the test compound at the screening concentration as well as at 2x the screening concentration; a no drug control was also included. The cultures were then continuously maintained, as in the first resistance induction method, under gradually increasing, sub-lethal concentrations of the test compound.

4.2.5 Resistance and cross-resistance profiling using the resazurin reduction assay

Resazurin reduction assays were conducted, exactly as described previously (Chapter 2.2.1), using the GJS-128 resistant R0.8 cell line and its parental *T. b. brucei* 427 wildtype strain to establish the EC₅₀ values for GJS-128 and a range of other compounds.

4.3 Results

4.3.1 Monitoring of the immediate cAMP response after treatment with potential PDE inhibitors

In order to establish whether the compounds inhibited the trypanosomal phosphodiesterase (PDE) enzymes in live trypanosomes, changes in intracellular cAMP levels were monitored after incubation with a selected panel of putative PDE inhibitors using a method based on the uptake of tritiated adenine and the isolation of [³H]-cAMP from cell extracts. A pre-experiment incubation period, where the cells are labelled with [³H]-adenine, allows the trypanosomes to take up and incorporate the radio-labelled adenine into its many metabolites including cAMP and its precursor ATP. After incubation with the putative PDE inhibitors the cAMP is separated from the rest of the tritiated adenine pool by a series of columns, as described above (4.2.2). The radioactivity of the cAMP sample is then appraised in relation to that of the whole adenine pool and this ratio can then be monitored in samples from the same experiment taken over time or compared to those of a control culture.

On incubation with GJS-128 at 0.3 μ M there is a statistically significant rise in the intracellular cAMP concentration over the first 10 minutes (Figure 4.1A), compared to the control which was incubated with the drug solvent (DMSO) only. After just 5 minutes incubation with GJS-128 the cAMP concentration has risen by approximately 2-fold compared to the control ($P < 0.01$; unpaired, 1-tailed Student's T-test) and after 10 minutes the cAMP is approximately 3 times higher than that of the control ($P < 0.001$).

Each of the GJS compounds show a statistically significant increase in the intracellular cAMP concentration after 20 minutes incubation at a concentration of 1 μ M compared to the control sample, with GJS-128 giving the largest rise (Figure 4.1B). Compounds 212 and Lmj-61 also significantly raised the cAMP levels over 20 minutes (Figure 4.1B); however, a much higher compound concentration, in comparison to that used for the GJS compounds, is required for an effect to be measurable.

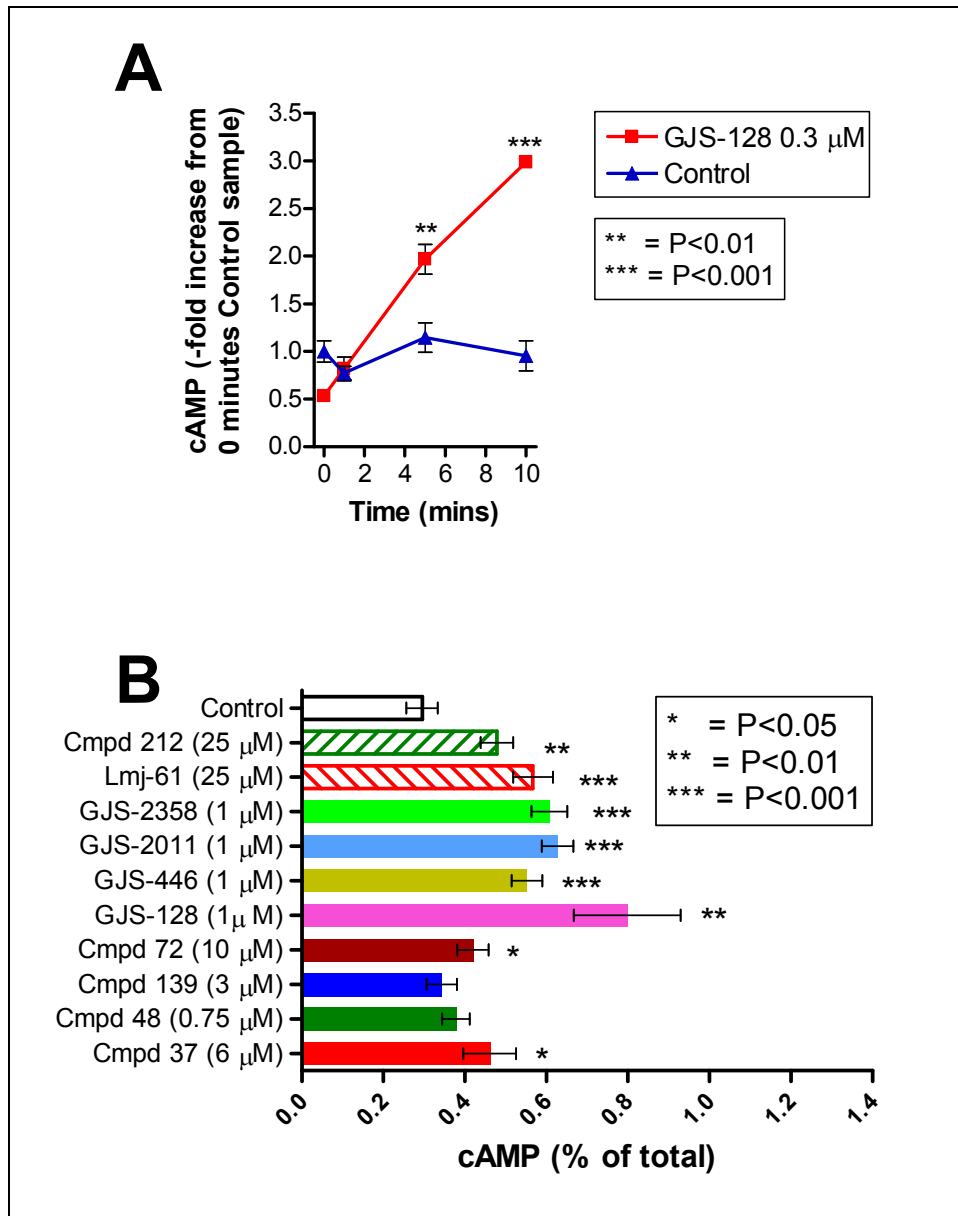


Figure 4.1: (A) Effect of 0.3 μ M GJS-128 on intracellular cAMP levels in bloodstream-form Tb427 wildtype trypanosomes pre-labelled for 2 hours with tritiated adenine. Intracellular cAMP was assessed by separating and comparing the tritiated cAMP to the total tritiated adenine pool by Dowex and alumina columns. The cells were incubated with or without GJS-128 at a cell density of 1×10^8 trypanosomes/ml in HMI-9 medium at 37 $^{\circ}$ C. The graph shown is representative of 3 separate experiments and the data expressed as -fold difference to the 0 minute Control value, with Standard Error bars for the triplicate data. The time-points showing statistically significant increases in cAMP from the control on average over the 3 experiments are also shown (asterisked), with the P-values calculated using the unpaired, 1-tailed, Student's T-test. **(B)** Bar-chart showing the average intracellular cAMP levels on incubation with various compounds for 20 minutes in bloodstream-form Tb427 wildtype cells, prepared as described in (A), at a cell density of 1×10^8 trypanosomes/ml in HMI-9 medium at 37 $^{\circ}$ C. The averages are from 3 separate experiments, sampled in triplicate, with Standard Error bars shown, with those compounds showing statistically significant increases in cAMP from the control asterisked. The P-values were calculated as described in (A) above. *, P<0.05; **, P<0.01; ***, P<0.001.

The concentrations used when assaying the Series 1 compounds were determined by the highest, but eventually lethal, concentration that the trypanosomes could tolerate for 3 hours under normal culturing conditions. Even with these

relatively high compound concentrations with regards to their *in vitro* trypanocidal activity, only moderate increases in the intracellular cAMP were measured and only Compounds 72 and 37 showed a statistically significant difference at the P-value threshold of 0.05 (Figure 4.1B).

4.3.2 Long-term effects of PDE inhibitors on intracellular cAMP

The tritiated adenine method of monitoring intracellular cAMP has a number of limitations that preclude its use for measuring cAMP concentrations over a period of hours. The most important of these is that after the trypanosomes have been removed from the pre-experiment incubation medium containing the [³H]-adenine, the radioactivity of the incorporated adenine pool diminishes by approximately one third every 30 minutes (personal observations). Conducting a cAMP monitoring experiment over a number of hours would result in radioactivity counts too low to provide accurate assessment unless an unfeasibly large cell number was sampled at each time-point.

In order to investigate the effects of the putative PDE inhibitors on the intracellular cAMP concentration over a longer period of time, enzyme-linked immuno-sorbent assay (ELISA) kits were used. These kits directly measure the concentration of cAMP in a sample from a standard curve made from known concentrations of cAMP thereby avoiding the need to radiolabel the adenine pool. As the kits measure the whole amount of cAMP in a sample instead of just the radio-labeled portion they can accurately quantify the intracellular concentration in a sample of trypanosomes of known quantity, which can be directly compared with results from separate experiments. The high sensitivity of the ELISA kits also means that a lower number of trypanosomes is needed for a detectable level of cAMP. This allows the cell density of the experimental culture to be greatly reduced, limiting environmental stress on the cells compared to the [³H]-adenine method.

A panel of putative trypanosomal PDE inhibitors, along with some known mammalian PDE inhibitors and trypanocides, were incubated with Tb427 wildtype trypanosomes for 3 hours, after which samples were assessed for cAMP content as described above (4.2.3). The control samples with just DMSO added, the solvent used to dissolve the test compounds, produced an average basal

intracellular cAMP content of 3.3 ± 0.2 pmol/ 10^8 trypanosomes (Table 4.1), which is consistent with data produced at other laboratories using similar methods (Zoraghi, R. and Seebeck, T., 2002; Oberholzer, M. et al, 2007). GJS-128 appears to be the most active compound tested with a 44-fold increase in intracellular cAMP (to 146 ± 12 pmol cAMP/ 10^8 trypanosomes) after incubation with $1 \mu\text{M}$ of the compound (Figures 4.2A and 4.2B; Table 4.1).

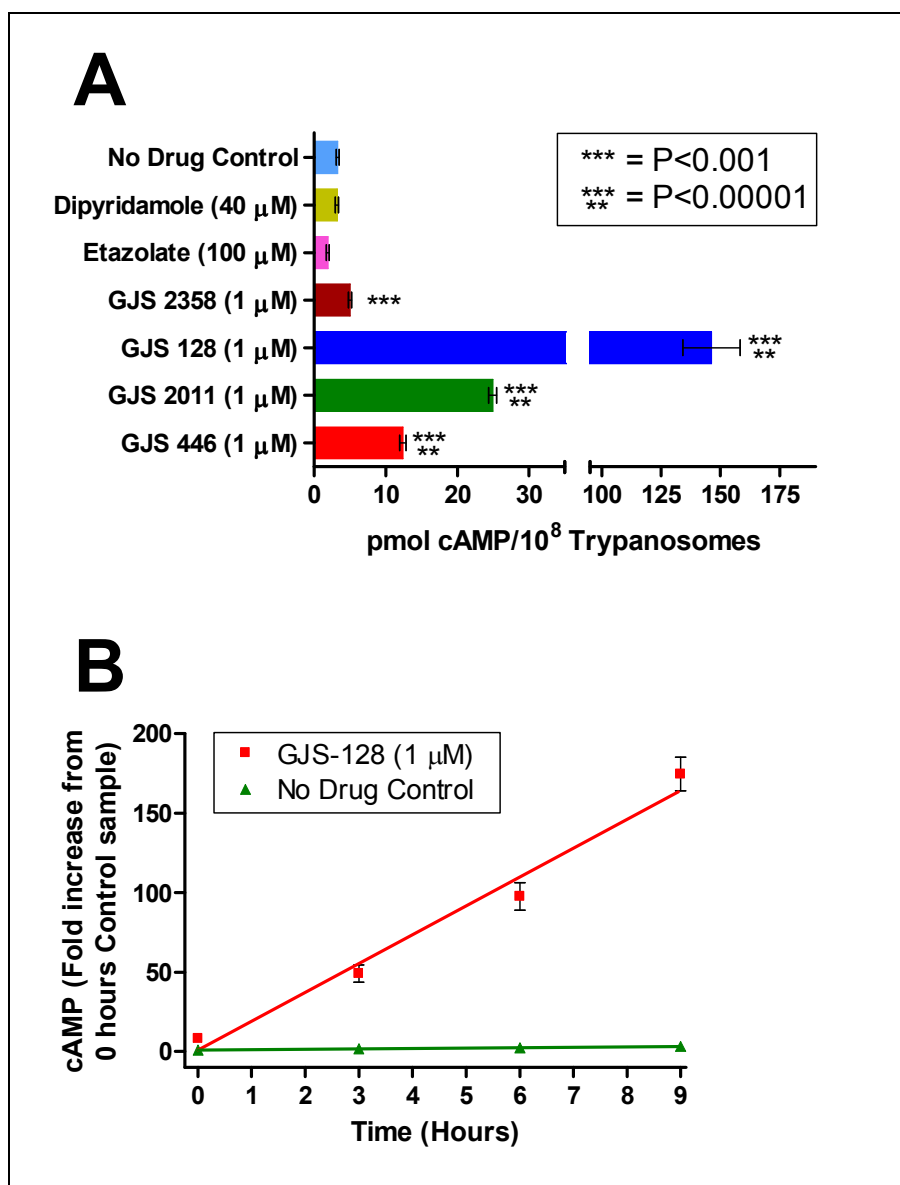


Figure 4.2: (A) Bar-chart showing the average intracellular cAMP concentration in bloodstream-form Tb427 wildtype cells incubated with various compounds for 3 hours. cAMP was measured in duplicate using an enzyme-linked immunosorbant assay (ELISA) kit as per kit instructions. The cells had been incubated with or without test compound at a cell density of 5×10^6 trypanosomes/ml in HMI-9 medium, at 37°C . Averages are from at least 3 independent experiments and the P-values were calculated using the 2-tailed, paired Student's T-Test. ***, $P < 0.001$; ****, $P < 0.00001$. (B) Graph showing the increase in intracellular cAMP in bloodstream-form Tb427 wildtype cells incubated with $1 \mu\text{M}$ GJS-128 in comparison with a control culture incubated with the test compound solvent DMSO only. The trypanosomes were incubated and cAMP measured under the same conditions as in (A). The data shown is the average of 3 independent experiments and analysed by linear regression using GraphPad Prism software. Error bars indicate Standard Errors.

University of Glasgow Compound Code	Concentration (μM)	cAMP concentration (pmol/ 10^8 cells)		Percentage of Control	P-values (Different from Control)
		Average	S. E.		
No Drug Control		3.3	0.2	100	
Etazolate	100	1.9	0.2	58	0.026
Dipyridamole	40	3.2	0.2	97	0.924
Dipyridamole	100	0.29	0.1	9	0.00025
GJS 446	1	12.4	0.4	377	<0.00001
GJS 446	0.1	4.8	0.3	146	0.0002
GJS 2011	1	24.9	0.6	758	<0.00001
GJS 2011	0.1	7.5	0.3	227	0.0001
GJS 128	1	146	12	4446	<0.00001
GJS 128	0.3	64.4	6.2	1958	<0.00001
GJS 128	0.1	40.6	2.4	1236	<0.00001
GJS 128	0.03	9.9	0.8	302	0.002
GJS 2358	1	5.0	0.2	152	0.0001
GJS 2358	0.1	3.0	0.3	90	0.359
37	6	2.1	0.1	63	0.005
37	0.6	1.4	0.1	41	0.0006
48	0.5	1.6	0.3	48	0.049
48	0.1	3.2	0.2	98	0.523
139	3	1.0	0.5	30	0.085
139	0.3	3.4	0.2	102	0.119
Pentamidine	1	3.1	0.1	93	0.993
Pentamidine	0.025	3.2	0.2	97	0.745
Melarsen Oxide	0.1	2.9	0.2	88	0.595
Melarsen Oxide	0.01	3.2	0.1	98	0.503
72	10	4.4	0.2	133	0.048
72	5	4.6	0.3	139	0.001
149	3	3.1	0.2	94	0.710
149	1	3.8	0.7	117	0.222
173	25	3.4	0.3	104	0.618
197	0.75	2.0	0.2	61	0.0004
197	0.15	3.1	0.3	94	0.093
197	0.015	3.1	0.3	95	0.343
198	0.75	3.7	0.1	112	0.314
198	0.15	3.0	0.4	90	0.101
200	100	1.5	0.1	46	0.002
201	25	3.7	0.2	113	0.043
201	5	3.4	0.2	103	0.619
204	25	4.7	0.3	142	0.006
204	5	3.8	0.6	115	0.212
Lmj-61	25	6.9	0.4	211	0.00001
212	25	3.7	0.3	112	0.00006

Table 4.1: Table showing the average intracellular cAMP concentration in bloodstream-form Tb427 wildtype trypanosomes after incubation with various compounds for 3 hours. cAMP was measured in duplicate using an ELISA kit as per manufacturer's instructions. Trypanosomes were incubated at 37 °C in HMI-9 at a starting cell density of 5×10^6 trypanosomes/ml. cAMP concentrations are averages of at least 3 independently performed experiments and the P-values are derived using the 2-tailed, paired Student's T-test for significant difference from the no drug Control: those values in green are significantly increased from Control and those in red are significantly decreased.

The rise in cAMP due to GJS-128 appears linear over 9 hours incubation at 1 μM ($P < 0.0001$; 2-tailed, paired Student's T-Test) (Figure 4.2B) with the intracellular cAMP concentration increasing 18 fold per hour (from 0 minute basal level) compared with an increase of just 1.24 fold per hour for the no drug control. The increase in cAMP after 3 hours incubation with GJS-128 is dose-dependent, with concentrations as low as just 30 nM enough to significantly raise the intracellular concentration 3 fold relative to the control (to 9.9 ± 0.8 pmol cAMP/ 10^8 trypanosomes, $P < 0.005$) (Table 4.1).

After 3 hours incubation at 1 μM , GJS-2011, -446 and -2358 also significantly increased intracellular cAMP, to 25 ± 0.6 , 12 ± 0.4 and 5.0 ± 0.2 pmol cAMP/ 10^8 trypanosomes respectively (Table 4.1), as did Lmj-61 and Compound 212 at 25 μM (6.9 ± 0.4 and 3.7 ± 0.3 pmol cAMP/ 10^8 trypanosomes respectively), as well as Compound 72 at 10 and 5 μM (4.4 ± 0.2 and 4.6 ± 0.3 pmol cAMP/ 10^8 trypanosomes, respectively). This confirms the increases observed over 20 minutes using the [^3H]-adenine method of monitoring cAMP changes. The only aberration from the radio-labeling method is with Compound 37 which appears to lower the intracellular cAMP concentration at 6 μM and also at 0.6 μM to 2.1 ± 0.1 and 1.4 ± 0.1 pmol cAMP/ 10^8 trypanosomes ($P < 0.005$ and < 0.001) respectively after 3 hours incubation.

Of the other Series 1 compounds tested only 201 and 204 showed a slight, but statistically significant increase in cAMP levels when incubated at 25 μM (3.7 ± 0.3 ($P < 0.05$) and 4.7 ± 0.4 ($P < 0.01$) pmol cAMP/ 10^8 trypanosomes, respectively).

The trypanocides pentamidine and melarsen oxide, compounds used in chemotherapy against African trypanosomiasis today, appeared to have no effect on cAMP concentrations at all, in spite of being assayed at concentrations many times their lethal threshold. Neither did the Series 1 compounds 139, 173 and 198. However Compounds 48, 197 and 200 each significantly lowered the cAMP concentration compared to the control at their highest concentrations tested to 1.6 ± 0.3 ($P < 0.05$); 2.0 ± 0.2 ($P < 0.0005$) and 1.5 ± 0.1 ($P < 0.005$) pmol cAMP/ 10^8 trypanosomes, respectively. Surprisingly, the mammalian phosphodiesterase inhibitors etazolate and dipyridamole, incubated at a concentration of 100 μM , also significantly lowered the intracellular cAMP levels in relation to the control

(to 1.9 ± 0.2 and 0.3 ± 0.1 pmol cAMP/ 10^8 trypanosomes ($P < 0.05$ and < 0.0005) respectively).

4.3.3 Induction of resistance to a panel of putative phosphodiesterase inhibitors.

After 2 years of continuous culturing in sub-lethal concentrations of test compound and attempting to gradually increase the tolerated concentration, no resistance to Compounds 72, 48 and 139 had developed. Only Compound 37 had induced a slight increase in the maximum tolerated concentration to, $1.4 \mu\text{M}$: just 4 times the EC_{50} value for that compound. However, when Compound 37 was assayed for its *in vitro* efficacy against this adapted culture, no significant difference from the parental Tb427 wildtype strain was observed (EC_{50} values = $1.0 \mu\text{M}$ versus $0.41 \mu\text{M}$, respectively; $P > 0.05$, unpaired Student's T-test).

Attempts to induce resistance to the Series 1 compounds by using the chemical mutagen methylmethanesulphonate (MMS) were also negative with no mutagenised trypanosomes surviving screening at the EC_{50} value for any of the compounds.

However, this method of inducing resistance was successful for GJS-128, with mutagenised trypanosomes surviving screening at $0.1 \mu\text{M}$ (GJS-128 EC_{50} value = $0.08 \mu\text{M}$). After just 2 months of continuously culturing the resistant cell line in sub-lethal, but gradually increasing concentrations, the maximum tolerated concentration for GJS-128 was above $0.8 \mu\text{M}$ (10-fold the EC_{50} value) and was termed the R0.8 cell line. After the resistant strain was cloned out by limiting dilutions under $0.8 \mu\text{M}$ drug pressure (2 clonal lines were obtained) and maintained with GJS-128 free medium, no loss of resistance was noted after 3 months of continuous culturing and experimenting. Resistance was also stable after storage in liquid nitrogen and subsequent thawing and culturing in HMI-9 medium. While biochemical and resistance characterization was performed with the R0.8 clonal line, further adaptation was attempted and after 4 months a culture tolerating $6.4 \mu\text{M}$ GJS-128 was obtained and stored in liquid nitrogen for future analysis.

4.3.4 Resistance and cross-resistance characterization of the GJS-128 resistant R0.8 cell line

University of Glasgow Compound Code	Tb427 WT EC ₅₀ Values (μM)		R0.8 EC ₅₀ Values (μM)		Resistance Factor	P-values (Different from Tb427 WT)
	Average	SE	Average	SE		
GJS-128	0.08	0.01	1.37	0.19	17.2	0.004
GJS-2358	0.37	0.02	5.39	1.55	14.7	0.045
GJS-2011	0.21	0.01	0.83	0.15	3.93	0.023
GJS-446	0.13	0.03	1.28	0.25	9.74	0.016
Dipyridamole	17.9	2.7	9.2	0.8	0.51	0.059
Dibutyl cAMP	263	13	1890	310	7.19	0.011
8-Bromo cAMP	271	8	1130	180	4.18	0.014
Chlorophenyl Thio cAMP	1.24	0.43	0.25	0.05	0.20	0.201
Suramin	0.021	0.001	0.016	0.000	0.74	0.001
Diminazene	0.022	0.007	0.011	0.001	0.48	0.133
Pentamidine	0.0016	0.0004	0.0014	0.0002	0.85	0.683
Cymelarsen	0.0038	0.0004	0.0038	0.0003	1.00	1.000
Phenylarsine Oxide	0.0008	0.0001	0.0009	0.0001	1.06	0.783
Nifurtimox	2.01	0.24	1.61	0.08	0.80	0.247
48	0.008	0.001	0.005	0.001	0.62	0.262
72	0.62	0.05	0.22	0.03	0.36	0.005
37	0.16	0.02	0.13	0.02	0.82	0.441
139	0.100	0.004	0.048	0.003	0.48	0.002
73	1.21	0.22	1.05	0.23	0.87	0.362
149	6.19	0.37	6.39	0.14	1.03	0.595
153	6.14	1.79	5.68	0.44	0.92	0.839
154	6.49	0.46	5.90	0.32	0.91	0.250
155	23.8	4.7	28.2	0.3	1.19	0.525
156	25.7	3.8	16.2	2.4	0.63	0.334
157	2.01	0.14	1.66	0.07	0.83	0.209
158	0.52	0.02	0.49	0.00	0.94	0.440
159	1.84	0.04	1.59	0.03	0.87	0.084
160	16.0	1.5	12.6	0.9	0.79	0.371

Table 4.2: *In vitro* efficacy values of putative phosphodiesterase inhibitors, and a range of known trypanocides and cAMP analogues, against Tb427 wildtype and the GJS-128-resistant R0.8 strain, as assessed by the resazurin reduction method. Trypanosomes were incubated with doubly diluted concentrations of the test compound for 48 hours in HMI-9 at 37 °C and 5% CO₂. Resazurin was then added and plates were incubated for a further 24 hours before fluorescence was measured. Data was graphed and EC₅₀ values (effective concentration that reduces fluorescence (resazurin metabolism) by 50%) were calculated using a non-linear regression sigmoidal curve fit (variable slope) on GraphPad Prism software. EC₅₀ values shown are averages of at least 3 independent experiments. Also shown is the fold-resistance displayed by the R0.8 cell line for each compound; P-values were calculated using the two-tailed, paired Student's T-Test (values shown in green are significantly resistant compared to the Tb427 wildtype and those in red are significantly sensitized).

To investigate the level of resistance achieved by the Tb427 wildtype-derived R0.8 cell line and to establish the presence, or otherwise, of cross-resistance to any known trypanosomiasis chemotherapies, *in vitro* efficacy values were

obtained using the resazurin reduction assays for both the parental and resistant strains against a panel of test compounds.

The R0.8 cell line displayed significant resistance to each of the GJS compounds: unsurprisingly the highest resistance was displayed against GJS-128, showing a 17.2-fold increase in the EC_{50} value from $0.079 \pm 0.01 \mu\text{M}$ against Tb427 wildtype to $1.4 \pm 0.2 \mu\text{M}$ against the R0.8 strain ($P < 0.005$) (Table 4.2). The compound showing the next highest increase in EC_{50} was GJS-2358 with a 14.7-fold increase from $0.37 \pm 0.02 \mu\text{M}$ to $5.4 \pm 1.5 \mu\text{M}$ in the R0.8 line ($P < 0.05$); GJS-446 and GJS-2011 displayed a 9.7 and 3.9-fold resistance, respectively ($P < 0.05$ for both).

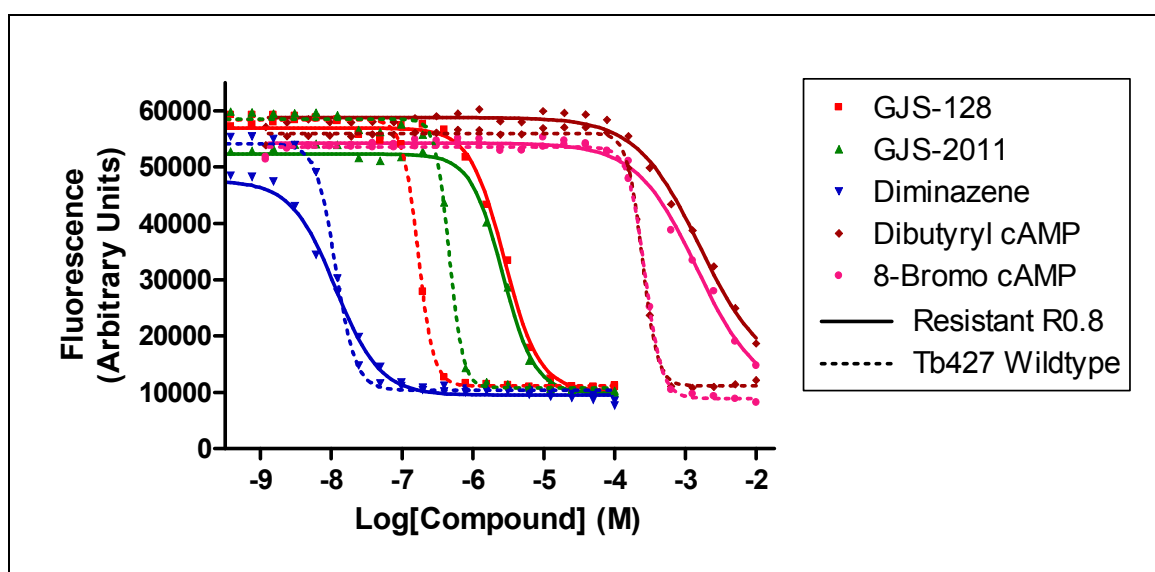


Figure 4.3: Graph of *in vitro* efficacy of selected compounds against the GJS-128 resistant R0.8 cell line and the parental Tb427 wildtype strain. Cell viability at various concentrations of test compound was assessed by measuring the fluorescence due to the reduction of the non-fluorescent resazurin by living cells to its fluorescent resorufin metabolite. Trypanosomes were incubated for 48 hours at 37 °C, 5% CO₂ in the presence of drug, after which resazurin was added with a further incubation of 24 hours under the same conditions before fluorescence was measured. Data was analysed by non-linear regression using a sigmoidal curve fit (variable slope) using GraphPad Prism software. The graph shown is representative of at least 3 independent experiments for each trypanosome strain with data generated from the resistant R0.8 cell line represented by a solid line and for the Tb427 wildtype by a dashed line.

Figure 4.3 shows a representative graph of the *in vitro* efficacy data from which the EC_{50} values were derived, with curves from the parental Tb427 wildtype and the R0.8 strains shown side by side for some selected compounds. For GJS-128 and GJS-2011 the curves produced when assayed against the R0.8 cell line have clearly shifted to the right compared to those from the Tb427 wildtype signifying an increase in the concentration of the compounds required to kill, or inhibit the growth of, the cells. The curves for the cAMP analogues dibutyryl cAMP and 8-

bromo cAMP for the R0.8 line have also moved markedly to the right: these compounds showed a 7.2 and 4.2-fold increase in EC_{50} values, respectively (Table 4.2) rising from $260 \mu\text{M} \pm 13$ against Tb427 wildtype to $1900 \pm 310 \mu\text{M}$ for dibutyryl cAMP ($P < 0.05$) and from $270 \pm 8 \mu\text{M}$ to $1100 \pm 190 \mu\text{M}$ for 8-bromo cAMP ($P < 0.05$). Curiously, another cAMP analogue, chlorophenyl-thio cAMP, appeared to show a 5-fold increase in sensitivity against the R0.8 trypanosomes. However, this proved not to be statistically different from the Tb427 wildtype data ($P > 0.2$).

There was no significant cross-resistance shown by the R0.8 trypanosomes to any of the current trypanosomiasis chemotherapies. However, a slight but statistically significant increase in sensitivity to suramin was observed, with the EC_{50} value reduced from $0.021 \pm 0.001 \mu\text{M}$ against the Tb427 wildtype to $0.016 \pm 0.0005 \mu\text{M}$ against R0.8 ($P < 0.005$).

Of the Series 1 compounds assayed against the R0.8 line there appeared to be no significant resistance displayed, however an increased sensitivity by the resistant strain was apparent with Compounds 72 and 139 ($P < 0.005$ for both) (Table 4.2).

4.3.5 cAMP response in T. b. brucei lines adapted to high concentrations of GJS-128

Since GJS compounds dramatically increase the intracellular cAMP concentration it was speculated that the resistance shown by the R0.8 line may have come about by an adaptation that allowed the strain to better control the cAMP levels on exposure to these compounds. To investigate whether this was the case the intracellular cAMP levels in the resistant trypanosomes and their parental Tb427 wildtype strain were determined after exposure to the GJS compounds as described, using the same ELISA-based protocol as before (4.2.3).

On incubation with various concentrations of GJS-128 over 3 hours there appeared to be no significant difference between the resistant and the Tb427 wildtype cell lines with respect to the levels of cAMP attained, nor in the speed with which they were reached (Figure 4.4A).

In a separate experiment, no statistical difference in cAMP levels in WT and R0.8 lines was observed after 3 hours incubation with a concentration of $1 \mu\text{M}$ of any

of the GJS compounds (Figure 4.4B). Yet, in both lines increases in cAMP levels compared to the no-drug control were highly significant, and similar to increases observed earlier (4.3.2). Incubations with both cell lines were performed in parallel so as to minimise inter-assay variation and there was no significant difference between the basal cAMP levels of the control samples for each strain. Also as before, the intracellular cAMP levels in both lines were unaffected by 3 hour incubations with 40 μM of the mammalian PDE inhibitor etazolate

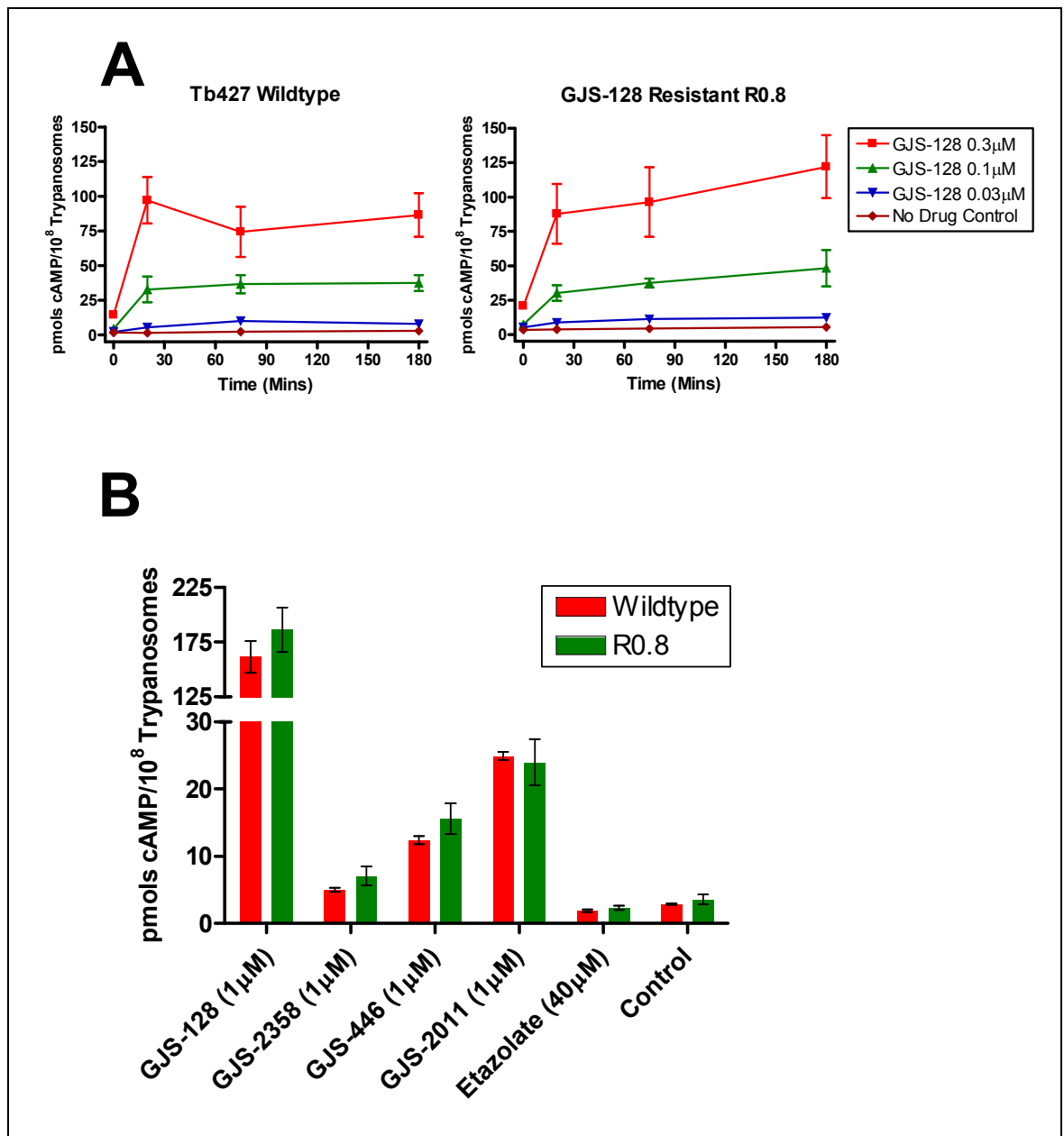


Figure 4.4: (A) The effect of various concentrations of GJS-128 on the intracellular cAMP concentration in Tb427 wildtype (left panel) and the GJS-128 resistant R0.8 cell line (right panel) over 3 hours. Graphs shown are representative of 3 paired, independent experiments performed in parallel. (B) Bar-chart showing the intracellular cAMP concentration in Tb427 wildtype (red bars) and GJS-128-resistant R0.8 trypanosomes (green bars) after 3 hours incubation with various compounds at specified concentrations. cAMP concentrations shown are averages of at least 3 independently performed experiments. For both (A) and (B) cAMP was measured in duplicate using an ELISA kit as per manufacturer's instructions. Trypanosomes were incubated at 37 $^{\circ}\text{C}$ in HMI-9 at a starting cell density of 5×10^6 trypanosomes/ml.

4.4 Discussion

It is apparent from the long and short term monitoring of intracellular cAMP concentrations that the majority of Series 1 compounds tested do not increase cAMP levels, even when incubated at concentrations lethal to trypanosomes. This strongly indicates that they are not phosphodiesterase enzyme inhibitors and kill trypanosomes via an alternative target. Of the four that did manage to significantly raise cAMP levels above that of the control the maximum increase was only around 40% (Table 4.1). For Compounds 72, 201 and 204 the concentration required to bring about the slight cAMP elevation was many times that of their *in vitro* EC₅₀ values, suggesting that, while they may inhibit PDEs at high concentrations, this is not their primary mode of action in the trypanosome. Although Compound 212 does inhibit recombinant TbrPDEB2 (Dr. Yasmin Shakur, Otsuka Maryland Medicinal Laboratories, personal communication), the fact that 25 µM only raised intracellular cAMP levels by 12% after 3 hours of incubation (Table 4.1), combined with an *in vitro* EC₅₀ value greater than 100 µM (Appendix 1), indicates that this compound may have difficulty entering the cell and reaching the PDEs inside the trypanosome.

Four Series 1 compounds significantly reduced the intracellular cAMP concentration compared to the control, suggesting that they either inhibited the production of cAMP by the adenylyl cyclases or stimulated its degradation by the phosphodiesterases. An alternative explanation, however, is that these compounds, while not at a concentration that would kill the cells over the length of the incubation, may have caused enough damage to a proportion of the trypanosomes to render them incapable of withstanding the stress of centrifugation after sampling. This would result in the content of these cells being lost to the ELISA measurement thereby lowering the apparent cAMP level of the sample.

Attempts to induce resistance to a panel of Series 1 compounds, by gradually increasing the maximum concentration tolerated by trypanosomes in *in vitro* culture, was unsuccessful after more than 2 years of continuous passaging. Even the use of chemical mutagens to increase the mutation rate did not result in resistance arising. This suggests that either there are multiple targets for these compounds - meaning that more than one mutation would have to occur

simultaneously for resistance to develop - or that the target(s) of these compounds is/are essential to parasitic survival. Clearly, if any of these compounds are deployed as clinical chemotherapies, the difficulty inducing resistance *in vitro* indicates resistance is unlikely to arise quickly in the field.

In contrast to those from Series 1, all four GJS compounds significantly raised intracellular cAMP concentrations in bloodstream form trypanosomes. These compounds were identified from a series developed at ALTANA Pharma for the inhibition of *T. b. brucei* PDEB1 and PDEB2, and displayed high affinity for the target recombinant enzyme which correlated very well with *in vitro* trypanocidal activity (conducted by Dr. Herrmann Tenor, ALTANA Pharma, and Prof. Thomas Seebeck, University of Bern; data not shown).

These data led to the testing of the effects of a subset of these compounds (GJS compounds) on intracellular cAMP levels and found that their dose-dependent effects (Table 4.1) again correlated well with their TbrPDEB2 K_i values (data not shown) and anti-trypanosomal EC_{50} values *in vitro* (Table 4.2 and Chapter 2, Table 2.6). GJS-128 acts quickly on the trypanosomes, significantly increasing cAMP levels after just 5 minutes incubation at 1 μ M, with the other GJS compounds significantly raising cAMP after 20 minutes incubation at the same concentration (Figures 4.1A and 4.1B). This indicates that the compounds can rapidly enter the cell to reach the trypanosomal PDEs. The rise in cAMP concentration is maintained for over 3 hours of incubation (Figure 4.2A and Table 4.1), and increases in an apparently linear manner over at least 9 hours with GJS-128 (Figure 4.2B) raising the intracellular cAMP concentration to levels only seen when both PDEB1 and PDEB2 are simultaneously knocked down by RNAi in bloodstream form trypanosomes (Oberholzer, M. et al, 2007).

This leads to the conclusion that the GJS compounds are genuine inhibitors of trypanosomal PDEs and that this inhibition results in an uncontrolled increase in cAMP, eventually leading to the death of the trypanosome. The fact that none of the Series 1 compounds, or known trypanocides such as pentamidine and melarsen oxide, do not increase cAMP, reinforces the conclusion that the effect seen by the GJS compounds is not just a response to general toxic stress. The lack of increase in cAMP levels by the mammalian PDE inhibitors dipyridamole and etazolate, even at very high concentrations, highlights the inherent

differences between the PDEs of the host and parasite cells. The observation that compound Lmj-61 also has an effect on trypanosomal cAMP levels (Figure 4.1B and Table 4.1) raises the possibility of the development of a chemotherapy effective against a broad spectrum of kinetoplastid species. Lmj-61 is an inhibitor of *Leishmania major* PDEs that was identified *in silico* by docking compound structures into the active site of the three-dimensional model developed from the crystal structure of *Leishmania major* PDEB2 (Prof. Hengming Ke, University of North Carolina, Chapel Hill, NC, USA: personal communication; Wang, H. et al, 2007).

Although an initial low level of resistance to GJS-128 was induced by heavily mutagenising a culture of trypanosomes with the mutagen MMS, passaging the resultant mutant line in gradually increasing concentrations of GJS-128 resulted in additional resistance arising remarkably quickly in comparison to the Series 1 compounds. After just two months of continuous culturing, a cell line (termed R0.8) was developed that could tolerate more than 10-fold the original *in vitro* EC₅₀ value, and after four months the maximum tolerated concentration was 80-fold that of the EC₅₀. This suggests that major resistance to a PDE inhibitor-based chemotherapy in the field might be problematic fairly quickly, however, for a more accurate assessment the induction of resistance to GJS-128 would need to be repeated without the assistance of the chemical mutagen.

The R0.8 cell line was characterised further, demonstrating that the resistance to GJS-128 was stable without drug pressure and not merely the result of a metabolic adaptation to the toxic stress. The cross-resistance profiling using the whole-cell *in vitro* efficacy assay indicates that all the GJS compounds likely hit the same target protein since resistance to GJS-128 results in resistance to the other GJS compounds as well (Table 4.2). No cross-resistance was observed for a panel of current trypanocides, or for the Series 1 compounds, which might open up the possibility of using a GJS compound in a combination therapy in endemic areas where resistance to current chemotherapies is prevalent.

Interestingly, significant resistance is displayed by the R0.8 line to the cAMP analogues dibutyryl cAMP and 8-bromo cAMP (Table 4.2 and Figure 4.3). This provides some evidence that the modification in R0.8 that gives resistance to GJS-128 may lie downstream of the phosphodiesterase enzymes in the cAMP

signalling pathway. If it were the enzymatic properties of the PDE enzymes that were altered in R0.8, then the hydrolysis-resistant cAMP analogues that bypass PDEs should have the same effect on the GJS-128 resistant trypanosome as against the wildtype. Further support for the source of resistance not coming from the PDEs comes from the examination of the cAMP profiles of the R0.8 and wildtype trypanosomes on addition of GJS-128 over 3 hours. There is no significant difference in increase of intracellular cAMP between the resistant and sensitive cell lines with 1 μ M GJS-128 at any of the time points sampled (Figures 4.4A and 4.4B) (2-tailed, paired Student's T-test). Neither is there any significant difference for any of the other GJS compounds after 3 hours incubation with 1 μ M, nor between the no-drug controls (Figure 4.4B). If resistance in the R0.8 line to the PDE inhibitor had arisen by modification to the PDE enzymes then one would expect either no, or a reduced, increase in intracellular cAMP on incubation with GJS-128 or the other GJS compounds. Since the speed of accumulation of cAMP appears to be the same in the resistant and wildtype trypanosomes one might assume that total adenylyl cyclase activity is also acting unaltered.

A further point of interest from the monitoring of intracellular cAMP on addition of GJS-128 is the difference in the dynamics of the response produced when sampled over different timescales. In Figure 4.2B the increase in cAMP concentration is apparently linear over 9 hours, however, for both the wildtype and the R0.8 cell lines the increase in cAMP appears to plateau after just 20 minutes (Figure 4.4A). One explanation for this apparent discrepancy is that there are two types of adenylyl cyclases activity present at the same time: one regulated by a negative feedback system, as seen for adenylyl cyclase A (ACA) in *Dictyostelium* (Saran, S. et al, 2003), and one that is not. The graphs in Figure 4.4A might depict the former AC type: when the cAMP rises rapidly on addition of the PDE inhibitor a negative feedback is activated, halting the production of further cyclic nucleotide. This would result in a plateau in cAMP concentration, rather than a return to basal levels, since the PDEs can no longer degrade it. The second AC type appears to produce cAMP more slowly than the first, or is merely the basal activity of the downregulated adenylyl cyclase. The resulting, slower rise in cAMP by this AC activity, once the PDEs are inhibited, is only detected when the former AC activity is deactivated, and measurements taken over long periods of time.

Chapter V

5 Further investigations into the mode of action of a panel of compounds & mode of resistance of the GJS-128 resistant R0.8 cell line

5.1 Introduction

This chapter investigates the effects of selected compounds on the cell cycle of bloodstream form trypanosomes, as well as on the gross intracellular morphology of the cells. Further examinations into the mode of resistance of the R0.8 strain of Tb427 trypanosomes, that is resistant to the PDE inhibitor GJS-128, are also undertaken.

Flow cytometry and fluorescent microscopy were performed to assess the impact on the replication cycle of trypanosomes exposed to selected test compounds. Flow cytometry is an automated method which, in this case, assesses the DNA content of individual fixed cells in samples stained with propidium iodide. The amount of fluorescence generated by propidium iodide binding to DNA is proportional to the amount of DNA contained within the cell. Trypanosomes maintain DNA in two organelles: the nucleus and the kinetoplast. Flow cytometry can quantify the proportion of cells in particular phases of cell replication; however it cannot distinguish between DNA in the nucleus and DNA in the kinetoplast. Using this method, trypanosomes are categorised into replication phases based on DNA replication of the nucleus outlined in Figure 5.1A. G1 is the non-dividing phase, S is where the DNA is replicated, G2/M is where the DNA segregate into the two nuclei and kinetoplasts before cytokinesis returns the mother and daughter cells to the G1 phase (McKean, P. G., 2003; Hammarton, T. C. et al, 2003).

In order to probe the effects of test compounds on kinetoplast replication, fixed trypanosomes were stained with DAPI and assessed for the configuration of the DNA containing organelles in relation to the rest of the dividing cell using a fluorescent microscope. Cells were categorised according to the number of nuclei and kinetoplasts as well as progression of the cleavage furrow as shown in Figure 5.1B.

The effect of the test compounds on the intracellular organelles was investigated using transmission electron microscopy. The trypanosomes were incubated with lethal concentrations of the compounds and cells were sampled before the trypanosomes were killed by the toxic effects of the compounds and fixed using a protocol based on standard methods (Hammarton, T. C. et al,

2007). Sections were viewed for gross abnormalities in the organelles or cytoplasm for clues as to the specific target(s) of the test compounds.

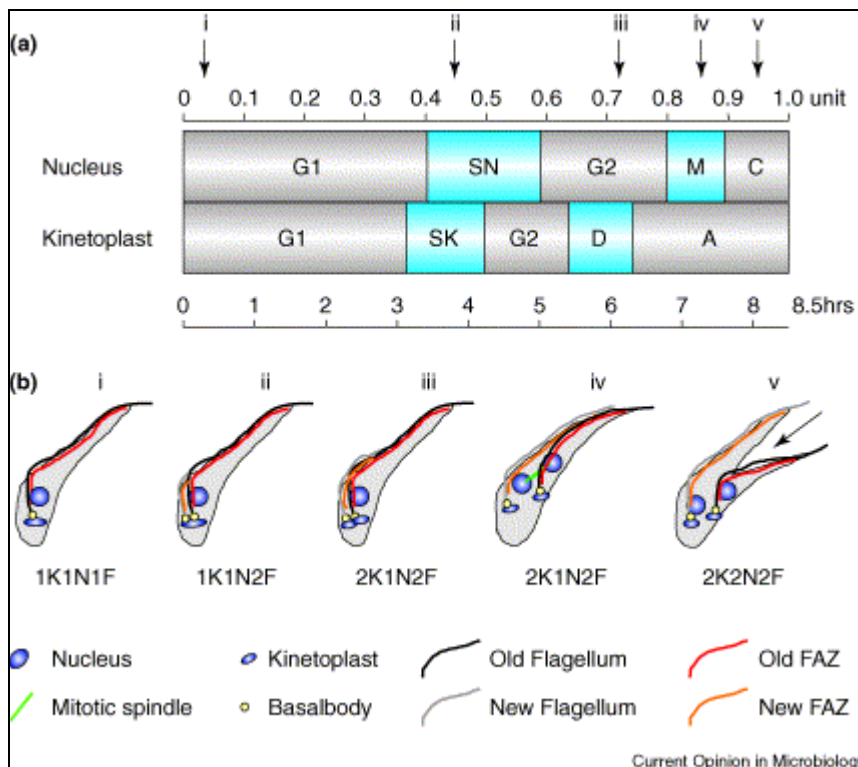


Figure 5.1: Cell division in procyclic form *Trypanosoma brucei*. Reproduced from McKean, P. G., 2003. (a) The trypanosome cell cycle is separated into nuclear and kinetoplast components. Cell cycle duration for exponentially growing procyclic trypanosomes is 8.5 h. Kinetoplast replication (SK) initiates before the nuclear phase (SN), but is considerably shorter and consequently kinetoplast segregation (D) occurs before the onset of nuclear mitosis (M). The phase annotated on the kinetoplast cycle as 'A' refers to the 'apportioning' phase during which basal bodies continue to move apart. (b) Schematic representations of trypanosome cells taken from various time points through the cell cycle. The black arrow indicates the direction and position of the cleavage furrow.

Finally, the phosphodiesterase B genes were both sequenced in the GJS-128 resistant R0.8 trypanosome strain. Evidence from Chapter 4 suggested the adaptation resulting in resistance to the PDE inhibitor lay downstream of the phosphodiesterase enzymes. In order to confirm this, the genes of the target proteins were cloned and sequenced and compared to those from the parental wildtype strain for any mutations that might affect enzyme function or inhibitor binding.

5.2 Materials & Methods

5.2.1 *Electron microscopy*

Tb427 wildtype bloodstream-form trypanosomes were cultured under normal conditions (37 °C, 5% CO₂) in a large volume of HMI-9 until the late logarithmic phase of population growth was achieved (approximately 1-2 x 10⁶ trypanosomes/ml). The cells were washed once by centrifugation at room temperature and 610 rcf, after which the cell pellet was resuspended in fresh HMI-9 to give a final cell density of 1 x 10⁶ trypanosomes/ml. After 15 minutes incubation at 37 °C and 5% CO₂ to allow the cells to recover, the culture was aliquoted into 150 cm² tissue culture flasks and the relevant volume of test compound dissolved in dimethylsulphoxide (DMSO) was added and mixed well to give the desired final compound concentration. For the control culture, an equal volume of DMSO without test compound was added to the flask. Series 1 compounds 37, 72, 48 and 139 were incubated at 0.625 μM, 1 μM, 0.25 μM and 0.5 μM respectively; GJS-128 was also incubated at 1 μM. The trypanosome cultures were then maintained at 37 °C and 5% CO₂ overnight.

After 20 and 24 hours incubation, a 10 ml sample of each culture was centrifuged at room temperature and 610 rcf, in a 15 ml tissue culture centrifuge tube, and the supernatant carefully removed. In a fume hood, 0.5 ml of 2.5% gluteraldehyde (diluted from 25% stock; Sigma) in 0.1 M phosphate buffer was carefully added down the wall of the tube (to avoid resuspension of the cell pellet) and left at room temperature for 10 minutes. The pellet was then gently detached from the wall of the tube and carefully agitated in the fixative before being left for a further 30 minutes at room temperature, after which the fixative was removed by pipette and 0.5 ml of the 0.1 M phosphate buffer added to rinse the pellet of any remaining gluteraldehyde fixative and the samples were stored overnight at 4 °C.

Further sample preparation was carried out by the Integrated Microscopy Facility within the university. The fixed pellet was broken into < 1 mm pieces, rinsed in fix buffer twice to remove aldehyde and fixed in 1% aqueous osmium tetroxide for 1 hour. Non-bound osmium residues were removed with several distilled water washes over 15 minutes, and 0.5% aqueous uranyl acetate added for 30

minutes. Cells were washed briefly in distilled water, dehydrated via an alcohol series (30,50,70,90 - 100% ethanol, 10 minutes each) then finally infiltrated in Epon/Araldite epoxy resin overnight, rotating at 200 °C. This was followed by fresh resin embedding and polymerisation of cells at 600 °C for 24 hours in silicon block moulds. 60 - 80 nm thick sections were routinely stained in uranyl and lead solutions and were then inspected by transmission electron microscopy (TEM) using a 120 kV Zeiss 912 energy filtering Transmission Electron Microscope.

5.2.2 Cell cycle analysis using flow cytometry

Tb427 wildtype trypanosomes were cultured under normal conditions until the late logarithmic phase of growth was reached. The cells were then washed once by centrifugation at room temperature for 10 minutes at 610 rcf, removal of the supernatant and resuspension of the cell pellet in HMI-9 with the cell density adjusted to 1×10^6 trypanosomes/ml.

After the cells had recovered for 15 minutes under normal culturing conditions, the experiment was started by the addition of the relevant concentration of test compound dissolved in DMSO (or equal volume of DMSO solvent without test compound for the control culture) and a 1 ml sample taken. The test culture was then maintained at 37 °C and 5% CO₂ for the duration of the experiment, except to allow further sampling. The sample was then centrifuged at 855 rcf for 10 minutes and at 4 °C in a Heraeus Biofuge centrifuge, after which the supernatant was removed and the pellet resuspended in a 1 ml solution of 70% methanol and 30% PBS straight from the fridge in order to fix the cells. Samples were taken at subsequent time-points and treated as described above and stored at 4 °C.

After storage, the samples were washed twice by centrifugation at 855 rcf for 10 minutes at room temperature, the removal of the supernatant and resuspension of the cell pellet in PBS. After the final centrifugation the cell pellet was resuspended in PBS containing 10 µg/ml of propidium iodide and RNaseA and incubated protected from light at room temperature for an hour. Flow cytometry analysis was performed using a Becton Dickinson FACSCalibur and using the FL2-A detector with an AmpGain of 1.75. Some data was further analysed using the ModFit LT software (Verity Software House).

5.2.3 DNA configuration assessment using fluorescence microscopy

Tb427 wildtype cells, cultured at 37 °C and 5% CO₂, were taken at the late logarithmic phase of growth and centrifuged at 610 rcf for 10 minutes at room temperature, the supernatant removed and the cell pellet resuspended in HMI-9 to give a cell density of 1 x 10⁶ trypanosomes/ml.

After recovering for 15 minutes, the experiment was started by the addition of the test compound dissolved in DMSO at the required concentration (or equal volume of DMSO solvent only for the control cultures). 50 µl samples were taken at regular time points and spread onto a glass microscope slide using a coverslip and allowed to air-dry. Once dry they were submerged in methanol at -20 °C in a Copelin jar and left to fix over night, after which the slides were removed, the methanol allowed to evaporate and stored in a slide box at 4 °C.

When required for DNA configuration assessment, the slides were rehydrated with approximately 1 ml of PBS for 10 minutes then the excess liquid was removed by tilting the slide onto a paper towel. 50 µl of PBS containing 1 µg/ml 4,6-diamidino-2-phenylindole (DAPI) and 1% (w/v) 1,4-diazabicyclo[2.2.2]octane (DABCO) was added to the slide and spread over the surface by affixing a coverslip and sealing with clear nail varnish. Slides were examined using a Zeiss Axioskop microscope with the requisite filters and images processed by a Hamamatsu digital camera with Openlab software. More than 500 trypanosomes in each sample were scored for their DNA configuration and placed into the following categories: 1N1K - having 1 nucleus and 1 kinetoplast; 1N2K - having 1 nucleus and 2 kinetoplasts; 2N2K (Early) - having 2 distinct nuclei and kinetoplasts but without an apparent cleavage furrow starting to divide mother and daughter cells; 2N2K (Late) - having 2 distinct nuclei and kinetoplasts, and with the cleavage furrow having made progress to division of mother and daughter cells but not having achieved full cytokinesis; and >2N2K - were cells have more than 2 nuclei and 2 kinetoplasts.

5.2.4 Sequencing of the *TbrPDEB1* and *TbrPDEB2* genes in the R0.8 cell line and its parental *T. b. brucei* 427 wildtype strain

5.2.4.1 Genomic DNA extraction

To provide cultures of trypanosomes that had been derived from a single parasite the *T. b. brucei* strain 427 wildtype and the R0.8 cell line were cloned out by limiting serial dilutions, with that of the R0.8 cell line conducted under selective pressure of 0.4 μM GJS-128. The genomic DNA was extracted from both strains in exactly the same way: a 50 ml culture was centrifuged at 610 rcf and resuspended in 1 ml HMI-9 before being transferred to a 1.5 ml eppendorf; this was centrifuged again at 380 rcf for 10 minutes. The supernatant was discarded and the pellet gently resuspended in 150 μl of TELT lysis buffer (50 mM Tris-HCl (pH 8.0), 62.5 mM EDTA (pH 9.0), 2.5 M LiCl, 4% (v/v) Triton X-100) and left for 5 minutes at room temperature. 150 μl equilibrated phenol:chloroform (Sigma-Aldrich) was added and mixed, then the eppendorf was centrifuged at 16060 rcf for 5 minutes. The upper, aqueous phase was removed and placed in a new eppendorf to which 300 μl of absolute ethanol was added, gently swirled and left for 5 minutes to precipitate the DNA. The eppendorf was then centrifuged at 16060 rcf for 10 minutes and the supernatant removed; the pellet was washed once with 70% (v/v) ethanol and re-pelleted at 16060 rcf for 10 minutes after which the ethanol was removed by pipette and the pellet left to air dry. The DNA was then dissolved in 100 μl TE buffer (10 mM Tris-HCl (pH 8.0), 1 mM EDTA (pH 8.0)) with RNaseA then quantified using a Nanodrop spectrophotometer (Thermo Fisher Scientific) and stored at 4 °C.

5.2.4.2 Amplification of *TbrPDEB1* and *TbrPDEB2*

Primers to amplify each gene by polymerase chain reaction (PCR) were designed by using the genome sequence for *Trypanosoma brucei* strain TREU927/4 GUTat10.1 from GeneDB as a reference sequence, since that of the 427 strain had not been completed. The sequences of both genes (+/- 500 bp) was downloaded and sections of DNA, approximately 20 bp in length, upstream and downstream of the genes were identified that gave only one region of 100% identity when the *T. brucei* contigs database was searched using BLAST. These sequences were used as the forward and reverse primers to amplify *TbrPDEB1*

and TbrPDEB2. For TbrPDEB1 the primer sequences were 5'-GAGCATCGGCAGCATAACCT-3' and 5'-TACATCTACCACCGGTCAAC-3' for forward and reverse primers respectively, with the forward primer's DNA annealing site located 89 bp upstream of the gene's open reading frame (ORF) and that of the reverse primer's located 38 bp downstream. For the amplification of TbrPDEB2, the forward primer sequence used was 5'-TGCAGATCCAGATAGCTGGGA-3', which annealed 34 bp upstream of the ORF, and that of the reverse primer was 5'-GCCTATCTTCGTCAACCAGG-3', which annealed 42 bp downstream.

The PCR reaction conditions were optimized so as to give a single product when run on an agarose gel by electrophoresis and the proof-reading polymerase enzyme KOD (Novagen) was used to limit the possibility of introducing errors into the product amplification. The exact reaction conditions differed only at the annealing temperatures for the amplification of each of the two genes (TbrPDEB1: 54.3 °C; TbrPDEB2: 56.7 °C) and closely followed the supplier's suggested reaction conditions with the addition of one extra step: after the final cycle, 0.2 µl of Taq polymerase was added to the reaction mix and maintained at 72 °C for 10 minutes. This final step was included because KOD produces a DNA reaction product with blunt ends, making it more difficult to ligate into a convenient vector; the inclusion of Taq for 10 minutes results in the addition of an 'A-overhang' allowing a simple ligation into the efficient vector pGEMT-easy, without compromising the fidelity of the proof-reading enzyme's amplification.

The PCR reactions' products were separated from the primers and visualized by electrophoresis on a 1% (w/v) agarose gel; the appropriate bands were then excised after confirming the DNA was of the expected size. The DNA was purified from the gel using a Gel purification kit from Qiagen, exactly as per the manufacturer's instructions, and ligated into the vector pGEMT-easy (Promega), again, as per the supplier's instructions. *E. coli* JM109 bacteria (Stratagene) were transformed with the pGEMT-easy vector containing the TbrPDEB1 or TbrPDEB2 gene, as directed by the suppliers, and plated out onto a Petri dish containing LB media agar supplemented with a selective concentration of ampicillin (Sigma) at 100 µg/ml. This resulted in only those bacteria transformed with the insert being able to tolerate the antibiotic and grow to form a colony overnight. Multiple colonies were picked and screened by PCR with Taq polymerase for the inclusion of TbrPDEB1 or TbrPDEB2, as appropriate, with the

positive colonies grown overnight in 5ml LB broth. The cultures were pelleted and the plasmid DNA extracted and purified using the 'mini-prep' function on a Qiacube robot, after which the product was again screened for the presence of the appropriate TbrPDE gene of interest by PCR.

5.2.4.3 Sequencing of the amplified TbrPDEB1 and TbrPDEB2 DNA

Samples of the purified plasmid DNA were prepared as directed and sent to Eurofins-MWG-Operon for sequencing. The maximum length of DNA they could sequence in one reaction was approximately 900 - 1000 bp so to sequence the genes in their entirety 4 over-lapping reactions were required for both TbrPDEB1 and TbrPDEB2. The first sequencing reactions were carried out using MWG's standard T7 and SP6 primers (T7: TAATACGACTCACTATAGGG; SP6: CATTAGGTGACTATAG), which anneal to the pGEMT-easy vector DNA that flank the insertion site of the ligated DNA. More primers were designed from the sequences that were returned for both genes to allow the completion of the sequencing of the full open reading frames. Sequencing Primer A (5'-TGGCCCGTGACAATCTTGATGAA-3') anneals to TbrPDEB1 starting at base-pair 683 of the ORF and Sequencing Primer C (5'-GATTACCACGCCTCTACGATGC-3') anneals to TbrPDEB2 starting at base-pair 550 of it's ORF. Due to the high degree of identity between TbrPDEB1 and TbrPDEB2, Sequencing Primer B (5'-GGCATAATCCACAACATGGT-3') bound to both genes (base-pair 2015 - 2035) and so was used in both sets of sequencing reactions for the two genes (see Figures 5.13 and 5.14 for diagrams showing the relative annealing positions for each primer).

In order to obtain the sequences of both alleles of the two genes the full open reading frame was sequenced from 9 bacterial clones containing the TbrPDEB1 and 9 clones with TbrPDEB2 from the R0.8 cell line; and from 9 clones containing the Tb427 wildtype TbrPDEB1 and 8 clones with TbrPDEB2. Each set of 4 sequence fragments was contig-ed and aligned using the Vector NTI Advance 10 software suite (Invitrogen).

5.3 Results

5.3.1 *Electron Microscopy*

The morphology of Tb427 wildtype bloodstream form trypanosomes incubated with lethal concentrations of test compounds was examined by transmission electron microscopy (TEM) in an attempt to identify any particular organelle or cellular process specifically targeted by the compound. After 24 hours of incubation under normal culturing conditions samples were taken and fixed, as described above (5.2.1), and delivered to the Integrated Microscopy Facility within the Biological and Life Sciences Faculty for specimen sectioning and staining. The ultrastructure of the treated trypanosomes was then inspected for any obvious intracellular disruption.

Figure 5.3 shows an electron micrograph of a trypanosome incubated with 0.625 μM Compound 37 for 20 hours, and is representative of a large number of cells inspected. The two most obvious aspects of the cell that appear abnormal are the massively enlarged flagellar pocket and the area of gross cellular disruption immediately to its right. A normal flagellar pocket and cytosol can be observed in the control image taken of trypanosomes incubated with DMSO only (Figure 5.2). It appears that incubation with Compound 37 induces the flagellar pocket to swell massively and also for part of the cytosol to become disorganised, possibly due to disruption to the acidocalcisomes, with evidence of their structural integrity being compromised at the bottom of figure 5.3.

Inspection of samples of trypanosomes incubated with 0.25 μM Compound 48 and 1 μM Compound 72 for 24 hours did not yield any pathology to the intracellular morphology (Figures 5.4 and 5.5). All of the sections investigated showed the organelles apparently intact and seemingly unaffected by exposure to a lethal concentration of the respective compounds, with those treated with Compound 72 apparently capable of undergoing cell division (Figure 5.5). However, cells incubated with 0.5 μM Compound 139 for 24 hours did show some disruption in the cytosol (Figure 5.6), but none of the organelles appeared affected.

1 μM GJS-128 has a very clear affect on the ultrastructure of trypanosomes. After 20 hours incubation a large number of cells displayed the components of

one or more flagellum inside the cytosol instead of extending out of the trypanosome from the flagellar pocket. Figure 5.7 shows an example of a cell incubated with GJS-128: the paraflagellar rod (PFR) and associated axoneme (A) of a flagellum can clearly be seen in longitudinal section towards the bottom left of the micrograph. Apparently separate PFR and axoneme assemblies can be identified at the extreme bottom and top of the cell. However, they all may be from the same flagellum undulating in and out of the section. Also observable are what appear to be microtubules from the flagellar attachment zone (FAZ) completely disassociated from both the flagellum and the subpellicular microtubule array. Another abnormal feature present is the large round vacuole-like structure in the centre of the image: this could be an enlarged flagellar pocket like that shown in figure 5.3 but not displaying its associated flagellum due to the angle of the section.

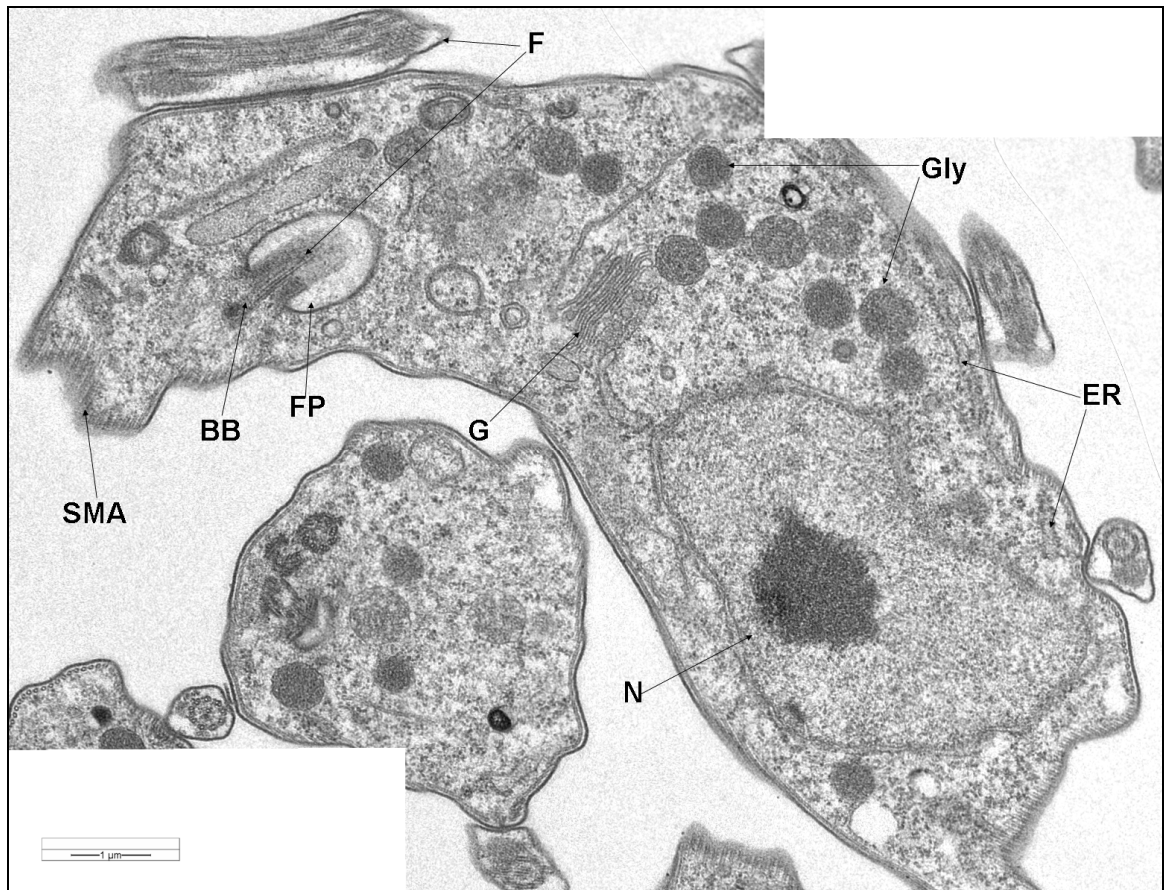


Figure 5.2: Transmission electron micrograph of a Tb427 wildtype bloodstream form trypanosome incubated for 20 hours with DMSO only as a No-Drug Control. (F) flagellum, (FP) flagellar pocket, (BB) basal body (Gly) glycosome, (ER) endoplasmic reticulum, (SMA) subpellicular microtubule array, (G) Golgi apparatus, (N) nucleus. Magnification: x 4000.

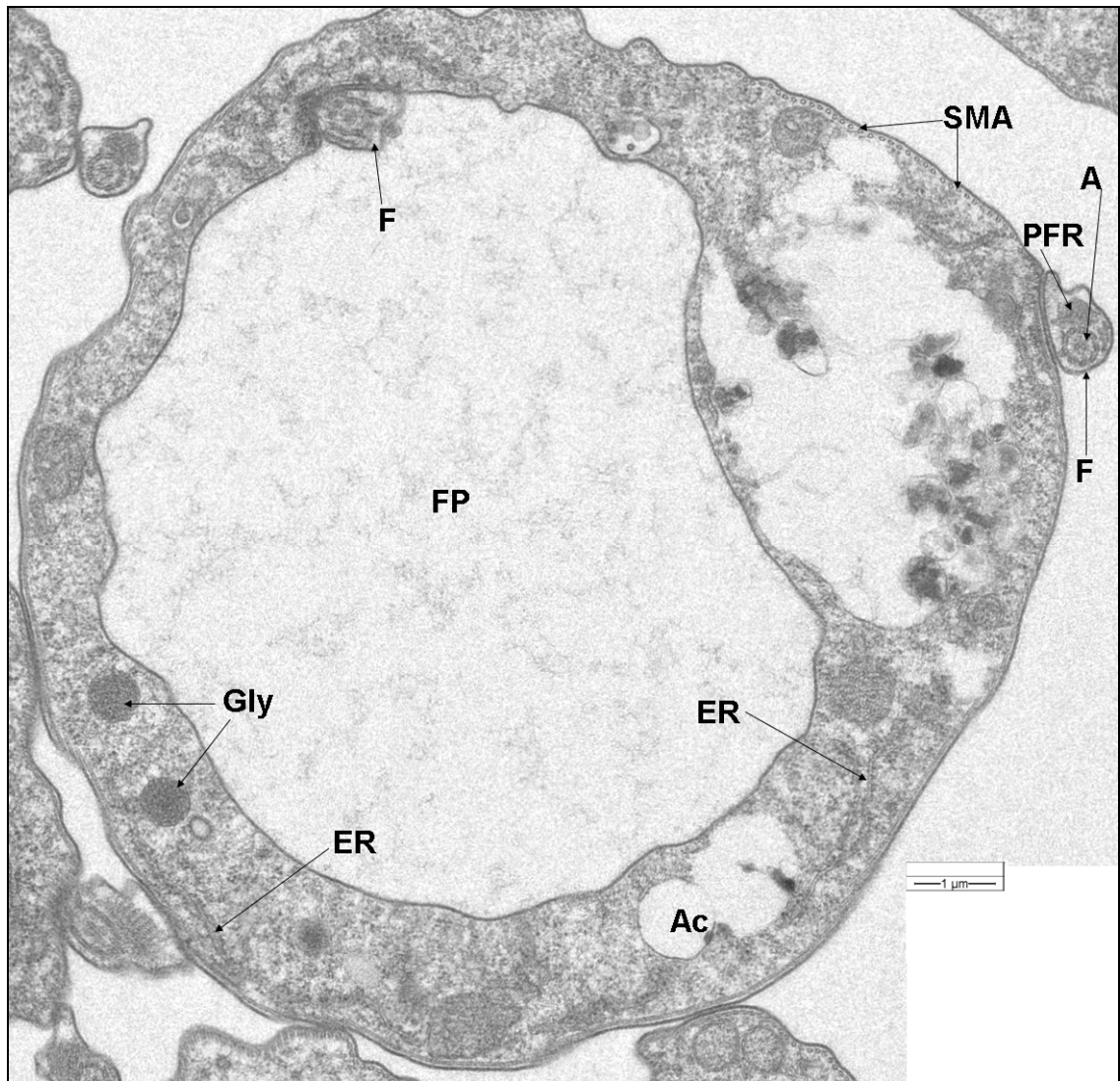


Figure 5.3: Transmission electron micrograph of a Tb427 wildtype bloodstream form trypanosome incubated for 20 hours with 0.625 μM Compound 37. (F) flagellum, (SMA) subpellicular microtubule array, (A) axoneme (PFR) paraflagellar rod, (FP) flagellar pocket, (Gly) glycosome, (ER) endoplasmic reticulum, (AC) acidocalcisome. Magnification: x 4000.

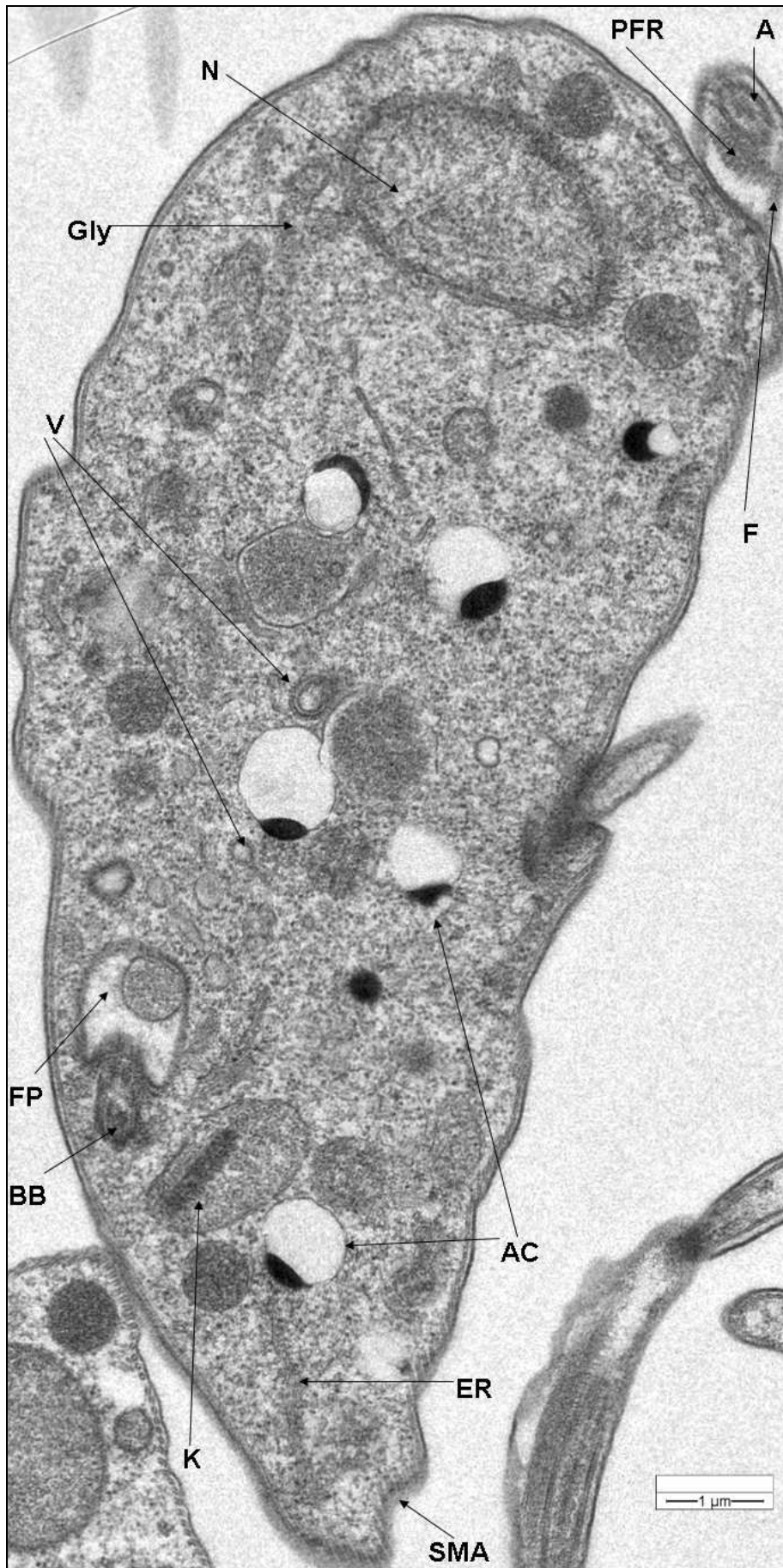


Figure 5.4: Transmission electron micrograph of a Tb427 wildtype bloodstream form trypanosome incubated for 24 hours with 0.25 μM Compound 48. (F) flagellum, (BB) basal body, (A) axoneme (PFR) paraflagellar rod, (FP) flagellar pocket, (K) kinetoplast, (N) nucleus, (V) clathrin coated vesicle, (Gly) glycosome, (ER) endoplasmic reticulum, (AC) acidocalcisome, (SMA) subpellicular microtubule array. Magnification: x 4000.

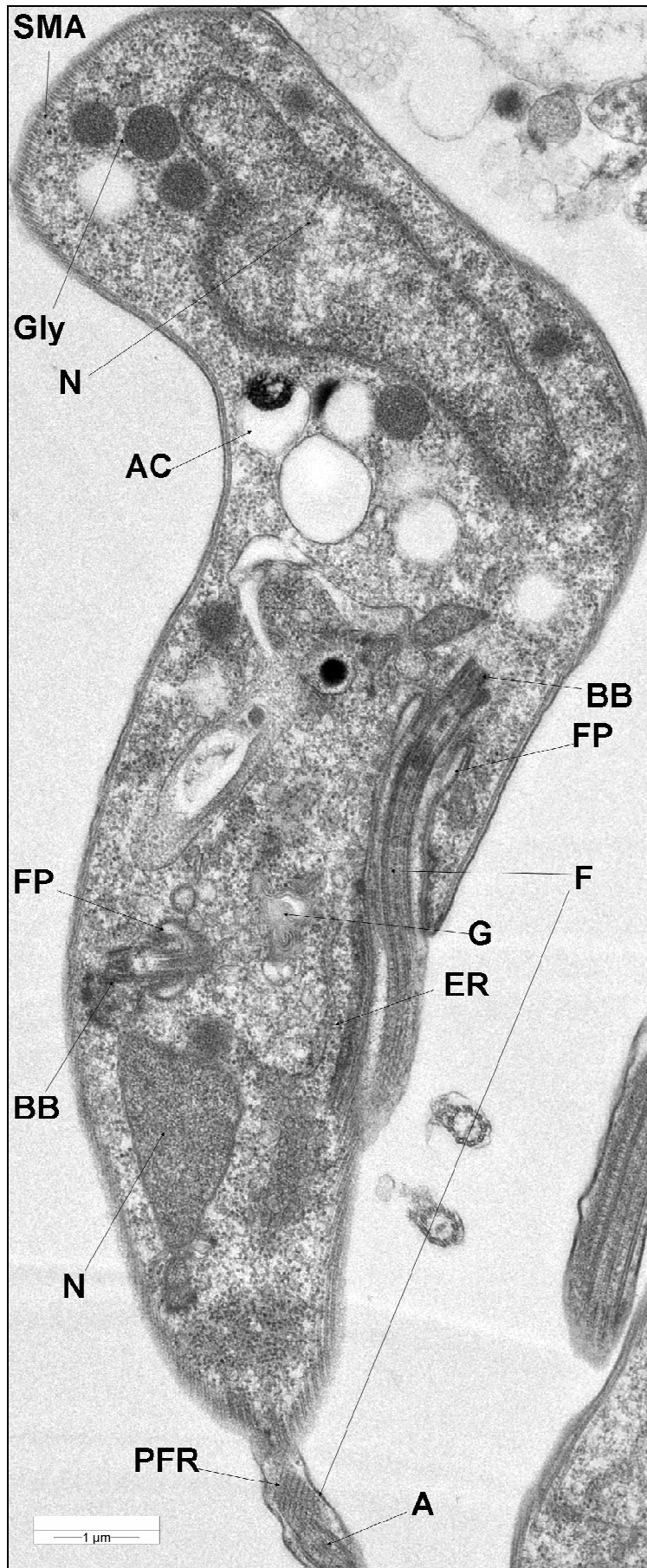


Figure 5.5: Transmission electron micrograph of a Tb427 wildtype bloodstream form trypanosome incubated for 24 hours with 1 μ M Compound 72 and undergoing cell division with two nuclei and basal bodies of separate flagella apparent. (F) flagellum, (BB) basal body, (A) axoneme (PFR) paraflagellar rod, (FP) flagellar pocket, (G) Golgi apparatus, (N) nucleus, (Gly) glycosome, (ER) endoplasmic reticulum, (AC) acidocalcisome, (SMA) subpellicular microtubule array. Magnification: x 4000.

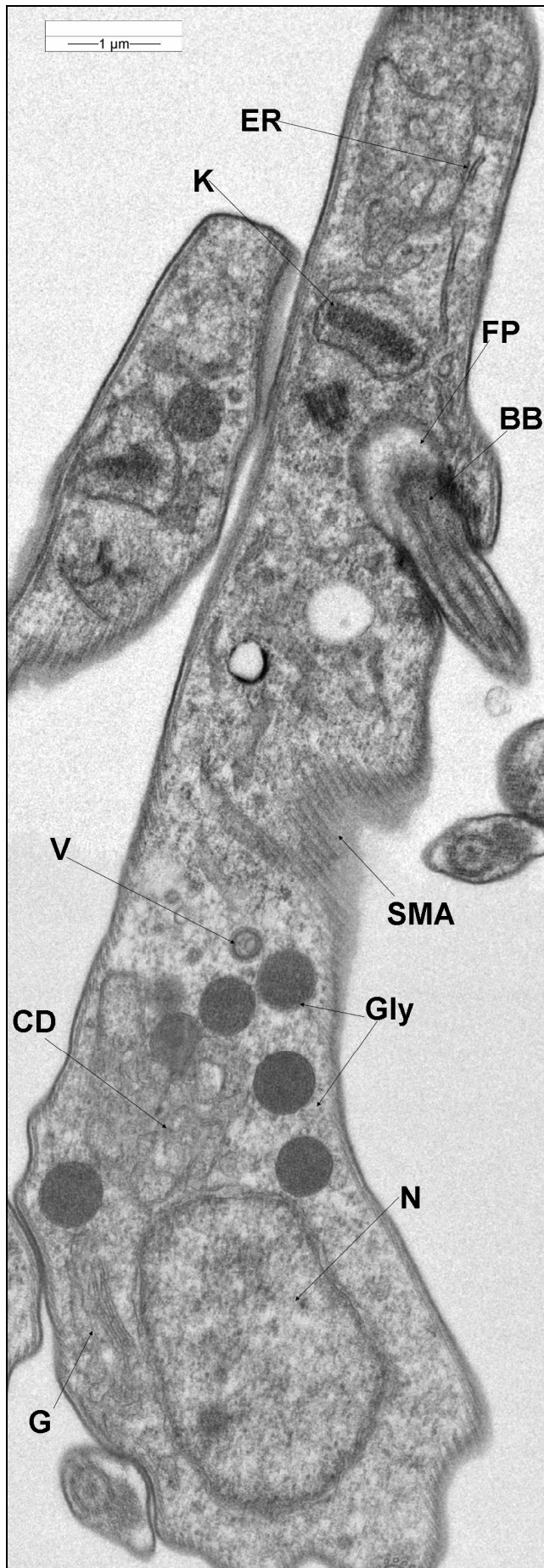


Figure 5.6: Transmission electron micrograph of a Tb427 wildtype bloodstream form trypanosome incubated for 24 hours with 0.5 μM Compound 139. (BB) basal body, (FP) flagellar pocket, (K) kinetoplast, (N) nucleus, (V) clathrin coated vesicle, (Gly) glycosome, (ER) endoplasmic reticulum, (SMA) subpellicular microtubule array, (G) Golgi apparatus, (CD) cytosolic disruption. Magnification: x 4000.

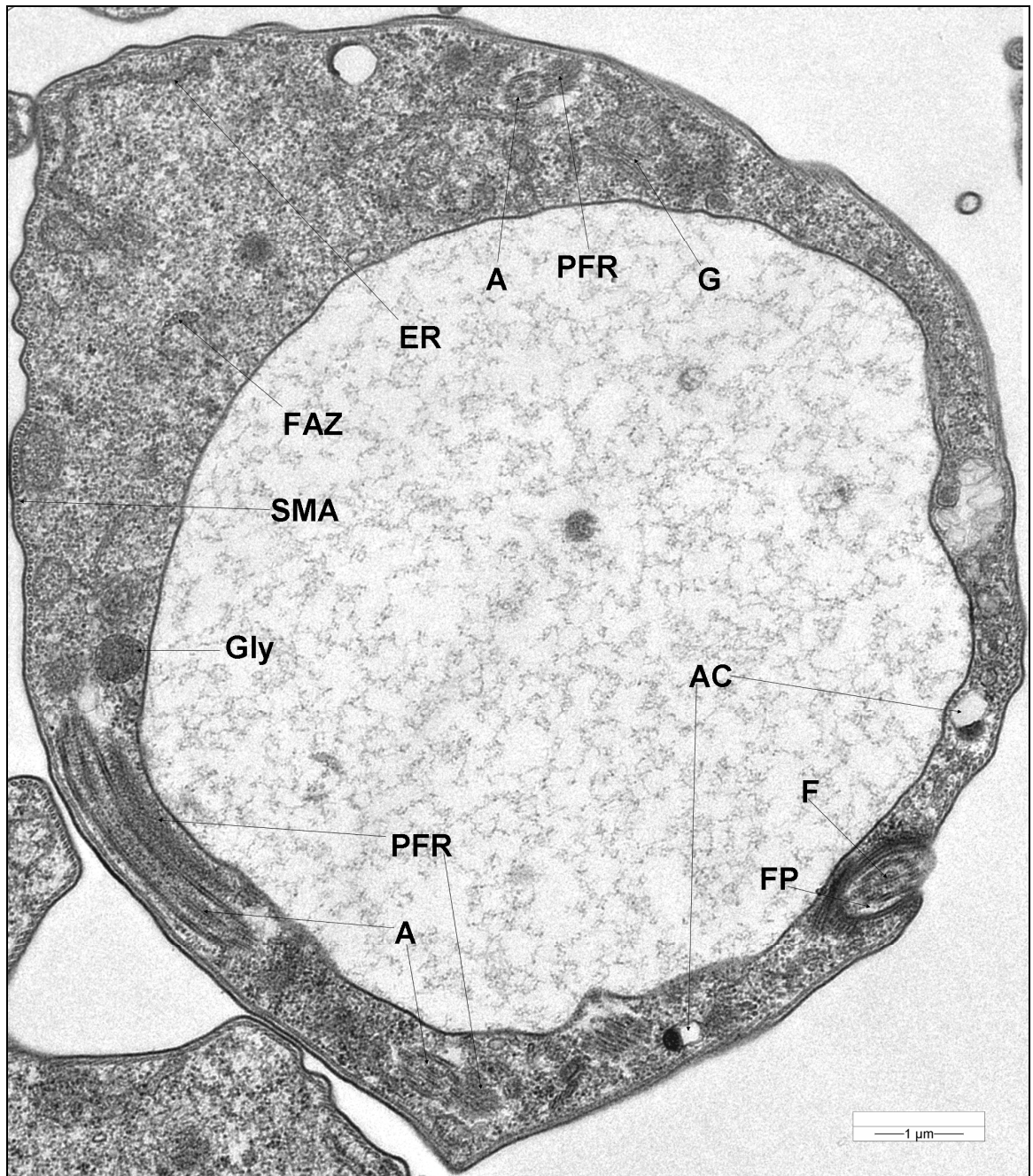


Figure 5.7: Transmission electron micrograph of a Tb427 wildtype bloodstream form trypanosome incubated for 20 hours with 1 μ M GJS-128. (F) flagellum, (A) axoneme (PFR) paraflagellar rod, (FP) flagellar pocket, (Gly) glycosome, (ER) endoplasmic reticulum, (AC) acidocalcisome, (SMA) subpellicular microtubule array, (FAZ) flagellar attachment zone (G) Golgi apparatus. Magnification: x 4000.

5.3.2 Cell cycle analysis using flow cytometry

In order to establish whether the Series 1 and GJS compounds had an effect on the cell cycle of trypanosomes the DNA content of Tb427 wildtype trypanosomes was monitored over time, with and without a panel of test compounds, using flow cytometry. Tb427 bloodstream form trypanosomes have a doubling time of around 6 hours (Forsythe, G. R., et al, 2009) but the cultures are asynchronous

with regards to cell-cycle stage so any block or specific disruption to replication may affect each individual cell at different incubation times. To account for this, samples were taken from test cultures up to 16 hours, and in some cases 24 hours, after the addition of test compound. The trypanosomes were assayed at a cell density of 1×10^6 cells/ml and, after the cells were fixed overnight with a methanol/phosphate-buffered saline solution, stained with propidium iodide. Propidium iodide binds to the nucleic acids of a cell and the intensity of its fluorescence is correlated to the amount of DNA, as the fixed cells are treated with RNase.

In Figure 5.8 the Tb427 wildtype cells were incubated with the highest, ultimately lethal concentration of Series 1 compound that did not kill the cells within 16 hours (Compound 48: $0.25 \mu\text{M}$; Compound 72: $1 \mu\text{M}$; Compound 139: $0.5 \mu\text{M}$), with the no drug control receiving an equal volume of the solvent, DMSO. After 16 hours incubation samples were taken and DNA content was assessed.

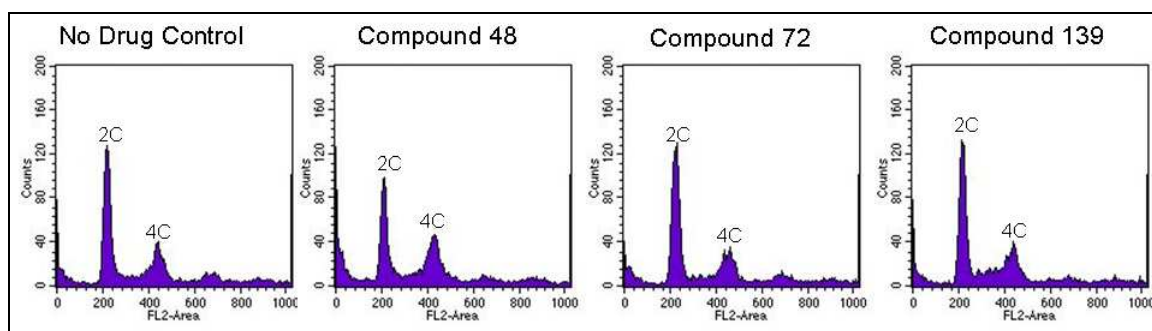


Figure 5.8: Flow cytometry analysis of the DNA content of Tb427 wildtype trypanosomes treated and untreated with $0.25 \mu\text{M}$ Compound 48, $1 \mu\text{M}$ Compound 72 and $0.5 \mu\text{M}$ Compound 139 and incubated under normal culturing conditions for 16 hours. The histograms show the number of cells with a particular fluorescence intensity which correlates with the amount of DNA in the cell. The peaks labelled 2C represent the number of cells in the sample with a complete diploid complement of DNA, having 2 copies of the genome; the peaks labelled 4C represent the cells which have replicated their DNA but not yet undergone cell division therefore having 4 copies of the genome.

Compounds 72 and 139 appear to have no direct impact on DNA replication after 16 hours incubation at a lethal concentration (Figure 5.8). Both the peaks corresponding to cells with one complete diploid genome (G_1 phase of the cell cycle corresponding to the 2C peak) and those having completed a round of DNA replication and are undergoing mitosis (G_2/M phase corresponding to the 4C peak) are very similar to those produced by the control culture.

Compound 48, however, appears to have a decreased 2C peak with a fractionally larger 4C peak compared to the control. This might suggest an impediment in the cell cycle during mitosis, resulting in trypanosomes in the G_2/M phase increasing in number and those in G_1 phase being depleted as cells progressing into S phase are not being replaced fast enough by others completing mitosis. Unfortunately further sampling of the Compound 48 culture was not possible due to the compound's toxic effects killing the trypanosomes shortly after 16 hours of incubation. This being the case it seems unlikely that the relatively minor effect on cell division itself caused the death of the cell population. Rather, it may be that cells in G_1 phase are more sensitive to Compound 48 than those undergoing mitosis.

In Figure 5.9 it is shown that Compound 37 has a very different DNA content profile from the other Series 1 compounds tested. Over a period of 16 hours of incubation at $0.625 \mu\text{M}$ the 2C peak has been drastically reduced, compared to the no drug control, with the 4C peak appearing larger. There is also a large peak at the left-hand side of the histogram which is not present in the control data. This probably represents DNA debris from cells too structurally weakened to withstand the centrifugation steps of the sample preparation; however, it may be caused by a proportion of the cell population having gone through cytokinesis before proper DNA segregation occurred resulting in cells without a full diploid genome. Alternatively, this could reflect extensive DNA degradation. Even after just four hours incubation with Compound 37 the 4C peak is noticeably larger than that of the no drug control's; a picture mirrored at 8 and 12 hours incubation, with the 2C peak gradually diminishing and the 'debris peak' ($<2n$ chromosomes) increasing.

These data suggest that Compound 37 disrupts the cell cycle of trypanosomes resulting in an accumulation of the cell population in the G_2/M phase. This may lead to cell death through blocked, or improper, DNA segregation and cell division. The incubation time of at most two replication cycles is not long enough to assess whether longer treatment with this compound would lead to the appearance of cells with higher ploidy but the increasing prominence of the $<2C$ peak makes this seem unlikely. One assessment of these data is that cell division was disrupted because of extensive damage/fragmentation of nuclear DNA, rather than the other way around.

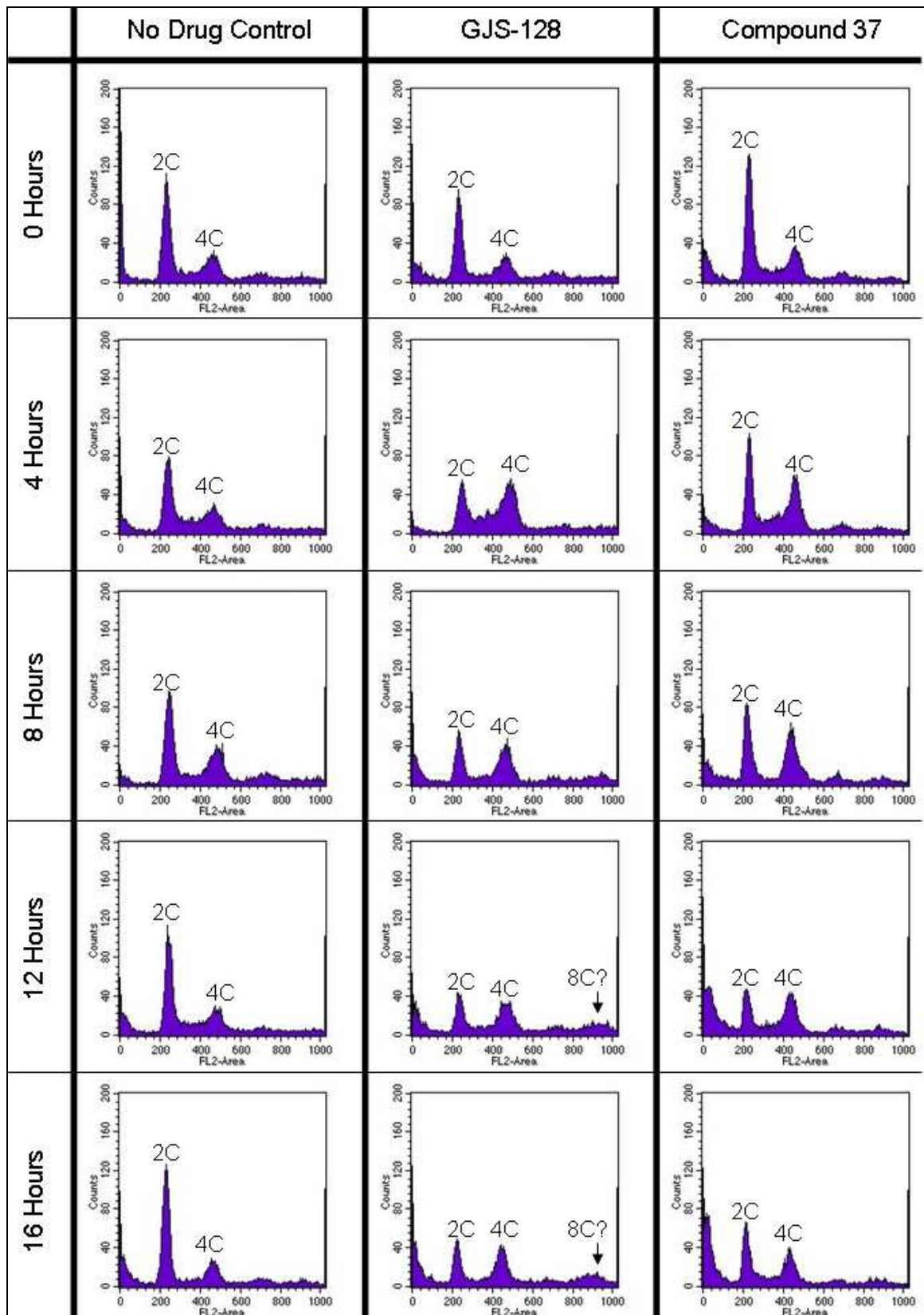


Figure 5.9: Flow cytometry analysis of the DNA content of Tb427 wildtype trypanosomes treated and untreated with 1 μ M GJS-128 and 0.625 μ M Compound 37, incubated under normal culturing conditions with samples taken every 4 hours for 16 hours. The histograms show the number of cells with a particular fluorescence intensity which correlates with the amount of DNA in the cell. The peaks labelled 2C represent the number of cells in the sample with a complete diploid complement of DNA, having 2 copies of the genome; the peaks labelled 4C represent the cells which have replicated their DNA but not yet undergone cytokinesis therefore having 4 copies of the genome. The peaks that are suggestive of cells with 8 copies of the genome are labelled 8C? and arrowed.

When incubated with 1 μM GJS-128 the G_1 phase (2C) peak is reduced after just 4 hours (Figure 5.9), in comparison with the no drug control, with a marked increase in the 4C G_2/M phase peak. After 8 hours the two peak sizes have remained approximately the same size with perhaps a slight increase in the debris peak at the left-hand side. At 12 hours incubation both the 2C and 4C peaks appear reduced relative to the 4 hour time point and the 2C peak is now only a small fraction of the corresponding peak in the control sample. However, this is not attributed to cell death as a shallow peak is beginning to emerge towards the right-hand side of the histogram at the expected intensity for 8C ploidy. This third peak is more pronounced after 16 hours incubation, with the 2C, 4C and debris peaks remaining approximately the same size as at 8 hours.

The rapid increase in the 4C peak combined with the decrease in the 2C peak relative to the no drug control after 4 and 8 hours incubation with GJS-128 suggest that this compound also disrupts the cell cycle; however, the appearance of the third peak after 12 hours incubation indicate that the DNA synthesis component of the cell cycle has not been halted but that either mitosis or cytokinesis, or both, have been skipped over. This would result in a proportion of the cells having gone through one round of DNA replication, then had mitosis and/or cytokinesis disrupted, halting physical cell division, but not a further round of DNA replication. This implies that a trypanosome affected by GJS-128 might replicate its diploid genome from 2C to 4C, and then undergo further DNA replication from 4C to 8C without finishing the cell division as expected.

Further analysis of the flow cytometry data by ModFit LT software (Verity Software House), which can model the histogram peaks to find the percentages of the population in diploid and other ploidy cell cycle phases, was carried out to shed further light on the particular stage of cell replication disruption.

The modelled percentages of the trypanosome population in diploid (2C), tetraploid (4C) and aneuploid (less than 2C, or less than a multiple of 2C) cell cycles were plotted for those cells incubated with and without GJS-128 (Figure 5.10A) and with and without Compound 37 (Figure 5.10B) against time. Cultures treated with 1 μM GJS-128 show that the percentage of trypanosomes in a normal diploid state declines over the course of 24 hours, falling from almost 95% to just over 30%; while the percentage of tetraploid cells steadily rises from

4% to nearly 60% over the same period. Tetraploid cells become the dominant cell cycle state in the culture after approximately 16 hours exposure to the compound. In contrast, in the control culture the percentage of trypanosomes in a diploid cell cycle barely drops below 70% over the 24 hour period, with those cells in a tetraploid cell cycle reaching a maximum of 27% after 16 hours incubation before falling again. For both the cultures the percentage of the cells in an aneuploid cell cycle does not differ greatly from each other: rising gradually from a negligible percentage to around 10% of the population after 24 hours.

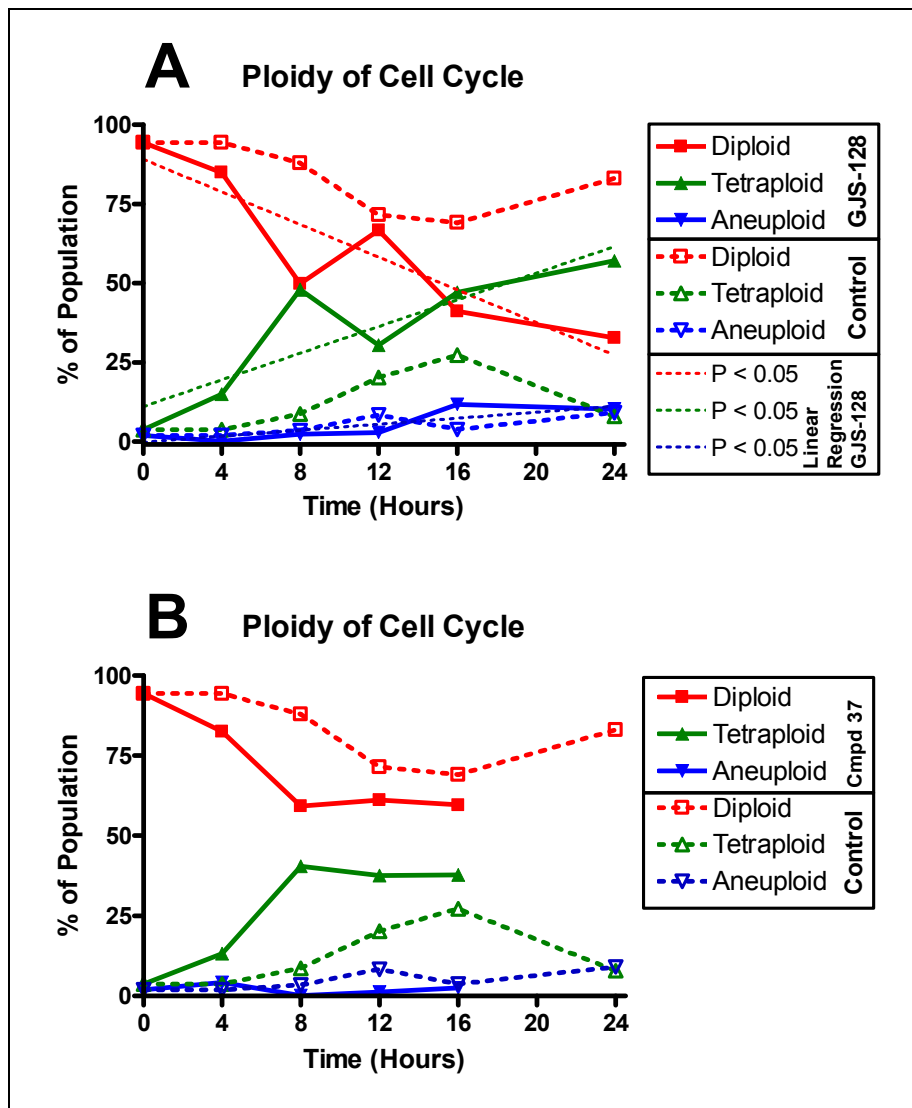


Figure 5.10: Graphs showing the percentage of the Tb427 wildtype culture in particular ploidy cell cycles. Diploid (red), tetraploid (green) or aneuploid (blue) cell cycle after incubation with or without 1 μ M GJS-128 (A) or 0.625 μ M Compound 37 (B) over 24 hours. The continuous lines with filled symbols represent the test compound treated cultures and the dashed lines with empty symbols represent the no-drug control culture. In graph A the thin dotted lines represent the linear regression of the GJS-128 treated culture's data with their respective P values for significance boxed on the right.

Cultures treated with 0.625 μM Compound 37 also show a more rapid decrease in the proportion of cells in a diploid cell cycle in comparison with the control, having fallen from 95% to 60% after 8 hours incubation compared to a decline to 88% for the control. The percentage of the culture in a tetraploid cell cycle also rises much faster than the control, reaching nearly 40% after 8 hours compared to just 9% for the control. The percentages in the Compound 37 treated culture then remain at the 8 hour levels for at least the next 8 hours; the samples taken after 16 hours had too much cell debris to allow for reliable modelling by the ModFit LT software.

The ModFit LT analysis suggest that GJS-128 and Compound 37 both have an affect on the cell cycle of Tb427 wildtype trypanosomes but act on the cell cycle in different ways. Compound 37 appears to block the cell cycle of the trypanosomes by disrupting either mitosis or cytokinesis after the genome of the cell has been replicated. The trypanosomes then stay in the 4C state until cell death, or die as a result of DNA damage. As a considerable percentage of Compound 37-treated cells remain diploid it is likely that DNA degradation rather than the block in cell division causes the demise of the trypanosome population. GJS-128 also appears to impede the cell cycle at either mitosis or cytokinesis however, instead of stopping the cell cycle, the trypanosomes appear to be able to undergo a further round of DNA replication without the mother and daughter cells dividing, resulting in the diminishing diploid cell population and an increasing number of tetraploid cells.

5.3.3 Assessment of DNA configuration using the fluorescent stain DAPI

In an attempt to pinpoint more precisely the location of the disruption to the cell cycle, the configuration of the nuclei and kinetoplasts in trypanosomes was investigated after incubation with the test compounds.

Tb427 wild-type trypanosomes were incubated with and without test compound for 12 hours under normal culturing conditions. Samples were then fixed onto a microscope slide and stained with 4,6-diamidino-2-phenylindole (DAPI) which fluoresces when bound to DNA. The samples were then inspected using a fluorescent microscope fitted with the appropriate filters, and the fixed

trypanosomes then assessed for the configuration and number of nuclei and kinetoplasts. The cells were scored and counted in the following categories: 1N1K - having 1 nucleus and 1 kinetoplast; 1N2K - having 1 nucleus and 2 kinetoplasts; 2N2K (Early) - having 2 distinct nuclei and 2 kinetoplasts but without an apparent cleavage furrow starting to divide mother and daughter cells; 2N2K (Late) - having 2 distinct nuclei and 2 kinetoplasts, and with the cleavage furrow having almost divided the mother and daughter cells, but not having achieved full cytokinesis; and >2N2K - cells with more than 2 nuclei and 2 kinetoplasts (see Figure 5.11 for examples).

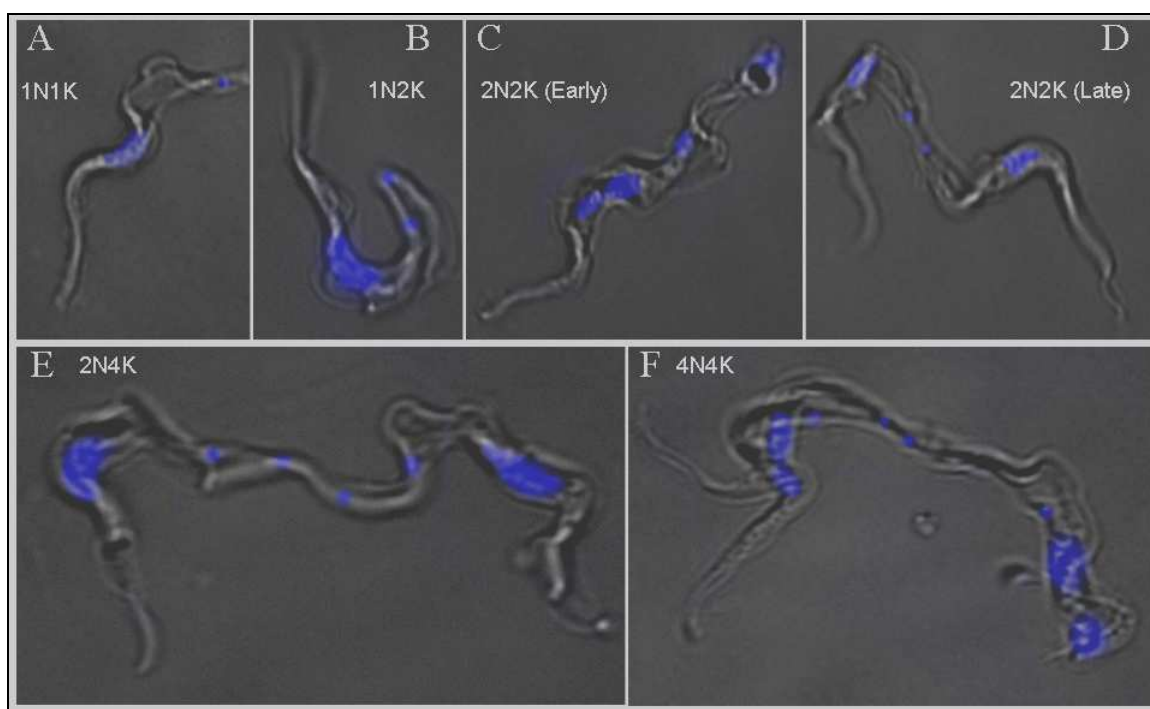


Figure 5.11: Example images of Tb427 wildtype trypanosomes, and the categories they were scored as, with their DNA stained with DAPI and inspected by fluorescent microscope. (A) Shows a trypanosome with 1 nucleus and 1 kinetoplast; (B) a trypanosome with 1 nucleus and 2 kinetoplasts; (C) a cell with 2 nuclei and 2 kinetoplasts but before an cleavage furrow has started to divide the mother and daughter cells; (D) another cell with 2 nuclei and 2 kinetoplasts but with the cleavage furrow having almost completed its progress to cell division; (E) an undivided cell with pronounced cleavage furrow, apparently halted close to completion, with 2 nuclei and 4 kinetoplasts; (F) a cell with 4 nuclei and 4 kinetoplasts with an cleavage furrow apparently halted near completion and at least one more (left side of image) having made progress to dividing the cell further.

The number and configuration of nuclei and kinetoplasts was significantly different from the control for those cultures incubated with GJS-128, Compound 37 and Compound 48 for 12 hours ($P < 0.001$; Chi-squared test). For trypanosomes incubated with GJS-128, the percentage of cells in the 1N1K category was reduced, in comparison to the control, from 74.4% to 34% after 12 hours incubation (Figure 5.12) however, the percentages of the 2N2K (Late) and

>2N2K both increased, from 8.7% and 1% respectively, in the control culture, to 39.3% and 17.8% respectively, in the GJS-128 treated population. When the categories that correspond to the diploid cell cycle are combined (1N1K, 1N2K and 2N2K (Early)) there is a statistically significant decrease, compared to the control, from a total of 90.3% to 42.9% in the GJS-128 incubated culture; this results in a corresponding increase in the percentage of cells in a tetraploid (or greater) cell cycle (2N2K (Late) + >2N2K) in the compound treated culture from 9.7% in the control to 57.1%.

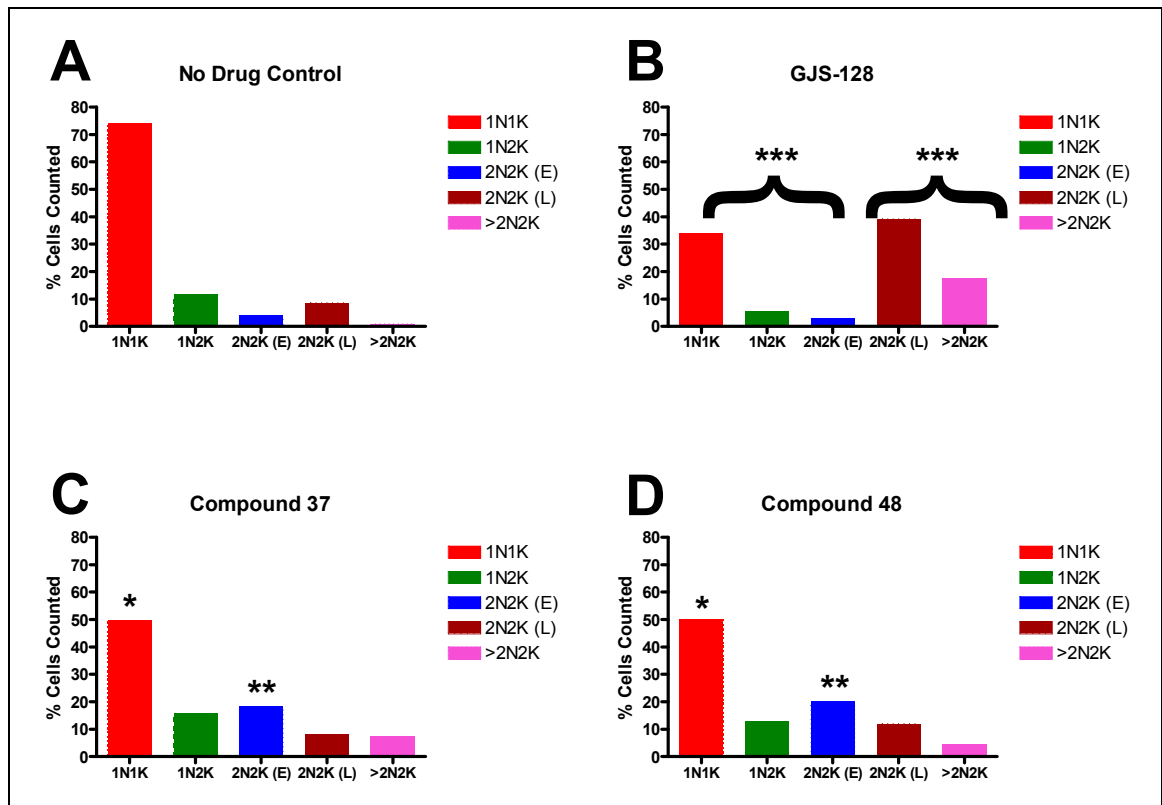


Figure 5.12: Graphs showing the percentage of Tb427 wildtype trypanosomes, in categories scored for number and configuration of nuclei and kinetoplasts, after 12 hours of incubation with or without test compound. From each culture more than 500 cells were assessed and scored for content of nuclei and kinetoplasts. (A) Control culture incubated with no test compound; (B) incubated with 1 μ M GJS-128; (C) incubated with 0.625 μ M Compound 37 and (D) incubated with 0.25 μ M Compound 48. N = nuclei, K = kinetoplasts, (E) = early stage before cleavage furrow, (L) = late stage after cleavage furrow halted near complete cell division. *** = P-value is less than 0.001 for no significant difference between the bracketed categories combined from those of the control; ** = P-value is less than 0.01 for no significant difference from control; * = P-value is less than 0.05 for no significant difference from control. P-values were calculated by using the Chi-squared statistical test.

These data indicate that treating trypanosomes with GJS-128 results in a specific block in the cytokinesis stage of the cell cycle. DNA replication, and segregation into two nuclei and two kinetoplasts during mitosis, appears to have occurred as normal; the cell has begun the process of physically dividing its contents with the cleavage furrow forming two compartments, each containing one nucleus

and one kinetoplast as well as a flagellum each (Figure 5.11D), and are apparently connected by only a very small region of cell membrane. On further incubation the cell can undergo another round of apparently co-ordinated DNA replication, with the third and fourth nuclei never appearing without the third and fourth kinetoplasts (personal observations; Figures 5.11E and 5.11F); the cell then tries to physically divide itself again with more cleavage furrows beginning to progress towards division (Figure 5.11F). Following the number and configuration of nuclei and kinetoplasts beyond the 12 hour time-point was not feasible as accurate scoring of the cells was compromised by the sheer number of nuclei obscuring other nuclei, as well as the much smaller kinetoplasts; however, it was apparent further DNA replication did take place but it was not possible to say if it was by co-ordinated replication followed by an orderly mitosis (personal observations).

Treatment with either Compound 37 or 48 significantly increased the percentage of trypanosomes with two nuclei and two kinetoplasts but no visible cleavage furrow (2N2K (Early)), compared to that of the control culture (Figure 5.12). There was also a significantly lower percentage with one nucleus and one kinetoplast (1N1K) compared to the control, but the other categories remained broadly the same. This suggests that for both Compounds 37 and 48 the disruption to the cell cycle lies after the replicated DNA has been segregated into the mother and daughter nuclei and kinetoplasts, but before the cleavage furrow starts to physically divide the cell, since the 2N2K (Late) percentages remained roughly the same.

5.3.4 Comparison of the gene sequences of *TbrPDEB1* and *TbrPDEB2* between the resistant R0.8 cell line and its parental *Tb427* wildtype strain

The loss of sensitivity of the GJS-128 resistant R0.8 cell line to two cAMP analogues (4.3.4), combined with the apparent lack of a change in the profile of the production or degradation of cAMP on incubation with GJS-128 (4.3.5) suggest that the adaptation resulting in increased tolerance to the GJS compounds (and the resultant increased cAMP concentration) lies, at least in part, downstream of the phosphodiesterase enzymes in the cAMP signalling cascade. If, however, the mode of resistance is solely due to changes to the

target trypanosomal PDE enzymes then one would expect to find those changes in the DNA sequences of the genes coding for them. To investigate this hypothesis further the open reading frames of the two essential trypanosomal PDEs (TbrPDEB1 and TbrPDEB2) were sequenced in the R0.8 cell line and compared to that of the parental Tb427 wildtype strain for any possible mutations that may result in a change in the action of the proteins.

The R0.8 and the Tb427 wildtype cell lines were cloned out by serial dilutions in 96-well plates so that cultures of each strain were obtained that had been derived from a single trypanosome. Primers flanking TbrPDEB1 and TbrPDEB2 were designed from the GeneDB *Trypanosoma brucei* genome sequence (which is that of strain TREU927/4 GUTat10.1) and used to amplify the genes of interest from the R0.8 and Tb427 wildtype strains by the proof-reading polymerase KOD. After ligation into the pGEMT-easy vector and transformation into JM109 *E. coli*, the plasmid DNA containing the respective genes was extracted by mini-prep and samples sent to Eurofins-MWG-Operon for sequencing. According to GeneDB (www.genedb.org/genedb/tryp/) the *T. b. brucei* genome contains only one copy each of PDEB1 and PDEB2. In order to be confident of obtaining sequences for both possible alleles of the genes, plasmid DNA from multiple bacteria clones screened for the insertion of TbrPDEB1 or TbrPDEB2 was sent for sequencing.

The data returned was analysed using the Vector Nti Advance 10 software suite which allowed the short, over-lapping partial DNA sequences to be 'contig-ed', or stitched together, to form the full open reading frame for the entire gene. The sequences from the multiple bacterial clones can be seen in Appendices 3 to 6 with those from the R0.8 strain and the Tb427 wildtype aligned alongside the reference sequence from GeneDB for both TbrPDEB1 and TbrPDEB2. A diagram of both genes showing the relative positions of specific features can be seen in Figures 5.13 and 5.14.

The sequences for TbrPDEB1 from the R0.8 and Tb427 wildtype strains differ from each other in just three base-pairs (Appendix 3). At base-pair 738 of the ORF the base is guanine for all of the bacteria clones transformed with DNA from R0.8, while for the Tb427 wildtype, five out of nine clones have a cytosine with the other four clones matching the R0.8 and having guanine. Similarly, at base-pair 1602 all the R0.8 clones have guanine while the same five out of nine Tb427

wildtype clones have cytosine with the remaining four having guanine; and at base-pair 1362 the R0.8 clones have thymine while the same five out of nine Tb427 clones have guanine and the remainder, again matching the R0.8, thymine. This strongly suggests that in the Tb427 wildtype strain there are two heterozygous alleles of the TbrPDEB1 gene, with the allelic variation apparent in the DNA sequence at base-pairs 738, 1362 and 1602 (Figure 5.13); whereas R0.8 has two homozygous alleles that match identically with one of the Tb427 wildtype's. When the DNA sequences are translated into their corresponding amino acid sequence (Appendix 4) only one of the three base-pair variations results in a change in amino acid: the change at base pair 1602 from guanine to cytosine changes the amino acid at residue 534 from a glutamic acid to the similarly charged aspartic acid.

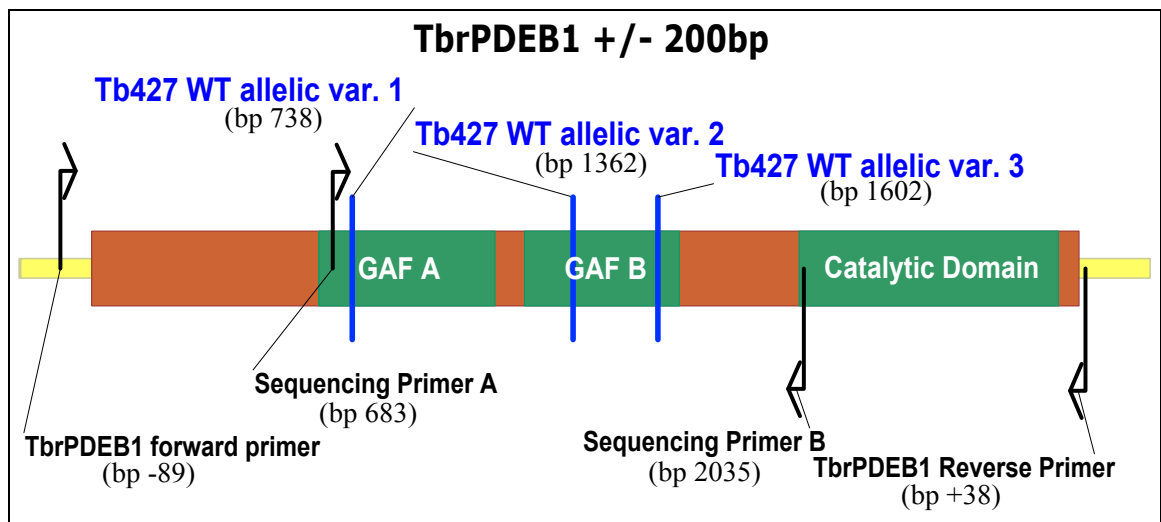


Figure 5.13: Diagram showing the open reading frame of TbrPDEB1 (+/- 200 base pairs). Black arrows indicate the annealing positions of the primers used in amplifying the gene for sequencing the versions in the Tb427 wildtype and the GJS-128 resistant R0.8 cell lines. Blue bars indicate the position of allelic variations present in the Tb427 wildtype gene but absent in the R0.8 line. The catalytic domain and GAF domains are represented by green blocks. The figures in brackets are the location of each feature relative to the starting base pair in the open reading frame (- or + indicate feature locations upstream or downstream of the open reading frame).

There are two other slight discrepancies observed in the sequences of the R0.8 and Tb427 wildtype TbrPDEB1 gene when all the clones are aligned. At bp 2338 there is a guanine in all clones except one, which has an adenine; and at bp 2658 one out of the 18 clones has an extra thymine inserted that results in a frame shift and corresponding amino acid changes (Appendices 3 & 4). Since these differences only appear in a single clone they are probably the result of an error

either in the sequencing reaction or in the initial PCR amplification by the polymerase enzyme. The differences between the sequences of the GeneDB strain and that of the R0.8 or Tb427 wildtype merely reflect the adaptations made by the diverging TREU927 and Tb427 strains of *Trypanosoma brucei* and would have no impact on the mode of resistance in the R0.8 cell line compared to the Tb427 wildtype.

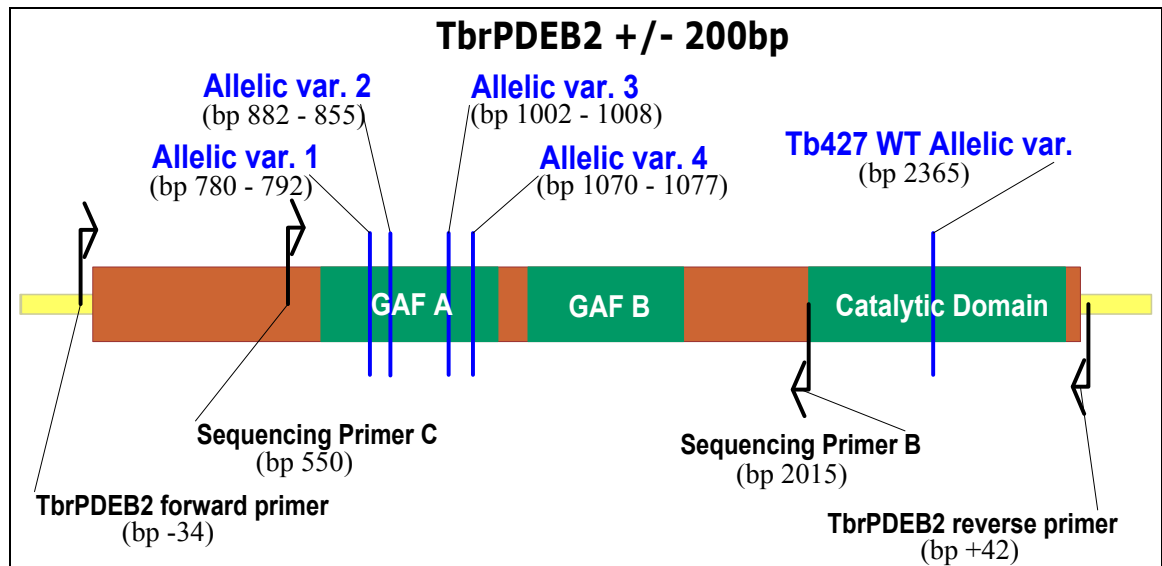


Figure 5.14: Diagram showing the open reading frame of TbrPDEB2 (+/- 200 base pairs). Black arrows indicate the annealing positions of the primers used in amplifying the gene for sequencing the versions in the Tb427 wildtype and the GJS-128 resistant R0.8 cell lines. Blue bars indicate the position of allelic variations. The catalytic domain and GAF domains are represented by green blocks. The figures in brackets are the location of each feature relative to the starting base pair in the open reading frame (- or + indicate feature locations upstream or downstream of the open reading frame).

For TbrPDEB2, two alleles (A and B) were also detected (Appendices 5 and 6), indicating heterozygosity; however they are both unambiguously present in the R0.8 and the Tb427 wildtype. The allelic sequence variations appear to cluster into four distinct regions. The first region begins at base-pair 780 and ends at bp 792 with allele A's sequence being **CAGGGGTGACGTA** and B's being **GAAAGACGACAAG**, having eight out of the thirteen bases different (red text). The second region is just 28 base-pairs downstream beginning at bp 822 and ending at bp 855 with the sequence of allele A being **TGTTACAATCCCTAGGGGTGCAGGTATTGCCGGA** and allele B being **CGTTTCCATACCCAAGGGAACAGGCATTGTAGGG**, with 13 out of 34 bases differing (red text). The other two regions are much smaller being just 7 and 8 base-pairs in length with just three differences each: allelic region 3 begins at bp 1002 and

ends at 1008 (allele A: **TGCCCAA**; allele B: **AACCCAG**) and region 4 beginning at bp 1070 and ending at bp 1077 (allele A: **GGCGTGAT**; allele B: **AACGTGAC**).

When the TbrPDEB2 open reading frame has been translated (appendix 6) the single letter amino acid code for region one is **RGDV** for allele A and **KDDK** for allele B; the amino acid sequence for region two is **TIPRGAGIA** for allele A and **SIPKGTGIV** for allele B. The remaining two regions of allelic variation result in just one amino acid difference each when translated: region three has an alanine in allele A and a threonine in allele B at position 335; region four has an arginine in allele A and a lysine in allele B at position 357. Interestingly, all four of these regions of allelic variation lie within the GAF A domain (Figure 5.14).

Tb427 wildtype has one further allelic difference in sequence which the R0.8 line appears to have lost: a single base variation at bp 2365 which lies almost in the middle of the catalytic domain (Figure 5.14). In allele A the base is adenine, but in allele B it is thymine; in the R0.8 line the base pair in allele B has reverted to the adenine of allele A in that position. This allelic difference results in the amino acid sequence changing from a cysteine to a serine at residue 789, a relatively conservative substitution, however.

There are four other discrepancies in the sequences where only a single clone from all of those sequenced has a difference at a single base position: bp 1656 (G - A); bp 2160 (C - T); bp 2162 (A - C) and bp 2174 (A - T). These differences are probably a result of sequencing error or PCR error by the polymerase.

5.4 Discussion

Electron microscopy, analysis of DNA and cell replication identify two different types of toxic action for Compound 37. The microscopy observes severe enlargement of the flagellar pocket and disruption in the cytosol, whereas the flow cytometry analysis and DAPI staining indicate that Compound 37 blocks the cell cycle after DNA replication. While Compound 37 may have multiple targets within the trypanosome, one possible pathway that interference of which might give rise to both phenotypes is intracellular transport. The flagellar pocket is the only site of endocytosis and exocytosis in trypanosomes (Ralston, K. S. and Hill, K. L., 2008) and actin has been demonstrated to play an important role in these cellular processes (McPherson, P. S., 2002; Qualmann, B. et al, 2000). RNAi knockdown of actin in bloodstream form trypanosomes appeared to block the normal formation of vesicles from the flagellar pocket membrane and resulted in the flagellar pocket swelling dramatically (Garcia-Salcedo, J. A. et al, 2004). In the same study it was also observed that cell division ceased within 24 hours of induction of the actin RNAi. The similarities in cellular pathology between actin RNAi and Compound 37 suggest that this Series 1 compound may inhibit actin, or another key protein in the endo/exocytic pathway.

In contrast to Compound 37, GJS-128 appears to block the cell replication cycle at a more specific point. The flow cytometry analyses demonstrate that while incubation with 1 μ M GJS-128 results in a build up of trypanosomes with two diploid genomes, suggesting a block after DNA replication, prolonged incubation with the compound gives rise to another peak with a higher ploidy, possibly four diploid genomes. This suggests that while GJS-128 inhibits cell replication, DNA synthesis is apparently unaffected.

Staining trypanosomes exposed to GJS-128 with DAPI and assessing the configuration of the DNA-containing organelles by fluorescence microscopy allowed us to determine the precise stage of the cell cycle being inhibited. While the uninterrupted DNA replication revealed by flow cytometry was confirmed, the microscopic assessment showed that the duplicated DNA also segregated into two separate nuclei and kinetoplasts as normal, allowing the formation of apparently complete daughter cells. However, repeating the microscopy with a panel of stains specific for individual organelles would help to

determine if all the single organelles are also replicated and segregated as normal. After DNA replication, the trypanosomes then attempted to physically divide the mother and daughter cells, with the cleavage furrow moving along the flagella. The division of the cells proceeded right up until the point of abscission, with only a very small section of plasma membrane connecting the two almost separated trypanosomes, before the process was halted. This type of cell cycle block appears to be unique and suggests that the uncontrolled elevation of cAMP inhibits a specific process, as yet undocumented, that completes cytokinesis.

The prolonged exposure to GJS-128 eventually resulted in the breakdown of normal flagellar replication, as observed by electron microscopy. This process is strictly coordinated and is supposed to progress along a path defined by the old flagellum (Ralston, K. S. and Hill, K. L., 2008). The presence of unattached components of a flagellum within the cytosol indicates that by this stage of PDE inhibitor exposure the replication of organelles has broken down. The flagella of a replicating cell are intimately linked with organelle segregation as well as initiation and progression of cytokinesis (Ralston, K. S. and Hill, K. L., 2008). If cAMP signalling plays a role in cytokinesis, and the PDE targets of GJS-128 are localised to the flagellum (Oberholzer, M. et al, 2007), then disruption to flagellar replication is not an inconsistent phenotype.

Since RNAi studies of the PDEB genes in *T. brucei* demonstrated that both PDEB1 and PDEB2 had to be disrupted to result in elevated intracellular cAMP concentrations and eventual cell death (Oberholzer, M. et al, 2007; Zoraghi, R. and Seebeck, T., 2002), a mutation in just one of these enzymes, making it insensitive to GJS-128, could give rise to significant resistance. As a means of determining whether the resistance displayed by the R0.8 trypanosome cell line to GJS-128 was due to mutation of either PDEB, TbrPDEB1 and TbrPDEB2 were cloned and sequenced from both the parental Tb427 wildtype and the R0.8 strains. Two alleles were identified for TbrPDEB2 in both the wildtype and R0.8 strains and are in excellent agreement with those published by Kunz, S. et al, 2009, with the GAF-A domain of TbrPDEB1 appearing to have been duplicated in allele B of TbrPDEB2. The two alleles of PDEB2 appear to be identical in both the resistant cell line and the wildtype except for a single allelic variation at base pair 2365, resulting in the substitution of serine to cysteine in allele B of R0.8,

making it the same as allele A. While this amino acid residue is located in the catalytic domain of the enzyme, it is unlikely to affect the kinetic properties of the enzyme for a number of reasons. The first is that the substitution is relatively conservative with serine and cysteine being neutral, rather hydrophobic, and of similar size. The second is that, although located in the catalytic domain of PDEB2, the residue is found towards the start of a 24 amino acid sequence divergent in all of the PDEB enzymes yet sequenced in kinetoplastids (Johner, A. et al, 2006). In the crystal structure of PDEB1 in *Leishmania major*, the homologous residue is found in helix 12 which is orientated towards the surface of the protein and does not appear to interact with the active site (Wang, H. et al, 2007). All of the above suggests that this region does not need to be absolutely conserved for the correct functioning of the protein. The final reason is that the substitution merely reverts the sequence from allele B to that of allele A, both of which are found in the GJS-128-sensitive wildtype strain.

The sequence of TbrPDEB1 in the resistant R0.8 strain is identical to that of one of the alleles of the wildtype's gene, having apparently lost the other, and becoming homozygous. There are just three base pairs different between the two PDEB1 alleles with only one resulting in an amino acid substitution. Again, this substitution is relatively conservative, and, being located well outside the catalytic domain, is unlikely to affect protein function.

Loss of heterozygosity is usually the result of either a loss of part of the chromosome due to mis-segregation or double-stranded break of the DNA, or caused by a recombination event. The loss of heterozygosity for PDEB1, and in the catalytic domain of PDEB2, observed in the R0.8 strain may be the result of the method used to induce the initial resistance to GJS-128. Methyl methane sulphonate (MMS) damages DNA by methylating the bases and one method of repairing the damage is by homologous recombination (Wyatt, M. D. and Pittman, D. L., 2006). This can result in the transfer of DNA sequence from one allele to the other. However, this process is not always a two-way exchange of DNA and can result in the loss of part or all of an allele by a short patch gene conversion that replaces a missing section (Paques, F. and Haber, J. E., 1999), or by break-induced replication that duplicates one strand of the chromosome from a double stranded break right to the telomere (Malkova, A. et al, 1996). As the

sequences of PDEB1 and PDEB2 in the resistant R0.8 line are also found in the wildtype, the loss of heterozygosity is unlikely to have contributed to the resistance, although the possibility that one of the alleles in the wildtype is defective cannot be formally excluded without cloning each allele and purifying the encoded product for the determination of its PDE activity.

Since there is also no compelling evidence of a mutation having changed the activity or inhibitor binding of the PDEs, the tentative conclusion from these data is that the adaptation in R0.8 is located downstream of the phosphodiesterase enzymes, with the effect of making the trypanosome much less sensitive to high levels of cAMP. However, this needs to be formally demonstrated with the whole-cell PDE activity determination of both strains from cell lysates, as well as showing there has been no change to the expression levels of any of the trypanosomal PDEs in the resistant line - this work is currently in progress. The hypothesis that the source of resistance in the R0.8 strain is not found in the phosphodiesterase enzymes is supported by the cross-resistance of the R0.8 line to the hydrolysis-resistant cAMP analogues (Chapter 4.2.4). Also, the almost identical profile of cAMP concentration increase in response to PDE inhibition by GJS-128 strongly suggests there is no change to the adenylyl cyclase capacity (Chapter 4.2.5). This leaves the possibility that the adaptation that gives resistance lies in one of the downstream regulatory proteins in the cAMP pathway, for example a putative cAMP-binding PKA-regulatory subunit. Although PKA-like phosphorylating activity has been identified in *T. brucei*, the only isolated and characterised PKA-regulatory subunit from the parasite appears to bind cGMP instead of cAMP (Shalaby, T. et al, 2001). However, since trypanosomes express a multitude of receptor-like adenylyl cyclases, and phosphodiesterases, and since changes in the cAMP concentration have such serious effects on the trypanosome, a protein that transduces that signal to effector and regulatory proteins is essential in some form. As in *T. brucei*, PKA catalytic activity has been observed in the closely related organisms *Trypanosoma cruzi* and *Leishmania* species (Ulloa, R. M. et al, 1988; Ochatt, C. M. et al, 1993; Banerjee, C. and Sarkar, D., 1992; Siman-Tov, M. M. et al, 2002). A PKA-regulatory subunit has been characterised from *T. cruzi* and it was demonstrated that cAMP can restore phosphorylating activity to the PKA-catalytic domain after inhibition by PKA-R. Although, a cAMP-binding regulatory domain has not yet been identified in *Leishmania*, cAMP has also been

shown to modulate PKA activity in *Leishmania amazonensis* (Genestra, M. et al, 2004). This suggests that the R0.8 cell line could prove to be a vital tool in identifying downstream effectors in the cAMP signalling pathway in *Trypanosoma brucei* for the first time.

Chapter VI

6 General Discussion

There is an urgent need for new chemotherapies for African trypanosomiasis. Current treatments can be extremely toxic to the patient, for example: 10% of those treated with the melaminophenyl arsenical class of drug, melarsoprol, enduring sometimes fatal reactive encephalopathy (Fairlamb, A. H., 2003). The treatment regimens can also be costly and difficult to administer and, to make a bad situation intolerable, refractory strains have been reported and resistance to the few drugs available appears to be growing (Delespaux, V. and De Koning, H. P., 2007; Anene, B. M. et al, 2006).

After the turn of the millennium, phosphodiesterase enzymes were demonstrated to be essential to the survival of bloodstream form trypanosomes. RNA-interference, resulting in the knockdown of the PDEB family induced a massive rise in intracellular cAMP concentration in procyclic forms and was lethal to the mammalian life cycle stage (Zoraghi, R. and Seebeck, T., 2002; Oberholzer, M. et al, 2007). However, none of the inhibitors active against mammalian PDEs could inhibit recombinantly expressed kinetoplastid PDEs with high affinity (see review of kinetoplastid PDEs; Chapter 1.4.1), nor inhibit native trypanosome or leishmania PDE activity from cell lysates (Goncalves, M. F. et al, 1980; Al-Chalabi, K. A. K. et al, 1989; Rascon, A. et al, 2000). While this suggests there is enough divergence between the mammalian and kinetoplastid PDEs to allow the development of specific inhibitors that target the parasite only, it also means that there were no suitable positive control compounds that can reliably inhibit bloodstream form trypanosome PDEs. The change in cAMP concentrations due to RNAi knock down of PDEB had been measured in procyclic form *T. brucei* and before this project started, there were no publications showing what effects should be expected on intracellular cAMP concentrations by disrupting or inhibiting bloodstream form trypanosomal PDEs, should such a compound be identified. Nor were there defined cellular effects of cAMP elevation in these cells, or ways to manipulate cAMP production as no receptor agonists or antagonists are known for the putative receptor adenylate cyclases and the cells do not express classical G-proteins that could be manipulated.

Well in excess of 200 putative phosphodiesterase inhibitors were provided from two sources for assessment of activity against trypanosomes *in vitro*. In order for any potential new chemotherapy against African trypanosomiasis to be effective, there must be no cross-resistance to the lead compound by strains refractory to

current treatments. To test this, not only were all the compounds assayed against wildtype *T. brucei*, but each was also assayed against the TbAT1 knockout strain. This strain shows marked resistance to most of the diamidine class compounds, as well as minor resistance to pentamidine and melaminophenyl arsenical class compounds (Matovu, E. et al, 2003) due to the disruption of a purine transporter that actively accumulates the drugs. For the majority of compounds no significant resistance was shown, with those that did show a statistical increase in EC₅₀ value showing only minor resistance in comparison to diminazene being over 20-fold less active against the TbAT1 knock out strain (Chapter 2.3.1). A panel of compounds was also tested against the wildtype and diminazene resistant veterinary parasite *T. equiperdum* (Barrett, M. et al, 1995) showing a similar lack of cross-resistance - as did a panel tested against a TbAT1 knockout strain made further resistant to pentamidine that also shows significant resistance to melaminophenyl arsenicals (Bridges, D. J. et al, 2007). These results demonstrate that the putative PDE inhibitors tested in this study do not enter the cell via the same transporters as the current chemotherapies, nor kill the trypanosomes by disrupting the same intracellular target.

Analysing the effects of large numbers of test compounds highlighted the need for a high-throughput method of determining the speed of action of each compound, at various concentrations, on live trypanosomes. Methods utilized previously, such as using a haemocytometer to manually count the number of cells in a culture, or a light absorbance-based assay had numerous disadvantages. Cell counts were extremely time-consuming, limiting the number of conditions tested at a time, and was not accurate over relatively short intervals. The light absorbance assay relied on high initial cell densities not obtained in normal *in vitro* culturing, possibly affecting results, as well as not being able to distinguish between loss of cell motility and cell lysis. During this project, a protocol based around the fluorescence of propidium iodide when bound to DNA was successfully developed (Chapter 3). Propidium iodide is a compound that cannot cross intact cell membranes; however, once the membrane has been compromised, and the compound enters the cell, it binds to DNA and fluoresces under certain conditions. The breaking up of the cell membrane is a definitive indicator of cell death, so when propidium iodide is incubated with live cells the fluorescence due to the compound binding DNA is a

proxy for cell death that can be easily detected and quantified at relatively low cell densities. This allows the monitoring of the lethal effects of a test compound on the population of a cell culture. The protocol was optimised to a 96-well plate format allowing the automating of fluorescence measuring, as well as resulting in the monitoring of the effects of many different compounds or test conditions in a single assay. This new assay saves time and provides accurate and relevant information to allow the efficient design of protocols for future biochemical investigations of the effects of test compounds.

A small number of compounds were identified that rapidly increase the intracellular cAMP concentration in bloodstream form trypanosomes, the most active of which was GJS-128 (Chapter 4.3.1; 4.3.2). Work conducted by Dr. Herrmann Tenor of ALTANA Pharma, The Netherlands, and Prof. Thomas Seebeck at the University of Bern, Switzerland, demonstrated that GJS-128 inhibits recombinant trypanosomal PDEB enzymes with K_i values consistent with its *in vitro* EC_{50} value against live trypanosomes. This gives a clear and consistent link between the cause of cAMP rise (inhibition of PDEB by GJS-128) and the effect of that concentration on bloodstream form trypanosomes (cell death). GJS-128 chemically validates phosphodiesterase enzymes as good drug targets for developing new lead compounds against African trypanosomiasis.

The downstream effects on the bloodstream form trypanosomes of elevating the intracellular cAMP levels were investigated by electron microscopy for gross intracellular disruption, as well as by flow cytometry analysis and DAPI staining for effects on the cell cycle (Chapter 5.3.1; 5.3.2; 5.3.3). The flow cytometry and DAPI staining of DNA-containing organelles showed that raising cAMP concentrations result in the cell cycle being blocked in cytokinesis, where the DNA has replicated and segregated into new nuclei and kinetoplasts and cell division has been initiated with the cleavage furrow having progressed between the mother and daughter flagella almost to separation. At this point, the moment of abscission, cell division has been halted with just a small section of plasma membrane connecting the two almost separated trypanosomes. While physical cell division has been blocked, DNA replication has not, with further rounds of DNA synthesis and segregation into nuclei and kinetoplasts observed in the mother and daughter cells, as well as secondary cleavage furrows along the new flagella which is again halted at the point of abscission. This specific mode

of blocking the cell cycle appears to be unique for a chemical action and implies a precise role for cAMP signalling in the process of terminating the physical separation of the replicating cells. The multiple flagella observed in the fluorescent microscopy, and the disruption to the flagellar assembly and swelling of the flagella pocket observed by electron microscopy, are all consistent with the phenotype of the bloodstream form trypanosomes noted after RNAi against TbrPDEB1 and TbrPDEB2 (Oberholzer, M. et al, 2007) - further confirmation that the defects in cell cycle seen is due to GJS-128 inhibiting phosphodiesterases and not a secondary, off-target effect.

As a means of examining the mode of action of GJS-128 further, resistance to the PDE inhibitor was induced in bloodstream form trypanosomes. A high degree of resistance was generated, resulting in the R0.8 strain which displayed cross-resistance to the other GJS compounds suggesting a common protein target. No cross-resistance was observed for current chemotherapies, consistent with the lack of cross-resistance to GJS compounds from the TbAT1 knockout and B48 clonal strains. This is strong additional evidence that the GJS compounds act via a different mode from the current drugs and suggests the possibility of a combination therapy between PDE inhibitors and diamidines or melaminophenyl arsenicals being effective against resistant strains already in the field. As a first step we are currently investigating whether the GJS compounds and diamidines act in an additive or in a synergistic way.

The mode of resistance in the R0.8 strain was investigated by examining the cAMP generation profile, on incubation with GJS-128, between the resistant and parental wildtype strains, as well as by sequencing the PDEB genes in both strains to identify mutations. While a loss of heterozygosity was observed in the R0.8 strain for PDEB1 and part of PDEB2, no base substitutions were found in the R0.8 DNA sequences that could not be found in one or other of the wildtype alleles in both genes. This, along with the strikingly similar cAMP profiles of the two strains on incubation with GJS-128, suggest that the adaptation giving resistance to PDE inhibitors in R0.8 is not located in the PDE genes. The comparison of PDE activity in cell lysates from both strains, as well as comparing expression levels of the PDE genes, is underway to fully confirm this hypothesis. Not only do the cAMP profiles of the R0.8 and wildtype strains suggest that there has been no change in the affinity of GJS-128 for the phosphodiesterase

enzymes, but it also infers there is no change to the adenylyl cyclase production of cAMP.

This leaves the effector proteins downstream of the PDE enzymes in the cAMP signalling pathway as most likely to harbour the adaptation giving PDE inhibitor resistance. A compound that inhibits trypanosomal phosphodiesterase enzymes both recombinantly and in live trypanosomes, as well as a cell line that has adaptations in the effector proteins could prove to be the vital tool required to uncover the identity and function of these elusive proteins for the first time in kinetoplastids.

Appendix 1:

Average EC₅₀ values for all Series 1 compounds against Tb427 wild type and TbAT1 knockout bloodstream form trypanosomes, with standard errors. Values were derived from whole-cell *in vitro* efficacy assays and calculated from sigmoidal dose-response curves, with variable slopes, using GraphPad Prism software. Averages are taken from at least 3 independent experiments. Also shown is the resistance factor of the TbAT1 knockout strain compared to Tb427 wild type for each compound. Statistical significance was calculated after an F-test was conducted to determine which one-tailed, unpaired Student's T-test was most appropriate: that for equal or unequal variances. Those compounds for which the TbAT1 knockout strain is statistically resistant are highlighted with red text.

University of Glasgow Compound Code	EC ₅₀ Value (M) Tb427 WT		EC ₅₀ Value (M) TbAT1 KO		TbAT1 KO Resistance Factor	P Value: Significantly Resistant
	Average	S.E.	Average	S.E.		
129	5.8E-09	3.4E-09	7.8E-09	4.2E-09	1.3	0.373
197	1.2E-08	2.1E-09	5.2E-08	1.8E-08	4.4	0.103
140	3.3E-08	1.8E-08	3.0E-08	1.6E-08	0.90	
141	3.6E-08	2.1E-08	3.2E-08	1.8E-08	0.89	
48	7.0E-08	2.8E-08	4.2E-08	2.9E-08	0.60	
82	7.0E-08	1.6E-08	4.7E-08	1.4E-08	0.67	
137	8.1E-08	4.3E-08	7.2E-08	4.1E-08	0.89	
Diminazene	8.6E-08	1.2E-08	1.8E-06	1.1E-07	21	0.000
138	1.2E-07	1.4E-08	9.1E-08	2.5E-08	0.75	
143	1.6E-07	1.9E-08	5.7E-07	5.0E-08	3.6	0.002
198	1.6E-07	2.1E-08	2.6E-07	4.7E-08	1.6	0.064
124	1.8E-07	2.4E-08	7.0E-07	4.4E-08	4.0	0.000
199	1.8E-07	3.0E-08	1.5E-07	4.2E-09	0.84	
128	1.9E-07	9.7E-08	3.1E-07	3.3E-08	1.6	0.169
114	2.0E-07	2.3E-08	4.7E-07	4.7E-09	2.4	0.004
142	2.0E-07	9.8E-09	3.3E-07	5.1E-08	1.7	0.078
139	2.3E-07	4.3E-08	1.9E-07	4.7E-09	0.84	
113	2.6E-07	2.7E-09	6.4E-07	2.5E-08	2.5	0.003
80	2.7E-07	2.9E-08	3.5E-07	3.6E-08	1.3	0.113
79	2.9E-07	4.5E-08	3.1E-07	6.2E-08	1.1	0.421
104	3.4E-07	4.1E-08	5.3E-07	4.8E-08	1.6	0.033
37	3.5E-07	7.5E-08	3.3E-07	8.0E-08	0.93	
111	3.9E-07	3.8E-08	4.9E-07	1.5E-08	1.3	0.058
83	4.4E-07	1.9E-08	5.1E-07	3.6E-08	1.2	0.126
107	4.4E-07	4.7E-09	4.9E-07	2.2E-08	1.1	0.093
130	4.8E-07	6.8E-08	4.3E-07	2.4E-08	0.89	
158	5.7E-07	4.5E-08	5.3E-07	1.1E-08	0.92	
72	5.8E-07	4.2E-08	8.5E-07	4.8E-08	1.5	0.013
105	5.9E-07	9.7E-08	8.5E-07	7.2E-08	1.4	0.080
103	6.6E-07	8.6E-08	1.1E-06	1.6E-07	1.6	0.069
77	7.6E-07	7.1E-08	5.7E-07	7.5E-08	0.75	
10	8.3E-07	1.7E-07	9.5E-07	2.0E-07	1.2	0.354
121	9.2E-07	7.3E-08	1.2E-06	2.2E-08	1.3	0.022
6	1.0E-06	2.3E-07	1.4E-06	4.7E-07	1.3	0.314
74	1.0E-06	4.7E-08	8.9E-07	1.1E-08	0.86	
152	1.1E-06	7.1E-08	1.6E-06	5.1E-08	1.4	0.006
151	1.2E-06	6.5E-08	1.7E-06	6.3E-08	1.4	0.005
131	1.2E-06	1.9E-07	1.3E-06	2.2E-07	1.1	0.376
145	1.3E-06	1.1E-07	1.4E-06	1.2E-07	1.1	0.284
112	1.5E-06	7.8E-08	1.2E-06	1.8E-08	0.83	
4	1.6E-06	3.1E-07	1.4E-06	2.4E-07	0.91	
122	1.6E-06	6.3E-08	1.6E-06	3.2E-08	1.0	0.471
84	1.7E-06	1.9E-08	1.9E-06	9.5E-08	1.1	0.103

University of Glasgow Compound Code	EC ₅₀ Value (M) Tb427 WT		EC ₅₀ Value (M) TbAT1 KO		TbAT1 KO Resistance Factor	P Value: Significantly Resistant
	Average	S.E.	Average	S.E.		
165	1.8E-06	7.5E-08	1.8E-06	3.0E-07	0.99	
186	1.9E-06	4.7E-07	1.6E-06	3.3E-07	0.82	
73	1.9E-06	7.2E-09	2.0E-06	6.4E-08	1.1	0.154
5	1.9E-06	1.7E-07	1.4E-06	3.9E-07	0.75	
161	1.9E-06	1.3E-07	1.5E-06	1.1E-07	0.77	
164	2.0E-06	7.4E-08	1.9E-06	2.0E-07	0.92	
63	2.1E-06	4.0E-07	2.4E-06	1.7E-07	1.2	0.288
27	2.1E-06	2.7E-08	4.4E-06	6.0E-07	2.2	0.041
64	2.1E-06	4.3E-07	2.4E-06	2.2E-07	1.2	0.294
159	2.1E-06	2.0E-07	1.7E-06	2.2E-07	0.79	
7	2.2E-06	9.9E-07	1.9E-06	5.4E-07	0.87	
136	2.3E-06	1.0E-07	2.7E-06	2.0E-07	1.2	0.118
192	2.3E-06	5.9E-08	2.4E-06	5.7E-08	1.1	0.089
157	2.3E-06	1.7E-07	2.1E-06	2.2E-07	0.93	
110	2.3E-06	2.8E-07	3.3E-06	3.2E-07	1.4	0.076
98	2.5E-06	5.8E-08	4.3E-06	4.2E-07	1.7	0.034
117	2.5E-06	1.3E-07	2.7E-06	3.8E-07	1.1	0.353
109	2.5E-06	2.4E-07	3.2E-06	3.4E-07	1.3	0.127
162	2.7E-06	1.0E-07	2.1E-06	2.5E-07	0.80	
166	2.7E-06	1.1E-07	2.3E-06	2.3E-07	0.83	
62	2.8E-06	2.0E-06	2.1E-06	1.5E-06	0.78	
119	2.8E-06	1.1E-07	3.8E-06	1.8E-08	1.4	0.008
106	2.9E-06	3.1E-07	3.0E-06	1.7E-07	1.1	0.370
127	2.9E-06	3.2E-07	2.7E-06	7.8E-08	0.92	
118	2.9E-06	7.1E-08	3.9E-06	4.1E-08	1.3	0.000
120	2.9E-06	3.3E-08	5.3E-06	5.2E-08	1.8	0.000
180	3.0E-06	9.6E-08	2.6E-06	3.6E-07	0.84	0.199
204	3.1E-06	5.0E-08	3.5E-06	2.1E-07	1.1	0.067
55	3.1E-06	6.5E-07	3.5E-06	7.9E-07	1.1	0.447
66	3.3E-06	6.7E-07	4.6E-06	7.7E-07	1.4	0.147
179	3.3E-06	2.8E-07	2.1E-06	2.8E-07	0.63	
168	3.4E-06	6.7E-08	2.7E-06	2.9E-07	0.80	
167	3.4E-06	5.7E-08	2.9E-06	2.3E-07	0.83	
69	3.5E-06	1.5E-07	5.6E-06	5.6E-07	1.6	0.021
149	3.5E-06	1.4E-07	2.7E-06	1.8E-07	0.77	
60	3.6E-06	1.4E-07	4.4E-06	2.0E-07	1.2	0.027
163	3.7E-06	1.6E-07	2.9E-06	3.4E-07	0.79	
115	3.9E-06	3.4E-07	4.4E-06	3.5E-07	1.1	0.223
2	4.0E-06	5.1E-07	1.2E-05	3.8E-06	3.0	0.112
135	4.0E-06	1.7E-07	4.5E-06	4.1E-07	1.1	0.219
102	4.0E-06	1.2E-07	6.7E-06	2.5E-07	1.7	0.001
68	4.2E-06	2.2E-06	5.0E-06	2.4E-06	1.2	0.417
123	4.2E-06	1.4E-07	4.9E-06	4.2E-07	1.1	0.160
96	4.4E-06	9.8E-08	4.7E-06	1.6E-07	1.1	0.092
133	5.1E-06	2.1E-07	5.7E-06	5.5E-07	1.1	0.198
201	5.1E-06	1.2E-07	5.7E-06	3.2E-07	1.1	0.091
24	5.4E-06	1.6E-06	5.2E-06	1.4E-06	0.97	
43	5.7E-06	1.9E-06	6.4E-06	2.1E-06	1.1	0.428
189	5.9E-06	1.5E-07	6.0E-06	1.7E-07	1.0	0.335
190	6.0E-06	2.4E-07	6.7E-06	3.8E-07	1.1	0.084
18	6.0E-06	1.0E-06	5.6E-06	1.1E-06	0.95	
132	6.2E-06	3.1E-07	5.3E-06	2.8E-07	0.85	
8	6.3E-06	1.1E-06	7.3E-06	2.5E-06	1.2	0.389

University of Glasgow Compound Code	EC ₅₀ Value (M) Tb427 WT		EC ₅₀ Value (M) TbAT1 KO		TbAT1 KO Resistance Factor	P Value: Significantly Resistant
	Average	S.E.	Average	S.E.		
25	6.3E-06	8.4E-07	6.8E-06	1.6E-07	1.1	0.349
116	7.0E-06	6.8E-08	9.1E-06	4.5E-07	1.3	0.029
153	7.0E-06	1.2E-06	7.1E-06	2.0E-07	1.0	0.485
154	7.3E-06	6.8E-07	7.5E-06	3.4E-07	1.0	0.418
20	7.7E-06	1.4E-06	1.0E-05	2.2E-06	1.3	0.381
93	7.7E-06	2.4E-07	7.3E-06	1.5E-07	0.94	
125	7.8E-06	2.5E-07	9.7E-06	3.0E-07	1.2	0.008
38	8.2E-06	1.8E-07	9.0E-06	7.0E-07	1.1	0.207
195	9.3E-06	1.8E-07	8.7E-06	7.1E-08	0.93	
173	9.7E-06	4.8E-07	9.7E-06	4.8E-07	1.0	0.492
34	9.8E-06	5.4E-07	8.3E-06	1.0E-06	0.84	
188	9.9E-06	3.1E-07	9.0E-06	2.8E-07	0.91	
41	1.0E-05	2.9E-07	1.1E-05	1.8E-07	1.1	0.056
61	1.0E-05	9.2E-07	9.0E-06	1.3E-06	0.87	
187	1.0E-05	4.7E-07	1.2E-05	5.0E-07	1.1	0.110
150	1.1E-05	2.6E-07	1.2E-05	1.2E-07	1.2	0.003
16	1.1E-05	2.7E-06	9.1E-06	2.3E-06	0.86	
71	1.1E-05	3.7E-07	1.4E-05	4.9E-07	1.2	0.015
40	1.1E-05	3.5E-07	1.2E-05	1.5E-07	1.1	0.128
70	1.1E-05	5.9E-07	1.5E-05	9.5E-07	1.3	0.027
44	1.2E-05	3.3E-06	1.2E-05	3.1E-06	0.97	
33	1.3E-05	4.2E-07	1.3E-05	5.6E-07	1.0	0.456
11	1.3E-05	2.9E-06	9.8E-06	1.7E-06	0.75	
53	1.3E-05	2.9E-06	1.2E-05	2.2E-06	0.89	
56	1.4E-05	4.0E-06	1.4E-05	4.7E-06	1.1	0.427
126	1.4E-05	5.1E-07	1.5E-05	6.7E-07	1.1	0.218
32	1.4E-05	9.3E-07	1.3E-05	7.3E-07	0.94	
108	1.4E-05	2.7E-07	1.5E-05	3.7E-07	1.1	0.125
206	1.5E-05	5.1E-07	1.5E-05	4.2E-07	1.0	
51	1.5E-05	3.7E-06	8.1E-06	2.2E-06	0.54	
134	1.6E-05	5.6E-07	1.6E-05	4.6E-07	1.0	0.430
101	1.6E-05	4.8E-07	2.2E-05	7.6E-07	1.4	0.003
200	1.6E-05	6.8E-07	1.2E-05	2.6E-07	0.79	
97	1.6E-05	6.4E-08	1.7E-05	3.1E-07	1.0	0.112
42	1.7E-05	8.1E-06	1.5E-05	7.5E-06	0.91	
21	1.7E-05	4.2E-06	2.2E-05	6.1E-06	1.3	0.310
160	1.7E-05	1.7E-06	1.5E-05	9.0E-07	0.85	
191	1.8E-05	3.7E-07	1.7E-05	6.0E-07	0.95	
100	1.8E-05	6.6E-07	2.0E-05	1.0E-06	1.1	0.152
19	1.9E-05	4.7E-06	2.5E-05	3.6E-06	1.3	0.219
169	1.9E-05	1.0E-06	1.3E-05	9.2E-07	0.68	
176	1.9E-05	5.8E-07	2.0E-05	1.4E-06	1.0	0.413
95	2.0E-05	1.6E-06	1.6E-05	3.3E-07	0.79	
193	2.0E-05	1.0E-06	1.8E-05	1.3E-06	0.90	
12	2.1E-05	8.0E-06	1.2E-05	2.0E-06	0.58	
54	2.1E-05	2.2E-06	2.3E-05	3.0E-06	1.1	0.127
76	2.2E-05	4.0E-06	3.1E-05	5.8E-06	1.4	0.173
202	2.3E-05	2.6E-07	2.1E-05	4.7E-07	0.91	
45	2.3E-05	6.7E-06	2.3E-05	6.6E-06	0.97	
81	2.4E-05	2.8E-06	2.6E-05	4.8E-06	1.1	0.378
177	2.4E-05	8.0E-06	3.7E-05	2.1E-06	1.6	0.147
59	2.4E-05	7.5E-06	2.2E-05	6.7E-06	0.91	
9	2.5E-05	2.6E-06	2.6E-05	9.6E-06	1.1	0.446

University of Glasgow Compound Code	EC ₅₀ Value (M) Tb427 WT		EC ₅₀ Value (M) TbAT1 KO		TbAT1 KO Resistance Factor	P Value: Significantly Resistant
	Average	S.E.	Average	S.E.		
75	2.5E-05	3.6E-06	3.4E-05	4.1E-06	1.3	0.131
17	2.6E-05	4.1E-06	2.5E-05	3.4E-06	0.95	
205	2.6E-05	2.2E-06	2.1E-05	1.2E-06	0.83	
181	2.6E-05	1.0E-06	1.8E-05	2.5E-06	0.67	
175	2.7E-05	4.5E-07	2.6E-05	1.2E-06	0.97	
15	2.7E-05	6.7E-06	2.7E-05	5.7E-06	1.0	
155	2.7E-05	3.0E-06	1.4E-05	1.4E-06	0.52	
52	2.8E-05	6.0E-06	2.7E-05	6.4E-06	0.94	
46	2.9E-05	9.1E-06	2.5E-05	8.4E-06	0.89	
194	2.9E-05	4.2E-07	2.6E-05	1.0E-06	0.91	
92	3.0E-05	1.2E-06	3.1E-05	7.5E-08	1.0	0.373
57	3.1E-05	9.7E-06	2.4E-05	8.0E-06	0.78	
196	3.4E-05	1.3E-06	3.0E-05	4.3E-07	0.89	
22	3.4E-05	8.3E-06	3.6E-05	6.4E-06	1.1	0.491
174	3.4E-05	2.3E-06	2.9E-05	1.4E-06	0.86	
26	3.4E-05	7.5E-06	3.9E-05	7.6E-06	1.1	0.466
58	3.4E-05	8.2E-06	3.8E-05	8.7E-06	1.1	0.462
30	3.8E-05	3.0E-06	4.2E-05	4.5E-06	1.1	0.273
49	3.8E-05	8.7E-06	3.5E-05	8.1E-06	0.91	
156	3.8E-05	8.9E-06	2.5E-05	2.2E-06	0.64	
3	4.0E-05	9.2E-06	2.3E-05	9.1E-06	0.57	
23	4.0E-05	1.1E-05	4.5E-05	8.3E-06	1.1	0.493
13	4.1E-05	1.9E-05	6.4E-05	1.9E-05	1.6	0.417
31	4.4E-05	7.8E-06	5.6E-05	1.3E-05	1.3	0.250
86	4.4E-05	2.1E-06	4.4E-05	1.1E-06	1.0	0.452
203	4.4E-05	3.0E-06	3.2E-05	1.5E-06	0.73	
184	4.5E-05	2.6E-06	3.8E-05	3.6E-06	0.84	
171	4.6E-05	1.7E-06	5.1E-05	3.9E-06	1.1	0.150
67	4.8E-05	7.7E-06	7.2E-05	4.4E-06	1.5	0.045
185	4.8E-05	2.6E-06	3.5E-05	5.3E-06	0.74	
29	5.0E-05	6.2E-06	5.0E-05	2.5E-06	1.0	
172	5.1E-05	7.5E-06	4.6E-05	1.2E-05	0.90	
89	5.6E-05	1.7E-06	6.2E-05	4.1E-06	1.1	0.220
14	6.1E-05	3.9E-05	6.7E-05	3.6E-05	1.1	0.470
170	6.1E-05	2.4E-06	5.7E-05	3.5E-06	0.92	
146	7.1E-05	2.3E-06	6.0E-05	5.0E-06	0.84	
178	7.1E-05	6.1E-06	6.2E-05	7.5E-06	0.87	
28	7.2E-05	7.4E-06	8.2E-05	7.2E-06	1.1	0.243
94	7.5E-05	9.2E-06	4.4E-05	4.0E-06	0.59	
144	7.6E-05	1.1E-06	6.9E-05	2.5E-06	0.91	
39	7.7E-05	1.3E-05	8.9E-05	1.6E-05	1.2	0.313
99	7.8E-05	9.1E-06	7.5E-05	5.8E-06	0.97	
85	8.4E-05	7.7E-07	7.5E-05	8.8E-06	0.90	
207	8.4E-05	4.0E-06	1.9E-04	1.2E-05	2.2	0.001
1	8.8E-05	1.1E-05	9.0E-04	6.6E-04	10.2	0.210
91	8.9E-05	2.2E-06	8.3E-05	1.3E-06	0.94	
183	9.4E-05	1.6E-06	8.7E-05	6.7E-06	0.93	
148	9.5E-05	1.9E-06	6.4E-05	2.8E-06	0.67	
147	9.7E-05	1.5E-06	1.0E-04	2.7E-07	1.1	0.043
182	9.8E-05	1.3E-06	8.9E-05	7.4E-06	0.91	
90	1.0E-04	4.6E-07	1.0E-04	3.4E-06	0.98	
208	1.0E-04	2.8E-06	6.3E-05	2.9E-06	0.60	
211	1.1E-04	1.1E-06	6.3E-05	1.8E-06	0.56	

University of Glasgow Compound Code	EC ₅₀ Value (M) Tb427 WT		EC ₅₀ Value (M) TbAT1 KO		TbAT1 KO Resistance Factor	P Value: Significantly Resistant
	Average	S.E.	Average	S.E.		
210	1.1E-04	1.0E-06	7.0E-05	1.5E-06	0.61	
209	1.2E-04	1.6E-06	6.5E-05	1.8E-06	0.55	
212	1.2E-04	2.1E-06	7.3E-05	1.1E-06	0.62	
35	Not Soluble					
36	Not Soluble					
65	Not Soluble					
47	Not Soluble					
50	Not Soluble					
78	Not Soluble					
87	Not Soluble					
88	Not Soluble					

Appendix 2:

Average EC₅₀ values for a panel of Series 1 compounds against *Trypanosoma equiperdum* wild type and the diminazene resistant PBR strain bloodstream form trypanosomes, with standard errors. Values were derived from whole-cell *in vitro* efficacy assays and calculated from sigmoidal dose-response curves, with variable slopes, using GraphPad Prism software. Averages are taken from at least 3 independent experiments. Also shown is the resistance factor of the PBR strain compared to *T. equiperdum* wild type, as well as the efficacy factor between species, comparing the average EC₅₀ values against Tb427 and *T. equiperdum* wild type strains for each compound. Statistical significance for the presence of resistance was calculated using the one-tailed, unpaired Student's T-test after an F-test was conducted to determine which was most appropriate: that for equal or unequal variances. A two-tailed, unpaired Student's T-test was carried out to determine the presence of significant differences between species, again after the use of the F-test to determine the correct T-test to use. Those compounds for which the PBR strain is statistically resistant are highlighted in red text, and those showing significant inter-species difference in EC₅₀ values are highlighted in blue.

University of Glasgow Compound Code	EC ₅₀ Value (M) <i>T. equiperdum</i> WT		EC ₅₀ Value (M) <i>T. equiperdum</i> PBR		PBR Resistance Factor	P Value: Significantly Resistant	Efficacy Factor (Tb427 WT / <i>T. equiperdum</i> WT)	P Value: Significantly Different
	Average	S.E.	Average	S.E.				
82	3.5E-09	2.1E-09	3.7E-09	9.8E-10	1.0	0.478	20	0.077
48	5.4E-09	1.3E-09	5.7E-09	1.6E-09	1.1	0.452	13	0.140
80	1.9E-08	1.9E-09	2.0E-08	4.7E-09	1.1	0.420	14	0.019
111	1.9E-08	2.9E-09	2.5E-08	8.2E-10	1.3	0.088	20	0.015
Diminazene	2.8E-08	4.9E-09	2.0E-06	2.9E-07	71	0.003	3.1	0.002
107	3.2E-08	1.4E-08	2.9E-08	1.2E-08	0.90		14	0.000
197	3.5E-08	1.4E-08	2.5E-08	2.2E-09	0.73		0.35	0.326
79	4.2E-08	6.8E-09	4.3E-08	2.7E-09	1.0	0.445	6.9	0.043
199	6.2E-08	8.9E-09	6.0E-08	4.6E-09	0.97		2.9	0.037
139	1.1E-07	4.9E-09	1.0E-07	3.2E-09	0.98		2.1	0.144
72	1.1E-07	2.0E-08	1.7E-07	1.3E-08	1.5	0.045	5.4	0.000
112	1.3E-07	1.4E-08	1.4E-07	1.4E-08	1.0	0.442	11	0.004
83	1.6E-07	2.1E-08	1.4E-07	2.3E-08	0.90		2.8	0.001
104	2.0E-07	1.5E-08	1.5E-07	4.7E-09	0.76		1.7	0.058
198	2.0E-07	3.2E-09	1.8E-07	2.0E-08	0.88		0.80	0.151
84	2.2E-07	2.7E-09	2.3E-07	5.4E-09	1.0	0.125	7.7	0.000
114	2.3E-07	2.0E-08	2.1E-07	1.8E-08	0.94		0.87	0.466
37	2.5E-07	1.4E-08	2.9E-07	2.5E-08	1.2	0.160	1.4	0.323
110	2.5E-07	4.3E-08	2.6E-07	3.3E-08	1.0	0.469	9.3	0.023
10	3.6E-07	1.4E-08	4.5E-07	2.7E-09	1.3	0.015	2.3	0.151
74	3.9E-07	9.0E-08	3.7E-07	7.4E-08	0.94		2.7	0.004
103	4.1E-07	1.2E-07	4.7E-07	1.0E-07	1.1	0.388	1.6	0.247
105	4.3E-07	1.2E-07	3.7E-07	7.7E-08	0.85		1.4	0.437
64	4.4E-07	3.6E-08	6.4E-07	4.8E-08	1.4	0.028	4.8	0.086
4	4.9E-07	4.7E-08	6.7E-07	5.0E-08	1.4	0.052	3.2	0.103
77	5.2E-07	1.2E-07	4.9E-07	1.3E-07	0.94		1.5	0.234
113	5.2E-07	3.7E-08	6.6E-07	1.2E-08	1.3	0.022	0.49	0.027
98	5.3E-07	3.8E-08	8.1E-07	5.9E-08	1.5	0.014	4.7	0.000
6	8.1E-07	1.9E-07	9.3E-07	1.6E-07	1.1	0.352	1.3	0.547
158	8.3E-07	3.4E-08	8.8E-07	3.9E-08	1.1	0.254	0.69	0.014
63	8.5E-07	9.3E-08	1.0E-06	1.1E-07	1.2	0.206	2.4	0.072
7	1.0E-06	6.0E-08	1.0E-06	3.3E-08	0.99		2.1	0.436
27	1.3E-06	4.4E-08	1.6E-06	1.4E-07	1.3	0.060	1.6	0.000
204	1.3E-06	9.1E-08	1.4E-06	4.1E-08	1.1	0.251	2.4	0.000
73	1.6E-06	3.1E-07	1.7E-06	2.0E-07	1.0	0.473	1.2	0.454
192	1.8E-06	5.0E-08	1.9E-06	2.0E-08	1.1	0.088	1.3	0.003
186	2.1E-06	4.3E-08	2.1E-06	1.4E-07	1.0	0.435	0.91	0.732
165	2.2E-06	1.0E-07	2.3E-06	1.5E-07	1.0	0.406	0.83	0.050
164	2.2E-06	1.7E-07	2.1E-06	1.1E-07	0.96		0.92	0.408
159	2.3E-06	1.1E-07	2.5E-06	5.6E-08	1.1	0.121	0.91	0.544
157	2.5E-06	9.3E-08	2.6E-06	1.5E-07	1.0	0.388	0.91	0.394
179	2.7E-06	2.0E-07	2.5E-06	2.4E-07	0.94		1.2	0.212
161	2.7E-06	1.5E-07	2.8E-06	9.8E-08	1.0	0.338	0.72	0.026
166	2.7E-06	2.4E-07	2.7E-06	6.2E-08	1.0	0.468	1.0	0.975
201	2.8E-06	1.0E-07	2.8E-06	6.2E-08	0.99		1.8	0.000
180	2.9E-06	4.5E-08	3.0E-06	6.2E-08	1.0	0.181	1.0	0.425
162	3.3E-06	4.3E-08	3.4E-06	1.1E-07	1.0	0.183	0.82	0.010
163	3.7E-06	1.9E-07	4.0E-06	1.0E-07	1.1	0.169	1.0	0.864
167	4.0E-06	9.8E-08	4.1E-06	1.2E-07	1.0	0.350	0.86	0.006
168	4.2E-06	1.5E-07	4.3E-06	8.7E-08	1.0	0.383	0.81	0.007
190	6.0E-06	9.0E-07	4.5E-06	5.5E-07	0.75		1.0	0.981

University of Glasgow Compound Code	EC ₅₀ Value (M) <i>T. equiperdum</i> WT		EC ₅₀ Value (M) <i>T. equiperdum</i> PBR		PBR Resistance Factor	P Value: Significantly Resistant	Efficacy Factor (Tb427 WT / <i>T. equiperdum</i> WT)	P Value: Significantly Different
	Average	S.E.	Average	S.E.				
189	6.3E-06	1.7E-07	5.7E-06	6.0E-07	0.90		0.93	0.154
200	7.2E-06	4.4E-07	7.3E-06	3.5E-07	1.0	0.485	2.2	0.000
154	7.3E-06	8.1E-07	6.5E-06	1.1E-06	0.88		1.0	0.995
195	8.7E-06	2.7E-07	7.5E-06	1.2E-06	0.86		1.1	0.144
173	1.3E-05	1.3E-07	9.8E-06	3.8E-07	0.75		0.75	0.004
153	1.3E-05	8.2E-07	1.1E-05	3.0E-07	0.85		0.54	0.020
55	1.5E-05	1.7E-07	1.6E-05	1.2E-06	1.1	0.326	0.21	0.000
208	1.0E-04	2.8E-06	5.4E-05	2.7E-06	0.52		1.0	0.763
211	1.1E-04	1.6E-06	5.7E-05	2.4E-06	0.54		1.1	0.063
209	1.1E-04	2.1E-06	6.6E-05	3.1E-06	0.58		1.0	0.429
210	1.2E-04	3.0E-06	6.4E-05	1.3E-06	0.56		0.99	0.835
212	1.2E-04	1.5E-06	6.2E-05	1.5E-06	0.53		1.0	0.720

Appendix 3:

The nucleotide sequences of TbrPDEB1 from all the cloned sequences taken from the GJS-128 resistant R0.8 strain and parental wildtype. Sequences are divided by the published sequence for TbrPDEB1 from GeneDB.

		1		100
R0-8 PDE-B1 Clone A1	(1)	ATGTTTCATGAACAAGCCCTTTGGCAGCAAGCGCTGCGAACCCCTCCACGAGTCGGAGCACCTTTGTGAGGCGTTTGCCATCACTGAAGCAATCCTCGCTC		
R0-8 PDE-B1 Clone A2	(1)	ATGTTTCATGAACAAGCCCTTTGGCAGCAAGCGCTGCGAACCCCTCCACGAGTCGGAGCACCTTTGTGAGGCGTTTGCCATCACTGAAGCAATCCTCGCTC		
R0-8 PDE-B1 Clone A3	(1)	ATGTTTCATGAACAAGCCCTTTGGCAGCAAGCGCTGCGAACCCCTCCACGAGTCGGAGCACCTTTGTGAGGCGTTTGCCATCACTGAAGCAATCCTCGCTC		
R0-8 PDE-B1 Clone A4	(1)	ATGTTTCATGAACAAGCCCTTTGGCAGCAAGCGCTGCGAACCCCTCCACGAGTCGGAGCACCTTTGTGAGGCGTTTGCCATCACTGAAGCAATCCTCGCTC		
R0-8 PDE-B1 Clone A5	(1)	ATGTTTCATGAACAAGCCCTTTGGCAGCAAGCGCTGCGAACCCCTCCACGAGTCGGAGCACCTTTGTGAGGCGTTTGCCATCACTGAAGCAATCCTCGCTC		
R0-8 PDE-B1 Clone A6	(1)	ATGTTTCATGAACAAGCCCTTTGGCAGCAAGCGCTGCGAACCCCTCCACGAGTCGGAGCACCTTTGTGAGGCGTTTGCCATCACTGAAGCAATCCTCGCTC		
R0-8 PDE-B1 Clone A7	(1)	ATGTTTCATGAACAAGCCCTTTGGCAGCAAGCGCTGCGAACCCCTCCACGAGTCGGAGCACCTTTGTGAGGCGTTTGCCATCACTGAAGCAATCCTCGCTC		
R0-8 PDE-B1 Clone A8	(1)	ATGTTTCATGAACAAGCCCTTTGGCAGCAAGCGCTGCGAACCCCTCCACGAGTCGGAGCACCTTTGTGAGGCGTTTGCCATCACTGAAGCAATCCTCGCTC		
R0-8 PDE-B1 Clone B1	(1)	ATGTTTCATGAACAAGCCCTTTGGCAGCAAGCGCTGCGAACCCCTCCACGAGTCGGAGCACCTTTGTGAGGCGTTTGCCATCACTGAAGCAATCCTCGCTC		
GeneDB TbrPDEB1	(1)	ATGTTTCATGAACAAGCCCTTTGGCAGCAAGCGCTGCGAACCCCTCCACGAGTCGGAGCACCTTTGTGAGGCGTTTGCCATCACTGAAGCAATCCTCGCTC		
WT PDE-B1 Clone B1	(1)	ATGTTTCATGAACAAGCCCTTTGGCAGCAAGCGCTGCGAACCCCTCCACGAGTCGGAGCACCTTTGTGAGGCGTTTGCCATCACTGAAGCAATCCTCGCTC		
WT PDE-B1 Clone A1	(1)	ATGTTTCATGAACAAGCCCTTTGGCAGCAAGCGCTGCGAACCCCTCCACGAGTCGGAGCACCTTTGTGAGGCGTTTGCCATCACTGAAGCAATCCTCGCTC		
WT PDE-B1 Clone A3	(1)	ATGTTTCATGAACAAGCCCTTTGGCAGCAAGCGCTGCGAACCCCTCCACGAGTCGGAGCACCTTTGTGAGGCGTTTGCCATCACTGAAGCAATCCTCGCTC		
WT PDE-B1 Clone A4	(1)	ATGTTTCATGAACAAGCCCTTTGGCAGCAAGCGCTGCGAACCCCTCCACGAGTCGGAGCACCTTTGTGAGGCGTTTGCCATCACTGAAGCAATCCTCGCTC		
WT PDE-B1 Clone A8	(1)	ATGTTTCATGAACAAGCCCTTTGGCAGCAAGCGCTGCGAACCCCTCCACGAGTCGGAGCACCTTTGTGAGGCGTTTGCCATCACTGAAGCAATCCTCGCTC		
WT PDE-B1 Clone A2	(1)	ATGTTTCATGAACAAGCCCTTTGGCAGCAAGCGCTGCGAACCCCTCCACGAGTCGGAGCACCTTTGTGAGGCGTTTGCCATCACTGAAGCAATCCTCGCTC		
WT PDE-B1 Clone A5	(1)	ATGTTTCATGAACAAGCCCTTTGGCAGCAAGCGCTGCGAACCCCTCCACGAGTCGGAGCACCTTTGTGAGGCGTTTGCCATCACTGAAGCAATCCTCGCTC		
WT PDE-B1 Clone A6	(1)	ATGTTTCATGAACAAGCCCTTTGGCAGCAAGCGCTGCGAACCCCTCCACGAGTCGGAGCACCTTTGTGAGGCGTTTGCCATCACTGAAGCAATCCTCGCTC		
WT PDE-B1 Clone A7	(1)	ATGTTTCATGAACAAGCCCTTTGGCAGCAAGCGCTGCGAACCCCTCCACGAGTCGGAGCACCTTTGTGAGGCGTTTGCCATCACTGAAGCAATCCTCGCTC		
		101		200
R0-8 PDE-B1 Clone A1	(101)	GCTATCAGCGTGGGAAACGCAGCTTTACGTCTCCGAAAAAAGTGGACTGGCAGCCCTTATCAAACGTATTCCCTTATGATATCCTTGTGAGGTTCTCGA		
R0-8 PDE-B1 Clone A2	(101)	GCTATCAGCGTGGGAAACGCAGCTTTACGTCTCCGAAAAAAGTGGACTGGCAGCCCTTATCAAACGTATTCCCTTATGATATCCTTGTGAGGTTCTCGA		
R0-8 PDE-B1 Clone A3	(101)	GCTATCAGCGTGGGAAACGCAGCTTTACGTCTCCGAAAAAAGTGGACTGGCAGCCCTTATCAAACGTATTCCCTTATGATATCCTTGTGAGGTTCTCGA		
R0-8 PDE-B1 Clone A4	(101)	GCTATCAGCGTGGGAAACGCAGCTTTACGTCTCCGAAAAAAGTGGACTGGCAGCCCTTATCAAACGTATTCCCTTATGATATCCTTGTGAGGTTCTCGA		
R0-8 PDE-B1 Clone A5	(101)	GCTATCAGCGTGGGAAACGCAGCTTTACGTCTCCGAAAAAAGTGGACTGGCAGCCCTTATCAAACGTATTCCCTTATGATATCCTTGTGAGGTTCTCGA		
R0-8 PDE-B1 Clone A6	(101)	GCTATCAGCGTGGGAAACGCAGCTTTACGTCTCCGAAAAAAGTGGACTGGCAGCCCTTATCAAACGTATTCCCTTATGATATCCTTGTGAGGTTCTCGA		
R0-8 PDE-B1 Clone A7	(101)	GCTATCAGCGTGGGAAACGCAGCTTTACGTCTCCGAAAAAAGTGGACTGGCAGCCCTTATCAAACGTATTCCCTTATGATATCCTTGTGAGGTTCTCGA		
R0-8 PDE-B1 Clone A8	(101)	GCTATCAGCGTGGGAAACGCAGCTTTACGTCTCCGAAAAAAGTGGACTGGCAGCCCTTATCAAACGTATTCCCTTATGATATCCTTGTGAGGTTCTCGA		
R0-8 PDE-B1 Clone B1	(101)	GCTATCAGCGTGGGAAACGCAGCTTTACGTCTCCGAAAAAAGTGGACTGGCAGCCCTTATCAAACGTATTCCCTTATGATATCCTTGTGAGGTTCTCGA		
GeneDB TbrPDEB1	(101)	GCTATCAGCGTGGGAAACGCAGCTTTACGTCTCCGAAAAAAGTGGACTGGCAGCCCTTATCAAACGTATTCCCTTATGATATCCTTGTGAGGTTCTCGA		
WT PDE-B1 Clone B1	(101)	GCTATCAGCGTGGGAAACGCAGCTTTACGTCTCCGAAAAAAGTGGACTGGCAGCCCTTATCAAACGTATTCCCTTATGATATCCTTGTGAGGTTCTCGA		
WT PDE-B1 Clone A1	(101)	GCTATCAGCGTGGGAAACGCAGCTTTACGTCTCCGAAAAAAGTGGACTGGCAGCCCTTATCAAACGTATTCCCTTATGATATCCTTGTGAGGTTCTCGA		
WT PDE-B1 Clone A3	(101)	GCTATCAGCGTGGGAAACGCAGCTTTACGTCTCCGAAAAAAGTGGACTGGCAGCCCTTATCAAACGTATTCCCTTATGATATCCTTGTGAGGTTCTCGA		
WT PDE-B1 Clone A4	(101)	GCTATCAGCGTGGGAAACGCAGCTTTACGTCTCCGAAAAAAGTGGACTGGCAGCCCTTATCAAACGTATTCCCTTATGATATCCTTGTGAGGTTCTCGA		
WT PDE-B1 Clone A8	(101)	GCTATCAGCGTGGGAAACGCAGCTTTACGTCTCCGAAAAAAGTGGACTGGCAGCCCTTATCAAACGTATTCCCTTATGATATCCTTGTGAGGTTCTCGA		
WT PDE-B1 Clone A2	(101)	GCTATCAGCGTGGGAAACGCAGCTTTACGTCTCCGAAAAAAGTGGACTGGCAGCCCTTATCAAACGTATTCCCTTATGATATCCTTGTGAGGTTCTCGA		
WT PDE-B1 Clone A5	(101)	GCTATCAGCGTGGGAAACGCAGCTTTACGTCTCCGAAAAAAGTGGACTGGCAGCCCTTATCAAACGTATTCCCTTATGATATCCTTGTGAGGTTCTCGA		
WT PDE-B1 Clone A6	(101)	GCTATCAGCGTGGGAAACGCAGCTTTACGTCTCCGAAAAAAGTGGACTGGCAGCCCTTATCAAACGTATTCCCTTATGATATCCTTGTGAGGTTCTCGA		
WT PDE-B1 Clone A7	(101)	GCTATCAGCGTGGGAAACGCAGCTTTACGTCTCCGAAAAAAGTGGACTGGCAGCCCTTATCAAACGTATTCCCTTATGATATCCTTGTGAGGTTCTCGA		

Appendix 4:

The amino acid sequences of TbrPDEB1 from all the cloned sequences taken from the GJS-128 resistant R0.8 strain and parental wildtype. Sequences are divided by the published sequence for TbrPDEB1 from GeneDB.

			1	100											
R0-8 PDE-B1 Clone A1	(1)	MFMNKFFGSKRCEPFHESEHLCEAFAITEAILARYQRGKRSFTSSEKSGLAALIKRIPYDILVEVLDQSGFTPTS	NATPPVDYLAMMEHTMTHGASITHA												
R0-8 PDE-B1 Clone A2	(1)	MFMNKFFGSKRCEPFHESEHLCEAFAITEAILARYQRGKRSFTSSEKSGLAALIKRIPYDILVEVLDQSGFTPTS	NATPPVDYLAMMEHTMTHGASITHA												
R0-8 PDE-B1 Clone A3	(1)	MFMNKFFGSKRCEPFHESEHLCEAFAITEAILARYQRGKRSFTSSEKSGLAALIKRIPYDILVEVLDQSGFTPTS	NATPPVDYLAMMEHTMTHGASITHA												
R0-8 PDE-B1 Clone A4	(1)	MFMNKFFGSKRCEPFHESEHLCEAFAITEAILARYQRGKRSFTSSEKSGLAALIKRIPYDILVEVLDQSGFTPTS	NATPPVDYLAMMEHTMTHGASITHA												
R0-8 PDE-B1 Clone A5	(1)	MFMNKFFGSKRCEPFHESEHLCEAFAITEAILARYQRGKRSFTSSEKSGLAALIKRIPYDILVEVLDQSGFTPTS	NATPPVDYLAMMEHTMTHGASITHA												
R0-8 PDE-B1 Clone A6	(1)	MFMNKFFGSKRCEPFHESEHLCEAFAITEAILARYQRGKRSFTSSEKSGLAALIKRIPYDILVEVLDQSGFTPTS	NATPPVDYLAMMEHTMTHGASITHA												
R0-8 PDE-B1 Clone A7	(1)	MFMNKFFGSKRCEPFHESEHLCEAFAITEAILARYQRGKRSFTSSEKSGLAALIKRIPYDILVEVLDQSGFTPTS	NATPPVDYLAMMEHTMTHGASITHA												
R0-8 PDE-B1 Clone A8	(1)	MFMNKFFGSKRCEPFHESEHLCEAFAITEAILARYQRGKRSFTSSEKSGLAALIKRIPYDILVEVLDQSGFTPTS	NATPPVDYLAMMEHTMTHGASITHA												
R0-8 PDE-B1 Clone B1	(1)	MFMNKFFGSKRCEPFHESEHLCEAFAITEAILARYQRGKRSFTSSEKSGLAALIKRIPYDILVEVLDQSGFTPTS	NATPPVDYLAMMEHTMTHGASITHA												
GeneDB TbrPDEB1	(1)	MFMNKFFGSKRCEPFHESEHLCEAFAITEAILARYQRGKRSFTSSEKSGLAALIKRIPYDILVEVLDQSGFTPTS	NATPPVDYLAMMEHTMTHGASITHA												
WT PDE-B1 Clone B1	(1)	MFMNKFFGSKRCEPFHESEHLCEAFAITEAILARYQRGKRSFTSSEKSGLAALIKRIPYDILVEVLDQSGFTPTS	NATPPVDYLAMMEHTMTHGASITHA												
WT PDE-B1 Clone A1	(1)	MFMNKFFGSKRCEPFHESEHLCEAFAITEAILARYQRGKRSFTSSEKSGLAALIKRIPYDILVEVLDQSGFTPTS	NATPPVDYLAMMEHTMTHGASITHA												
WT PDE-B1 Clone A3	(1)	MFMNKFFGSKRCEPFHESEHLCEAFAITEAILARYQRGKRSFTSSEKSGLAALIKRIPYDILVEVLDQSGFTPTS	NATPPVDYLAMMEHTMTHGASITHA												
WT PDE-B1 Clone A4	(1)	MFMNKFFGSKRCEPFHESEHLCEAFAITEAILARYQRGKRSFTSSEKSGLAALIKRIPYDILVEVLDQSGFTPTS	NATPPVDYLAMMEHTMTHGASITHA												
WT PDE-B1 Clone A8	(1)	MFMNKFFGSKRCEPFHESEHLCEAFAITEAILARYQRGKRSFTSSEKSGLAALIKRIPYDILVEVLDQSGFTPTS	NATPPVDYLAMMEHTMTHGASITHA												
WT PDE-B1 Clone A2	(1)	MFMNKFFGSKRCEPFHESEHLCEAFAITEAILARYQRGKRSFTSSEKSGLAALIKRIPYDILVEVLDQSGFTPTS	NATPPVDYLAMMEHTMTHGASITHA												
WT PDE-B1 Clone A5	(1)	MFMNKFFGSKRCEPFHESEHLCEAFAITEAILARYQRGKRSFTSSEKSGLAALIKRIPYDILVEVLDQSGFTPTS	NATPPVDYLAMMEHTMTHGASITHA												
WT PDE-B1 Clone A6	(1)	MFMNKFFGSKRCEPFHESEHLCEAFAITEAILARYQRGKRSFTSSEKSGLAALIKRIPYDILVEVLDQSGFTPTS	NATPPVDYLAMMEHTMTHGASITHA												
WT PDE-B1 Clone A7	(1)	MFMNKFFGSKRCEPFHESEHLCEAFAITEAILARYQRGKRSFTSSEKSGLAALIKRIPYDILVEVLDQSGFTPTS	NATPPVDYLAMMEHTMTHGASITHA												
		101		200											
R0-8 PDE-B1 Clone A1	(101)	LQYLN	DLMTKCTGCGP	GIRTYHNP	NDDV	LADPV	HDTAAL	IDETTAVGKSVVTKQYLN	IAGAHYIPLIHG	DIVVGC	VEVPRF	SGNLEK	LPSF	FPSLI	RAVTC
R0-8 PDE-B1 Clone A2	(101)	LQYLN	DLMTKCTGCGP	GIRTYHNP	NDDV	LADPV	HDTAAL	IDETTAVGKSVVTKQYLN	IAGAHYIPLIHG	DIVVGC	VEVPRF	SGNLEK	LPSF	FPSLI	RAVTC
R0-8 PDE-B1 Clone A3	(101)	LQYLN	DLMTKCTGCGP	GIRTYHNP	NDDV	LADPV	HDTAAL	IDETTAVGKSVVTKQYLN	IAGAHYIPLIHG	DIVVGC	VEVPRF	SGNLEK	LPSF	FPSLI	RAVTC
R0-8 PDE-B1 Clone A4	(101)	LQYLN	DLMTKCTGCGP	GIRTYHNP	NDDV	LADPV	HDTAAL	IDETTAVGKSVVTKQYLN	IAGAHYIPLIHG	DIVVGC	VEVPRF	SGNLEK	LPSF	FPSLI	RAVTC
R0-8 PDE-B1 Clone A5	(101)	LQYLN	DLMTKCTGCGP	GIRTYHNP	NDDV	LADPV	HDTAAL	IDETTAVGKSVVTKQYLN	IAGAHYIPLIHG	DIVVGC	VEVPRF	SGNLEK	LPSF	FPSLI	RAVTC
R0-8 PDE-B1 Clone A6	(101)	LQYLN	DLMTKCTGCGP	GIRTYHNP	NDDV	LADPV	HDTAAL	IDETTAVGKSVVTKQYLN	IAGAHYIPLIHG	DIVVGC	VEVPRF	SGNLEK	LPSF	FPSLI	RAVTC
R0-8 PDE-B1 Clone A7	(101)	LQYLN	DLMTKCTGCGP	GIRTYHNP	NDDV	LADPV	HDTAAL	IDETTAVGKSVVTKQYLN	IAGAHYIPLIHG	DIVVGC	VEVPRF	SGNLEK	LPSF	FPSLI	RAVTC
R0-8 PDE-B1 Clone A8	(101)	LQYLN	DLMTKCTGCGP	GIRTYHNP	NDDV	LADPV	HDTAAL	IDETTAVGKSVVTKQYLN	IAGAHYIPLIHG	DIVVGC	VEVPRF	SGNLEK	LPSF	FPSLI	RAVTC
R0-8 PDE-B1 Clone B1	(101)	LQYLN	DLMTKCTGCGP	GIRTYHNP	NDDV	LADPV	HDTAAL	IDETTAVGKSVVTKQYLN	IAGAHYIPLIHG	DIVVGC	VEVPRF	SGNLEK	LPSF	FPSLI	RAVTC
GeneDB TbrPDEB1	(101)	LQYLN	DLMTKCTGCGP	GIRTYHNP	NDDV	LADPV	HDTAAL	IDETTAVGKSVVTKQYLN	IAGAHYIPLIHG	DIVVGC	VEVPRF	SGNLEK	LPSF	FPSLI	RAVTC
WT PDE-B1 Clone B1	(101)	LQYLN	DLMTKCTGCGP	GIRTYHNP	NDDV	LADPV	HDTAAL	IDETTAVGKSVVTKQYLN	IAGAHYIPLIHG	DIVVGC	VEVPRF	SGNLEK	LPSF	FPSLI	RAVTC
WT PDE-B1 Clone A1	(101)	LQYLN	DLMTKCTGCGP	GIRTYHNP	NDDV	LADPV	HDTAAL	IDETTAVGKSVVTKQYLN	IAGAHYIPLIHG	DIVVGC	VEVPRF	SGNLEK	LPSF	FPSLI	RAVTC
WT PDE-B1 Clone A3	(101)	LQYLN	DLMTKCTGCGP	GIRTYHNP	NDDV	LADPV	HDTAAL	IDETTAVGKSVVTKQYLN	IAGAHYIPLIHG	DIVVGC	VEVPRF	SGNLEK	LPSF	FPSLI	RAVTC
WT PDE-B1 Clone A4	(101)	LQYLN	DLMTKCTGCGP	GIRTYHNP	NDDV	LADPV	HDTAAL	IDETTAVGKSVVTKQYLN	IAGAHYIPLIHG	DIVVGC	VEVPRF	SGNLEK	LPSF	FPSLI	RAVTC
WT PDE-B1 Clone A8	(101)	LQYLN	DLMTKCTGCGP	GIRTYHNP	NDDV	LADPV	HDTAAL	IDETTAVGKSVVTKQYLN	IAGAHYIPLIHG	DIVVGC	VEVPRF	SGNLEK	LPSF	FPSLI	RAVTC
WT PDE-B1 Clone A2	(101)	LQYLN	DLMTKCTGCGP	GIRTYHNP	NDDV	LADPV	HDTAAL	IDETTAVGKSVVTKQYLN	IAGAHYIPLIHG	DIVVGC	VEVPRF	SGNLEK	LPSF	FPSLI	RAVTC
WT PDE-B1 Clone A5	(101)	LQYLN	DLMTKCTGCGP	GIRTYHNP	NDDV	LADPV	HDTAAL	IDETTAVGKSVVTKQYLN	IAGAHYIPLIHG	DIVVGC	VEVPRF	SGNLEK	LPSF	FPSLI	RAVTC
WT PDE-B1 Clone A6	(101)	LQYLN	DLMTKCTGCGP	GIRTYHNP	NDDV	LADPV	HDTAAL	IDETTAVGKSVVTKQYLN	IAGAHYIPLIHG	DIVVGC	VEVPRF	SGNLEK	LPSF	FPSLI	RAVTC
WT PDE-B1 Clone A7	(101)	LQYLN	DLMTKCTGCGP	GIRTYHNP	NDDV	LADPV	HDTAAL	IDETTAVGKSVVTKQYLN	IAGAHYIPLIHG	DIVVGC	VEVPRF	SGNLEK	LPSF	FPSLI	RAVTC

801

900

R0-8 PDE-B1 Clone A1 (801) DQSSDEAAFHRMTMEIILKAGDISNVTKPFDISRQWAMAVTEEFYRQGDMEKERGVEVLPMFDRSKNMELAKGQIGFIDFVAAPFFQKIVDA CLOGMQWT

R0-8 PDE-B1 Clone A2 (801) DQSSDEAAFHRMTMEIILKAGDISNVTKPFDISRQWAMAVTEEFYRQGDMEKERGVEVLPMFDRSKNMELAKGQIGFIDFVAAPFFQKIVDA CLOGMQWT

R0-8 PDE-B1 Clone A3 (801) DQSSDEAAFHRMTMEIILKAGDISNVTKPFDISRQWAMAVTEEFYRQGDMEKERGVEVLPMFDRSKNMELAKGQIGFIDFVAAPFFQKIVDA CLOGMQWT

R0-8 PDE-B1 Clone A4 (801) DQSSDEAAFHRMTMEIILKAGDISNVTKPFDISRQWAMAVTEEFYRQGDMEKERGVEVLPMFDRSKNMELAKGQIGFIDFVAAPFFQKIVDA CLOGMQWT

R0-8 PDE-B1 Clone A5 (801) DQSSDEAAFHRMTMEIILKAGDISNVTKPFDISRQWAMAVTEEFYRQGDMEKERGVEVLPMFDRSKNMELAKGQIGFIDFVAAPFFQKIVDA CLOGMQWT

R0-8 PDE-B1 Clone A6 (801) DQSSDEAAFHRMTMEIILKAGDISNVTKPFDISRQWAMAVTEEFYRQGDMEKERGVEVLPMFDRSKNMELAKGQIGFIDFVAAPFFQKIVDA CLOGMQWT

R0-8 PDE-B1 Clone A7 (801) DQSSDEAAFHRMTMEIILKAGDISNVTKPFDISRQWAMAVTEEFYRQGDMEKERGVEVLPMFDRSKNMELAKGQIGFIDFVAAPFFQKIVDA CLOGMQWT

R0-8 PDE-B1 Clone A8 (801) DQSSDEAAFHRMTMEIILKAGDISNVTKPFDISRQWAMAVTEEFYRQGDMEKERGVEVLPMFDRSKNMELAKGQIGFIDFVAAPFFQKIVDA CLOGMQWT

R0-8 PDE-B1 Clone B1 (801) DQSSDEAAFHRMTMEIILKAGDISNVTKPFDISRQWAMAVTEEFYRQGDMEKERGVEVLPMFDRSKNMELAKGQIGFIDFVAAPFFQKIVDA CLOGMQWT

GeneDB ThrPDEB1 (801) DQSSDEAAFHRMTMEIILKAGDISNVTKPFDISRQWAMAVTEEFYRQGDMEKERGVEVLPMFDRSKNMELAKGQIGFIDFVAAPFFQKIVDA CLOGMQWT

WT PDE-B1 Clone B1 (801) DQSSDEAAFHRMTMEIILKAGDISNVTKPFDISRQWAMAVTEEFYRQGDMEKERGVEVLPMFDRSKNMELAKGQIGFIDFVAAPFFPEDS--CIPARDAM

WT PDE-B1 Clone A1 (801) DQSSDEAAFHRMTMEIILKAGDISNVTKPFDISRQWAMAVTEEFYRQGDMEKERGVEVLPMFDRSKNMELAKGQIGFIDFVAAPFFQKIVDA CLOGMQWT

WT PDE-B1 Clone A3 (801) DQSSDEAAFHRMTMEIILKAGDISNVTKPFDISRQWAMAVTEEFYRQGDMEKERGVEVLPMFDRSKNMELAKGQIGFIDFVAAPFFQKIVDA CLOGMQWT

WT PDE-B1 Clone A4 (801) DQSSDEAAFHRMTMEIILKAGDISNVTKPFDISRQWAMAVTEEFYRQGDMEKERGVEVLPMFDRSKNMELAKGQIGFIDFVAAPFFQKIVDA CLOGMQWT

WT PDE-B1 Clone A8 (801) DQSSDEAAFHRMTMEIILKAGDISNVTKPFDISRQWAMAVTEEFYRQGDMEKERGVEVLPMFDRSKNMELAKGQIGFIDFVAAPFFQKIVDA CLOGMQWT

WT PDE-B1 Clone A2 (801) DQSSDEAAFHRMTMEIILKAGDISNVTKPFDISRQWAMAVTEEFYRQGDMEKERGVEVLPMFDRSKNMELAKGQIGFIDFVAAPFFQKIVDA CLOGMQWT

WT PDE-B1 Clone A5 (801) DQSSDEAAFHRMTMEIILKAGDISNVTKPFDISRQWAMAVTEEFYRQGDMEKERGVEVLPMFDRSKNMELAKGQIGFIDFVAAPFFQKIVDA CLOGMQWT

WT PDE-B1 Clone A6 (801) DQSSDEAAFHRMTMEIILKAGDISNVTKPFDISRQWAMAVTEEFYRQGDMEKERGVEVLPMFDRSKNMELAKGQIGFIDFVAAPFFQKIVDA CLOGMQWT

WT PDE-B1 Clone A7 (801) DQSSDEAAFHRMTMEIILKAGDISNVTKPFDISRQWAMAVTEEFYRQGDMEKERGVEVLPMFDRSKNMELAKGQIGFIDFVAAPFFQKIVDA CLOGMQWT

901

932

R0-8 PDE-B1 Clone A1 (901) VDRIKSNRAQWERVLETRLSTSSGNSSTR--

R0-8 PDE-B1 Clone A2 (901) VDRIKSNRAQWERVLETRLSTSSGNSSTR--

R0-8 PDE-B1 Clone A3 (901) VDRIKSNRAQWERVLETRLSTSSGNSSTR--

R0-8 PDE-B1 Clone A4 (901) VDRIKSNRAQWERVLETRLSTSSGNSSTR--

R0-8 PDE-B1 Clone A5 (901) VDRIKSNRAQWERVLETRLSTSSGNSSTR--

R0-8 PDE-B1 Clone A6 (901) VDRIKSNRAQWERVLETRLSTSSGNSSTR--

R0-8 PDE-B1 Clone A7 (901) VDRIKSNRAQWERVLETRLSTSSGNSSTR--

R0-8 PDE-B1 Clone A8 (901) VDRIKSNRAQWERVLETRLSTSSGNSSTR--

R0-8 PDE-B1 Clone B1 (901) VDRIKSNRAQWERVLETRLSTSSGNSSTR--

GeneDB ThrPDEB1 (901) VDRIKSNRAQWERVLETRLSTSSGNSSTR--

WT PDE-B1 Clone B1 (899) DSRPYQIEPRTVGASSGNKINEFWQQQYSL

WT PDE-B1 Clone A1 (901) VDRIKSNRAQWERVLETRLSTSSGNSSTR--

WT PDE-B1 Clone A3 (901) VDRIKSNRAQWERVLETRLSTSSGNSSTR--

WT PDE-B1 Clone A4 (901) VDRIKSNRAQWERVLETRLSTSSGNSSTR--

WT PDE-B1 Clone A8 (901) VDRIKSNRAQWERVLETRLSTSSGNSSTR--

WT PDE-B1 Clone A2 (901) VDRIKSNRAQWERVLETRLSTSSGNSSTR--

WT PDE-B1 Clone A5 (901) VDRIKSNRAQWERVLETRLSTSSGNSSTR--

WT PDE-B1 Clone A6 (901) VDRIKSNRAQWERVLETRLSTSSGNSSTR--

WT PDE-B1 Clone A7 (901) VDRIKSNRAQWERVLETRLSTSSGNSSTR--

Appendix 5:

The nucleotide sequences of TbrPDEB2 from all the cloned sequences taken from the GJS-128 resistant R0.8 strain and parental wildtype. Sequences are divided by the published sequence for TbrPDEB2 from GeneDB.

		1		100
R0-8 PDE-B2 Clone B1	(1)	ATGACACACAACGGTGGTCGTCATCTGCTTGAGGCGGTTACGCTATGCGGGTCCATTCTTAC	CGCTATAAGCGGAGCAACATGAAGCTCGACGAAGCTG	
R0-8 PDE-B2 Clone A1	(1)	ATGACACACAACGGTGGTCGTCATCTGCTTGAGGCGGTTACGCTATGCGGGTCCATTCTTAC	CGCTATAAGCGGAGCAACATGAAGCTCGACGAAGCTG	
R0-8 PDE-B2 Clone A2	(1)	ATGACACACAACGGTGGTCGTCATCTGCTTGAGGCGGTTACGCTATGCGGGTCCATTCTTAC	CGCTATAAGCGGAGCAACATGAAGCTCGACGAAGCTG	
R0-8 PDE-B2 Clone A3	(1)	ATGACACACAACGGTGGTCGTCATCTGCTTGAGGCGGTTACGCTATGCGGGTCCATTCTTAC	CGCTATAAGCGGAGCAACATGAAGCTCGACGAAGCTG	
R0-8 PDE-B2 Clone A4	(1)	ATGACACACAACGGTGGTCGTCATCTGCTTGAGGCGGTTACGCTATGCGGGTCCATTCTTAC	CGCTATAAGCGGAGCAACATGAAGCTCGACGAAGCTG	
R0-8 PDE-B2 Clone A5	(1)	ATGACACACAACGGTGGTCGTCATCTGCTTGAGGCGGTTACGCTATGCGGGTCCATTCTTAC	CGCTATAAGCGGAGCAACATGAAGCTCGACGAAGCTG	
R0-8 PDE-B2 Clone A6	(1)	ATGACACACAACGGTGGTCGTCATCTGCTTGAGGCGGTTACGCTATGCGGGTCCATTCTTAC	CGCTATAAGCGGAGCAACATGAAGCTCGACGAAGCTG	
R0-8 PDE-B2 Clone A7	(1)	ATGACACACAACGGTGGTCGTCATCTGCTTGAGGCGGTTACGCTATGCGGGTCCATTCTTAC	CGCTATAAGCGGAGCAACATGAAGCTCGACGAAGCTG	
R0-8 PDE-B2 Clone A8	(1)	ATGACACACAACGGTGGTCGTCATCTGCTTGAGGCGGTTACGCTATGCGGGTCCATTCTTAC	CGCTATAAGCGGAGCAACATGAAGCTCGACGAAGCTG	
GeneDB ThrPDEB2	(1)	ATGACACACAACGGTGGTCGTCATCTGCTTGAGGCGGTTACGCTATGCGGGTCCATTCTTAC	CGCTATAAGCGGAGCAACATGAAGCTCGACGAAGCTG	
WT PDE-B2 Clone A1	(1)	ATGACACACAACGGTGGTCGTCATCTGCTTGAGGCGGTTACGCTATGCGGGTCCATTCTTAC	CGCTATAAGCGGAGCAACATGAAGCTCGACGAAGCTG	
WT PDE-B2 Clone A2	(1)	ATGACACACAACGGTGGTCGTCATCTGCTTGAGGCGGTTACGCTATGCGGGTCCATTCTTAC	CGCTATAAGCGGAGCAACATGAAGCTCGACGAAGCTG	
WT PDE-B2 Clone A3	(1)	ATGACACACAACGGTGGTCGTCATCTGCTTGAGGCGGTTACGCTATGCGGGTCCATTCTTAC	CGCTATAAGCGGAGCAACATGAAGCTCGACGAAGCTG	
WT PDE-B2 Clone A4	(1)	ATGACACACAACGGTGGTCGTCATCTGCTTGAGGCGGTTACGCTATGCGGGTCCATTCTTAC	CGCTATAAGCGGAGCAACATGAAGCTCGACGAAGCTG	
WT PDE-B2 Clone A5	(1)	ATGACACACAACGGTGGTCGTCATCTGCTTGAGGCGGTTACGCTATGCGGGTCCATTCTTAC	CGCTATAAGCGGAGCAACATGAAGCTCGACGAAGCTG	
WT PDE-B2 Clone A6	(1)	ATGACACACAACGGTGGTCGTCATCTGCTTGAGGCGGTTACGCTATGCGGGTCCATTCTTAC	CGCTATAAGCGGAGCAACATGAAGCTCGACGAAGCTG	
WT PDE-B2 Clone A7	(1)	ATGACACACAACGGTGGTCGTCATCTGCTTGAGGCGGTTACGCTATGCGGGTCCATTCTTAC	CGCTATAAGCGGAGCAACATGAAGCTCGACGAAGCTG	
WT PDE-B2 Clone B1	(1)	ATGACACACAACGGTGGTCGTCATCTGCTTGAGGCGGTTACGCTATGCGGGTCCATTCTTAC	CGCTATAAGCGGAGCAACATGAAGCTCGACGAAGCTG	
		101		200
R0-8 PDE-B2 Clone B1	(101)	AGGTAAGGGCATTAAAGGAGTTATTCGAGAAGTATCAAGATATCCTCGTGGATGGATCCCCTGGTTTGCCACCCACGCTAGCGGGCCCATGATCCAGCC		
R0-8 PDE-B2 Clone A1	(101)	AGGTAAGGGCATTAAAGGAGTTATTCGAGAAGTATCAAGATATCCTCGTGGATGGATCCCCTGGTTTGCCACCCACGCTAGCGGGCCCATGATCCAGCC		
R0-8 PDE-B2 Clone A2	(101)	AGGTAAGGGCATTAAAGGAGTTATTCGAGAAGTATCAAGATATCCTCGTGGATGGATCCCCTGGTTTGCCACCCACGCTAGCGGGCCCATGATCCAGCC		
R0-8 PDE-B2 Clone A3	(101)	AGGTAAGGGCATTAAAGGAGTTATTCGAGAAGTATCAAGATATCCTCGTGGATGGATCCCCTGGTTTGCCACCCACGCTAGCGGGCCCATGATCCAGCC		
R0-8 PDE-B2 Clone A4	(101)	AGGTAAGGGCATTAAAGGAGTTATTCGAGAAGTATCAAGATATCCTCGTGGATGGATCCCCTGGTTTGCCACCCACGCTAGCGGGCCCATGATCCAGCC		
R0-8 PDE-B2 Clone A5	(101)	AGGTAAGGGCATTAAAGGAGTTATTCGAGAAGTATCAAGATATCCTCGTGGATGGATCCCCTGGTTTGCCACCCACGCTAGCGGGCCCATGATCCAGCC		
R0-8 PDE-B2 Clone A6	(101)	AGGTAAGGGCATTAAAGGAGTTATTCGAGAAGTATCAAGATATCCTCGTGGATGGATCCCCTGGTTTGCCACCCACGCTAGCGGGCCCATGATCCAGCC		
R0-8 PDE-B2 Clone A7	(101)	AGGTAAGGGCATTAAAGGAGTTATTCGAGAAGTATCAAGATATCCTCGTGGATGGATCCCCTGGTTTGCCACCCACGCTAGCGGGCCCATGATCCAGCC		
R0-8 PDE-B2 Clone A8	(101)	AGGTAAGGGCATTAAAGGAGTTATTCGAGAAGTATCAAGATATCCTCGTGGATGGATCCCCTGGTTTGCCACCCACGCTAGCGGGCCCATGATCCAGCC		
GeneDB ThrPDEB2	(101)	AGGTAAGGGCATTAAAGGAGTTATTCGAGAAGTATCAAGATATCCTCGTGGATGGATCCCCTGGTTTGCCACCCACGCTAGCGGGCCCATGATCCAGCC		
WT PDE-B2 Clone A1	(101)	AGGTAAGGGCATTAAAGGAGTTATTCGAGAAGTATCAAGATATCCTCGTGGATGGATCCCCTGGTTTGCCACCCACGCTAGCGGGCCCATGATCCAGCC		
WT PDE-B2 Clone A2	(101)	AGGTAAGGGCATTAAAGGAGTTATTCGAGAAGTATCAAGATATCCTCGTGGATGGATCCCCTGGTTTGCCACCCACGCTAGCGGGCCCATGATCCAGCC		
WT PDE-B2 Clone A3	(101)	AGGTAAGGGCATTAAAGGAGTTATTCGAGAAGTATCAAGATATCCTCGTGGATGGATCCCCTGGTTTGCCACCCACGCTAGCGGGCCCATGATCCAGCC		
WT PDE-B2 Clone A4	(101)	AGGTAAGGGCATTAAAGGAGTTATTCGAGAAGTATCAAGATATCCTCGTGGATGGATCCCCTGGTTTGCCACCCACGCTAGCGGGCCCATGATCCAGCC		
WT PDE-B2 Clone A5	(101)	AGGTAAGGGCATTAAAGGAGTTATTCGAGAAGTATCAAGATATCCTCGTGGATGGATCCCCTGGTTTGCCACCCACGCTAGCGGGCCCATGATCCAGCC		
WT PDE-B2 Clone A6	(101)	AGGTAAGGGCATTAAAGGAGTTATTCGAGAAGTATCAAGATATCCTCGTGGATGGATCCCCTGGTTTGCCACCCACGCTAGCGGGCCCATGATCCAGCC		
WT PDE-B2 Clone A7	(101)	AGGTAAGGGCATTAAAGGAGTTATTCGAGAAGTATCAAGATATCCTCGTGGATGGATCCCCTGGTTTGCCACCCACGCTAGCGGGCCCATGATCCAGCC		
WT PDE-B2 Clone B1	(101)	AGGTAAGGGCATTAAAGGAGTTATTCGAGAAGTATCAAGATATCCTCGTGGATGGATCCCCTGGTTTGCCACCCACGCTAGCGGGCCCATGATCCAGCC		

Appendix 6:

The amino acid sequences of TbrPDEB2 from all the cloned sequences taken from the GJS-128 resistant R0.8 strain and parental wildtype. Sequences are divided by the published sequence for TbrPDEB2 from GeneDB.

		1	100
R0-8 PDE-B2 Clone B1	(1)	MTHNGGRHLLAEAVTLCGSLTRYKRSNMKLDEAEVRALKELFEKYQDILVDGSPGLPTHASGPMIQQPVVNMVAPYDSPDTIVKFVEGTINLQRPIVEV	
R0-8 PDE-B2 Clone A1	(1)	MTHNGGRHLLAEAVTLCGSLTRYKRSNMKLDEAEVRALKELFEKYQDILVDGSPGLPTHASGPMIQQPVVNMVAPYDSPDTIVKFVEGTINLQRPIVEV	
R0-8 PDE-B2 Clone A2	(1)	MTHNGGRHLLAEAVTLCGSLTRYKRSNMKLDEAEVRALKELFEKYQDILVDGSPGLPTHASGPMIQQPVVNMVAPYDSPDTIVKFVEGTINLQRPIVEV	
R0-8 PDE-B2 Clone A3	(1)	MTHNGGRHLLAEAVTLCGSLTRYKRSNMKLDEAEVRALKELFEKYQDILVDGSPGLPTHASGPMIQQPVVNMVAPYDSPDTIVKFVEGTINLQRPIVEV	
R0-8 PDE-B2 Clone A4	(1)	MTHNGGRHLLAEAVTLCGSLTRYKRSNMKLDEAEVRALKELFEKYQDILVDGSPGLPTHASGPMIQQPVVNMVAPYDSPDTIVKFVEGTINLQRPIVEV	
R0-8 PDE-B2 Clone A5	(1)	MTHNGGRHLLAEAVTLCGSLTRYKRSNMKLDEAEVRALKELFEKYQDILVDGSPGLPTHASGPMIQQPVVNMVAPYDSPDTIVKFVEGTINLQRPIVEV	
R0-8 PDE-B2 Clone A6	(1)	MTHNGGRHLLAEAVTLCGSLTRYKRSNMKLDEAEVRALKELFEKYQDILVDGSPGLPTHASGPMIQQPVVNMVAPYDSPDTIVKFVEGTINLQRPIVEV	
R0-8 PDE-B2 Clone A7	(1)	MTHNGGRHLLAEAVTLCGSLTRYKRSNMKLDEAEVRALKELFEKYQDILVDGSPGLPTHASGPMIQQPVVNMVAPYDSPDTIVKFVEGTINLQRPIVEV	
R0-8 PDE-B2 Clone A8	(1)	MTHNGGRHLLAEAVTLCGSLTRYKRSNMKLDEAEVRALKELFEKYQDILVDGSPGLPTHASGPMIQQPVVNMVAPYDSPDTIVKFVEGTINLQRPIVEV	
GeneDB TbrPDEB2	(1)	MTHNGGRHLLAEAVTLCGSLTRYKRSNMKLDEAEVRALKELFEKYQDILVDGSPGLPTHASGPMIQQPVVNMVAPYDSPDTIVKFVEGTINLQRPIVEV	
WT PDE-B2 Clone A1	(1)	MTHNGGRHLLAEAVTLCGSLTRYKRSNMKLDEAEVRALKELFEKYQDILVDGSPGLPTHASGPMIQQPVVNMVAPYDSPDTIVKFVEGTINLQRPIVEV	
WT PDE-B2 Clone A2	(1)	MTHNGGRHLLAEAVTLCGSLTRYKRSNMKLDEAEVRALKELFEKYQDILVDGSPGLPTHASGPMIQQPVVNMVAPYDSPDTIVKFVEGTINLQRPIVEV	
WT PDE-B2 Clone A3	(1)	MTHNGGRHLLAEAVTLCGSLTRYKRSNMKLDEAEVRALKELFEKYQDILVDGSPGLPTHASGPMIQQPVVNMVAPYDSPDTIVKFVEGTINLQRPIVEV	
WT PDE-B2 Clone A4	(1)	MTHNGGRHLLAEAVTLCGSLTRYKRSNMKLDEAEVRALKELFEKYQDILVDGSPGLPTHASGPMIQQPVVNMVAPYDSPDTIVKFVEGTINLQRPIVEV	
WT PDE-B2 Clone A5	(1)	MTHNGGRHLLAEAVTLCGSLTRYKRSNMKLDEAEVRALKELFEKYQDILVDGSPGLPTHASGPMIQQPVVNMVAPYDSPDTIVKFVEGTINLQRPIVEV	
WT PDE-B2 Clone A6	(1)	MTHNGGRHLLAEAVTLCGSLTRYKRSNMKLDEAEVRALKELFEKYQDILVDGSPGLPTHASGPMIQQPVVNMVAPYDSPDTIVKFVEGTINLQRPIVEV	
WT PDE-B2 Clone A7	(1)	MTHNGGRHLLAEAVTLCGSLTRYKRSNMKLDEAEVRALKELFEKYQDILVDGSPGLPTHASGPMIQQPVVNMVAPYDSPDTIVKFVEGTINLQRPIVEV	
WT PDE-B2 Clone B1	(1)	MTHNGGRHLLAEAVTLCGSLTRYKRSNMKLDEAEVRALKELFEKYQDILVDGSPGLPTHASGPMIQQPVVNMVAPYDSPDTIVKFVEGTINLQRPIVEV	
		101	200
R0-8 PDE-B2 Clone B1	(101)	LHVMNEHLSLVLRAKNTHVFYVDPVNNLLYDPIHGVAALDESSPIGKAIVSGERLNVAGTLYIPIISEGMPLGCVLSPCGRADYHASTMLESSLRVI	
R0-8 PDE-B2 Clone A1	(101)	LHVMNEHLSLVLRAKNTHVFYVDPVNNLLYDPIHGVAALDESSPIGKAIVSGERLNVAGTLYIPIISEGMPLGCVLSPCGRADYHASTMLESSLRVI	
R0-8 PDE-B2 Clone A2	(101)	LHVMNEHLSLVLRAKNTHVFYVDPVNNLLYDPIHGVAALDESSPIGKAIVSGERLNVAGTLYIPIISEGMPLGCVLSPCGRADYHASTMLESSLRVI	
R0-8 PDE-B2 Clone A3	(101)	LHVMNEHLSLVLRAKNTHVFYVDPVNNLLYDPIHGVAALDESSPIGKAIVSGERLNVAGTLYIPIISEGMPLGCVLSPCGRADYHASTMLESSLRVI	
R0-8 PDE-B2 Clone A4	(101)	LHVMNEHLSLVLRAKNTHVFYVDPVNNLLYDPIHGVAALDESSPIGKAIVSGERLNVAGTLYIPIISEGMPLGCVLSPCGRADYHASTMLESSLRVI	
R0-8 PDE-B2 Clone A5	(101)	LHVMNEHLSLVLRAKNTHVFYVDPVNNLLYDPIHGVAALDESSPIGKAIVSGERLNVAGTLYIPIISEGMPLGCVLSPCGRADYHASTMLESSLRVI	
R0-8 PDE-B2 Clone A6	(101)	LHVMNEHLSLVLRAKNTHVFYVDPVNNLLYDPIHGVAALDESSPIGKAIVSGERLNVAGTLYIPIISEGMPLGCVLSPCGRADYHASTMLESSLRVI	
R0-8 PDE-B2 Clone A7	(101)	LHVMNEHLSLVLRAKNTHVFYVDPVNNLLYDPIHGVAALDESSPIGKAIVSGERLNVAGTLYIPIISEGMPLGCVLSPCGRADYHASTMLESSLRVI	
R0-8 PDE-B2 Clone A8	(101)	LHVMNEHLSLVLRAKNTHVFYVDPVNNLLYDPIHGVAALDESSPIGKAIVSGERLNVAGTLYIPIISEGMPLGCVLSPCGRADYHASTMLESSLRVI	
GeneDB TbrPDEB2	(101)	LHVMNEHLSLVLRAKNTHVFYVDPVNNLLYDPIHGVAALDESSPIGKAIVSGERLNVAGTLYIPIISEGMPLGCVLSPCGRADYHASTMLESSLRVI	
WT PDE-B2 Clone A1	(101)	LHVMNEHLSLVLRAKNTHVFYVDPVNNLLYDPIHGVAALDESSPIGKAIVSGERLNVAGTLYIPIISEGMPLGCVLSPCGRADYHASTMLESSLRVI	
WT PDE-B2 Clone A2	(101)	LHVMNEHLSLVLRAKNTHVFYVDPVNNLLYDPIHGVAALDESSPIGKAIVSGERLNVAGTLYIPIISEGMPLGCVLSPCGRADYHASTMLESSLRVI	
WT PDE-B2 Clone A3	(101)	LHVMNEHLSLVLRAKNTHVFYVDPVNNLLYDPIHGVAALDESSPIGKAIVSGERLNVAGTLYIPIISEGMPLGCVLSPCGRADYHASTMLESSLRVI	
WT PDE-B2 Clone A4	(101)	LHVMNEHLSLVLRAKNTHVFYVDPVNNLLYDPIHGVAALDESSPIGKAIVSGERLNVAGTLYIPIISEGMPLGCVLSPCGRADYHASTMLESSLRVI	
WT PDE-B2 Clone A5	(101)	LHVMNEHLSLVLRAKNTHVFYVDPVNNLLYDPIHGVAALDESSPIGKAIVSGERLNVAGTLYIPIISEGMPLGCVLSPCGRADYHASTMLESSLRVI	
WT PDE-B2 Clone A6	(101)	LHVMNEHLSLVLRAKNTHVFYVDPVNNLLYDPIHGVAALDESSPIGKAIVSGERLNVAGTLYIPIISEGMPLGCVLSPCGRADYHASTMLESSLRVI	
WT PDE-B2 Clone A7	(101)	LHVMNEHLSLVLRAKNTHVFYVDPVNNLLYDPIHGVAALDESSPIGKAIVSGERLNVAGTLYIPIISEGMPLGCVLSPCGRADYHASTMLESSLRVI	
WT PDE-B2 Clone B1	(101)	LHVMNEHLSLVLRAKNTHVFYVDPVNNLLYDPIHGVAALDESSPIGKAIVSGERLNVAGTLYIPIISEGMPLGCVLSPCGRADYHASTMLESSLRVI	

801

900

R0-8 PDE-B2 Clone B1 (801) **TSYNVDDSDHRQMTMDVLMKAGDISNVTKPFDISRQWAMAVTEEFYRQGDMEKERGVEVLPMPFDRSKNMELAKGQIGFIDFVAAPFFQKIVDAQLQGMQW**

R0-8 PDE-B2 Clone A1 (801) **TSYNVDDSDHRQMTMDVLMKAGDISNVTKPFDISRQWAMAVTEEFYRQGDMEKERGVEVLPMPFDRSKNMELAKGQIGFIDFVAAPFFQKIVDAQLQGMQW**

R0-8 PDE-B2 Clone A2 (801) **TSYNVDDSDHRQMTMDVLMKAGDISNVTKPFDISRQWAMAVTEEFYRQGDMEKERGVEVLPMPFDRSKNMELAKGQIGFIDFVAAPFFQKIVDAQLQGMQW**

R0-8 PDE-B2 Clone A3 (801) **TSYNVDDSDHRQMTMDVLMKAGDISNVTKPFDISRQWAMAVTEEFYRQGDMEKERGVEVLPMPFDRSKNMELAKGQIGFIDFVAAPFFQKIVDAQLQGMQW**

R0-8 PDE-B2 Clone A4 (801) **TSYNVDDSDHRQMTMDVLMKAGDISNVTKPFDISRQWAMAVTEEFYRQGDMEKERGVEVLPMPFDRSKNMELAKGQIGFIDFVAAPFFQKIVDAQLQGMQW**

R0-8 PDE-B2 Clone A5 (801) **TSYNVDDSDHRQMTMDVLMKAGDISNVTKPFDISRQWAMAVTEEFYRQGDMEKERGVEVLPMPFDRSKNMELAKGQIGFIDFVAAPFFQKIVDAQLQGMQW**

R0-8 PDE-B2 Clone A6 (801) **TSYNVDDSDHRQMTMDVLMKAGDISNVTKPFDISRQWAMAVTEEFYRQGDMEKERGVEVLPMPFDRSKNMELAKGQIGFIDFVAAPFFQKIVDAQLQGMQW**

R0-8 PDE-B2 Clone A7 (801) **TSYNVDDSDHRQMTMDVLMKAGDISNVTKPFDISRQWAMAVTEEFYRQGDMEKERGVEVLPMPFDRSKNMELAKGQIGFIDFVAAPFFQKIVDAQLQGMQW**

R0-8 PDE-B2 Clone A8 (801) **TSYNVDDSDHRQMTMDVLMKAGDISNVTKPFDISRQWAMAVTEEFYRQGDMEKERGVEVLPMPFDRSKNMELAKGQIGFIDFVAAPFFQKIVDAQLQGMQW**

GeneDB ThrPDEB2 (801) **TSYNVDDSDHRQMTMDVLMKAGDISNVTKPFDISRQWAMAVTEEFYRQGDMEKERGVEVLPMPFDRSKNMELAKGQIGFIDFVAAPFFQKIVDAQLQGMQW**

WT PDE-B2 Clone A1 (801) **TSYNVDDSDHRQMTMDVLMKAGDISNVTKPFDISRQWAMAVTEEFYRQGDMEKERGVEVLPMPFDRSKNMELAKGQIGFIDFVAAPFFQKIVDAQLQGMQW**

WT PDE-B2 Clone A2 (801) **TSYNVDDSDHRQMTMDVLMKAGDISNVTKPFDISRQWAMAVTEEFYRQGDMEKERGVEVLPMPFDRSKNMELAKGQIGFIDFVAAPFFQKIVDAQLQGMQW**

WT PDE-B2 Clone A3 (801) **TSYNVDDSDHRQMTMDVLMKAGDISNVTKPFDISRQWAMAVTEEFYRQGDMEKERGVEVLPMPFDRSKNMELAKGQIGFIDFVAAPFFQKIVDAQLQGMQW**

WT PDE-B2 Clone A4 (801) **TSYNVDDSDHRQMTMDVLMKAGDISNVTKPFDISRQWAMAVTEEFYRQGDMEKERGVEVLPMPFDRSKNMELAKGQIGFIDFVAAPFFQKIVDAQLQGMQW**

WT PDE-B2 Clone A5 (801) **TSYNVDDSDHRQMTMDVLMKAGDISNVTKPFDISRQWAMAVTEEFYRQGDMEKERGVEVLPMPFDRSKNMELAKGQIGFIDFVAAPFFQKIVDAQLQGMQW**

WT PDE-B2 Clone A6 (801) **TSYNVDDSDHRQMTMDVLMKAGDISNVTKPFDISRQWAMAVTEEFYRQGDMEKERGVEVLPMPFDRSKNMELAKGQIGFIDFVAAPFFQKIVDAQLQGMQW**

WT PDE-B2 Clone A7 (801) **TSYNVDDSDHRQMTMDVLMKAGDISNVTKPFDISRQWAMAVTEEFYRQGDMEKERGVEVLPMPFDRSKNMELAKGQIGFIDFVAAPFFQKIVDAQLQGMQW**

WT PDE-B2 Clone B1 (801) **TSYNVDDSDHRQMTMDVLMKAGDISNVTKPFDISRQWAMAVTEEFYRQGDMEKERGVEVLPMPFDRSKNMELAKGQIGFIDFVAAPFFQKIVDAQLQGMQW**

901

926

R0-8 PDE-B2 Clone B1 (901) **TVDRTKSNRAQWERVLEARSTGASS-**

R0-8 PDE-B2 Clone A1 (901) **TVDRTKSNRAQWERVLEARSTGASS-**

R0-8 PDE-B2 Clone A2 (901) **TVDRTKSNRAQWERVLEARSTGASS-**

R0-8 PDE-B2 Clone A3 (901) **TVDRTKSNRAQWERVLEARSTGASS-**

R0-8 PDE-B2 Clone A4 (901) **TVDRTKSNRAQWERVLEARSTGASS-**

R0-8 PDE-B2 Clone A5 (901) **TVDRTKSNRAQWERVLEARSTGASS-**

R0-8 PDE-B2 Clone A6 (901) **TVDRTKSNRAQWERVLEARSTGASS-**

R0-8 PDE-B2 Clone A7 (901) **TVDRTKSNRAQWERVLEARSTGASS-**

R0-8 PDE-B2 Clone A8 (901) **TVDRTKSNRAQWERVLEARSTGASS-**

GeneDB ThrPDEB2 (901) **TVDRTKSNRAQWERVLEARSTGASS-**

WT PDE-B2 Clone A1 (901) **TVDRTKSNRAQWERVLEARSTGASS-**

WT PDE-B2 Clone A2 (901) **TVDRTKSNRAQWERVLEARSTGASS-**

WT PDE-B2 Clone A3 (901) **TVDRTKSNRAQWERVLEARSTGASS-**

WT PDE-B2 Clone A4 (901) **TVDRTKSNRAQWERVLEARSTGASS-**

WT PDE-B2 Clone A5 (901) **TVDRTKSNRAQWERVLEARSTGASS-**

WT PDE-B2 Clone A6 (901) **TVDRTKSNRAQWERVLEARSTGASS-**

WT PDE-B2 Clone A7 (901) **TVDRTKSNRAQWERVLEARSTGASS-**

WT PDE-B2 Clone B1 (901) **TVDRTKSNRAQWERVLEARSTGASS-**

References:

- Abel, P. M., Kiala, G., Loa, V., Behrend, M., Musolf, J., Fleischmann, H., Théophile, J., Krishna, S., Stich, A., 2004. **Retaking sleeping sickness control in Angola.** *Tropical Medicine and International Health*, Vol. 9, No. 1, P 141-148.
- al-Chalabi, K. A., Ziz, L. A., al-Khayat, B., 1989. **Presence and properties of cAMP phosphodiesterase from promastigote forms of *Leishmania tropica* and *Leishmania donovani*.** *Comparative Biochemistry and Physiology. B, Comparative Biochemistry*, Vol. 93, Iss. 4, P 789-792.
- Akaki, M., Nakano, Y., Ito, Y., Nagayasu, E., Aikawa, M., 2002. **Effects of dipyridamole on *Plasmodium falciparum*-infected erythrocytes.** *Parasitology Research*, Vol. 88, Iss. 12, P 1044-1050.
- Alexandre, S., Paindavoine, P., Tebabi, P., Pays, A., Halleux, S., Steinert, M., Pays, E., 1990. **Differential expression of a family of putative adenylate/guanylate cyclase genes in *Trypanosoma brucei*.** *Molecular and Biochemical Parasitology*, Vol. 43, Iss. 2, P 279-288.
- Alonso, G. D., Schoijet, A. C., Torres, H. N., Flawiá, M. M., 2006. **TcPDE4, a novel membrane-associated cAMP-specific phosphodiesterase from *Trypanosoma cruzi*.** *Molecular and Biochemical Parasitology*, Vol. 145, Iss. 1, P 40-49.
- Alonso, G. D., Schoijet, A. C., Torres, H. N., Flawiá, M. M., 2007. **TcrPDEA1, a cAMP-specific phosphodiesterase with atypical pharmacological properties from *Trypanosoma cruzi*.** *Molecular and Biochemical Parasitology*, Vol. 152, Iss. 1, P 72-79.
- Al-Salabi, M. I., De Koning, H. P., 2005. **Purine nucleobase transport in amastigotes of *Leishmania mexicana*: involvement in allopurinol uptake.** *Antimicrobial Agents and Chemotherapy*, Vol. 49, Iss. 9, P 3682-3689.
- Aravind, L., Ponting, C. P., 1997. **The GAF domain: an evolutionary link between diverse phototransducing proteins.** *Trends in Biochemical Sciences*, Vol. 22, Iss. 12, P 458-459.

Banerjee, C., Sarkar, D., 1992. Isolation and characterization of a cyclic nucleotide-independent protein kinase from *Leishmania donovani*. *Molecular and Biochemical Parasitology*, Vol, 52, Iss. 2, P 195-205.

Banerjee, C., Sarkar, D., 2001. The cAMP-binding proteins of *Leishmania* are not the regulatory subunits of cAMP-dependent protein kinase. *Comparative Biochemistry and Physiology. Part B, Biochemistry & Molecular Biology*, Vol. 130, Iss. 2, P 217-226.

Bao, Y., Weiss, L. M., Braunstein, V. L., Huang, H., 2008. Role of protein kinase A in *Trypanosoma cruzi*. *Infection and Immunity*, Vol. 76, Iss. 10, P 4757-5763.

Barrett, M. P. 1999., The fall and rise of sleeping sickness. *The Lancet*, Vol. 353, Iss. 9159, P 1113-1114.

Barrett, M. P., Zhang, Z. Q., Denise, H., Giroud, C., Baltz, T., 1995. A diamidine-resistant *Trypanosoma equiperdum* clone contains a P2 purine transporter with reduced substrate affinity. *Molecular and Biochemical Parasitology*, Vol. 73, P 223-229.

Barry, J. D., McCulloch, R., 2001. Antigenic Variation in Trypanosomes: Enhanced Phenotypic Variation in a Eukaryotic Parasite. In 'Advances in Parasitology', Baker, J. R., Muller, R., Rollinson, D. (Editors). Academic Press, Vol. 49, P 1-70.

Batkin, M., Schvartz, I., Shaltiel, S., 2000. Snapping of the carboxyl terminal tail of the catalytic subunit of PKA onto its core: characterization of the sites by mutagenesis. *Biochemistry*, Vol. 39, Iss. 18, P 5366-5373.

Bellofatto, V., Fairlamb, A.H., Henderson, G.B., Cross, G.A.M., 1987. Biochemical changes associated with alpha-difluoromethylornithine uptake and resistance in *Trypanosoma brucei*. *Molecular and Biochemical Parasitology*, Vol. 25, P 227-238.

Beraldo, F. H., Almeida, F. M., da Silva, A. M., Garcia, C. R., 2005. **Cyclic AMP and calcium interplay as second messengers in melatonin-dependent regulation of *Plasmodium falciparum* cell cycle.** The Journal of Cell Biology, Vol. 170, Iss. 4, P 551-557.

Berger, B. J., Carter, N. S., Fairlamb, A. H., 1995. **Characterization of pentamidine-resistant *Trypanosoma brucei brucei*.** Molecular and Biochemical Parasitology, Vol. 69, Iss. 2, P 289-298.

Berriman M, Ghedin E, Hertz-Fowler C, Blandin G, Renauld H, Bartholomeu DC, Lennard NJ, Caler E, Hamlin NE, Haas B, Böhme U, Hannick L, Aslett MA, Shallom J, Marcello L, Hou L, Wickstead B, Alsmark UC, Arrowsmith C, Atkin RJ, Barron AJ, Bringaud F, Brooks K, Carrington M, Cherevach I, Chillingworth TJ, Churcher C, Clark LN, Corton CH, Cronin A, Davies RM, Doggett J, Djikeng A, Feldblyum T, Field MC, Fraser A, Goodhead I, Hance Z, Harper D, Harris BR, Hauser H, Hostetler J, Ivens A, Jagels K, Johnson D, Johnson J, Jones K, Kerhornou AX, Koo H, Larke N, Landfear S, Larkin C, Leech V, Line A, Lord A, Macleod A, Mooney PJ, Moule S, Martin DM, Morgan GW, Mungall K, Norbertczak H, Ormond D, Pai G, Peacock CS, Peterson J, Quail MA, Rabbinowitsch E, Rajandream MA, Reitter C, Salzberg SL, Sanders M, Schobel S, Sharp S, Simmonds M, Simpson AJ, Tallon L, Turner CM, Tait A, Tivey AR, Van Aken S, Walker D, Wanless D, Wang S, White B, White O, Whitehead S, Woodward J, Wortman J, Adams MD, Embley TM, Gull K, Ullu E, Barry JD, Fairlamb AH, Opperdoes F, Barrell BG, Donelson JE, Hall N, Fraser CM, Melville SE, El-Sayed NM. 2005. **The genome of the African trypanosome *Trypanosoma brucei*.** Science, Vol. 309, Iss. 5733, P 416-422.

Bhattacharya, A., Biswas, A., Das, P. K., 2008. **Role of intracellular cAMP in differentiation-coupled induction of resistance against oxidative damage in *Leishmania donovani*.** Free Radical Biology and Medicine, Vol. 44, Iss. 5, P 779-794.

Bieger, B., Essen, L. O., 2000. **Crystallization and preliminary X-ray analysis of the catalytic domain of the adenylate cyclase GRESAG4.1 from *Trypanosoma brucei*.** Acta crystallographica. Section D, Biological crystallography, Vol. 56, Pt. 3, P 359-362.

Bieger, B., Essen, L. O., 2001. **Structural analysis of adenylate cyclases from *Trypanosoma brucei* in their monomeric state.** The EMBO Journal, Vol. 20, Iss. 3, P 433-445.

Billker, O., Lindo, V., Panico, M., Etienne, A. E., Paxton, T., Dell, A., Rogers, M., Sinden, R. E., Morris, H. R., 1998. **Identification of xanthurenic acid as the putative inducer of malaria development in the mosquito.** Nature, Vol. 392, Iss. 6673, P 227-228.

Bouteille, B., Oukem, O., Bisser, S., Dumas, M., 2003. **Treatment perspectives for human African trypanosomiasis.** Fundamental & Clinical Pharmacology, Vol. 17, P 171-181.

Bowles, D. J., Voorheis, H. P., 1982. **Release of the surface coat from the plasma membrane of intact bloodstream forms of *Trypanosoma brucei* requires Ca²⁺.** FEBS Letters, Vol. 139, Iss. 1, P 17-21.

Bridges, D., Gould, M. K., Nerima, B., Mäser, P., Burchmore, R. J. S., De Koning, H. P., 2007. **Loss of the High Affinity Pentamidine Transporter is responsible for high levels of cross-resistance between arsenical and diamidine drugs in African trypanosomes.** Molecular Pharmacology, Vol 71, P 1098-1108.

Brun, R., Schumacher, R., Schmid, C., Kunz, C., Burri, C., 2001. **The phenomenon of treatment failures in Human African Trypanosomiasis.** Tropical Medicine and International Health, Vol. 6, Iss. 11, P 906-914.

Burri, C., Brun, R., 2003. **Eflornithine for the treatment of human African trypanosomiasis.** Parasitology Research, Vol. 90, Suppl. 1, P 49-52.

Carter, N. S., Fairlamb, A. H., 1993. **Arsenical resistant trypanosomes lack an unusual adenosine transporter.** Nature, Vol. 361, No. 6408, P 173-175.

Carucci, D. J., Witney, A. A., Muhia, D. K., Warhurst, D. C., Schaap, P., Meima, M., Li, J. L., Taylor, M. C., Kelly, J. M., Baker, D. A., 2000. **Guanylyl cyclase activity associated with putative bifunctional integral membrane proteins in *Plasmodium falciparum*.** The Journal of Biological Chemistry, Vol. 275, Iss. 29, P 22147-22156.

Cerqueira, G. C., Bartholomeu, D. C., DaRocha, W. D., Hou, L., Freitas-Silva, D. M., Machado, C. R., El-Sayed, N. M., Teixeira, S. M., 2008. **Sequence diversity and evolution of multigene families in *Trypanosoma cruzi***. *Molecular and Biochemical Parasitology*, Vol. 157, Iss. 1, P 65-72.

Changtam, C., De Koning, H. P., Ibrahim, H., El-Sabbagh, N., Sajid, S., Gould, M. K., and Sukamrarn, A., 2009. **Curcuminoid analogues with potent activity against *Trypanosoma* and *Leishmania* species**. *European Journal of Medicinal Chemistry*, in press.

Chappuis, F., Loutan, L., Simarro, P., Lejon, V., Büscher, P., 2005. **Options for Field Diagnosis of Human African Trypanosomiasis**. *Clinical Microbiology Reviews*, Vol. 18, No. 1, P 133-146.

Coso, O. A., Díaz Añel, A., Martinetto, H., Muschietti, J. P., Kazanietz, M., Fraidenraich, D., Torres, H. N., Flawia, M. M., 1992. **Characterization of a Gi-protein from *Trypanosoma cruzi* epimastigote membranes**. *The Biochemical Journal*, Vol. 287, Pt. 2, P 443-446.

Dal Piaz, V., Castellana, M. C., Vergelli, C., Giovannoni, M. P., Gavaldà, A., Segarra, V., Beleta, J., Ryder, H., Palacios, J. M., 2002. **Synthesis and evaluation of some pyrazolo[3,4-d]pyridazinones and analogues as PDE 5 inhibitors potentially useful as peripheral vasodilator agents**. *Journal of Enzyme Inhibition and Medicinal Chemistry*, Vol. 17, Iss. 4, P 227-233.

D'Angelo, M. A., Montagna, A. E., Sanguineti, S., Torres, H. N., Flawiá, M. M., 2002. **A novel calcium-stimulated adenylyl cyclase from *Trypanosoma cruzi*, which interacts with the structural flagellar protein paraflagellar rod**. *The Journal of Biological Chemistry*, Vol. 277, Iss. 38, P 35025-35034.

D'Angelo, M. A., Sanguineti, S., Reece, J. M., Birnbaumer, L., Torres, H. N., Flawiá, M. M., 2004. **Identification, characterization and subcellular localization of TcPDE1, a novel cAMP-specific phosphodiesterase from *Trypanosoma cruzi***. *The Biochemical Journal*, Vol. 378, Pt. 1, P 63-72.

De Koning, H. P., 2001. **Uptake of pentamidine in *Trypanosoma brucei brucei* is mediated by three distinct transporters. Implications for cross-resistance with arsenicals.** *Molecular Pharmacology*, Vol. 59, Iss. 3, P 586-592.

De Koning, H. P., Jarvis, S. M., 1999. **Adenosine Transporters in Bloodstream Forms of *Trypanosoma brucei brucei*: Substrate Recognition Motifs and Affinity for Trypanocidal Drugs.** *Molecular Pharmacology*, Vol. 56, Iss. 6, P 1162-1170.

De Koning, H. P., Stewart, M., Anderson, L., Burchmore, R., Wallace, L. J. M., Barrett, M. P., 2004. **The trypanocide diminazene aceturate is accumulated predominantly through the TbAT1 purine transporter; additional insights in diamidine resistance in African trypanosomes.** *Antimicrobial Agents and Chemotherapy*, Vol. 48, P 1515-1519.

De Koning, H. P., Watson, C. J., Jarvis, S. M., 1998. **Characterization of a nucleoside/proton symporter in procyclic *Trypanosoma brucei brucei*.** *Journal of Biological Chemistry*, Vol. 273, Iss. 16, P 9486-9494.

Delespaux, V., De Koning, H. P., 2007. **Drugs and drug resistance in African trypanosomiasis.** *Drug Resistance Updates*, Vol. 10, P 30-50.

Denise, H., Barret, M. P., 2001. **Uptake and mode of action of drugs used against sleeping sickness.** *Biochemical Pharmacology*, Vol. 61, Iss. 1, P 1-5.

Díaz-Benjumea, R., Laxman, S., Hinds, T. R., Beavo, J. A., Rascón, A., 2006. **Characterization of a novel cAMP-binding, cAMP-specific cyclic nucleotide phosphodiesterase (TcrPDEB1) from *Trypanosoma cruzi*.** *The Biochemical Journal*, Vol. 399, Iss. 2, P 305-314.

Docampo, R., Moreno, S. N. J., 2003. **Current chemotherapy of human African trypanosomiasis.** *Parasitology Research*, Vol. 90, Suppl. 1, P 10-13.

Eichler, H., 1934. **Der Nachweis der hydrosulfite (sulfoxylate) und des nachierenden Wasserstoffs mit Resazurin.** *Fresenius' Journal of Analytical Chemistry*, Vol. 99, P 270-272.

Eisenschlos, C., Flawiá, M. M., Torruella, M., Torres, H. N., 1986. **Interaction of *Trypanosoma cruzi* adenylate cyclase with liver regulatory factors.** The Biochemical Journal, Vol. 236, Iss. 1, P 185-191.

Emes, R. D., Yang, Z., 2008. **Duplicated paralogous genes subject to positive selection in the genome of *Trypanosoma brucei*.** PLoS One, Vol. 3, Iss. 5, P e2295.

Fairlamb, A. H., 2003. **Chemotherapy of human African trypanosomiasis: current and future prospects.** Trends in Parasitology, Vol. 19, No. 11, P 488-494.

Fairlamb, A. H., Carter, N. S., Cunningham, M., Smith, K., 1992. **Characterisation of melarsen-resistant *Trypanosoma brucei brucei* with respect to cross-resistance to other drugs and trypanothione metabolism.** Molecular and Biochemical Parasitology, Vol. 53, P 213-222.

Ferlini, C., Di Cesare, S., Rainaldi, G., Malorni, W., Samoggia, P., Biselli, R., Fattorossi, A., 1996. **Flow cytometric analysis of the early phases of apoptosis by cellular and nuclear techniques.** Cytometry, Vol. 24, Iss. 2, P 106-115.

Forsythe, G. R., McCulloch, R., Hammarton, T. C., 2009. **Hydroxyurea-induced synchronisation of bloodstream stage *Trypanosoma brucei*.** Molecular and Biochemical Parasitology, Vol. 164, Iss. 2, P 131-136.

Foucher, A. L., 2003, **A proteomic approach to the investigation of cymelarsan resistance in *Trypanosoma brucei*.** PhD thesis, University of Glasgow, UK.

Fraidenraich, D., Peña, C., Isola, E. L., Lammel, E. M., Coso, O., Añel, A. D., Pongor, S., Baralle, F., Torres, H. N., Flawia, M. M., 1993. **Stimulation of *Trypanosoma cruzi* adenyl cyclase by an alpha D-globin fragment from *Triatoma hindgut*: effect on differentiation of epimastigote to trypomastigote forms.** Proceedings of the National Academy of Sciences of the United States of America, Vol. 90, Iss. 21, P 10140-10144.

- Galán-Caridad, J. M., Calabokis, M., Uzcanga, G., Aponte, F., Bubis, J., 2004. **Identification of casein kinase 1, casein kinase 2, and cAMP-dependent protein kinase-like activities in *Trypanosoma evansi*.** Memórias do Instituto Oswaldo Cruz, Vol. 99, Iss. 8, P 845-854.
- Garcia, E. S., Gonzalez, M. S., de Azambuja, P., Baralle, F. E., Fraidenraich, D., Torres, H. N., Flawiá, M. M., 1995. **Induction of *Trypanosoma cruzi* metacyclogenesis in the gut of the hematophagous insect vector, *Rhodnius prolixus*, by hemoglobin and peptides carrying alpha D-globin sequences.** Experimental Parasitology, Vol. 81, Iss. 3, P 255-261.
- Garcia, G. E., Wirtz, R. A., Barr, J. R., Woolfitt, A., Rosenberg, R., 1998. **Xanthurenic acid induces gametogenesis in *Plasmodium*, the malaria parasite.** The Journal of Biological Chemistry, Vol. 273, Iss. 20, P 12003-12005.
- Garcia, L. S., 2001. **Diagnostic Medical Parasitology (4th Edition).** ASM Press, Chapter 9, P 235-264.
- García-Salcedo, J. A., Pérez-Morga, D., Gijón, P., Dilbeck, V., Pays, E., Nolan, D. P., 2004. **A differential role for actin during the life cycle of *Trypanosoma brucei*.** The EMBO Journal, Vol. 23, Iss. 4, P 780-789.
- Genestra, M., Cysne-Finkelstein, L., Leon, L., 2004. **Protein kinase A activity is associated with metacyclogenesis in *Leishmania amazonensis*.** Cell Biochemistry and Function, Vol. 22, Iss. 5, P 315-320.
- Gilles, H. M., (Editor), 1999. **Protozoal Diseases.** Arnold publishers, Chapter 3, P 249-305.
- Gillingwater, K., Büscher, P., Brun, R., 2007. **Establishment of a panel of reference *Trypanosoma evansi* and *Trypanosoma equiperdum* strains for drug screening.** Veterinary Parasitology, Vol. 148, Iss. 2, P 114-121.
- Gonçalves, M. F., Zingales, B., Colli, W., 1980. **cAMP phosphodiesterase and activator protein of mammalian cAMP phosphodiesterase from *Trypanosoma cruzi*.** Molecular and Biochemical Parasitology, Vol. 1, Iss. 2, P 107-118.

- Gong, K. W., Kunz, S., Zoraghi, R., Kunz Renggli, C., Brun, R., Seebeck, T., 2001. **cAMP-specific phosphodiesterase TbPDE1 is not essential in *Trypanosoma brucei* in culture or during midgut infection of tsetse flies.** *Molecular and Biochemical Parasitology*, Vol. 116, Iss. 2, P 229-232.
- Gonzalez, R. J., Tarloff, J. B., 2001. **Evaluation of hepatic subcellular fractions for Alamar blue and MTT reductase activity.** *Toxicology In Vitro*, Vol. 15, Iss. 3, P 257-259.
- Hammarton, T. C., 2007. **Cell cycle regulation in *Trypanosoma brucei*.** *Molecular and Biochemical Parasitology*, Vol. 153, Iss. 1, P 1-8.
- Hammarton, T. C., Engstler, M., Mottram, J. C., 2004. **The *Trypanosoma brucei* cyclin, CYC2, is required for cell cycle progression through G1 phase and for maintenance of procyclic form cell morphology.** *Journal of Biological Chemistry*, Vol. 279, Iss. 23, P 24757-24764.
- Hertelendy, F., Toth, M., Fitch, C. D., 1979. **Malaria enhances cyclic AMP production by immature erythrocytes *in vitro*.** *Life Sciences*, Vol. 25, Iss. 5, P 451-455.
- Hirai, M., Arai, M., Kawai, S., Matsuoka, H., 2006. **PbGCbeta is essential for *Plasmodium ookinete* motility to invade midgut cell and for successful completion of parasite life cycle in mosquitoes.** *Journal of Biochemistry*, Vol. 140, Iss. 5, P 747-757.
- Hotta, C. T., Gazarini, M. L., Beraldo, F. H., Varotti, F. P., Lopes, C., Markus, R. P., Pozzan, T., Garcia, C. R. 2000. **Calcium-dependent modulation by melatonin of the circadian rhythm in malarial parasites.** *Nature Cell Biology*, Vol. 2, Iss. 7, P 466-468.
- Huang, H., Weiss, L. M., Nagajyothi, F., Tanowitz, H. B., Wittner, M., Orr, G. A., Bao, Y., 2006. **Molecular cloning and characterization of the protein kinase A regulatory subunit of *Trypanosoma cruzi*.** *Molecular and Biochemical Parasitology*, Vol. 149, Iss. 2, P 242-245.

- Huang, H., Werner, C., Weiss, L. M., Wittner, M., Orr, G. A., 2002. **Molecular cloning and expression of the catalytic subunit of protein kinase A from *Trypanosoma cruzi***. International Journal for Parasitology, Vol. 32, Iss. 9, P 1107-1115.
- Iizumi, K., Mikami, Y., Hashimoto, M., Nara, T., Hara, Y., Aoki, T., 2006. **Molecular cloning and characterization of ouabain-insensitive Na(+)-ATPase in the parasitic protist, *Trypanosoma cruzi***. Biochimica et Biophysica Acta, Vol. 1758, Iss. 6, P 738-746.
- Inselburg, J., 1983. **Stage-specific inhibitory effect of cyclic AMP on asexual maturation and gametocyte formation of *Plasmodium falciparum***. The Journal of Parasitology, Vol. 69, Iss. 3, P592-597.
- Iten, M., Mett, H., Evans, A., Enyaru, J. C. K., Brun, R., Kaminsky, R., 1997. **Alterations in ornithine decarboxylase characteristics account for tolerance of *Trypanosoma brucei rhodesiense* to DL-alpha-difluoromethylornithine**. Antimicrobial Agents and Chemotherapy, Vol. 41, P 1922-1925.
- Johner, A., Kunz, S., Linder, M., Shakur, Y., Seebeck, T., 2006. **Cyclic nucleotide specific phosphodiesterases of *Leishmania major***. BMC Microbiology, Vol. 6:25.
- Kaushal, D. C., Carter, R., Miller, L. H., Krishna, G., 1980. **Gametocytogenesis by malaria parasites in continuous culture**. Nature, Vol. 286, Iss. 5772, P 490-492.
- Kawamoto, F., Alejo-Blanco, R., Fleck, S. L., Kawamoto, Y., Sinden, R. E., 1990. **Possible roles of Ca²⁺ and cGMP as mediators of the exflagellation of *Plasmodium berghei* and *Plasmodium falciparum***. Molecular and Biochemical Parasitology, Vol. 42, Iss. 1, P 101-108.
- Kennedy, P. G. E. 2004. **Human African trypanosomiasis of the CNS: current issues and challenges**. Journal of Clinical Investigation, Vol. 113, No. 4, P 496-504.

Khare, S., Saxena, J. K., Sen, A. B., Ghatak, S., 1984. **Erythrocyte membrane-bound enzymes in *Mastomys natalensis* during *Plasmodium berghei* infection.** The Australian Journal of Experimental Biology and Medical Science, Vol. 62, Pt. 2, P137-143.

Kunz, S., Beavo, J. A., D'Angelo, M. A., Flawia, M. M., Francis, S. H., Johner, A., Laxman, S., Oberholzer, M., Rascon, A., Shakur, Y., Wentzinger, L., Zoraghi, R., Seebeck, T., 2006. **Cyclic nucleotide specific phosphodiesterases of the kinetoplastida: a unified nomenclature.** Molecular and Biochemical Parasitology, Vol. 145, Iss, 1, P 133-135.

Kunz, S., Kloeckner, T., Essen, L. O., Seebeck, T., Boshart, M., 2004. **TbPDE1, a novel class I phosphodiesterase of *Trypanosoma brucei*.** European Journal of Biochemistry/FEBS, Vol. 271, Iss. 3, P 437-647.

Kunz, S., Luginbuehl, E., Seebeck, T., 2009. **Gene Conversion Transfers the GAF-A Domain of Phosphodiesterase TbrPDEB1 to One Allele of TbrPDEB2 of *Trypanosoma brucei*.** PLoS Neglected Tropical Diseases, Vol. 3, Iss. 6, P e455.

Kunz, S., Oberholzer, M., Seebeck, T., 2005. **A FYVE-containing unusual cyclic nucleotide phosphodiesterase from *Trypanosoma cruzi*.** The FEBS Journal, Vol. 272, Iss. 24, P 6412-6422.

Laloo, D. G., 2004. **African Trypanosomiasis.** In 'Infectious Diseases' (2nd Edition), Cohen, J., Powderly, W. G., et al, (Editors). Mosby, Vol. 2, Chapter 157, P 1525-1529.

Lanham, S. M., 1968. **Separation of trypanosomes from the blood of infected rats and mice by anion-exchangers.** Nature, Vol. 218, Iss. 5148, P 1273-1274.

Lanteri, C. A., Stewart, M. L., Brock, J. M., Alibu, V. P., Meshnick, S. R., Tidwell, R. R., Barrett, M. P., 2006. **Roles for the *Trypanosoma brucei* P2 transporter in DB75 uptake and resistance.** Molecular Pharmacology, Vol. 70, Iss. 5, P 1585-1592.

- Laxman, S., Beavo, J. A., 2007. **Cyclic nucleotide signaling mechanisms in trypanosomes: possible targets for therapeutic agents.** *Molecular Interventions*, Vol. 7, Iss. 4, P203-215.
- Laxman, S., Rascón, A., Beavo, J. A., 2005. **Trypanosome cyclic nucleotide phosphodiesterase 2B binds cAMP through its GAF-A domain.** *Journal of Biological Chemistry*, Vol. 280, Iss. 5, P 3771-3779.
- Legros, D., Ollivier, G., Gastellu-Etchegorry, M., Paquet, C., Burri, C., Jannin, J., Büscher, P., 2002. **Treatment of human African trypanosomiasis - present situation and needs for research and development.** *The Lancet Infectious Diseases*, Vol. 2, P 437-440.
- Linder, J. U., Engel, P., Reimer, A., Krüger, T., Plattner, H., Schultz, A., Schultz, J. E., 1999. **Guanylyl cyclases with the topology of mammalian adenylyl cyclases and an N-terminal P-type ATPase-like domain in *Paramecium*, *Tetrahymena* and *Plasmodium*.** *The EMBO Journal*, Vol. 18, Iss. 15, P 4222-4232.
- Liu, Y., Ruoho, A. E., Rao, V. D., Hurley, J. H., 1997. **Catalytic mechanism of the adenylyl and guanylyl cyclases: modeling and mutational analysis.** *Proceedings of the National Academy of Sciences of the United States of America*, Vol. 94, Iss. 25, P 13414-13419.
- Loomis, W. F., 1998. **Role of PKA in the timing of developmental events in *Dictyostelium* cells.** *Microbiology and Molecular Biology Reviews*, Vol. 62, Iss. 3, P 684-694.
- Malki-Feldman, L., Jaffe, C. L., 2009. ***Leishmania major*: effect of protein kinase A and phosphodiesterase activity on infectivity and proliferation of promastigotes.** *Experimental Parasitology*, Vol. 123, Iss. 1, P 39-44.
- Malkova, A., Ivanov, E. L., Haber, J. E., 1996. **Double-strand break repair in the absence of RAD51 in yeast: a possible role for break-induced DNA replication.** *Proceedings of the National Academy of Science of the United States of America*, Vol. 93, Iss. 14, P 7131-7136.

- Mancini, P. E., Patton, C. L., 1981. **Cyclic 3',5'-adenosine monophosphate levels during the developmental cycle of *Trypanosoma brucei brucei* in the rat.** *Molecular and Biochemical Parasitology*, Vol. 3, Iss. 1, P 19-31.
- Martin, S. K., Miller, L. H., Nijhout, M. M., Carter, R., 1978. ***Plasmodium gallinaceum*: induction of male gametocyte exflagellation by phosphodiesterase inhibitors.** *Experimental Parasitology*, Vol. 44, Iss. 2, P 239-242.
- Martin, B.R., Voorheis, H. P., Kennedy, E. L., 1978. **Adenylate cyclase in bloodstream forms of *Trypanosoma (Trypanozoon) brucei* sp.** *The Biochemical Journal*, Vol. 175, Iss. 1, P 207-212.
- Mäser, P., Lüscher, A., Kaminsky, R., 2003. **Drug transport and drug resistance in African trypanosomes.** *Drug Resistance Updates*, Vol. 6, Iss. 5, P 281-290.
- Matovu, E., Enyaru, J. C. K., Schmid, V., Seebeck, T., Kaminsky, R., 2001. **Melarsoprol refractory *T. b gambiense* from Omugo, north-western Uganda.** *Tropical Medicine and International Health*, Vol. 6, Iss. 5, P 407-411.
- McKean, P. G., 2003. **Coordination of cell cycle and cytokinesis in *Trypanosoma brucei*.** *Current Opinion in Microbiology*, Vol. 6, Iss. 6, P 600-607.
- McPherson, P. S., 2002. **The endocytic machinery at an interface with the actin cytoskeleton: a dynamic, hip intersection.** *Trends in Cell Biology*, Vol. 12, Iss. 7, P312-315.
- McRobert, L., Taylor, C. J., Deng, W., Fivelman, Q. L., Cummings, R. M., Polley, S. D., Billker, O., Baker, D. A., 2008. **Gametogenesis in malaria parasites is mediated by the cGMP-dependent protein kinase.** *PLoS Biology*, Vol. 6, Iss. 6, P e139.
- Medina-Acosta, E., Cross, G. A., 1993. **Rapid isolation of DNA from trypanosomatid protozoa using a simple 'mini-prep' procedure.** *Molecular and Biochemical Parasitology*, Vol. 59, Iss. 2, P327-329.

Melville, S. E., Leech, V., Navarro, M., Cross, G. A., 2000. **The molecular karyotype of the megabase chromosomes of *Trypanosoma brucei* stock 427.** *Molecular and Biochemical Parasitology*, Vol. 111, Iss. 2, P 261-273.

Mikus, J., Steverding, D., 2000. **A simple colorimetric method to screen drug cytotoxicity against *Leishmania* using the dye Alamar Blue.** *Parasitology International*, Vol. 48, Iss. 3, P 265-269.

Milord, F., Loko, L., Ethier L., Mpia, B., Pépin, J., 1993. **Eflornithine concentrations in serum and cerebrospinal fluid in 63 patients treated for *Trypanosoma brucei gambiense* sleeping sickness.** *Transactions of the Royal Society for Tropical Medicine and Hygiene*, Vol. 87, Iss. 4, P 473-477.

Muhia, D. K., Swales, C. A., Eckstein-Ludwig, U., Saran, S., Polley, S. D., Kelly, J. M., Schaap, P., Krishna, S., Baker, D. A., 2003. **Multiple splice variants encode a novel adenylyl cyclase of possible plastid origin expressed in the sexual stage of the malaria parasite *Plasmodium falciparum*.** *The Journal of Biological Chemistry*, Vol. 278, Iss. 24, P 22014-22022.

Muhia, D. K., Swales, C. A., Deng, W., Kelly, J. M., Baker, D. A., 2001. **The gametocyte-activating factor xanthurenic acid stimulates an increase in membrane-associated guanylyl cyclase activity in the human malaria parasite *Plasmodium falciparum*.** *Molecular Microbiology*, Vol. 42, Iss. 2, P 553-560.

Naula, C., Schaub, R., Leech, V., Melville, S., Seebeck, T., 2001. **Spontaneous dimerization and leucine-zipper induced activation of the recombinant catalytic domain of a new adenylyl cyclase of *Trypanosoma brucei*, GRESAG4.4B.** *Molecular and Biochemical Parasitology*, Vol. 112, Iss. 1, P 19-28.

Neva, F. A., Brown, H. W., 1994. **Basic Clinical Parasitology (6th Edition).** Prentice-Hall International Inc, P 57-65.

Nok, A. J., 2003. **Arsenicals (melarsoprol), pentamidine and suramin in the treatment of human African trypanosomiasis.** *Parasitology Research*, Vol, 90, Iss. 1, P 71-79.

Nolan, D. P., Rolin, S., Rodriguez, J. R., Van Den Abbeele, J., Pays, E., 2000. **Slender and stumpy bloodstream forms of *Trypanosoma brucei* display a differential response to extracellular acidic and proteolytic stress.** European Journal of Biochemistry/FEBS, Vol. 267, Iss. 1, P 18-27.

O'Beirne, C., Lowry, C. M., Voorheis, H. P., 1998. **Both IgM and IgG anti-VSG antibodies initiate a cycle of aggregation-disaggregation of bloodstream forms of *Trypanosoma brucei* without damage to the parasite.** Molecular and Biochemical Parasitology, Vol. 91, Iss. 1, P 165-193.

Oberholzer, M., Marti, G., Baresic, M., Kunz, S., Hemphill, A., Seebeck, T., 2007. **The *Trypanosoma brucei* cAMP phosphodiesterases TbrPDEB1 and TbrPDEB2: flagellar enzymes that are essential for parasite virulence.** The FASEB Journal, Vol. 21, Iss. 3, P 720-731.

O'Brien, J., Wilson, I., Orton, T., Pognan, F., 2000. **Investigation of the Alamar Blue (resazurin) fluorescent dye for the assessment of mammalian cell cytotoxicity.** European Journal of Biochemistry/FEBS, Vol. 267, Iss. 17, P 5421-5426.

Ochatt, C. M., Ulloa, R. M., Torres, H. N., Téllez-Iñón, M. T., 1993. **Characterization of the catalytic subunit of *Trypanosoma cruzi* cyclic AMP-dependent protein kinase.** Molecular and Biochemical Biochemistry, Vol. 57, Iss. 1, p 73-81.

O'Hara, B. P., Wilson, S. A., Lee, A. W., Roe, S. M., Siligardi, G., Drew, R. E., Pearl, L. H., 2000. **Structural adaptation to selective pressure for altered ligand specificity in the *Pseudomonas aeruginosa* amide receptor, amiC.** Protein Engineering, Vol. 13, Iss. 2, P 129-132.

Ono, T., Cabrita-Santos, L., Leitao, R., Bettiol, E., Purcell, L. A., Diaz-Pulido, O., Andrews, L. B., Tadakuma, T., Bhanot, P., Mota, M. M., Rodriguez, A., 2008. **Adenylyl cyclase alpha and cAMP signaling mediate *Plasmodium* sporozoite apical regulated exocytosis and hepatocyte infection.** PLoS Pathogens, Vol. 4, Iss. 2, P e1000008.

- Paindavoine, P., Rolin, S., Van Assel, S., Geuskens, M., Jauniaux, J. C., Dinsart, C., Huet, G., Pays, E., 1992. **A gene from the variant surface glycoprotein expression site encodes one of several transmembrane adenylate cyclases located on the flagellum of *Trypanosoma brucei*.** *Molecular and Cellular Biology*, Vol. 12, Iss. 3, P 1218-1225.
- Pal, A., Hall, B. S., Field, M. C., 2002. **Evidence for a non-LDL-mediated entry route for the trypanocidal drug suramin in *Trypanosoma brucei*.** *Molecular and Biochemical Parasitology*, Vol. 122, Iss. 2, P 217-221.
- Papageorgiou, I. G., Yakob, L., Al Salabi, M. I., Dhallinas, G., Soteriadou, K. P., De Koning, H. P., 2005. **Identification of the first pyrimidine nucleobase transporter in *Leishmania*: similarities with the *Trypanosoma brucei* U1 transporter and antileishmanial activity of uracil analogues.** *Parasitology*, Vol, 130, Pt. 3, P 275-283.
- Pâques, F., Haber, J. E., 1999. **Multiple pathways of recombination induced by double-strand breaks in *Saccharomyces cerevisiae*.** *Microbiology and Molecular Biology Reviews*, Vol. 63, Iss. 2, P 349-404.
- Pays, E., Tebabi, P., Pays, A., Coquelet, H., Revelard, P., Salmon, D., Steinert, M., 1989. **The genes and transcripts of an antigen gene expression site from *T. brucei*.** *Cell*, Vol. 57, Iss. 5, P 835-845.
- Pépin, J., 2000. **African Trypanosomiasis.** In 'Hunter's Tropical Medicine and Emerging Infectious Diseases' (8th Edition), Strickland, G. T., et al. (Editor). W. B. Saunders Company, Chapter 93, P 643-653.
- Pépin, J., Méda, H. A., 2001. **The Epidemiology and Control of Human African Trypanosomiasis.** In 'Advances in Parasitology', Baker, J. R., Muller, R., Rollinson, D. (Editors). Academic Press, Vol. 49, P 71-132.
- Pépin, J., Milord, F., 1994. **The Treatment of Human African Trypanosomiasis.** In 'Advances in Parasitology', Baker, J. R., Muller, R., Rollinson, D. (Editors). Academic Press, Vol. 33, P 1-47.

Pereira, N. M., Timm, S. L., Da Costa, S. C., Rebello, M. A., De Souza, W., 1978. ***Trypanosoma cruzi*: isolation and characterization of membrane and flagellar fractions.** Experimental Parasitology, Vol. 46, Iss. 2, P 225-234.

Pfaller, M. A., Vu, Q., Lancaster, M., Espinel-Ingroff, A., Fothergill, A., Grant, C., McGinnis, M. R., Pasarell, L., Rinaldi, M. G., Steele-Moore, L., 1994. **Multisite reproducibility of colorimetric broth microdilution method for antifungal susceptibility testing of yeast isolates.** Journal of Clinical Microbiology, Vol. 32, P 1625-1628.

Phillips, M. A., Wang, C. C., 1987. **A *Trypanosoma brucei* mutant resistant to alpha-difluoromethylornithine.** Molecular and Biochemical Parasitology, Vol. 22, P 9-17.

Pozzan, T., Rizzuto, R., Volpe, P., Meldolesi, J. 1994. **Molecular and cellular physiology of intracellular calcium stores.** Physiological Reviews, Vol. 74, Iss. 3, P 595-636.

Qualmann, B., Kessels, M. M., Kelly, R. B., 2000. **Molecular links between endocytosis and the actin cytoskeleton.** The Journal of Cell Biology, Vol. 150, Iss. 5, P F111-116.

Ralston, K. S., Hill, K. L., 2008. **The flagellum of *Trypanosoma brucei*: new tricks from an old dog.** International Journal for Parasitology, Vol. 38, P 869-884.

Rascón, A., Soderling, S. H., Schaefer, J. B., Beavo, J. A., 2002. **Cloning and characterization of a cAMP-specific phosphodiesterase (TbPDE2B) from *Trypanosoma brucei*.** Proceedings of the National Academy of Science of the United States of America, Vol. 99, Iss. 7, P 4714-4719.

Rascón, A., Vilorio, M. E., De-Chiara, L., Dubra, M. E., 2000. **Characterization of cyclic AMP phosphodiesterases in *Leishmania mexicana* and purification of a soluble form.** Molecular and Biochemical Parasitology, Vol. 106, Iss. 2, P 283-292.

Rätz, B., Iten, M., Grether-Bühler, Y., Kaminsky, R., Brun, R., 1997. **The Alamar Blue assay to determine drug sensitivity of African trypanosomes (*T.b. rhodesiense* and *T.b. gambiense*) in vitro.** Acta Tropica Vol. 69, Iss. 2, P 139-147.

Read, L. K., Mikkelsen, R. B., 1991a. ***Plasmodium falciparum*-infected erythrocytes contain an adenylate cyclase with properties which differ from those of the host enzyme.** Molecular and Biochemical Parasitology, Vol. 45, Iss. 1, P 109-119.

Read, L. K., Mikkelsen, R. B., 1991b. **Comparison of adenylate cyclase and cAMP-dependent protein kinase in gametocytogenic and nongametocytogenic clones of *Plasmodium falciparum*.** The Journal of Parasitology, Vol. 77, Iss. 3, P 346-352.

Roberts, L. S., Janovy, J., 2000. **Foundations of Parasitology (6th Edition).** The McGraw-Hill Companies Inc, Chapter 5, P 55-81.

Rodenko, B., van der Burg, A. M., Wanner, M. J., Kaiser, M., Brun, R., Gould, M., De Koning, H. P., Koomen, G. J., 2007. **2,N6-disubstituted adenosine analogs with antitrypanosomal and antimalarial activities.** Antimicrobial Agents and Chemotherapy, Vol. 51, Iss. 11, P 3796-3802.

Rohloff, P., Montalvetti, A., Docampo, R., 2004. **Acidocalcisomes and the contractile vacuole complex are involved in osmoregulation in *Trypanosoma cruzi*.** The Journal of Biological Chemistry, Vol. 279, Iss. 50, P 52270-52281.

Rolin, S., Halleux, S., Van Sande, J., Dumont, J., Pays, E., Steinert, M., 1990. **Stage-specific adenylate cyclase activity in *Trypanosoma brucei*.** Experimental Parasitology, Vol. 71, Iss. 3, P 350-352.

Rolin, S., Hanocq-Quertier, J., Paturiaux-Hanocq, F., Nolan, D., Salmon, D., Webb, H., Carrington, M., Voorheis, P., Pays, E., 1996. **Simultaneous but independent activation of adenylate cyclase and glycosylphosphatidylinositol-phospholipase C under stress conditions in *Trypanosoma brucei*.** The Journal of Biological Chemistry, Vol. 271, Iss. 18, P 10844-10852.

- Rolin, S., Paindavoine, P., Hanocq-Quertier, J., Hanocq, F., Claes, Y., Le Ray, D., Overath, P., Pays, E., 1993. **Transient adenylate cyclase activation accompanies differentiation of *Trypanosoma brucei* from bloodstream to procyclic forms.** *Molecular and Biochemical Parasitology*, Vol. 61, Iss. 1, P 115-125.
- Rolón, M., Vega, C., Escario, J. A., Gómez-Barrio, A., 2006. **Development of resazurin microtiter assay for drug sensibility testing of *Trypanosoma cruzi* epimastigotes.** *Parasitology Research*, Vol, 99, Iss. 2, P 103-107.
- Ross, D. T., Raibaud, A., Florent, I. C., Sather, S., Gross, M. K., Storm, D. R., Eisen, H., 1991. **The trypanosome VSG expression site encodes adenylate cyclase and a leucine-rich putative regulatory gene.** *The EMBO Journal*, Vol. 10, Iss. 8, P 2047-2053.
- Salomon, Y., Londos, C., Rodbell, M. 1974. **A highly sensitive adenylate cyclase assay.** *Analytical Biochemistry*, Vol. 58, Iss. 2, P 541-548.
- Sanchez, M. A., Zeoli, D., Klamo, E. M., Kavanaugh, M. P., Landfear, S. M., 1995. **A family of putative receptor-adenylate cyclases from *Leishmania donovani*.** *The Journal of Biological Chemistry*, Vol. 270, Iss. 29, P 17551-17558.
- Saran, S., Meima, M. E., Alvarez-Curto, E., Weening, K. E., Rozen, D. E., Schaap, P., 2003. **cAMP signaling in *Dictyostelium*. Complexity of cAMP synthesis, degradation and detection.** *Journal of Muscle Research and Cell Motility*, Vol. 23, P 793-802.
- Schultz, J. E., Klumpp, S., Benz, R., Schürhoff-Goeters, W. J., Schmid, A., 1992. **Regulation of adenylate cyclase from *Paramecium* by an intrinsic potassium conductance.** *Science*, Vol. 255, Iss. 5044, P 600-603.
- Seebeck, T., Schaub, R., Johner, A., 2004. **cAMP signalling in the kinetoplastid protozoa.** *Current Molecular Medicine*, Vol. 4, Iss. 6, P 585-599.
- Seebeck, T., Gong, K., Kunz, S., Schaub, R., Shalaby, T., Zoraghi, R., 2001. **cAMP signalling in *Trypanosoma brucei*.** *International Journal for Parasitology*, Vol. 31, P 491-498.

Shalaby, T., Liniger, M., Seebeck, T., 2001. **The regulatory subunit of a cGMP-regulated protein kinase A of *Trypanosoma brucei***. *European Journal of Biochemistry/FEBS*, Vol. 268, Iss. 23, P 6197-6206.

Siman-Tov, M. M., Aly, R., Shapira, M., Jaffe, C. L., 1996. **Cloning from *Leishmania major* of a developmentally regulated gene, c-lpk2, for the catalytic subunit of the cAMP-dependent protein kinase**. *Molecular and Biochemical Parasitology*, Vol. 77, Iss. 2, P 201-215.

Siman-Tov, M. M., Ivens, A. C., Jaffe, C. L., 2002. **Molecular cloning and characterization of two new isoforms of the protein kinase A catalytic subunit from the human parasite *Leishmania***. *Gene*, Vol. 288, P 65-75.

Slaughter, M. R., Bugelski, P. J., O'Brien, J., 1999. **Evaluation of Alamar blue reduction for the *in vitro* assay of hepatocyte toxicity**. *Toxicology In Vitro*, Vol 13, P 567-569.

Smith, A. B., Esko, J. D., Hajduk, S. L., 1995. **Killing of trypanosomes by the human haptoglobin-related protein**. *Science*, Vol. 268, P 284-286.

Sternberg, J. M. 1998. **Immunobiology of African Trypanosomiasis**. In 'Immunology of Intracellular Parasitism', Liew, F. Y., Cox, F. E. G. (Editors). In *Chemical Immunology*. Karger, Vol. 70, P 186-199.

Strickler, J. E., Patton, C. L., 1975. **Adenosine 3',5'-monophosphate in reproducing and differentiated trypanosomes**. *Science*, Vol. 190, Iss. 4219, P 1110-1112.

Sunahara, R. K., Dessauer, C. W., Gilman, A. G., 1996. **Complexity and diversity of mammalian adenylyl cyclases**. *Annual Review of Pharmacology and Toxicology*, Vol. 36, P 461-480.

Taylor, C. J., McRobert, L., Baker, D. A., 2008. **Disruption of a *Plasmodium falciparum* cyclic nucleotide phosphodiesterase gene causes aberrant gametogenesis**. *Molecular Microbiology*, Vol. 69, Iss. 1, P 110-118.

Taylor, M. C., Muhia, D. K., Baker, D. A., Mondragon, A., Schaap, P. B., Kelly, J. M., 1999. ***Trypanosoma cruzi* adenyl cyclase is encoded by a complex multigene family.** *Molecular and Biochemical Parasitology*, Vol. 104, Iss. 2, P 205-217.

Téllez-Iñón, M. T., Ulloa, R. M., Torruella, M., Torres, H. N., 1985. **Calmodulin and Ca²⁺-dependent cyclic AMP phosphodiesterase activity in *Trypanosoma cruzi*.** *Molecular and Biochemical Parasitology*, Vol. 17, Iss. 2, P 143-153.

Torruella, M., Flawiá, M. M., Eisenschlos, C., Molina y Vedia, L., Rubinstein, C. P., Torres, H. N., 1986. ***Trypanosoma cruzi* adenylate cyclase activity. Purification and characterization.** *The Biochemical Journal*, Vol. 234, Iss. 1, P 145-150.

Ulloa, R. M., Mesri, E., Esteva, M., Torres, H. N., Téllez-Iñón, M. T., 1988. **Cyclic AMP-dependent protein kinase activity in *Trypanosoma cruzi*.** *The Biochemical Journal*, Vol. 255, Iss. 1, P 319-326.

van den Abbeele, J., Rolin, S., Claes, Y., Le Ray, D., Pays, E., Coosemans, M., 1995. ***Trypanosoma brucei*: stimulation of adenylate cyclase by proventriculus and esophagus tissue of the tsetse fly, *Glossina morsitans morsitans*.** *Experimental Parasitology*, Vol. 81, Iss. 4, P 618-620.

Vassella, E., Reuner, B., Yutzy, B., Boshart, M., 1997. **Differentiation of African trypanosomes is controlled by a density sensing mechanism which signals cell cycle arrest via the cAMP pathway.** *Journal of Cell Science*, Vol. 110, P 2661-2671.

Vickerman, K., Myler, P. J., Stuart, K., 1993. **African Trypanosomiasis.** In 'Immunology and molecular biology of parasitic infections,' Warren, K. S., (Editor). Blackwell Scientific Publications, Chapter 10, P 170-212.

Voorheis, H. P., Martin, B. R., 1980. **'Swell dialysis' demonstrates that adenylate cyclase in *Trypanosoma brucei* is regulated by calcium ions.** *European Journal of Biochemistry/FEBS*, Vol. 113, Iss. 3, P 223-227.

- Voorheis, H. P., Martin, B. R., 1981. **Characteristics of the calcium-mediated mechanism activating adenylate cyclase in *Trypanosoma brucei*.** European Journal of Biochemistry/FEBS, Vol. 116, Iss. 3, P 471-477.
- Voorheis, H. P., Bowles, D. J., Smith, G. A., 1982. **Characteristics of the release of the surface coat protein from bloodstream forms of *Trypanosoma brucei*.** Journal of Biological Chemistry, Vol. 257, Iss. 5, P 2300-2304.
- Voorheis, H. P., Martin, B. R., 1982. **Local anaesthetics including benzyl alcohol activate the adenylate cyclase in *Trypanosoma brucei* by a calcium-dependent mechanism.** European Journal of Biochemistry/FEBS, Vol. 123, Iss. 2, P 371-376.
- Wallace, L. J., Candlish, D., De Koning, H. P., 2002. **Different substrate recognition motifs of human and trypanosome nucleobase transporters. Selective uptake of purine antimetabolites.** Journal of Biological Chemistry, Vol. 277, Iss. 29, P 26149-26156.
- Walter, R. D., 1974. **Adenylate cyclase from *Trypanosoma gambiense*.** Hoppe-Seyler's Zeitschrift für physiologische Chemie, Vol. 355, P 427-430.
- Walter, R. D., Opperdoes, F. R., 1982. **Subcellular distribution of adenylate cyclase, cyclic-AMP phosphodiesterase, protein kinases and phosphoprotein phosphatase in *Trypanosoma brucei*.** Molecular and Biochemical Parasitology, Vol. 6, Iss. 5, P 287-295.
- Wang, H., Yan, Z., Geng, J., Kunz, S., Seebeck, T., Ke, H., 2007. **Crystal structure of the *Leishmania major* phosphodiesterase LmjPDEB1 and insight into the design of the parasite-selective inhibitors.** Molecular Microbiology, Vol. 66, Iss. 4, P 1029-1038.
- Weber, J. H., Vishnyakov, A., Hambach, K., Schultz, A., Schultz, J. E., Linder, J. U., 2004. **Adenylyl cyclases from *Plasmodium*, *Paramecium* and *Tetrahymena* are novel ion channel/enzyme fusion proteins.** Cellular Signalling, Vol. 16, Iss. 1, P 115-125.

Welburn, S. C., Odiit, M., 2002. **Recent developments in human African trypanosomiasis.** *Current Opinion in Infectious Diseases*, Vol. 15, P 477-484.

Wentzinger, L., Bopp, S., Tenor, H., Klar, J., Brun, R., Beck, H. P., Seebeck, T., 2008. **Cyclic nucleotide-specific phosphodiesterases of *Plasmodium falciparum*: PfPDEalpha, a non-essential cGMP-specific PDE that is an integral membrane protein.** *International Journal for Parasitology*, Vol. 38, Iss. 14, P 1627-1637.

Wentzinger, L., Seebeck, T., 2007. **Protozoal phosphodiesterases.** In: Beavo, J. A., Houslay, M. D., Francis, S. H. (Editors.), *Cyclic Nucleotide Phosphodiesterases in Health and Disease*. CRC Press, Boca Raton, FL, pp. 277-300.

White, M. J., DiCaprio, M. J., Greenberg, D. A., 1996. **Assessment of neuronal viability with Alamar blue in cortical and granule cell cultures.** *Journal of Neuroscience Methods*, Vol. 70, P 195-200.

Wilkinson, S. H., Taylor, M. C., Horn, D., Kelly, J. M., Cheeseman, I., 2008. **A mechanism for cross-resistance to nifurtimox and benznidazole in trypanosomes.** *Proceedings of the National Academy of Sciences of the United States of America*, Vol. 105, Iss. 13, P 5022-5027.

World Health Organisation, 2000. **Report on Global Surveillance of Epidemic-Prone Infectious Diseases - African Trypanosomiasis.** World Health Organization

World Health Organization, 2001. **African Trypanosomiasis or sleeping sickness.** World Health Organization, Fact sheet No. 259.

www.genedb.org/genedb/tryp/

Wyatt, M. D., Pittman, D. L., 2006. **Methylating agents and DNA repair responses: Methylated bases and sources of strand breaks.** *Chemical Research in Toxicology*, Vol. 19, Iss. 12, P 1580-1594.

Yuasa, K., Mi-Ichi, F., Kobayashi, T., Yamanouchi, M., Kotera, J., Kita, K., Omori, K., 2005. **PfPDE1, a novel cGMP-specific phosphodiesterase from the human malaria parasite *Plasmodium falciparum*.** The Biochemical Journal, Vol. 392, Pt. 1, P 221-229.

Zoraghi, R., Seebeck, T., 2002. **The cAMP-specific phosphodiesterase TbpPDE2C is an essential enzyme in bloodstream form *Trypanosoma brucei*.** Proceedings of the National Academy of Sciences of the United States of America, Vol. 99, Iss. 7, P 4343-4348.